Horbachevskyi National Medical University, Ternopil, Ukraine
Ivan Franko State Pedagogical University, Drohobych, Ukraine
Danylo Halytskyi National Medical University, Lviv, Ukraine
Nicolaus Copernicus University, Torun, Poland
Ukrainian SR Institute of Medicine of Transport, Odesa
Bohomolets Institute of Physiology of NAS, Kyïv, Ukraine

Mykhaylo M. Korda
Oksana A. Fihura
Oksana I. Melnyk
Ivan M. Klishch
Roman I. Yanchij
Walery A. Zukow
Sofiya V. Ruzhylo
Dariya V. Popovych
Igor L. Popovych

UKRAINIAN PHYTOCOMPOSITION «BALM TRUSKAVETS'», METABOLISM, PHYSICAL WORKING CAPACITY AND NEURO-ENDOCRINE-IMMUNE COMPLEX

LVIV
SVIT
2025

УДК 615.8:614.215]:615.45(477)(043.5)
U

Recommended for publication by the Academic Council
of Horbachevskyi National Medical University
(protocol No. 10 dated 30/08/2024)

Reviewers:

Regeda Mykhaylo S., MD, DS, Prof, head of the department of pathophysiology of the Danylo Halytskyi National Medical University, Lviv, Ukraine

Vastyanov Ruslan S., MD, DS, Prof, head of the department of general and clinical pathophysiology named after VV Podvysotskyi of the National Medical University, Odesa, Ukraine

Korda MM, Fihura OA, Melnyk OI, Klishch IM,
Yanchij RI, Zukow W, Ruzhylo SV, Popovych DV, Popovych IL.

U Ukrainian phytocomposition «Balm Truskavets'», metabolism, physical working capacity and neuro-endocrine-immune complex. Lviv. Svit; 2025: 328.

ISBN 978-966-914-477-5

The monograph highlights the results of priority experimental and clinical-physiological studies of the Ukrainian phytocomposition «Balm Truskavets'». Physiologically favorable modulating effects of the phytocomposition on the neuro-endocrine-immune complex, metabolism and physical performance, which are attributes of classic adaptogens, were revealed.

For physiologists, endocrinologists, immunologists, phytotherapists, medical rehabilitation specialists.

УДК 615.8:614.215]:615.45(477)(043.5)

ISBN 978-966-914-477-5

Authors

Mykhaylo M. Korda, MD, DS, Prof; Horbachevskyi National Medical University, Ternopil, Ukraine cordamm@yahoo.com; orcid.org/0000-0003-0676-336X

Oksana A. Fihura, MD; Ivan Franko State Pedagogical University, Drohobych, Ukraine oksanafigura08@gmail.com; orcid.org/0000-0002-5711-0484

Oksana I. Melnyk, MD, PhD; Danylo Halytskyi National Medical University, Lviv, Ukraine omelnyk7@gmail.com; orcid.org/0000-0001-7928-4760

Ivan M. Klishch, MD, DS, Prof; Horbachevskyi National Medical University, Ternopil, Ukraine klishch@tdmu.edu.ua; orcid.org/0000-0001-6226-4296

Roman I. Yanchij, DS, Prof; Bohomolets Institute of Physiology, Kyïv, Ukraine tas@biph.kiev.ua; orcid.org/0000-0001-7129-7698

Walery Zukow, MD, DS, Prof. hab.; Nicolaus Copernicus University, Torun, Poland w.zukow@wp.pl; orcid.org/0000-0002-7675-6117

Sofiya V. Ruzhylo, MD, DS; Ivan Franko State Pedagogical University, Drohobych, Ukraine doctor-0701@ukr.net; orcid.org/0000-0003-2944-8821

Dariya V. Popovych, MD, DS, Prof; Horbachevskyi National Medical University, Ternopil, Ukraine darakoz@yahoo.com; orcid.org/0000-0002-5142-2057

Igor L. Popovych, MD, PhD, senior res. fel.; Bohomolets Institute of Physiology, Kyïv, Ukraine; Kozyavkin International Rehabilitation Clinic, Truskavets', Ukraine; i.popovych@biph.kiev.ua; i.l.popovych@gmail.com; orcid.org/0000-0002-5664-5591



We dedicate the monograph to memory of Emmanuil N. Berger (1910-1999), Olena O. Markova (1930-2000) and Yurij I. Bondarenko (1936-2024) as the first (1957-1975), second (1975-2000) and fifth (2012-2018) Heads of the Department of Pathological Physiology of the Ternopil Medical Institute/University

CONTENT

Summary

The monograph presents the results of experimental and clinical-physiological studies of the influence of the Ukrainian phytocomposition "Balm Truskavets'" on the neuro-endocrine-immune complex, metabolism and physical performance with the aim of sanogenetic justification of its use to increase the effectiveness of rehabilitation of patients with maladaptation.

In an experiment on rats of both sexes, the authors found modulating effects of phytocomposition on post-stress changes in neuroendocrine-immune complex, metabolome, electrocardiogram (ECG), and gastric mucosa. First of all, it was confirmed that acute water- immersion and restraint stress (WIRS) causes in control animals an increase in sympathetic tone, blood levels of catecholamines and corticosterone, combined with a decrease in vagal tone and serum testosterone levels. Such a neuro-endocrine reaction is accompanied by damage to the myocardium and gastric mucosa, an increase in the percentage of macrophages, fibroblasts and Hassal's corpuscles in the thymus, entropy in the spleen, theophylline-resistant T-lymphocytes, natural killer cells and polymorphonuclear neutrophils in the blood, as well as the activity of serum alanine transaminase and creatine phosphokinase. Instead, the mass of the spleen and the percentage of lymphoblasts in it, theophylline-sensitive T-lymphocytes and eosinophils in the blood, the content of malondialdehyde and cholesterol in the serum, as well as the catalase activity of serum and erythrocytes, decrease. Preventive use of phytocomposition, first of all, to one degree or another minimizes adverse post-stress deviations from the norm of most of the listed parameters, and even completely prevents deviations of 5 parameters. Secondly, it initiates an increase in the level of PTH and the activity of serum acid phosphatase, the percentage of reticulocytes in the spleen and the intensity of phagocytosis of blood neutrophils, but at the same time a decrease in their bactericidal activity, as well as the percentage of monocytes and B-lymphocytes in the blood. Thirdly, it potentiates the post-stress increase in sympathetic tone and damage to the gastric mucosa, as well as natural killers, on the one hand, and the decrease in vagal tone, the level of testosterone and malondialdehyde in the serum, as

well as the mass of the spleen – on the other hand. Fourthly, it reverses the catalase activity of erythrocytes and the entropy of the splenocytogram. Thus, phytocomposition has a generally favorable adaptogenic effect on the post-stress state of the neuro-endocrine-immune complex, ECG and metabolome. However, there are certain adverse effects as the so-called adaptation fee.

The authors found that the severity of damage to gastric mucosa significantly correlates with changes in ECG parameters, in particular, depression of the T wave and S-T joint, which indicate myocardial dystrophy. Further, it was found that such a connection is caused by the damaging effect on both targets of increasing the level of parathyroid hormone, as well as the production of aldosterone and catecholamines by enlarged adrenal glands. In addition, an increase in the level of corticosterone and sympathetic tone with a simultaneous decrease in vagal tone as well as serum calcitonin and testosterone cause damage only to the gastric mucosa, but not to the myocardium. Such a constellation of neuro-endocrine reactions to stressors (cold, immobilization, hunger, etc.) determines the severity of damage to the gastric mucosa and myocardium by 73%. Thus, the condition of the gastric mucosa and myocardium as essential targets of stressors is determined by the damaging and protective effects of adaptive hormones and the autonomic nervous system.

Next, metabolic and immune accompaniments of ECG and damage to gastric mucosa parameters were analyzed. It was found that Serum levels of Phosphates, Catalase and α-LP Cholesterol as well as erythrocyte level of Potassium (as marker of Kalihistia) and Na,K-ATPase activity of the shadows of erythrocytes (as marker of membranes of myocardiocytes) are positively correlated with ECG markers of damage to myocardium such as T wave amplitude and ST junction, and negatively correlated with visual markers of damage to the gastric mucosa, i.e. reflect intactness (normality) of both targets of stressors – myocardium and gastric mucosa. Erythrocyte level of Sodium and serum levels of Potassium and Alkaline Phosphatase reflect the intactness of the gastric mucosa only. While serum level of Calcium reflects damage to the gastric mucosa. Taken together, the listed metabolic factors determine the morpho-functional state of the gastric mucosa and myocardium by 72% (R=0.851). Damage to the gastric mucosa and myocardium is more severe, the lower the bactericidal

activity of blood neutrophils, and the greater the mass of the thymus. The spleen mass and the content of fibroblasts in the thymus are negatively correlated only with the severity of damage to the gastric mucosa, while the percentages of reticulocytes and lymphoblasts in the spleen are positively correlated with it. Finally, the higher the percentage of macrophages in the thymus, the deeper the damage to the myocardium. The canonical correlation between the listed immune parameters and markers of the two targets of stressors is very strong (R=0.809). Thus, WIRS causes changes in the neuro-endocrine-immune complex, which lead to changes in the metabolome and damage to the gastric mucosa and myocardium.

The next goal was a detailed analysis of sexual dimorphism in these parameters in baseline and post stress situations. By the method of discriminant analysis was selected 23 variables (4 endocrines, 6 immune, 9 metabolic as well as 4 markers of damage in gastric mucosa and myocardium) whose constellation is characteristic for each group**.** The distance between the centroids of the major discriminant root of intact females and males as a measure of sexual dimorphism is 16.2 units. Acute stress increases it in control rats to 23.4 units, and in pretreated by phytoadaptogen – up to 29.4 units. Acute stress increases the severity of sexual dimorphism also in relation to variables, information about which is condensed in the minor root – from 0.99 to 2.29 units, while preventive use of phytoadaptogen limits it to 1.63 units. Thus, in intact rats, significant sex differences were found for a number of endocrine, immune, and metabolic variables, which increase under the influence of acute stress per se, and to an even greater extent against the background of preventive use of a phytoadaptogen.

In a separate experiment, the ability of phytocomposition to prevent the adverse actotropic effect of Naftussya bioactive water was investigated. It was found that the weekly use of Naftyssya bioactive water reduces the duration of swimming of rats to exhaustion by 30% compared to the daily water control. Addition of phytoadaptogen to Naftyssya softens its negative actotropic effect by up to -9%, and adding Balsam to daily water prolongs the maximum duration of swimming compared to the control by 11%. A positive correlation of the swimming test with 17-KS excretion and water diuresis was revealed, but a negative correlation with mineralocorticoid activity, spontaneous diuresis and

neutrophils phagocytosis. Thus, phytoadaptogen reverses the adverse effects of Naftussya bioactive water on dynamic muscle performance in healthy rats by mitigating the decrease in the excretion of 17-ketosteroids and increased mineralocorticoid activity.

At the preparatory stage of clinical and physiological studies, the authors supplemented previously known data on the close relationship between the parameters of gas discharge visualization (GDV, electrophotonic) and neuroendocrine-immune complex with their own data on the relationship of EEG parameters with the energy and asymmetry of virtual Chakras, reconstructed on the basis of GDV parameters. It was found that the coefficients of canonical correlation between the EEG parameters and virtual Chakras Energy are in the interval 0,415÷0,564 and 0,358÷0,528 when registering without a filter and with a filter, respectively. Additional inclusion of HRV and endocrine parameters increases the strength of the canonical correlation to 0,768 and 0,772, respectively. The coefficients of canonical correlation between the EEG parameters and individual virtual Chakras Asymmetry are in the interval 0,284÷0,634 and 0,152÷0,458 when registering without a filter and with a filter, respectively. Integral coefficient of the canonical correlation is 0,820. The above data, taken together with the previous ones, state that between parameters of neuroendocrine-immune complex and GDV in general and virtual Chakras in particular, exist strong canonical correlation suggesting suitability of the latter method.

The purpose of next study was relationships between levels of major adaptation hormones and EEG&HRV parameters at human with maladaptation. Using the method of canonical correlation analysis, it was found that the level of triiodothyronine is determined by the constellation of 17 EEGs and 4 HRVs parameters by 87,5%. The rate of determination of the cortisol level by 14 EEGs and 3 HRVs parameters is 83,7%, and aldosterone by the other 14 EEGs and 3 HRVs parameters is 80,0%. Neuromodulation of testosterone and calcitonin levels is characterized by sexual dimorphism. With the same coefficients of determination (92,4%), the regression model for testosteroneemia in women included 15 EEGs parameters and no HRV parameters, instead testosteroneemia in men is modulated by other 11 EEGs parameters and one HRV parameter. The level of calcitonin in women is determined by 86,2% by the constellation of 9

EEGs and 2 HRVs parameters, while in men by 83,5% by the other 5 EEGs and 4 HRVs parameters. Thus, levels of the main adaptation hormones are accompanied by specific patterns of EEG and HRV parameters.

At the next stage, the immediate effects of a single use of the phytocomposition "Balm Truskavets'" on HRV, EEG and GDV parameters at 12 women and 62 men with dysfunction of neuro-endocrine-immune complex were investigated. Discriminant analysis revealed 26 EEG, 6 HRV and 7 GDV parameters characteristic of the baseline state and after consumption of phytocomposition or tap water. The use of balm causes the normalizing decrease of increased sympathotonic markers and the increase of decreased vagotonic markers. Physiologically favorable vegetotropic effects of the balm are accompanied by a further increase in the initially increased activity of β-rhythm-generating cortical and subcortical structures as well as activation of θ-rhythm-generating and inhibition of α- and δ-rhythm-generating nuclei whose initial activity was within normal limits. Neurotropic effects are accompanied by a decrease in fractality and entropy and an increase in the area of gas discharge image, as well as the energy of the first, fourth, fifth and seventh virtual Chakras. Thus, Ukrainian phytocomposition "Balm Truskavets'" causes favorable immediate neurotropic and biophysic changes at patients with dysfunction of neuro-endocrine-immune complex.

This provided the basis for studying long-term (9-day course) effects on parameters of neuro-endocrine-immune complex and biophotonics at 16 women and 24 men with maladaptation. A noticeable effect of the phytocomposition on 38 parameters was revealed, grouped into 6 clusters, of which 4 are enhancing and 2 are reducing. In particular, the reduced levels of the adaptation index and phagocytosis parameters increase significantly, instead, the increased levels of the strain index, testosterone, triiodothyronine, LF band HRV as well as two biophotonics parameters decrease, that is, there is a normalizing/beneficial effect. At the same time, normal levels of HRV-markers of vagal tone decrease, and cortisol and circulating catecholamines as well as the activity of β- and α-rhythm generating neurons increase, but within the normal range. Finally, there is a further increase in the upper limit levels of activity of δ-rhythm generating neurons. Thus, Ukrainian phytocomposition "Balm Truskavets'" exerts classical adaptogenic effects on parameters of neuro-

endocrine-immune complex as well as biophotonics and acupuncture in humans with maladaptation.

The discovery of the adaptogenic properties of the phytocomposition provided the basis for studying its ability to increase the effectiveness of rehabilitation at the Truskavets' spa for patients with maladaptation. In the first study, it has been found that at patients with post-radiation encephalopathy standard balneotherapy increases the decreased level of T-helper lymphocytes, but further decreases the level of B-lymphocytes, glomerular filtration rate and PWC_{150}, in combination with increased normal levels of blood creatinine and urea, as well as decreased levels of diastolic blood pressure and heart rate. This is accompanied by a further increase in the sympathetic tone and the leveling of the increased of ULF band HRV as marker of level of catecholamines and glucocorticoids. Additional use of phytocomposition limits the adverse effects of standard balneotherapy by modulating EEG and HRV parameters. Thus, phytocomposition «Balm Truskavets'» limits the adverse effects of standard balneotherapy at the Truskavets' spa in patients with post-radiation encephalopathy.

The effect of standard balneotherapeutic complex of the Truskavets' Spa on the physical performance of both rats and resort patients is ambiguous. Therefore, the search for means of correcting its adverse or neutral actotropic effects remains relevant. The results of the experiment on rats provided the basis for clinical testing of the effectiveness of the phytocomposition. At the preparatory stage, the relationships between PWC and the parameters of neuro-endocrine regulation as well as sexual differences in such relationships were investigated. The object of observation were 30 women and 30 men with maladaptation. For estimation of PWC a two-stage bicycle ergometry used. Parameters of EEG, HRV and adaptation hormones levels registered twice with an interval of 4 or 7 days. It was found that PWC levels in men are generally downregulated by cortisol, triiodothyronine, sympathetic tone, and θ-rhythm generating neurons, but upregulated by testosterone, calcitonin, vagal tone, and related α-rhythm generating neurons. In women, PWC levels are borderline downregulated by cortisol and aldosterone, but significantly upregulated by circulating catecholamines and β-rhythm generating neurons.

The object of last observation were 40 women with chronic cholecystitis in remission phase, who came for rehabilitation at the Truskavets' Spa. Registered PWC_{150}, adaptation hormones levels, parameters of HRV, EEG, immunity, metabolism as well as GDV. Members of the control group received for two weeks standard balneotherapy: drinking of Naftussya bioactive water, application of Ozokerite, baths with mineral water. Members of the main group additionally received a phytoadaptogen. The analysis of individual changes revealed that normal levels of PWC in control group fell to the lower zone of the norm. Phytoadaptogen prevents PWC decrease. This is accompanied by the prevention of both a decrease in power spectral density (PSD) T4-θ EEG and VLF band HRV, leukocytes level as well as area and symmetry of GDV, as well as an increase in vagal tone and entropy of HRV as well as a rightward shift in the symmetry of the virtual first Chakra of GDV. In addition, phytoadaptogen reverses balneotherapy-induced moderate decrease in the frequency of α-rhythm, PSD O1-β, sympathetic tone, serum levels of catecholamines, testosterone and IgG, activity of Na,K-ATPase of erythrocyte shadows as well as Energy of the first, third and fourth virtual Chakras. Phytoadaptogen potentiates the reduction of PSD P4-β, IgM and cholesterol as well as initiates the reduction of δ-rhythm variability, PSD of α-rhythm in C3, C4, P4 and Fp2 loci, entropy in F4 locus as well as serum potassium while increasing in serum cortisol and calcitonin, blood B-lymphocytes levels as well as PSD Fp2-δ. Thus, the phytoadaptogen «Balm Truskavets'» prevents the adverse effect of the standard balneotherapeutic complex of the Truskavets' Spa on PWC by, apparently, its neuro-endocrine effects.

The materials of the monograph are reflected in the following publications of the authors

Ruzhylo SV, Fihura OA, Zukow W, Popovych IL. Immediate neurotropic effects of Ukrainian phytocomposition. Journal of Education, Health and Sport. 2015; 5(4): 415-427. DOI http://dx.doi.org/10.12775/JEHS.2015.05.04.042

Fihura OA, Ruzhylo SV, Żukow X, Popovych IL. Immediate effects of Ukrainian phytocomposition on biophotonics (GDV), EEG and HRV

parameters. Journal of Education, Health and Sport. 2021; 11(7): 349-365. DOI http://dx.doi.org/10.12775/JEHS.2021.11.07.035

Korda MM, Gozhenko AI, Fihura OA, Popovych DV, **Ż**ukow X, Popovych IL. Relationships between plasma levels of main adaptogene hormones and EEG&HRV parameters at human with dysadaptation. Journal of Education, Health and Sport. 2021; 11(12): 492-512.
DOI http://dx.doi.org/10.12775/JEHS.2021.11.12.040

Babelyuk VY, Tserkovniuk RG, Dubkova GI, Kruhliy YS, Korolyshyn TA, Babelyuk NV, Zukow W, Ruzhylo SV, Fihura OA, Gozhenko AI, Popovych IL. Relationships between the neuro-endocrine parameters and virtual chakras energy and asymmetry. Journal of Education, Health and Sport. 2022; 12(1): 235-249. DOI http://dx.doi.org/10.12775/JEHS.2022.12.01.020

Fihura OA, Ruzhylo SV, Popovych IL. Ukrainian adaptogenic phytocomposition "Balm Truskavets'" modulate EEG, HRV and biophotonics (GDV) parameters. Вісник морської медицини. 2022; 2(95): 99-108. DOI https://zenodo.org/record/6984227

Fihura OA, Ruzhylo SV, Zakalyak NR. Phytoadaptogen reverses the adverse effects of Naftussya bioactive water on dynamic muscle performance in healthy rats. Quality in Sport. 2022; 8(2): 45-55. DOI http://dx.doi.org/10.12775/QS.2022.08.02.004

Ruzhylo SV, Fihura OA, Zakalyak NR, Kovalchuk GY, **Ż**ukow X, Popovych DV. Sexual dimorphism in the neuro-endocrine regulation of bicycle ergometric test parameters in untrained individuals with dysfunction of the neuro-endocrine-immune complex. Journal of Education, Health and Sport. 2022; 12(9): 971-984. DOI http://dx.doi.org/10.12775/JEHS.2022.12.09.110

Fihura OA, Ruzhylo SV, Korda MM, Klishch IM, **Ż**ukow X, Popovych IL. The influence of the Ukrainian phytocomposition «Balm Truskavets'» on parameters of neuro-endocrine-immune complex and biophotonics in humans with maladaptation. Journal of Education, Health and Sport. 2023; 13(1): 326-337. DOI http://dx.doi.org/10.12775/JEHS.2023.13.01.048

Fihura OA. Amelioration by phytoadaptogene of effects of balneofactors of Truskavets' Spa on patients with post-radiation encephalopathy. Journal of Education, Health and Sport. 2023; 19(1): 36-58. DOI http://dx.doi.org/10.12775/JEHS.2023.19.01.005

Fihura OA, Melnyk OI, Ruzhylo SV, Zakalyak NR, Kondratska HD, Zukow W, Popovych IL. Relationships between neuro-endocrine, electrocardiogram, and gastric mucosal damage parameters in naïve and stressed rats. Journal of Education, Health and Sport. 2023; 18(1): 162-190. DOI http://dx.doi.org/10.12775/JEHS.2023.18.01.014

Zukow W, Fihura OA, Żukow X, Muszkieta R, Hagner-Derengowska M, Smoleńska O, Michalska A, Melnyk OI, Ruzhylo SV, Zakalyak NR, Kondratska HD, Voloshyn OR, Popovych IL. Prevention of adverse effects of balneofactors at Truskavets' Spa on gastroenterologic patients through phytoadaptogens and therapeutic physical education: mechanisms of rehabilitation. Journal of Physical Education and Sport. 2024; 24(4): 791-810. DOI 10.7752/jpes.2024.04093

Zukow W, Fihura OA, Korda MM, Klishch IM, Ruzhylo SV, Melnyk OI, Yanchij RI, Popovych IL. Modulating effects of Ukrainian phytocomposition "Balm Truskavets'" on post stress changes in neuroendocrine-immune complex, metabolome, electrocardiogram, and gastric mucosa at rats. Journal of Education, Health and Sport. 2024; 64: 55171. DOI https://dx.doi.org/10.12775/JEHS.2024.64.55171

Fihura OA, Korda MM, Klishch IM, Ruzhylo SV, Melnyk OI, Zukow W, Yanchij RI, Vorobienko AA, Plyska OI, Popovych IL. Metabolic and immune accompaniments of electrocardiographic and morphologic gastric mucosa parameters in naïve and stressed rats. Journal of Education, Health and Sport. 2024; 61: 54947. DOI https://dx.doi.org/10.12775/JEHS.2024.61.54947

Fihura O, Korda M, Klishch I, Ruzhylo S, Melnyk O, Zukow W, Yanchij R, Vorobienko A, Plyska O, Popovych D, Popovych I. Sexual dimorphism in basal and post stress parameters of neuro-endocrine-immune complex, metabolome, electrocardiogram, and gastric mucosa at rats. Journal of Education, Health and Sport. 2024; 72: 57566. DOI https://doi.org/10.12775/JEHS.2024.72.5756

Fihura OA, Korda MM, Popovych DV, Ruzhylo SV. Plasma levels of main adaptogene hormones and EEG&HRV parameters are closely correlated. В: Матер. XIII Всеукраїнської наук.-практ. конф. "Актуальні питання патології за умов дії надзвичайних факторів на організм" (Тернопіль, 26-28 жовтня 2022 р). Тернопіль; 2022: 81-81.

Fihura OA, Korda MM, Klishch IM, Ruzhylo SV, Melnyk OI, Zukow WA, Yanchij RI, Popovych IL. Modulating effects of Ukrainian phytocomposition “Balm Truskavets’” on post-stress changes at rats. В: Матер. XIV Всеукраїнської наук.-практ. конф. “Актуальні питання патології за умов дії надзвичайних факторів на організм” (Тернопіль, 23-25 жовтня 2024 р). Тернопіль; 2024:72-73.

Fihura OA, Korda MM, Klishch IM, Ruzhylo SV, Melnyk OI, Zukow W, Yanchij RI, Vorobienko AA, Plyska OI, Popovych IL. Metabolic and immune accompaniments of electrocardiographic and morphologic gastric mucosa parameters in naïve and stressed rats. Abstracts of the International Conference on Neuroscience and Scientific Readings Dedicated to Visceral Physiology and Pathophysiology, November 19-21, 2024. Fiziol. Zh. 2024;70(5S):111-112.

Fihura OA, Ruzhylo SV, Korda MM, Klishch IM, Żukow X. The influence of the Ukrainian phytocomposition “Balm Truskavets’” on parameters of neuro-endocrine-immune complex and biophotonics in humans with maladaptation. Abstracts of the International Conference on Neuroscience and Scientific Readings Dedicated to Visceral Physiology and Pathophysiology, November 19-21, 2024. Fiziol. Zh. 2024;70(5S):112-113.

INTRODUCTION

The researchers of the Truskavetsian Scientific School of Balneology have demonstrated the adaptogenic properties of the main curative factors of the Truskavets' Spa such as Naftussya bioactive water, Ozokerite and mineral baths, which together make up a standard balneotherapeutic complex [Flyunt IS et al., 2002; Popovych IL et al., 2003; Kostyuk PG et al., 2006; Flyunt IS et al., 2008; Popovych IL, 2011; Popovych IL et al., 2022].

However, in contrast to the beneficial effect of the latter on stress resistance and the neuro-endocrine-immune complex, the effect on the physical performance of both rats and resort patients is ambiguous [Popovych IL et al., 2005; Zukow W et al., 2020; Zukow W et al., 2021; Zukow W et al., 2022].

It is important to note that, firstly, various responses of fitness to balneofactors are accompanied by characteristic changes in metabolic, HRV, EEG, immune, and other parameters; secondly, based on the constellation of such initial parameters, first of all, the level of fitness, as well as lipids and electrolytes, it is possible to predict not only the direction, but also the severity of the fitness reaction [Popovych IL et al., 2005; Zukow W et al., 2021; Zukow W et al., 2022].

A detailed analysis of the causes of the adverse actotropic effect of balneotherapy revealed the following. In an experiment on female rats, it was found that after 3 weeks of Naftussya water use adverse changes in swimming time to fatigue were observed only in 4 rats with initial very high performance, ie a reduction in swimming time from 61±7 min to 39± 3 min. Instead, in 6 animals the performance increased from 13.0±1.4 min to 52.3±5.9 min, and in 8 animals did not change significantly (from 24.5± 3.9 min to 37.3±5.9 min; $p>0.05$). In 73 children and adolescents of both sexes aged 10-17 with maladaptation, who received Naftussya water together with ozokerite applications and mineral baths, three variants of actotropic effects were also revealed. In particular, PWC170, assessed by the step test, decreased only in 31.5% of children with a PWC170 level significantly higher than the sex-age norm: from 125.8±3.5% to 119.6±3.0% (direct difference: -6.2±1.1%). On the other hand, the normal level of PWC170 in 21.9% of children did not change, and in 46.6% it increased from 113.7±2.7% to 125.6±2.8% (direct difference: 11.9±1.8%). A similar pattern also occurred in 42 adult gastroenterology patients of both sexes. In particular, PWC150, assessed by two-stage bicycle ergometry, decreased from 2.82±0.32 W/kg to 2.42±0.26 W/kg (by 11.0±5.0%) in 26.2% of

patients, whereas in 47.6% of patients with lower work capacity, it increased from 2.32±0.18 W /kg to 2.45±0.14 W/kg (by 11.0±5.2%), and in another 26.2% it did not change significantly [Popovych IL et al., 2005]. The analysis of individual changes in another sample (19 men and 3 women with urate urolithiasis and chronic pyelonephritis) revealed that in 54.5% patients the normal level of fitness fell to the lower zone of the norm, however, in 45.5% patients reduced fitness was completely normalized [Zukow W et al., 2022].

This situation prompted researchers to additionally apply of aerobic training [Tserkovnyuk AV & Ruzhylo SV, 2001] and/or phytoadaptogens, both well-known (Ginseng, Bittner's balsam), and the Ukrainian phytocomposition "Balm Kryms'kyi" [Hrinchenko BV, 1998; Hrinchenko BV et al., 1999; Flyunt IS et al., 2002; Kostyuk PG et al., 2006].

Adaptogenic properties of "Balm Kryms'kyi" first discovered by representatives of the Truskavetsian Scientific School of Balneology [Panasyuk YM et al., 1994; Alyeksyeyev ***OI*** et al., 1996; Pat. 10271 Ukraine MKI A 61 K 31/00, 1996].

Previous experimental and clinical-physiological studies have shown that adaptogenic properties are manifested in both actotropic and vegetative, endocrine, immunotropic, coagulotropic, metabolic effects [Panasyuk YM et al., 1994; Alyeksyeyev ***OI*** et al., 1996; Markova OO et al., 1997; Flyunt IS et al., 2002; Hrinchenko BV et al., 2006; Kostyuk PG et al., 2006; Flyunt IS et al., 2008; Hrinchenko BV, 2008]. However, the neurotropic properties of this phytocomposition remain unclear. Endocrine, immunological and biochemical studies, primarily in the experiment, were not carried out in full. In the statistical processing of digital material, modern methods were not used.

Therefore, the study of the possibility of using phytoadaptogens to increase the effectiveness of rehabilitation at the Truskavets' Spa of patients with maladaptation remains relevant.

The subject of the new study was a new Ukrainian phytocomposition "Balm Truskavets'" produced by private research and production enterprise "Ukrainian Balms", Mykolaïv, Ukraine (ТУ У 15.8-24055046-005:2009). It is similar in composition to its predecessor, differing in the smaller number of medicinal plants included in the recipe.

Here are the components of the phytocomposition "Balm Truskavets'": *Nepeta cataria, Mentha×piperita, Salvia officinalis, Echinacea purpurea, Cichorium inthybus, Achillea millefolium, Artemisia balchanorum, Acorus calamus, Althaea officinalis, Silybum marianum, Rubus idaeus, Rosa majalis.*

Chapter 1

ADAPTOGENS, STRESS, METABOLISM AND THE NEUROENDOCRINE-IMMUNE COMPLEX (LITERATURE REVIEW)

The aim of this review is to summarize our knowledge about common concept relating to adaptogenic plants used as officinal medical preparations in the Western and in traditional Chinese medicine (TCM), Ayurveda, Kampo, and other traditional medical systems (TMS) and alternative medical systems, and to analyze how such preparations have been studied scientifically. This provides a basis for assessing the use of adaptogens in the treatment of stress-induced and aging-related disorders.

The term adaptogens is currently widely used in alternative and complementary medicine, as well as in pharmacognosy, phytomedicine, and phytotherapy research [Samuelsson G & Bohlin L, 2009]. The definition of adaptogens is continuously updated, incorporating the increasing body of scientific evidence related to understanding their pharmacological and molecular mechanisms of action [Panossian AG et al., 2021].

1. Adaptogens are medicinal substances causing the "state of nonspecifically increased resistance" of the organism [Lazarev NV, 1958; Lazarev NV et al., 1959].

2. Only those preparations that meet the following requirements may be included in the group of adaptogens: (a) An adaptogen should be innocuous and cause minimal disorders in the physiological functions of an organism; (b) The action of an adaptogen should be nonspecific, i.e., it should increase resistance to adverse influences of a wide range of factors of physical, chemical and biological nature, (c) An adaptogen may possess normalizing action irrespective of the direction of the foregoing pathologic changes [Brekhman II & Dardymov IV, 1969].

3. The adaptogens are nontoxic compounds with polyvalent mechanisms of action and pharmacological effects related to adaptability and survival [Farnsworth NR et al., 1986].

4. Adaptogens are substances, which elicit in an organism a state of nonspecifically raised resistance, allowing them to counteract stressor signals and to adapt to exceptional strain [Wagner H et al., 1994].

5. Adaptogens are metabolic regulators, which increase the ability of an organism to adapt to environmental factors and to avoid damage from such factors [Panossian A et al., 1999].

6. Plant adaptogens are agents, which reduce damaging effects of various stressors due to reduction of the reactivity of host defense system. They adapt organism to stress and have curative effect in stress-induced disorders [Panossian A et al., 1999a].

7. Adaptogenic substances have the capacity to normalize body functions and strengthen systems compromised by stress. They have a protective effect on health against a wide variety of environmental assaults and emotional conditions [EMEA/HMPC/102655/2007].

8. Adaptogens comprise a pharmacotherapeutic group of herbal preparations used to: increase attention and endurance in fatigue and prevent/mitigate/reduce stress-induced impairments and disorders related to neuro-endocrine and immune systems [Panossian A & Wikman G, 2009].

9. Botanical adaptogens are plant extracts, or specific constituents of plant extracts, which function to increase survival in animals and humans by stimulating their adaptability to stress by inducing adaptive responses [Panossian A, Amsterdam J, 2017].

10. Adaptogens are stress-response modifiers that increase an organism's nonspecific resistance to stress by increasing its ability to adapt and survive [Panossian A, 2017].

11. Botanical adaptogens are metabolic regulators that increase survival by increasing adaptability in stress [Panossian A, 2017].

12. Adaptogens are natural compounds or plant extracts that increase adaptability and survival of living organisms to stress [Panossian A et al., 2018].

Importantly, the term adaptogen is related to a physiological process – adaptation to environmental challenges, which is a multistep process including diverse mechanisms of extracellular and intracellular interactions. The renewed definition of adaptogens is supported by the results of recent studies on the molecular mechanisms of action of adaptogens in a variety of regulatory systems from the cellular to entire organism levels.

Similar to antioxidants and vitamins, adaptogens constitute a category of nutritional and herbal medicinal products essential for good health, adaptability, resilience, survival, and healthy aging. Regardless of the nature

of the stimulus (stressor), an adaptogen increases adaptability, resilience, and survival by activating adaptive signaling pathways of cellular and organismal defence systems (stress system e.g., neuroendocrine-immune complex). Furthermore, adaptogens trigger the generation of hormones (cortisol, corticotropin-releasing hormone [CRH] and gonadotropin-releasing hormones, urocortin, neuropeptide Y), playing key roles in metabolic regulation and homeostasis. Meanwhile, multitarget mechanisms of action and a wide range of pharmacological effects indicate their nonspecific pharmacological activity. Therefore, adaptogens are most likely effective for the prevention and treatment of stress-induced and adult-onset disorders such as chronic fatigue, memory impairment, depression, anxiety, sleep disturbance, diabetes, heart disease and high blood pressure, chronic inflammation and autoimmune diseases, cold and flu, infections, skin diseases, liver diseases, and cancer. This can be achieved due to their ability to activate the innate defence system, increase resistance to stress, adapt organisms to stress, increase recovery of stress-induced damages, provide energy to fight fatigue, reduce aging-associated decline of the neuroendocrine-immune system [Panossian AG et al., 2021].

Panossian AG et al. [2021] provides a summary of the general characteristics of adaptogens, which comprise a category of nutritional and herbal medicinal products.

Definition: Adaptogens are natural compounds or plant extracts that increase adaptability, resilience, and survival of organisms to stress.

Chemical class: Various, predominantly tetracyclic triterpenes, phenethyl-and phenylpropanoids glycosides, stilbenes, lignans, etc.

Pharmacological activity/health claims: adaptogenic.

Mechanism of action: Multitarget effects on neuroendocrine-immune system including:

(i) Triggering of intracellular and extracellular adaptive signaling pathways that promote cell survival and organismal resilience in stress;

(ii) Regulation of metabolism and homeostasis via effects on expression of stress hormones (corticotropin and gonadotropin-releasing hormones, urocortin, cortisol, neuropeptide Y, heat shock proteins Hsp70) and their receptors.

Indications for use: Stress-induced fatigue, mental and behavioral disorders, aging-associated diseases.

Key points of the adaptogenic concept defined by Brekhman II & Dardymov IV [1969] are in line with basic principles of the TMS of China, Korea, Japan, India (Ayurveda), and Middle Asia (Yunani). For instance, an assumption is that some adaptogens used in TCM, Kampo, and Ayurveda medicine (e.g., Ginseng, Ashwagandha, Andrographis, Bryony) must have normalizing effects, irrespective of the nature of the disease. Herbalists refer to adaptogens as restoratives, qi-tonics, rasayanas, or rejuvenating herbs. Tonic herbs are classified as the highest and most sought-after herbal remedies in many traditional systems of healing such as TCM and Ayurveda. Both traditional systems are based on holistic approaches to patients and treatment, suggesting that the patient is an individual and not a disease. Holistic medicine strives to consider the whole person, suggesting that one can only achieve optimal health by complex treatment of all imbalances (physical, emotional, or spiritual) induced by environmental factors. Consequently, multitarget therapy by herbal preparations have polyvalent actions on various mediators, effectors, and regulatory systems, presumably making it the most effective approach for the treatment of complex diseases. Both TMS have a similar notion of "life vital energy" and activating the body and mind: the *qi* in TCM and the *prana* in Ayurveda. Similar notions exist in various cultures including the Greek *pneuma*, the Armenian *zorutyun* (զորություն), the Polynesian *mana*, the German *od*, and the Hebrew *ruah*. Prana is also referred to as life force, subtle, or bioplasmic energy. Below are brief descriptions of the ethnopharmacological roots of the adaptogenic concept [Panossian AG et al., 2021].

In TCM, all known medicinal plants are divided into three categories: inferior, middle, and superior. The highest forms of medicine revered in China are the superior herbs (tonic herbs), which help everything to heal and nurtures life itself. Superior herbs are thought to possess restorative properties and are used as general tonics for the treatment of disease and in convalescence. The most well-known broad action medicinal plant in TCM is ginseng. The pharmacological activity of ginseng was first described in the 1st century by an unknown author. According to his records, ginseng improves mental activity and visual acuity, dispels pathogenic factors, enhances longevity with long-term intake tonifying five vital organs of the body (spleen, lung, heart, kidney, and liver). According to other ancient regards written by Hongjing Tao (AD 456–536), ginseng can be used to

enhance cognitive function; improve blood circulation; relieve thirst and feelings of solidity; and cure internal coldness, pain in the chest or abdomen, vomiting, and diarrhea. These and other beneficial effects of ginseng have also been described in other more complete and comprehensive medical textbooks including treatment for general weakness and fatigue [Ginseng Radix, 1999; Pharmacopoeia, 2017].

The concept of adaptogens is based on Hans Selye's theory of stress and homeostasis. The word "stress" is commonly used in numerous conditions and has quite different meanings in daily life. In this review, we used commonly accepted definitions of stress, homeostasis, adaptive stress response, and adaptive homeostasis [Davies KJ, 2016].

Definitions of stress, stress system, homeostasis, adaptation, adaptedness, adaptability, resilience, adaptive homeostasis, adaptive stress response (hormesis), adaptive stress system, and adaptive signaling pathways.

1. Stress is a state of threatened homeostasis Cannon WB [1935], depending on severity and duration, stress can have quite a different impact on the organism -from beneficial to harmful: chronic eustress (too little stress), acute stress (optimum stress) initiate beneficial adaptive stress response, while when stress increases beyond a certain level - acute distress (too much stress), and chronic stress (burnout) – it leads to harmful health effects and can cause numerous diseases. In this context, adaptogens act like chronic eustress activating adaptive stress response, resilience and overall survival. Repeated mild exposure or low doses of stress induce the increased resistance of cells and organisms to subsequent stress exposure, resulting in an adaptation favouring survival. This phenomenon of adaptation to repetitive low-level stress was first described by Hans Selye in 1936.

2. Stress system is the neuroendocrine-immune complex, Adaptive stress system includes all physiological systems involved in the process of adaptation to stress [Stratakis CA & Chrousos GP, 1995].

3. Homeostasis is a complex dynamic equilibrium/steady state, maintained by coordinated physiological processes in the organism [Cannon WB, 1935; Chrousos GP & Gold PW, 1992]. In other words, homeostasis is the ability of a living organism or cell to maintain the state of internal balance despite changes in the conditions around it, while stress – is temporary inability to maintain this steady state.

4. Adaptation as an active process of responding to challenges which includes behavioral, physiological, structural, and genetic changes upon environmental impacts that are beyond the biologically adequate ranges [Peck JR & Waxman D, 2018].

Survival of organisms and resistance to stress depends on adaptability, and adaptive homeostasis is the threshold that determines an organism's innate tolerance to a given level of stress.

In recent years our understanding of mechanisms underlying the health benefits of natural dietary compounds has improved considerably. Based on modern concepts, plants synthesize in their most susceptible parts (flowers, roots, and leaves) special secondary metabolites for self-protection against microorganisms, insects, and other pests, as well as to mitigate harmful environmental conditions [Mattson MP et al., 2007; Mattson MP, 2008; Murakami A, 2018]. In animals that use plants as their primary nutrition multiple mechanisms to counteract the potentially poisonous effects of phytotoxins have evolved. These natural compounds are not noxious in humans at lower doses but are able to induce mild cellular stress responses [Dhabhar FS, 2018]. The ability of plant secondary metabolites to activate the adaptive cellular stress response pathway in human body is one of their essential mechanisms of action [Mattson MP, 2008; Murakami A, 2018].

This phenomenon has been categorized as hormesis or as adaptive stress response, pre-conditioning [Calabrese EJ et al., 2007; Calabrese EJ et al., 2010]. The multiple mediators of the stress signaling system (the neuroendocrine-immune complex) including different growth factors, antioxidants, and stress-resistant proteins such as heat shock proteins (Hsps) are involved in stress-induced responses of the innate and adaptive defence systems [Mattson MP & Cheng A, 2006; Mattson MP, 2008; Panossian A et al., 2018].

Panossian A et al. [2018] suggest that adaptogens are the first line of plant secondary metabolites activating adaptive stress response pathways (Fig. 1).

Adaptive stress response is important in cell maturation, with initiation by mild stress of mechanisms of repair and maintenance to protect cells against subsequent stresses, while chronic stress induce progressive failure of these mechanisms, leading to cellular senescence, aging, and death [Thorin-Trescases N & Thorin E, 2010]. With cellular maintenance

on overdrive, the organism can continue to protect himself from chronic inflammation, which causes a range of serious illnesses, particularly aging-related diseases.

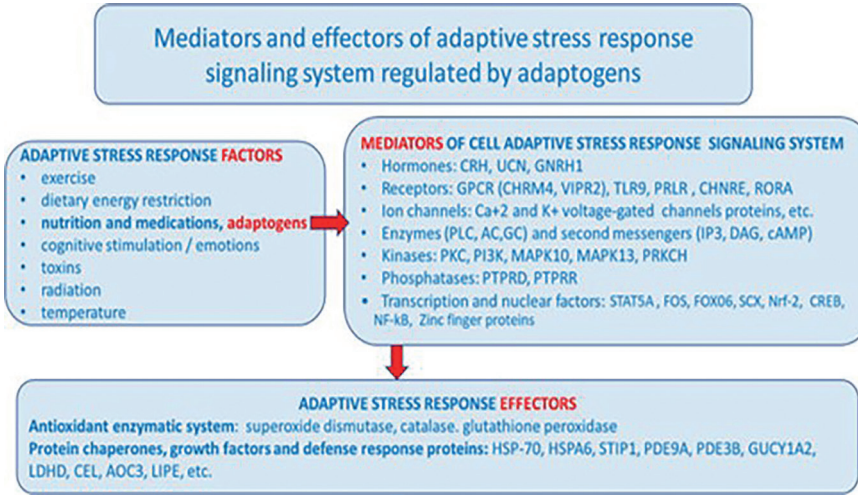

Fig. 1. Adaptive stress response factors, mediators, and effectors.
Adaptive stress response involves activation of intracellular and extracellular signaling pathways and increased expression of antiapoptotic proteins, neuropeptides, antioxidant enzymes, and defense response of an organism resulting in increased survival. One basic mechanism of action of adaptogens, that is, that they activate adaptive cellular stress response pathways in humans' brain cells (updated and adapted from: Mattson MP, Son TG, Camandola S [2007] and Panossian A et al. [2018]).

The adaptive stress response is a survival mechanism. All functions of the body systems (e.g., cardiovascular, immune, nervous, endocrine, gastrointestinal digestive) are regulated by about 30,000 genes and fragments of DNA, which are located in the nucleus of every single cell. The activity of genes depends on the signals/stimuli received from numerous receptors and various proteins located on the outside surface of the cell membrane. The receptors specifically trigger signals from extracellular molecules – stressors (Fig. 2) and transfer the signals to genes via many signaling cascades (adaptive signaling pathways), which can interact and influence each other in a complex molecular network (Fig. 3).

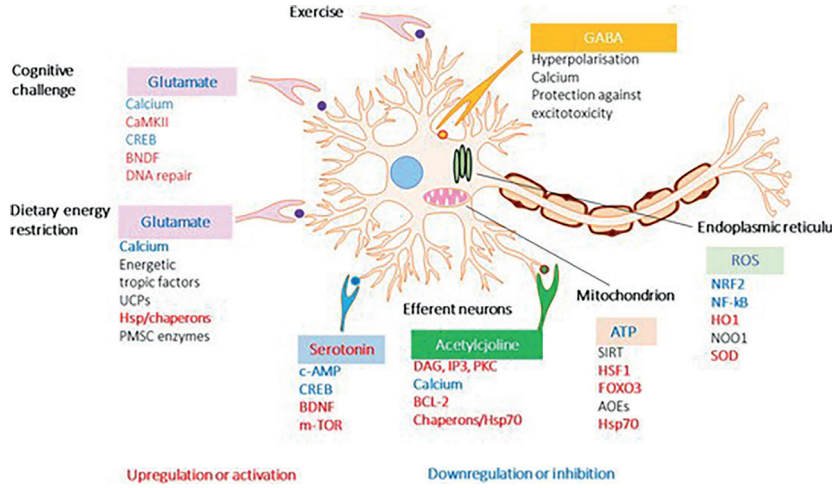

Fig. 2. Effects of adaptogens on adaptive stress response signaling pathways that promote synaptic plasticity and protect neurons against degeneration. Illustration of a glutamatergic neuron receiving excitatory signals from neurons activated in response to intellectual tasks, exercise, and dietary energy restriction. Postsynaptic receptors for glutamate, acetylcholine, and serotonin, are activated to trigger intracellular signaling pathways and transcription factors that activate the expression of neuroprotective proteins including antiapoptotic proteins, brain-mitochondrial uncoupling proteins (UCPs), and derived neurotrophic factor (BDNF). BDNF activates neuronal growth by stimulating the mammalian target of rapamycin (mTOR). Mild cellular stress resulting from dietary energy restriction and oxidative stress (ROS) activates adaptive stress response pathways including those that upregulate antioxidant enzymes (AOEs) and protein chaperones. CREB, cyclic AMP response element-binding protein; CaMKII, calcium/calmodulin kinase II; DAG, diacylglycerol; FOXO3, forkhead box protein O3; HO1, heme oxygenase 1; HSF1, heat shock factor 1; IP3 PKC, inositol trisphosphate 3 protein kinase C; NF-B, nuclear factor B; NRF2, nuclear regulatory factor 2 NQO1, NAD(P)H-quinone oxidoreductase 1 (updated and adapted from Stranahan AM & Mattson MP [2012] and Panossian A [2017a]).

Collectively, this stimulus-response system is known as the adaptive stress response system of the body responding to environmental stress [Mattson MP & Cheng A, 2006; Mattson MP et al., 2007; Mattson MP, 2008; Son TG et al., 2008; Panossian A, 2017a; Shen CY et al., 2017].

The principal active constituents of adaptogenic plants can be divided into three main chemical groups [Panossian A et al., 2021]:

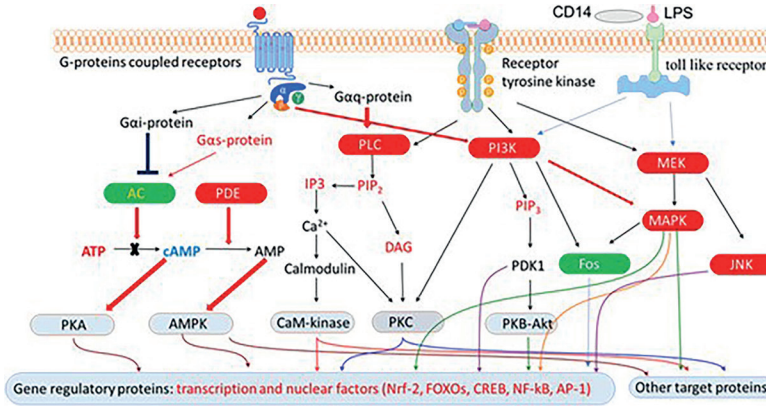

Fig. 3. Effects of adaptogens on adaptive stress response intracellular signaling pathways.

Activation of the PI3K/AKT/mTOR signaling pathway positively regulates cell cycle, proliferation, neural long-term potentiation (memory cognitive functions and longevity. AC, adenylate cyclase; AMPK, 5' AMP-activated protein kinase; AP-1, activator protein 1 transcription factor; CREB, cyclic AMP response element-binding protein; DAG, diacylglycerol; Fos, Fos proto-oncogene, AP-1 transcription factor subunit; FOXOs, forkhead box proteins; IP3, inositol 1,4,5-trisphosphate; JNK, c-Jun N-terminal kinases; MaM-kinase, Ca^{2+}/calmodulin-dependent protein kinase II; MAPK–MEK (MAPK/ERK), mitogen-activated protein kinases; NF-κB, nuclear factor kappa-light-chain-enhancer of activated B cells; NRF2, nuclear regulatory factor 2; PDE, 3',5'-cyclic-AMP phosphodiesterase; PI3K, phosphoinositide 3-kinase; PIP3, phosphatidylinositol (3,4,5)-trisphosphate; PIP2, phosphatidylinositol (4,5)-bisphosphate; PKA, cAMP-dependent protein kinase; PKB-Akt, serine/threonine-specific protein kinase; PKC, protein kinase C; PLC, phospholipase C (updated from Panossian A et al. [2018]).

1. Compounds with a tetracyclic skeleton like cortisol and testosterone – terpenoids ginsenosides, sitoindosides, cucurbitacines, and withanolides.

2. Structural analogues of catecholamines or tyrosine – lignans (schizandrin B from *S. chinensis*, eleutheroside E from *E. senticosus*); phenylpropane derivatives (rosavin from *R. rosea* and syringin from *E. senticosus*); phenylethane derivatives (tyrosol and salidroside from *R. rosea*).

3. Structural analogues of resolvins – oxylipins (polyhydroxylated polyunsaturated fatty acids).

The number of plants reported as being adaptogenic has increased exponentially during the past decades. However, it should be emphasized that only a few comply with the most important criterium – exhibiting

multitarget effects on the neuroendocrine-immune system. These effects include triggering intracellular and extracellular adaptive signaling pathways that promote cell survival and organismal resilience in stress; and regulating metabolism and homeostasis via effects on the expression of stress hormones (corticotropin- and gonadotropin-releasing hormones, urocortin, cortisol, melatonin, Hsp70, and neuropeptide Y) and their receptors [Asea A et al., 2013; Panossian A et al., 2018].

Various adaptogens and their active principles – for example, salidroside [Lin X et al., 2020], schisandrin A [Song F et al., 2016], schisandrin B [Dai X et al., 2018], withaferin A [Hsu JH et al., 2019], Ginsenoside 20(S)Rg3 [Li J et al., 2015], Ginsenoside 20(S)-Rh2 [Han S et al., 2016], compound K [Park S et al., 2011; Zhang X et al., 2018] and 20(S)-25-methoxy-protopanaxatriol [Ai HH et al., 2017; Kim D et al., 2020] – exhibit anticancer effects. It was found that compound K, an intestinal microbiome metabolite of ginsenoside Rb1 [Qi LW et al., 2011], one of the major ginsenosides of Panax ginseng, has much stronger cancer chemopreventive activity than its precursor (Rb1 in HCT-116 and HT-19).

Stress-protective and stimulating effects are characteristic and common pharmacological effects of adaptogens [Panossian AG, 2003; Panossian A & Wagner H, 2005; Boon-Niermeijer EK et al., 2012], which have been observed in many animals and humans' studies. The effects of adaptogens on cognitive functions and physical endurance in stress are summarized in several reviews [Wagner H et al., 1994; Panossian AG, 2003; Panossian A & Wikman G, 2010; Panossian A & Wagner H, 2011; Panossian A et al., 2012; Panossian A, 2013].

The main difference between adaptogens and conventional stimulants such as caffeine and amphetamine is that after prolonged use, the latter can cause the user to develop both tolerance and addiction [Panossian A & Wikman G, 2010; Panossian A et al., 2011].

Primarily, adaptogens have potential benefits in cases of behavior-related disorders, mental illness, stress-induced fatigue and cognitive function [Bogatova RI et al., 1997; Darbinyan V et al., 2000; Deyama T et al., 2001; Facchinetti F et al., 2002; Panossian AG, 2003; Hartz AJ et al., 2004; Yue PY et al., 2007; Olsson EM et al., 2009; Panossian A & Wikman G, 2010; Sarris J et al., 2011; Megna M et al., 2012; Panossian A, 2013; Jeong HG et al., 2015; Mao JJ et al., 2015; Bertoglio JC et al., 2016; Amsterdam JD & Panossian AG, 2016; Lopresti AL et al., 2019; Gannon JM et al., 2019; Baek JH et al., 2019; Cave AE et al., 2019] (Fig. 4).

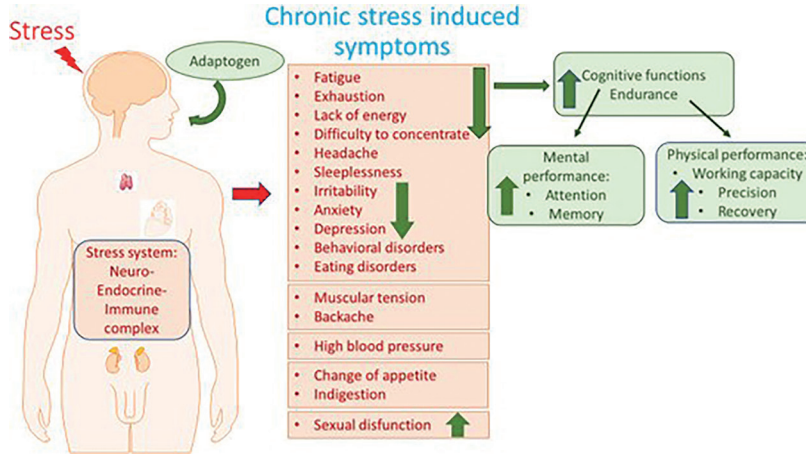

Fig. 4. Chronic stress-induced symptoms and effect of adaptogens (updated from Panossian A & Wikman G [2009])

In a number of clinical studies, the beneficial effects of adaptogens have been demonstrated on healthy subjects in stress conditions [Bogatova RI et al., 1997; Darbinyan V et al., 2000; Facchinetti F et al., 2002; Yue PY et al., 2007; Olsson EM et al., 2009; Aslanyan G et al., 2010; Panossian A & Wikman G, 2010; Megna M et al., 2012; Panossian A, 2013; Qi Z et al., 2016; Lopresti AL et al., 2019]. This is especially true of the mental and physical performance of fatigue and mental strain. Furthermore, the efficacy of adaptogens in mild and moderate depression has been demonstrated [Darbinyan V et al., 2007; Sarris J et al., 2011; Mao JJ et al., 2015; Jeong HG et al., 2015; Amsterdam JD & Panossian AG, 2016; Gannon JM et al., 2019].

Several systematic reviews and assessment reports have been conducted on the clinical efficacy and safety of *Ginseng* [Vogler BK et al., 1999; Coon JT & Ernst E, 2002; Lee NH & Son CG, 2011], *Eleutherococcus* [Li W et al., 2009], *Rhodiola* [Man C et al., 2020], *Withania* [Durg S et al., 2020; Ayati Z et al., 2020; Pérez-Gómez J et al., 2020].

The pathogenesis of complex diseases as well as the adaptive stress response, inflammation, and senescence are multistep processes which involve extracellular and intracellular communications at differing stages of stress regulation and cannot be limited to the few biochemical interactions that occur in the brain or other tissues. Clearly, for the description of the mechanism of action of adaptogens the reductionist model that assumes

a single drug-single receptor interaction is insufficient and not valid. Adaptogens have many molecular targets, involved in the metabolic regulation of homeostasis at both the cellular and systemic levels and play a role of stress response modifiers [Panossian A et al., 2021].

Network pharmacology with the use of the systems biology offers exciting new opportunities for understanding such complex systems [Panossian A, 2017; Panossian A et al., 2022]. During the past several decades, many molecules, signaling pathways, and networks targeted by adaptogens have been identified. They include stress hormones and some other important mediators of homeostasis regulation such as the molecular chaperons Hsp70, neuropeptide Y, G protein-coupled receptors (GPCRs), dopamine-cAMP-PKA-CERT, IP3, PLC, DAG, phosphoinositide 3-kinase (PI3K), nuclear factor kappa-light-chain-enhancer of activated B cells (NF-κB)-mediated signaling pathways, stress-activated kinase c-Jun N-terminal kinase (JNK), forkhead box protein O3 (FOXO3), cortisol, estrogens, and nitric oxide (NO) [Asea A et al., 2013; Panossian A, 2013; Panossian A et al., 2013; Panossian A, 2017; Panossian A et al., 2018; Mohanan P et al., 2018; Qi HY et al., 2018]. The mechanisms of action of adaptogens are mainly associated with metabolic regulation via extracellular communication of hypothalamic–pituitary–adrenal (HPA)-axis hormones and activation of intracellular adaptive stress response signaling pathways [Panossian A, 2017].

The hypothetical mechanism of adaptogens' action on HPA-axis hormones in stress is presented in Fig. 5. The HPA axis plays a pivotal role in regulating the majority of endocrine hormones associated with the CNS. Stress hormones regulate growth, appetite, blood pressure, emotion, sexual function, body temperature, sleep, biorhythms, and hydration. They are produced by the endocrine system, are secreted into the bloodstream, and target other tissues to regulate physiological functions. The main function of stress hormones is to maintain homeostasis to counteract stress.

Ginsenoside Rg1 directly interacts with glucocorticoid receptor (GR) ligand-binding sites and behaves as a partial agonist of GR. Ginsenoside Rb1 is a functional ligand of the estrogen receptor (ER). Along with CRH, another primary upstream mediator of extracellular communications stimulated by adaptogens is the stress hormone neuropeptide-Y (NPY) [Asea A et al., 2013; Panossian A et al., 2013]. Stimulation and release of NPY into the blood circulatory system are innate defence responses to mild stressors (adaptogens), which increase resistance to stress. This

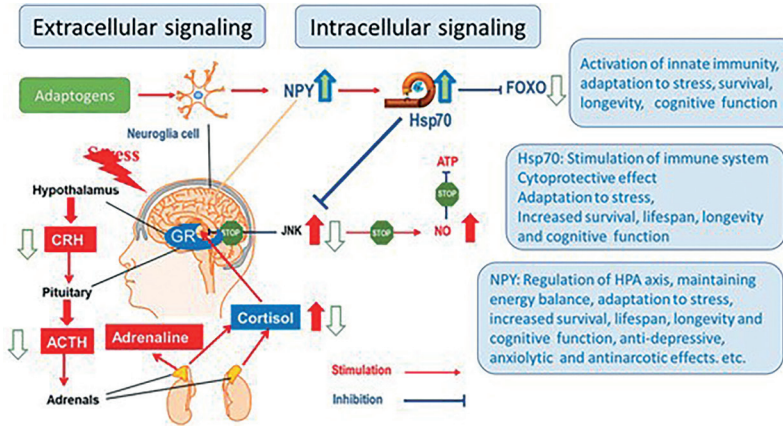

Fig. 5. Hypothetical mechanism of action underlying the effects of adaptogens on the adaptive stress response in the hypothalamic–pituitary–adrenal axis: forkhead box O, neuropeptide-Y (NPY), and Hsp70 signaling. Persistent chronic stress induces and blockage of negative feedback regulation of cortisol and disruption of ATP synthesis. During stress, corticotropin-releasing hormone (CRH) is released from the hypothalamus, followed by the release of adrenocorticotropic hormone (ACTH) from the pituitary, which stimulates the release of adrenal hormones and NPY. Feedback regulation of overreaction is triggered by cortisol release from the adrenal cortex, followed by binding to glucocorticoid receptors (GRs) in the brain, which halts the further release of brain hormones, resulting in decreases of cortisol to normal levels. Although mild stress (eustress) is a vital part of life, chronic and severe stress can cause depression associated with the production of active oxygen-containing molecules including nitric oxide, which inhibits ATP formation. The stress-induced signaling protein c-Jun N-terminal kinase (JNK) inhibits GRs. Subsequently, this feedback control is inhibited and the cortisol content in the bloodstream of depressed patients is permanently high, which is associated with impaired memory, decreased ability to concentrate, fatigue, among others. Adaptogens normalize increased cortisol/corticosterone levels in the bloodstream and saliva of humans or animals presumably due to direct interaction with GRs. Adaptogens also attenuate elevated JNK and cortisol levels during stress and activate the generation of Hsp70, which inhibits JNK. Therefore, the nitric oxide level no longer rises, and ATP production is not inhibited [Panossian A et al., 2021].

leads to stress-protective and adaptive effects via various elements of the endocrine, immune, central nervous, sympathetic, cardiovascular, and gastrointestinal systems. Both Hsp72 and NPY play essential roles in stress, and pathogenesis of aging-related diseases. The antinarcotic effects of adaptogens are mediated by NPY, which is an important intermediate involved in morphine tolerance and opioid dependence.

Although adaptogens at high concentrations are potent radical scavengers, in lower amounts, they may activate some intracellular adaptive stress response signaling pathways resulting in the expression of cytoprotective proteins including neurotrophic factors, protein chaperones, antioxidant and phase II enzymes, and antiapoptotic proteins. A possible cytoprotecting mechanisms of adaptogens related to drug toxicity, oxidative stress, chronic inflammation, and aging-related disorders include their effects on Hsp70 and FOXO expression (Fig. 6).

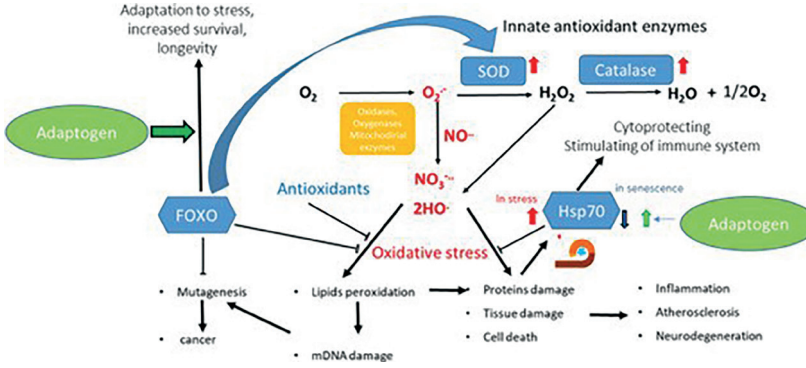

Fig. 6. Hypothetical mechanism of action of adaptogens in the regulation of the innate antioxidant system and oxidative stress-induced apoptosis in aging. According to the free radical theory of aging, the organisms are continuously exposed to reactive oxygen species containing molecules/species (ROS), which are produced as by-products of normal cellular metabolism. When the innate antioxidant system (glutathione peroxidase, superoxide dismutase, and catalase) incompletely deactivates ROS, increasing cellular oxidative damage induces irreversible functional changes leading to early senescence and to aging-associated diseases. Oxidative stress triggers many signaling pathways, including FOXO and Hsp70 mediated pathways. Adaptogens upregulate Hsp70, which directly regulates FOXO signaling and promote translocation of FOXO/DAF-16 to nucleus triggering activation antioxidant systems and antiaging programs (Updated from Panossian AG [2017]).

Adaptogens prevent stress-induced increases in NO, and as such, ATP production remains efficient and performance and endurance are increased. Putative mechanisms of ATP generation are shown in Fig. 7.

Adaptogens have pharmacologically pleiotropic effects, including antistress/antifatigue, stimulating, tonic, antidepressant, neuroprotective, cardioprotective, hepatoprotective, gastroprotective, antioxidant,

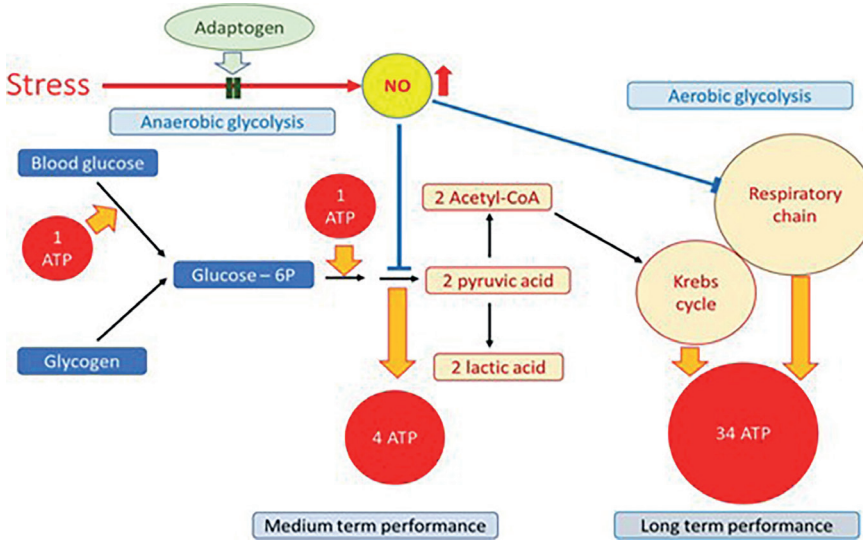

Fig. 7. Schematic representation of the potential molecular mechanism by which generation of nitric oxide (NO) strongly inhibits the production of cellular energy through two mechanisms: inhibition of mitochondrial respiration by reversible (from constitutive isoforms of nitric oxide synthase [NOS]) and irreversible (from inducible NOS [iNOS]) inhibition of cytochrome P450 [Brown GC, 2001] and glycolysis inhibition through modification of the SH-groups of glyceraldehyde 3-phosphate dehydrogenase [Hara MR et al., 2006]. In anaerobic glycolysis, muscle glycogen is converted to lactic acid via glucose-6-phosphate, yielding three ATP molecules for each glucose residue. Aerobic oxidation of glucose is required for the sustained exercise and provides 34 ATP molecules per glucose residue via the Krebs cycle and the respiratory chain, a process that occurs 1 min after anaerobic ATP generation. If a sufficient supply of ATP is not generated, anaerobic glycolysis is continued. NO levels increase during stress, consequently decreasing performance by inhibiting ATP production. Adaptogens prevent stress-induced increases in NO, and as such, ATP production remains efficient and performance and endurance are increased (Updated from Panossian AG [2013]).

autoinflammatory, immunomodulatory, antitumor, antiviral, antibacterial, and hypoglycemic activity. This polyvalent activity is due to their action on genes encoding hormones, transcription factors, and other regulatory proteins, which play a key role in the regulation of many canonical intracellular signaling pathways and molecular networks as well as extracellular communication in the neuroendocrine–immune system [Panossian AG et al., 2021; Panossian AG et al., 2022].

The specificity of the pharmacological action of various adaptogenic plants depends on both the chemical compositions of the extracts and the dose. Product-specific (or compound-specific) activity is theoretically possible to achieve in the smallest dose/concentration, when a compound selectively interacts with only one receptor type, which can trigger minimal signaling pathways in a molecular network. Although the effector (ligand) molecule at higher doses can nonspecifically interact with numerous molecules of several networks, this may cause both feedback downregulations and antagonistic interactions of various molecular networks, resulting in quite different pharmacological responses and toxic effects. At low and normal doses, adaptogens act as mild stress mimetics, increasing the homeostatic range and resulting in increased resistance to stress. At higher doses, they may suppress inflammation and therefore prevent premature aging and maintain health and vitality. This is the "specific" difference of adaptogens, which activate adaptive signaling pathways and increase survival and resiliency from stress, from some other natural compounds, the so-called PAINS (PAn-assay Interference compouNdS), such as toxoflavin, epigallocatechin gallate, genistein, and resveratrol. Quercetin, β-sitosterol, rutin, and curcumin do not comply with these criteria, despite nonspecific pleiotropic effects in numerous in vitro experiments [Bisson J et al., 2016].

Adaptogens stimulate neurogenesis and exhibit neuroprotective activity, suggesting their potential benefits in neurodegenerative disorders. Surprisingly, they trigger apoptotic signaling pathways associated with antitumor activity. Regulation of both stress-resistance and proapoptotic genes is not necessarily a paradox. Adaptogens stimulate mediators of the stress response and transcription factors, which may orchestrate different patterns of gene expression based on the dose of adaptogens, perhaps activating stress-resistance genes normal or small doses, but proapoptotic genes at high doses beyond a certain threshold. Possibly, adaptogens regulate different genes in different cell types, causing apoptosis in some cells (*e.g.*, cancer cells) while promoting survival in others (e.g., in neurons and glia cells). Importantly, the induction of apoptosis by adaptogens may cause the death of damaged or abnormal cells, which may extend the lifespan of the entire organism [Panossian AG et al., 2021].

The adaptogenic process is can be studied very well using "systems biology" and "network pharmacology" approaches, which has the potential to provide plant-based treatments for complex diseases, chronic

conditions, and syndromes. This is a remarkably complex system of synergistic interactions of molecular networks and cellular communication systems that quite literally add up to more than the sum of the parts. It also requires a detailed understanding of disease concepts, as we have outlined in this MS and second, the use of suitable pharmacological models to understand such effects. There can be no one to one correlation between use as an adaptogens and a specific model, and the suitability of a model needs to be assessed carefully before starting experimental approaches. Such approaches can help understanding these complex systems better and this is a key challenge in the future.

Adaptogens are distributed in all organs and tissues involved in the regulation neuroendocrine-immune system where they trigger the expression of hormones and key metabolic regulators of defense responses and cellular homeostasis. That is one of the likely explanations of the pleotropic effects of adaptogens. Finally, some adaptogens actively interact with gut microbiota that results in prevention of progression of chronic inflammatory diseases [Panossian AG et al., 2022].

Conclusion

The adaptogenic concept does not have a long history as analogues of TMS, even though adaptogenic plants have been used in TMS as rejuvenating herbs, qi tonics, rasayanas, and restoratives for centuries and are formally considered to be “traditional” by drug regulatory authorities in Europe and the United States. It is supported by an evidence-based approach and statistical assessments of pharmacological and clinical studies of efficacy and safety of standardized herbal medicinal products as well as their mechanisms of action. The efficacy of plants used in TMS has been investigated using modern theories and methods of system biology and network pharmacology. This review summarized our knowledge about common adaptogenic plants used as officinal medical preparations in USSR and in traditional Chinese medicine, Ayurveda medicine, and other TMS and alternative medical systems, and to provide a modern rationale for their use in the treatment of stress-induced and aging-related disorders. Overall, the basic principles of TMS are in line with those of the adaptogenic concept, which uses systems biology and network pharmacology models to understand the fundamentals of TMS such as “life vital energy” qi (Chinese), prana (Indian), pneuma (Greece), zorutyun (Armenian), od (German), ruah (Hebrew), and mana (Polynesian), which are related to

adaptability. Yin-yang balance can be interpreted as "homeostasis", whereas "shanghuo" – as a state of threatened homeostasis and decreased resistance to stress, which is increased by adaptogens.

Adaptogens play key roles in defending organisms against environmental challenges including harmful bacteria, diseases carried by insects, excessive ultraviolet rays from the sun, and challenges from pollution, excess heat and cold, and hypoxia. The key to understanding adaptogens is their role in establishing and maintaining adaptive homeostasis by building the body's natural resistance to stressors, which may be physical, chemical, biological, and psychological in nature. Adaptogens function like stress vaccines to activate the body's defence system and metabolic rate, reversing the negative physical effects of stress and restoring the body's balance and health. If the immune system is not functioning properly by overreacting or underreacting to challenges, adaptogens help restore the proper immune response. If the immune system is overly active, triggering allergies and asthma, rheumatoid arthritis or lupus, adaptogens lower the immune system's response and returns it to a normal level. If the immune system is underactive, leading to frequent colds, bronchitis, sinus or ear infections, and even pneumonia or causing anemia or digestive problems such as ulcers or chronic diarrhea, adaptogens can help strengthen the immune response, thereby ending the cycle of illness. If the brain chemistry is unbalanced, adaptogens can restore the balance, having profound effects on cognitive function, memory, and mood. The power of adaptogens goes far beyond the immune system. Adaptogens can correct imbalances in cellular division cycles that cause cells to divide in an uncontrolled manner, eventually causing cancer. Adaptogens have a potential to prevent or postpone chronic diseases associated with aging, recognizing their uncanny ability to fix what's wrong, boost what's right, keep the body in balance, and prevent the body's functions from deteriorating. Adaptogenic effects like those seen in *Ginseng, Rhodiola, Eleutherpcoccus, Withania*, and *Schisandra* have been scientifically validated as being effective against chronic inflammation, atherosclerosis, neurodegenerative cognitive impairment, metabolic disorders, diabetes, cancer and a host of other aging-related diseases.

The concept of adaptogens provides a scientific rationale for adaptogenic plants traditionally used in stress-induced and aging-related diseases. The basic principles of TMS are in line with those of the adaptogenic concept, which uses systems biology and network pharmacology models to understand the fundamentals of TMS.

Chapter 2

EXPERIMENTS ON RATS

2.1. The effect of preventive use of phytocomposition on the state of the neuroendocrine-immune complex, gastric mucosa, ECG and metabolome after acute stress

Summary

Introduction and aim. The list of important properties of adaptogens includes their stress-limiting effect, which is usually tested in an experiment. Therefore, the purpose of this study was to identify modulating effects of phytocomposition on post stress changes in neuroendocrine-immune complex, metabolome, electrocardiogram (ECG), and gastric mucosa at rats.

Material and methods. The experiment is at 18 male and 20 female rats Wistar line. 10 animals remained intact with free access to tap daily water. Rats of the control group for 7 days loaded through a tube with same tap daily water (2 mL once), while the animals of main groups received according to a similar scheme 0,1 mL of phytocomposition dissolved in 2 mL of daily water or bottled table water "Truskavetska". Over the next 10 days, one animal remained intact and 3 other rats were exposed to acute (4 hours) water-immersion and restraint stress. The next day after stressing, EEG, endocrine, immune and metabolic parameters as well as gastric mucosa injuries was recorded.

Results. Acute stress causes in control animals an increase in sympathetic tone, blood levels of catecholamines and corticosterone, combined with a decrease in vagal tone and serum testosterone levels. Such a neuro-endocrine reaction is accompanied by damage to the myocardium and gastric mucosa, an increase in the percentage of macrophages, fibroblasts and Hassal's corpuscles in the thymus, entropy in the spleen, theophylline-resistant T-lymphocytes, natural killer cells and polymorphonuclear neutrophils in the blood, as well as the activity of serum alanine transaminase and creatine phosphokinase. Instead, the mass of the spleen and the percentage of lymphoblasts in it, theophylline-sensitive T-lymphocytes and eosinophils in the blood, the content of malondialdehyde and cholesterol

in the serum, as well as the catalase activity of serum and erythrocytes, decrease. Preventive use of phytocomposition, first of all, to one degree or another minimizes adverse post-stress deviations from the norm of most of the listed parameters, and even completely prevents deviations of 5 parameters. Secondly, it initiates an increase in the level of PTH and the activity of serum acid phosphatase, the percentage of reticulocytes in the spleen and the intensity of phagocytosis of blood neutrophils, but at the same time a decrease in their bactericidal activity, as well as the percentage of monocytes and B-lymphocytes in the blood. Thirdly, it potentiates the post-stress increase in sympathetic tone and damage to the gastric mucosa, as well as natural killers, on the one hand, and the decrease in vagal tone, the level of testosterone and malondialdehyde in the serum, as well as the mass of the spleen – on the other hand. Fourthly, it reverses the catalase activity of erythrocytes and the entropy of the splenocytogram.

Conclusion. Ukrainian phytocomposition "Balm Truskavets" has a generally favorable adaptogenic effect on the post-stress state of the neuro-endocrine-immune complex, ECG and metabolome. However, there are certain adverse effects as the so-called adaptation fee.

The list of important properties of adaptogens includes their stress-limiting effect, which is usually tested in an experiment. Therefore, the purpose of this study was to identify modulating effects of phytocomposition on post stress changes in neuroendocrine-immune complex, metabolome, electrocardiogram, and gastric mucosa at rats.

Ethics approval

All animals were kept in room having temperature 22±2ºC, and relative humidity of 44-55% under 12/12 hours light and dark cycle with standard laboratory diet and water given ad libitum. Studies have been conducted in accordance with the rules and requirements of the "General Principles for the Work on Animals" approved by the I National Congress on Bioethics (Kyïv, Ukraine, 2001) and agreed with the provisions of the "European Convention for the Protection of Vertebrate Animals used for Experimental and other Scientific Purposes" (Council of Europe No 123, Strasbourg 1985), and the Law of Ukraine "On the Protection of Animals from Cruelty" of 26.02.2006. The removal of animals from the experiment was carried out under light inhalation (ether) anesthesia by decapitation.

Material and methods

Participants

The experiment is at 38 rats Wistar line: 18 males (Weight Mean= 227 g; SD=25 g) and 20 females (Mean=214 g; SD=27 g).

Study design and procedure

In a previous study, it was shown that the severity of post-stress changes in target organs are significantly determined by innate resistance to hypoxia and aerobic muscular performance [Ordynskyi YuM et al., 2017; Ordynskyi YuM et al., 2019; Fil VM et al, 2021; Zukow W et al., 2022; Melnyk OI et al., 2023]. Therefore, at the preparatory stage, all animals were first tested for resistance to hypoxic hypoxia by the classical method of Berezovskyi VYa [1975]. To do this, each rat was placed in a pressure chamber with a transparent lid, in which the pump created a vacuum of air equivalent to a rise to a height of 12 km (20 kPa) and recorded the time of the second agonal breath or seizure. One week later, aerobic muscular performance was determined by the duration of swimming (t^0 water 26^0 C) with a load (5% of body weight) to exhaustion (falling to the bottom of the bath) [Brekhman II, 1968]. After a week of recovery, under light ether anesthesia for 15-20 sec recorded electrocardiogram (ECG) in standard lead II (introducing needle electrodes subcutaneously) followed by calculation of HRV parameters: The Mode, Amplitude of Mode (AMo) and Variation scope (MxDMn) as markers of the so-called humoral channel of regulation, sympathetic and vagal tone respectively [Baevsky RM & Berseneva AP, 2008].

On the basis of the received data four qualitatively equivalent groups (equally females and males, practically identical average sizes and variances of swimming and hypoxic tests as well as HRV) were formed. 10 animals remained intact with free access to tap daily water. Rats of the control group (n=10) for 7 days loaded through a tube with same tap daily water (2 mL once), while the animals of main groups received according to a similar scheme 0,1 mL of Balm dissolved in 2 mL of daily water (n=8) or bottled table water “Truskavetska” (n=10).

Over the next 10 days, one animal remained intact and 3 other rats were exposed to water-immersion and restraint stress according to the method of Nakamura J et al. [1984] in the modification of Popovych IL [2007], which is to reduce the duration of stay of the rat in a fixed standing position in cold water (t^0 20-21^0 C) to the level of the xiphoid process from 8 to 4 hours. Prior to the experiments, rats were fasted for 24 h, but allowed access to tap water *ad libitum*.

The next day after stressing, a sample of peripheral blood (by incision of the tip of the tail) was taken for analysis of Leukocytogram (LCG), ie the percentage of lymphocytes (L), monocytes (M), eosinophils (Eo), basophils (Bas), rod-shaped (RN) and polymorphonucleary (PMNN) neutrophils. Based on these data, the Entropy of the Leukocytogram (hLCG) was calculated according to the equation derived by Popovych IL [2007] on the basis of the classical equation of Shannon CE [1948]:

$hLCG = – (L•\log_2 L+M•\log_2 M+Eo•\log_2 Eo+Bas•\log_2 Bas+RN•\log_2 RN+ PMNN•\log_2 PMNN)/\log_2 6$.

Then the ECG under light ether anesthesia was re-recorded, and right away the animals removed from the experiment by decapitation in order to remove the stomach, adrenal glands, thymus, spleen, and collect the maximum possible amount of blood in which was determined some endocrine, metabolic, and immune parameters.

Among endocrine parameters determined serum levels of main adaptation hormones such as corticosterone, aldosterone, testosterone, triiodothyronine, as well as parathyroid hormone and calcitonin (by ELISA, with the use of analyzer “RT-2100C” and corresponding sets of reagents from “Alkor Bio”, XEMA Co, Ltd and DRG International Inc).

On lipid metabolism judged by the level of triglycerides (metaperiodate-acetylacetone colorimetric method), total cholesterol (direct method by reaction Zlatkis-Zach) and its distribution as part of α-lipoprotein (applied enzymatic method Hiller G, 1987) after precipitation nonα-lipoproteins using dextransulfate/Mg^{2+}) as described in the manual [Goryachkovsiy AM, 1998]. State of lipid peroxidation assessed the content in the serum its products: diene conjugates (spectrophotometry of heptane phase of lipids extract [Gavrilov VB & Mishkorudnaya MI, 1983]) and malondyaldehide (test with thiobarbituric acid [Andreyeva LI et al., 1988]), as well as the activity of antioxidant enzymes: catalase of serum and erythrocytes (by the speed of decomposition hydrogen peroxide [Korolyuk MA et al., 1988]) and superoxide dismutase of erythrocytes (by the degree of inhibition of nitroblue tetrazolium recovery in the presence of N-methylphenazone metasulfate and NADH [Dubinina YY et al., 1988]). On electrolytes exchange judged by the level of calcium (by the reaction with arsenazo III), phosphate (phosphate molibdate method) and chloride (mercury rodanide method) in the serum, sodium and potassium in the serum and erythrocytes (flame photometry method) as described in the manual [Goryachkovsiy

AM, 1998]. In addition, the activity of Na,K-ATPase of the shadows of erythrocytes was determined (by the increase of Pi in the supernatant of the incubation medium [Makarenko YeV, 1988].

Alanine and asparagine aminotranspherase, alkaline and acid phosphatase as well as creatine phosphokinase determined by uniform methods as described in the manual [Goryachkovsiy AM, 1998].

Use analyzers «Tecan» (Oesterreich), «Pointe-180» («Scientific», USA), «Reflotron» («Boehringer Mannheim», BRD) and flame spectrophotometer.

The stomach was cut along the greater curvature, mounted it on gastroluminoscope and under a magnifying glass counted the amount of ulcers and their length was measured, evaluated erosive and ulcerative damage on scale by Popovych IL [2007]. This scale is based on the qualitative-quantitative Harrington EC [1965] scale.

The parameters of immunity were determined, as described in the manual [Perederiy VG et al., 1995]. The percentage of theophylline-resistant (TR) and theophylline-susceptible (TS) T-lymphocytes, B-lymphocytes, plasma cells (Pla), and natural killers (NK) were identified. For these components the Entropy of the Immunocytogram (hICG) was calculated by Popovych IL et al. [2020] equation:

$hICG = – (TR \bullet \log_2 TR + TS \bullet \log_2 TS + B \bullet \log_2 B + Pla \bullet \log_2 Pla + NK \bullet \log_2 NK + 0L \bullet \log_2 0L)/\log_2 6$.

About the condition of the phagocytic function of neutrophils (microphages) and monocytes (macrophages) were judged by the phagocytosis index (percentage of cells, in which found microbes), the microbial count (number of microbes absorbed by one phagocyte) and the killing index (percentage of dead microbes) for *Staphylococcus aureus* (ATCC N25423 F49) [Bilas VR & Popovych IL, 2009].

The Spleen and Thymus were weighed and made smears-imprints for counting Thymocytogram and Splenocytogram [Horizontov PD et al., 1983; Bilas VR et al., 2020]. The components of the Thymocytogram (TCG) are lymphocytes (Lc), lymphoblastes (Lb), reticulocytes (Ret), macrophages (Mac), basophiles (B), endotheliocytes (En), epitheliocytes (Ep), and Hassal's corpuscles (H). The Splenocytogram (SCG) includes lymphocytes (Lc), lymphoblastes (Lb), plasma cells (Pla), reticulocytes (R), macrophages (Ma), fibroblasts (F), microphages (Mi), and eosinophils (Eo).

For them Shannon's entropy was calculated too [Popovych IL, 2007; Popovych IL et al., 2020]:

$hTCG = -(Lc \bullet \log_2 Lc + Lb \bullet \log_2 Lb + Ret \bullet \log_2 Ret + Mac \bullet \log_2 Mac + B \bullet \log_2 B + En \bullet \log_2 En + Ep \bullet \log_2 Ep + H \bullet \log_2 H)/\log_2 8$;

$hSCG = -(Lc \bullet \log_2 Lc + Lb \bullet \log_2 Lb + Pla \bullet \log_2 Pla + R \bullet \log_2 R + Ma \bullet \log_2 Ma + F \bullet \log_2 F + Mi \bullet \log_2 Mi + Eo \bullet \log_2 Eo)/\log_2 8$.

Statistical analysis

Statistical processing was performed using a software package "Microsoft Excell" and "Statistica 6.4 StatSoft Inc" (Tulsa, OK, USA).

Results

Due to the purposeful formation of groups, the potential predictors of post-stress reactions of the neuro-endocrine-immune complex and the metabolome were almost identical both in mean values and, to a lesser extent, in variance (SD). In particular, the hypoxic test (sec) was: 136±59; 130±78, and 134±83; swimming test (min): 19±11; 18±14, and 19±19; HRV Stress index (units) as $(AMo/2 \bullet Mo \bullet MxDMn)^{1/3}$: 0,14±0,08, 0,14±0,03, and 0,14±0,06 in intact animals and those exposed to acute stress against the background of daily water or Balm consumption, respectively. This gave reason to believe that the possible differences in the post-stress state of the registered parameters are not related to the initial state of innate predictors of reactivity, but are caused only by the factor used in this study – the phytoadaptogen.

Adhering to the Truskavetsian Scientific School's analytical algorithm, in order to correctly compare variables expressed in different units and with different variability, the actual/raw parameters were normalized by recalculation by the equations:

$Z = 4 \bullet (V - N)/(Max - Min) = (V - N)/SD = (V/N - 1)/Cv$, where

V is the actual value; N is the normal (at intact animals) value; SD and Cv are the standard deviation and coefficient of variation respectively [Polovynko IS et al., 2016; Popovych IL et al., 2020).

By means of screening, a constellation of precisely such parameters, which are significantly different in intact rats and subjected to stress against the background of daily water and phytocomposition consumption, was selected (Fig. 2.1).

Further, the patterns were grouped into 8 clusters and for each cluster the essential (per se) effect of the phytocomposition was calculated as the algebraic difference between the post-stress variables in the main and

control groups (Fig. 2.2). It was found that the phytocomposition exerts enhancing effects on the post-stress variables condensed in 6 clusters, while on the other variables – weakening ones.

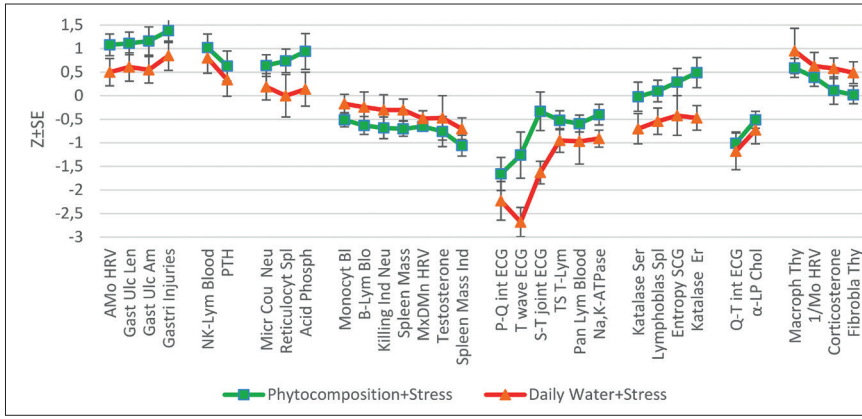

Fig. 2.1. Clusters of patterns of post-stress profiles of rats against the background of daily water and phytocomposition consumption

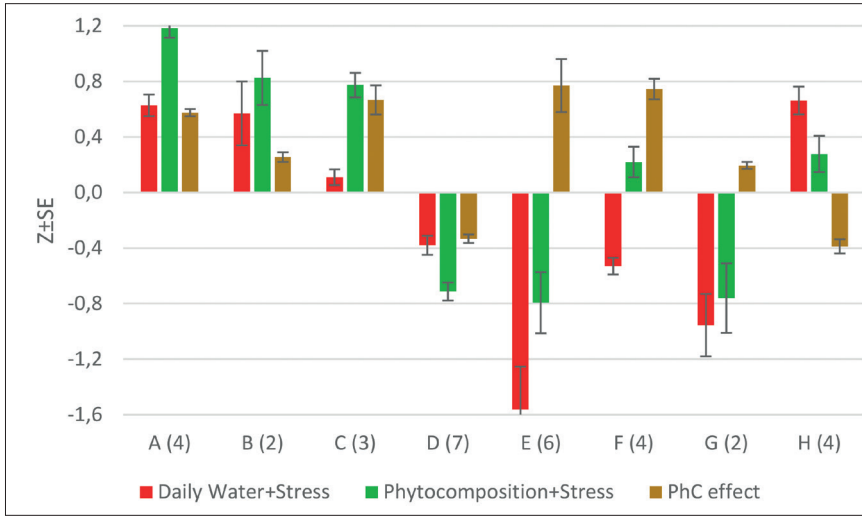

Fig. 2.2. Clusters of post-stress variables (n) of rats against the background of **daily water** and **phytocomposition** consumption. Essential (*per se*) effects of phytocomposition calculated as algebraic difference.

In order to identify exactly those post-stress parameters (variables) whose constellation is characteristic for each group, the available informational field was subjected to discriminant analysis by the method of forward stepwise [Klecka WR, 1989]. To include in the model (Tables 2.1 and 2.2), the program has selected 16 variables (3 **markers of gastric mucosa injuries**, 2 **ECGs**, 3 **metabolic**, 3 **neuro-endocrine**, as well as 5 **immune**).

Table 2.1. Discriminant Function Analysis Summary

	Groups (n)			Parameters of Wilks' Statistics				
Variables currently in the model	**Intact Rats (10)**	**CW+ Stress (10)**	**PhC+ Stress (18)**	**Wilks' Λ**	**Partial Λ**	**F-remove (5.6)**	**p-value**	**Tolerancy**
1	2	3	4	5	6	7	8	9
Gastric Ulcers Amount	0	1.0 0.5	2.1 0.5	0,050	0,663	5,090	0,016	0,072
Gastric Ulcers Length, mm	0	2.1 1.0	3.8 0.8	0,036	0,918	0,899	0,422	0,063
Gastric Mucosa Injury, points	0	0.21 0.08	0.34 0.06	0,066	0,503	9,884	0,001	0,099
T wave ECG, μV	131 3	61 8	98 13	0,052	0,641	5,605	0,012	0,138
S-T joint ECG, μV	54 5	13 6	45 10	0,042	0,786	2,729	0,090	0,155
Na,K-ATPase of Erythrocytes, M/L•h	0.77 0.06	0.60 0.03	0.69 0.04	0,068	0,485	10,64	0,001	0,180
Katalase of Erythrocytes, μM/L•h	227 17	202 14	253 17	0,050	0,659	5,171	0,015	0,507
Acid Phosphatase, IU/L	31.4 1.9	32.2 2.1	37.0 2.2	0,036	0,901	1,094	0,354	0,449
AMo HRV as Sympathetic tone, %	48 6	73 6	67 4	0,041	0,799	2,520	0,106	0,263
MxDMn HRV as Vagal tone, msec	51 14	16 3	32 5	0,043	0,770	2,995	0,073	0,212
Corticosterone, nM/L	354 35	407 31	375 27	0,041	0,803	2,458	0,111	0,162
Macrophages of Thymus, %	5.39 0.50	6.89 0.75	6.31 0.31	0,057	0,575	7,401	0,004	0,325
Microbial Count of Neutrophils, Bac/Phag	5.5 0.3	5.7 0.3	6.2 0.2	0,050	0,662	5,099	0,016	0,172

Table 2.1 (cont)

1	2	3	4	5	6	7	8	9
Killing Index of Neutrophils, %	47.5 2.9	44.7 3.0	41.1 2.1	0,039	0,851	1,751	0,199	0,506
Theophylline-susceptib-le T-Lymphocytes, %	15.3 1.1	11.9 0.9	13.4 0.7	0,039	0,853	1,723	0,204	0,636
B-Lymphocytes of Blood, %	13.4 0.8	12.8 0.8	11.8 0.5	0,050	0,654	5,285	0,014	0,327

Step 16, N of vars in model: 16; Grouping: 3 grps; Wilks' Λ: 0.033; appr. $F_{(32.4)}$=5.6; $p<10^{-6}$.

In each column, the top row is the average, the bottom is the standard error.

Table 2.2. Summary of Stepwise Analysis for Variables ranked by criterion Λ

Variables currently in the model	F to enter	p-level	Λ	F-value	p-level
Gastric Mucosa Injury, points	9,444	0,001	0,649	9,44	10^{-3}
S-T joint ECG, μV	6,649	0,004	0,467	7,88	10^{-4}
Na,K-ATPase of Erythrocytes, M/L•h	5,908	0,006	0,344	7,76	10^{-6}
Macrophages of Thymus, %	5,896	0,007	0,251	7,96	10^{-6}
Theophylline-susceptible T-Lymphocytes, %	4,370	0,021	0,196	7,81	10^{-6}
Katalase of Erythrocytes, μM/L•h	3,892	0,031	0,156	7,68	10^{-6}
Gastric Ulcers Amount	4,013	0,029	0,122	7,72	10^{-6}
T wave ECG, μV	2,475	0,102	0,104	7,38	10^{-6}
B-Lymphocytes of Blood, %	2,193	0,131	0,089	7,05	10^{-6}
AMo HRV as Sympathetic tone, %	4,787	0,017	0,065	7,59	10^{-6}
Microbial Count of Neutrophils, Bac/Phag	1,634	0,215	0,058	7,20	10^{-6}
MxDMn HRV as Vagal tone, msec	1,324	0,285	0,052	6,78	10^{-6}
Gastric Ulcers Length, mm	1,566	0,230	0,046	6,51	10^{-6}
Corticosterone, nM/L	1,150	0,335	0,041	6,16	10^{-6}
Killing Index of Neutrophils, %	1,349	0,281	0,037	5,92	10^{-6}
Acid Phosphatase, IU/L	1,094	0,354	0,033	5,63	10^{-6}

The rest of the registered variables were left out of the model (Table 2.3), although some of them carry discriminant (recognizable) information.

Table 2.3. Variables currently not in the model

	Groups (n)			Parameters of Wilks' Statistics				
Variables	Intact Rats (10)	CW+ Stress (10)	PhC+ Stress (18)	Wilks' Λ	Partial Λ	F to enter	p-value	Tolerancy
P-Q interval ECG, msec	55.6 0.8	45.4 1.9	48.0 1.6	0.032	0.992	0.790	0.496	0.405
Q-T interval ECG, msec	104.9 1.2	92.0 4.3	93.8 2.7	0.030	0.955	0.450	0.545	0.430
α-LP Cholesterol, mM/L	0.84 0.05	0.73 0.04	0.76 0.03	0.033	0.970	0.380	0.404	0.342
Katalase of Serum, μM/L•h	143 12	116 12	142 12	0,033	0,998	0,018	0,983	0,501
Mode HRV as inverse Catecholamines, msec	175 10	155 9	163 6	0.034	0.925	0.530	0.618	0.482
Parathyroid hormone normalized by sex, Z	0 0.32	0.30 0.30	0.56 0.30	0,032	0,961	0,386	0,685	0,345
Testosterone normalized by sex, Z	0 0.32	-0.74 0.58	-0.99 0.34	0.035	0.941	0.400	0.596	0.410
Spleen Mass, mg	773 58	718 42	644 30	0,033	0,996	0,036	0,965	0,350
Spleen Mass Index, mg/100 g Body Mass	375 25	320 18	292 17	0,033	0,997	0,027	0,974	0,450
Reticulocytes of Spleen, %	2.67 0.22	2.67 0.32	3.19 0.18	0,033	0,998	0,016	0,985	0,662
Lymphoblastes of Spleen, %	8.6 10	6.8 0.9	8.9 0.8	0,031	0,932	0,690	0,514	0,601
Entropy of Splenocytogram	0.534 0.019	0.552 0.018	0.509 0.025	0,032	0,969	0,300	0,744	0,589
Fibroblastes of Thymus, %	5.33 0.65	6.33 0.47	5.38 0.38	0,031	0,927	0,749	0,486	0,465
Pan Lymphocytes of Blood, %	51.8 1.5	47.2 2.3	49.0 0.9	0,030	0,920	0,824	0,454	0,485
Monocytes of Blood, %	6.20 0.73	5.81 0.46	5.02 0.35	0,033	0,985	0,147	0,864	0,572
NK-Lymphocytes of Blood, %	5.29 0.35	6.18 0.36	6.43 0.32	0.032	0.965	0.450	0.401	0.457

Note. Testosterone and parathyroid hormone levels are normalized by sex (41.8±1.7 vs 3.53±0.24 nM/L and 154±12 vs 185±3 ng/L in intact male vs female respectively).

Than the 16-dimensional space of discriminant variables transforms into 2-dimensional space of a canonical roots, which are a linear combination of discriminant variables. The discriminating ability of the root characterizes the canonical correlation coefficient as a measure of the degree of dependence between groups and a roots. It is for Root 1 0.906 (Wilks' Λ=0.033; $\chi^2_{(32)}$=94; $p<10^{-6}$), for Root 2 0.903 (Wilks' Λ=0.185; $\chi^2_{(15)}$=46; $p<10^{-4}$). The first root contains 51% of discriminative opportunities, the second 49%.

Table 4.4 presents raw (actual) and standardized (normalized) coefficients for discriminant variables. The raw coefficient gives information on the absolute contribution of this variable to the value of the discriminative function, whereas standardized coefficients represent the relative contribution of a variable independent of the unit of measurement. They make it possible to identify those variables that make the largest contribution to the discriminatory function value.

Table 2.4. Standardized and Raw Coefficients and Constants for Canonical Variables

Coefficients	**Standardized**		**Raw**	
Variables	**Root 1**	**Root 2**	**Root 1**	**Root 2**
1	2	3	4	5
Gastric Mucosa Injury, points	0,894	-2,316	0,785	-2,035
S-T joint ECG, μV	0,439	-1,226	0,014	-0,038
Na,K-ATPase of Erythrocytes, M/L•h	-0,768	1,710	-4,745	10,57
Macrophages of Thymus, %	0,749	-1,019	0,460	-0,625
Theophylline-susceptible T-Lymphocytes, %	0,116	0,520	0,037	0,167
Katalase of Erythrocytes, μM/L•h	0,609	0,672	0,010	0,011
Gastric Ulcers Amount	0,333	2,367	0,185	1,313
T wave ECG, μV	1,231	1,286	0,031	0,032
B-Lymphocytes of Blood, %	-0,867	-0,734	-0,380	-0,322
AMo HRV as Sympathetic tone, %	0,508	0,823	0,028	0,045

Table 2.4 (cont)

1	2	3	4	5
Microbial Count of Neutrophils, Bac/Phag	1,533	0,196	1,498	0,191
MxDMn HRV as Vagal tone, msec	1,099	-0,340	0,043	-0,013
Gastric Ulcers Length, mm	0,832	-0,960	0,279	-0,322
Corticosterone, nM/L	1,080	0,564	0,011	0,005
Killing Index of Neutrophils, %	-0,456	-0,389	-0,049	-0,042
Acid Phosphatase, IU/L	0,368	0,365	0,047	0,046
	Constants		-18,30	-9,442
	Eigenvalues		4,60	4,40
Cumulative Proportions			0.511	1

The third discriminant parameter is the full structural coefficients (Table 2.5), that is, the coefficients of correlation between the discriminant root and variables. The structural coefficient shows how closely variable and discriminant functions are related, that is, what is the portion of information about the discriminant function (root) contained in this variable. The calculation of the discriminant root values for each animal as the sum of the products of raw coefficients to the individual values of discriminant variables together with the constant enables the visualization of each rat in the information space of the roots.

Table 2.5. Correlations Variables-Canonical Roots, Means of Roots and Z-scores of Variables

Variables	**Correlations Variables-Canonical Roots**		**Intact Rats (10)**	**CW+ Stress (10)**	**PhC+ Stress (18)**	**Effectof PhC**	**Clus-ter on Fig. 1**
1	2	3	4	5	6	7	8
Root 1 (51%)	**Root 1**	**Root 2**	-2.41	-1.44	**2.14**		
AMo HRV as Sympathetic tone	**0.202**	-0.034	0	0.50 0.29	**1.08** **0.23**	0.58 0.23	A
Gastric Ulcers Length	**0.242**	-0.085	0	0.61 0.30	**1.11** **0.24**	0.50 0.24	A
Gastric Ulcers Amount	**0.230**	-0.060	0	0.55 0.28	**1.16** **0.30**	0.61 0.30	A

Table 2.5 (cont)

1	2	3	4	5	6	7	8
Gastric Mucosal Damage	**0.298**	-0.171	0	0.85 0.31	**1.38** **0.25**	0.53 0.25	A
NK-Lymphocytes of Blood			0	0.80 0.32	**1.02** **0.29**	0.22 0.29	B
Parathyroid hormone			0	0.30 0.30	**0.56** **0.30**	0.26 0.30	B
Microbial Count of Neutrophils	**0.145**	-0.010	0	0.19 0.28	**0.64** **0.23**	0.46 0.23	C
Reticulocytes of Spleen			0	0.00 0.45	**0.74** **0.25**	0.74 0.25	C
Acid Phosphatase	**0.149**	0.014	0	0.14 0.36	**0.94** **0.38**	0.80 0.38	C
Monocytes of Blood			0	-0.17 0.20	**-0.51** **0.15**	-0.34 0.15	D
B-Lymphocytes of Blood	**-0.140**	0.023	0	-0.24 0.32	**-0.63** **0.19**	-0.39 0.19	D
Killing Index of Neutrophils	**-0.137**	0.031	0	-0.30 0.32	**-0.68** **0.23**	-0.38 0.23	D
Spleen Mass			0	-0.30 0.23	**-0.70** **0.16**	-0.40 0.16	D
MxDMn HRV as Vagal tone	**-0.173**	0.094	0	-0.48 0.16	**-0.65** **0.08**	-0.17 0.08	D
Testosterone			0	-0.74 0,58	**-0.99** **0.34**	-0.25 0.34	D
Spleen Mass Index			0	-0.70 0.23	**-1.06** **0.22**	-0.36 0.22	D
Root 2 (49%)	**Root 1**	**Root 2**	2.41	**-3.06**	0.37		
P-Q interval ECG			0	**-2.23** **0.41**	-1.66 0.35	0.57 0.36	E
T wave ECG	-0.041	**0.312**	0	**-2.68** **0.31**	-1.26 0.49	1.43 0.49	E
S-T joint ECG	0.048	**0.239**	0	**-1.63** **0.24**	-0.33 0.41	1.30 0.41	E
Theophylline-susceptible T-Lymphocytes	-0.045	**0.192**	0	**-0.95** **0.25**	-0.52 0.20	0.43 0.20	E

Table 2.5 (cont)

1	2	3	4	5	6	7	8
Pan Lymphocytes of Blood			0	**-0.97 0.48**	-0.59 0.18	0.38 0.18	E
Na,K-ATPase of Erythrocytes	0.009	**0,216**	0	**-0,91 0,18**	-0,40 0,22	0,51 0,22	E
Catalase of Serum			0	**-0.70 0.32**	-0.02 0.31	0.68 0.31	F
Lymphoblastes of Spleen			0	**-0.54 0.28**	0.10 0.23	0.63 0.23	F
Entropy of Splenocytogram			0	**-0.42 0.42**	0.29 0.29	0,71 0.42	F
Catalase of Erythrocytes	0.134	**0.100**	0	**-0.47 0.26**	0.49 0.32	0.96 0.32	F
Q-T interval ECG			0	**-1.18 0.39**	-1.01 0.24	0.17 0.24	G
α-LP Cholesterol			0	**-0.73 0.29**	-0.51 0.18	0.22 0.18	G
Macrophages of Thymus	0.055	**-0.150**	0	**0.95 0.48**	0.59 0.20	-0.37 0.20	H
1/Mode HRV as Catecholamines			0	**0.63 0.29**	0.39 0.19	-0.25 0.19	H
Corticosterone	0.001	**-0.084**	0	**0.58 0.22**	0.11 0.29	-0.46 0.29	H
Fibroblastes of Thymus			0	**0.49 0.23**	0.02 0.19	-0.47 0.19	H

Localization of the cluster of animals exposed to stress against the background of daily water loads in the lowest zone of the axis of the second root (Fig. 2.3) reflects the maximum for the sample depression of the T wave and the S-T joint and the shortening of the P-Q and Q-T EEG intervals, a decrease the percentage of lymphocytes in general and theophylline-sensitive T-lymphocytes in particular in the blood, lymphoblasts in the Spleen and entropy of splenocytogram, cholesterol levels in α-lipoproteins, as well as erythrocyte Na,K-ATPase and catalase activity. On the other hand, the lowest localization of the cluster reflects the maximum rise of the percentage of macrophages and fibroblastes in the Thymus as well as catecholamines and corticosterone levels in the serum. The intermediate

position of rats of the main group relative to control and intact animals, and even partial mixing with the latter, reflects the minimization or even prevention of the effects of stress on the listed variables.

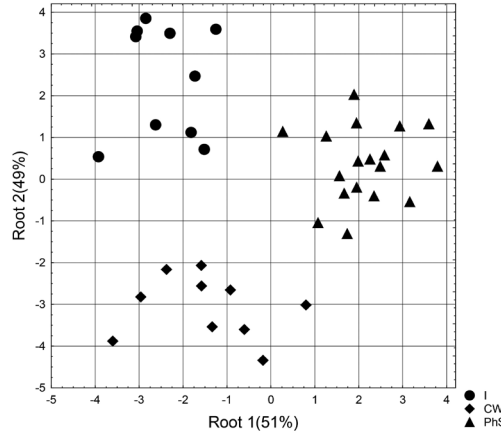

Fig. 2.3. Individual values of discriminative roots of **intact** rats and one day after acute stress, which was preceded by weekly administration of **daily (control) water** (CWS) and **phytocomposition** (PhS). The roots contain condensed information about 16 parameters

The shift along the first root axis of the cluster of rats of the main group to the right relative to the cluster of both intact and control animals reflects, firstly, the potentiation by phytocomposition the post-stress increase in sympathetic tone and the content of NK-lymphocytes in the blood, as well as damage to the gastric mucosa, on the one hand, and a decrease in vagal tone, the level of testosterone in the serum, and the mass index of the spleen – on the other hand. Secondly, such extreme localization reflects the initiation by the phytocomposition of an increase in the level of PTH and the activity of serum acid phosphatase, the intensity of phagocytosis of blood neutrophils and the percentage of reticulocytes in the Spleen, on the one hand, and a decrease in the bactericidal activity of blood neutrophils, the percentage of monocytes and B-lymphocytes in the blood as well as absolute mass of Spleen – on the other hand.

The apparent clear demarcation of clusters is documented by calculating Mahalanobis distances (Table 2.6).

Table 2.6. Squared Mahalanobis Distances between clusters (above the diagonal), F-values (df=16.2) and p-levels (under the diagonal)

Clusters	Intact Rats	CW + Stress	UPhCBT + Stress
Intact Rats (10)	0	30.9	24.9
CW + Stress (10)	5.5 0.0003	0	24.5
UPhCBT + Stress (18)	5.7 0.0002	5.6 0.0002	0

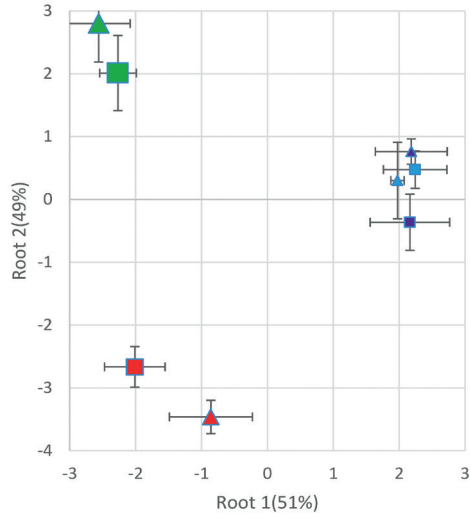

Fig. 2.4. Mean (M±SE) values of discriminant roots of female (triangles) and male (squares) rats **intact** and one day after acute stress, which was preceded by weekly administration of **daily water** and phytocomposition dissolved in **daily water** or "**Truskavetska" water**

The calculation of cluster centroids demonstrates, firstly, the absence of sexual differences both between intact rats and stressed female rats pretreated by the phytocomposition soluted in daily water; secondly, the moderate difference between the stressed male rats pretreated by the phytocomposition soluted in the "Truskavetska"™ bottled table water; thirdly, the moderate sexual difference between stressed rats pretreated by the daily water (Fig. 2.4).

The same discriminant parameters can be used to retrospective identify the belonging of one or another animal to one or another cluster. This purpose of discriminant analysis is realized with the help of classifying functions (Table 2.7). These functions are special linear combinations that maximize differences between groups and minimize dispersion within groups. The coefficients of the classifying functions are not standardized, therefore they are not interpreted. An object belongs to a group with the maximum value of a function calculated by summing the products of the values of the variables by the coefficients of the classifying functions plus the constant.

Table 2.7. Coefficients and Constants for Classification Functions

Clusters	Intact Rats (10)	CW + Stress (10)	UPhCBT + Stress (18)
Variables	p=0.263	p=0.263	p=0.474
Gastric Mucosa Injury, points	-15,668	-3,771	-7,945
S-T joint ECG, μV	-0,302	-0,080	-0,162
Na,K-ATPase of Erythrocytes, M/L•h	52,861	-9,596	9,705
Macrophages of Thymus, %	3,071	6,940	6,438
Theophylline-susceptible T-Lymphocytes, %	6,986	6,109	6,814
Katalase of Erythrocytes, μM/L•h	0,259	0,208	0,283
Gastric Ulcers Amount	16,118	9,117	14,282
T wave ECG, μV	0,860	0,716	0,934
B-Lymphocytes of Blood, %	-8,657	-7,270	-9,730
AMo HRV as Sympathetic tone, %	0,738	0,517	0,773
Microbial Count of Neutrophils, Bac/Phag	56,966	57,387	63,395
MxDMn HRV as Vagal tone, msec	1,045	1,160	1,269
Gastric Ulcers Length, mm	1,627	3,659	3,551
Corticosterone, nM/L	0,625	0,606	0,662
Killing Index of Neutrophils, %	-0,856	-0,674	-0,995
Acid Phosphatase, IU/L	2,851	2,643	2,969
Constants	-439,437	-405,625	-499,458

The accuracy of classification (retrospective recognition) is **100%**.

Thus, by applying the water-immersion and restraint stress model, we reproduced Selye's primary attributes of stress: an increase in the mass of the adrenal glands, an increase in the level of corticosterone, involution of lymphoid tissue (a decrease in the mass of the spleen and the content of lymphocytes as well as eosinophils in the blood) and erosive-ulcerative damage to the gastric mucosa, on the one hand, and Cannon's: an increase in the level of circulating catecholamines and sympathetic tone and a reciprocal decrease in vagal tone, which causes myocardial damage – on the other hand [Selye H, 1936; Berger EN, 1980; Zavodskaya IS & Moreva YeV, 1981; Horizontov PD et al., 1983; Markova OO et al., 1987; Szabo S et al., 2017]. The moderate severity of the main signs of stress is explained by our use of gentle stressor parameters (water temperature and duration of water immersion). However, the real picture has more colors, and the immune manifestations of stress are ambiguous.

The main goal of this study is to find out the essential effects of the phytocomposition. One of the approaches tested in our previous studies is the calculation of algebraic differences between the Z-scores of variable animals that received an aqueous solution of the phytocomposition and only water-solvent. The revealed effects of the phytocomposition were collected in 7 morpho-functional-metabolic clusters (Fig. 2.5).

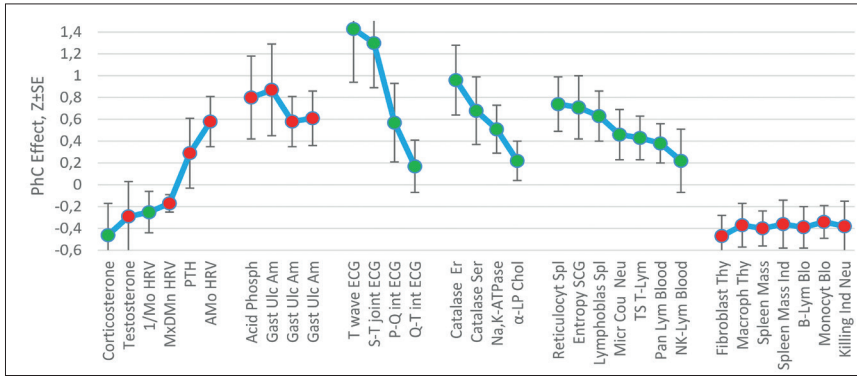

Fig. 2.5. Clusters of simulated **favorable** and **unfavorable** effects of phytocomposition per se (essentially) on post-stress parameters of rats. See please Table 2.5

Among the registered neuro-endocrine effectors of acute stress, the phytocomposition most significantly affected the serum corticosterone

level, which is an attribute of adaptogens [Dardymov IV, 1976; Jin W et al., 2020]. The inhibitory effects on testosterone, catecholamines and vagal tone levels were less noticeable. Instead, the sympathetic tone and the serum PTH level increased slightly. Such modulation by the phytocomposition of the post-stress constellation of neuro-endocrine factors has a noticeable cardioprotective effect (judging by the T wave and ST joint ECG), which is accompanied by a significant increase in the activity of catalase in both erythrocyte shadows (a marker of the membranes of myocardiocytes and other cells) and serum, but at the same time slightly burdens stressor damage to the gastric mucosa, which is accompanied by a significant increase in the activity of acid phosphatase (a marker of cytolysis), which is contrary to expectations [Sun XB et al., 1992; Lu S et al., 2019]. However, it should be kept in mind that under this model of acute stress, damage to the gastric mucosa was insignificant, while damage to the myocardium was pronounced (see please Fig. 2.1). Therefore, we consider the insignificant burden of phytoadaptogen damage to the gastric mucosa as a kind of payment (sacrifice) of the body [Meerson FZ, 1991] for appreciable minimization of myocardial damage.

The same interpretation applies to the combination of an increase in the percentage of reticulocytes and lymphoblasts in the spleen, T- and natural killer cells in the blood, as well as the intensity of phagocytosis of blood neutrophils with a decrease in the mass of the spleen, the percentage of fibroblasts and macrophages in the thymus, B-lymphocytes and monocytes in the blood, as well as completion of phagocytosis of blood neutrophils.

To what substances does this phytocomposition owe its adaptogenicity?

The most investigated medicinal herbs for their adaptogenic activity are *Panax ginseng, Eleutherococcus senticosus, Withania somnifera, Schisandra chinensis, Rhaponticum carthamoides, Lepidium meyenii, and Rhodiola spp.* The main phytochemical classes isolated from different plant parts were phytosteroids, phytosterols, flavoloids, flavolignans, alkaloids, glucosinolates, saponins, phenolic acids, salidroside, ginsenosides, andrographolide, methyl jasmonate, cucurbitacin R, dichotosin, dichotosininare and others that have shown a considerable adaptogenic activity. Flavonoids are substances with a phenolic structure, and over 8000 flavonoids are known. Flavonoids are divided into the subclasses flavonols, flavones, flavanones, catechins, and their glycosides. An important property of phenolic compounds is the ability to oxidize; they are especially easily

oxidized in an alkaline environment. Antioxidant activity is associated with the presence of a large number of hydroxyl groups in flavonoids. Flavonoids differ in the degree of oxidation: the most reduced of them are catechins, the most oxidized are flavonols. Others chemicals are Phenolic acids: Protocatechuic, Benzoic, Hydroxyphenylacetic, Hydroxybenzoic, Salicylic, Gentisic, Elagic, Chlorogenic, Vanillic, Coumaric, Synapic, Caffeic, Ferulic, Gallic, Syringic [reviews: Gerontakos SE et al., 2020; Todorova V et al., 2021; Sergeeva I et al., 2021; Esmaealzadeh N et al., 2022; Kumar P et al., 2023].

The principal active constituents of adaptogenic plants can be divided into three main chemical groups: compounds with a tetracyclic skeleton like cortisol and testosterone – terpenoids, ginsenosides, sitoindosides, cucurbitacines, and withanolides; structural analogues of catecholamines or tyrosine – lignans (schizandrin B, eleutheroside E), phenylpropane derivatives (rosavin and syringin), phenylethane derivatives (tyrosol and salidroside); structural analogues of resolvins – oxylipins (polyhydroxylated polyunsaturated fatty acids [review: Panossian A et al., 2021].

The ginsenosides act primarily on the hypothalamus and pituitary, stimulating ACTH secretion, followed by increased corticosterone biosynthesis in the adrenal cortex. On the contrary, ginseng has an inhibitory effect on the hyperactivity of the HPA axis induced by stresses and increased corticosterone levels associated with metabolic and psychiatric disorders, e.g., Ginsenoside Rd, inhibits corticosterone secretion in the cells, and inhibits ACTH-induced corticosterone biosynthesis through downregulation of proteins in the cAMP/PKA/CREB signaling pathway in adrenocortical cells. In other words, ginseng acts as a mild stressor ("stress vaccine"), increasing the range of adaptive homeostasis that adjusts the stress response in mental disorders and metabolic diseases. That is a typical adaptogenic activity to activate the body's defense system and metabolic rate resulting in increased resilience and survival in response to stressful factors, including infections. Key mechanisms of action of ginseng and other adaptogens are related to their effects on adaptive intracellular signaling pathways involved in the regulation of cell growth, differentiation, apoptosis, and survival under the stressful stimulus, factors including hormones, neurotransmitters, xenobiotics, pathogens, and physical factors (UV, osmotic, etc.) [reviews: Jin W et al., 2020; Panossian A & Efferth T, 2022].

Here are the components of the phytocomposition "Balm Truskavets'": *Nepeta cataria, Mentha×piperita, Salvia officinalis, Echinacea purpurea, Cichorium inthybus, Achillea millefolium, Artemisia balchanorum, Acorus calamus, Althaea officinalis, Silybum marianum, Rubus idaeus, Rosa majalis.*

Currently, we do not have data on its chemical composition. In the composition of its predecessor and analogue „Balm Kryms'kyi", polyphenols were detected in the amount of 4 mg/L compared to 7 mg/L in ginseng tincture (produced by „Lubnykhimfarm", Ukraine) [Alyeksyeyev OI et al., 2006]. It is interesting that polyphenols in amounts of 5.28 mg/L (alkylbenzene 1.55; alkenylbenzene 0.47; esters of aromatic acids 1.32; alkyl phenols 1.14; polyaromatic hydrocarbons 0.08; alkylnaphthalenes 0.53; unidentified polycyclic aromatic hydrocarbons 0,19) also found in the composition of Naftussya bioactive water [Datsko OR et al., 2008; Ivassivka SV, 1997; Zukow W et al., 2022], the adaptogenic properties of which have long been known [Popovych IL et al., 2003; Kostyuk PG et al., 2006; Popovych IL, 2011; Popovych IL et al., 2022].

In a comparative study of effects of the phytocomposition "Balm Truskavets'" and the bioactive Naftussya water on patients with maladaptation, 39 parameters (18 EEGs, 8 HRVs, 5 biophysical, 4 phagocytosis, as well as the Popovych's leukocytary adaptation index, triiodothyronine, testosterone and cortisol) were identified, the physiologically favorable changes of which are common to both adaptogenic means [Popovych IL, 2022].

The adrenomimetic effect of both «Balm Kryms'kyi» and ginseng tincture on the isolated heart of a frog [Alyeksyeyev OI et al., 2006], due to inhibition of catechol-o-methyltransferase activity [Lupandin AV, 1989], is associated with polyphenols. However, we are inclined to the neurogenic mechanism of the adreno-sympathomimetic effect of the phytocomposition revealed in this study. This is consistent with literature data on the direct neurotropic effect of phytoadaptogens in vitro and in vivo [Asea A et al., 2013; Panossian A & Wikman G, 2010; Panossian A et al., 2018; Panossian A et al., 2019; Panossian A et al., 2021], as well as our group data on changes in EEG parameters [Popovych IL, 2022].

In conclusion, we will consider the issue of receptors through which the effects of physiologically active chemicals of adaptogens are realized. Based on the structural analogue [Panossian A et al., 2021], the corresponding chemicals act through cortisol, testosterone, catecholamines, and polyunsaturated fatty acids receptors. However, the most authoritative

group on the study of adaptogens, led by Panossian A, to our surprise, ignored both the very existence of the aryl hydrocarbon receptors (AhR) and their role in the effects of the favorite adaptogen ginseng.

As a preamble, we note that although AhR was initially recognized as a receptor that mediates the pathological effects of dioxins and other environmental pollutants [Nebert DW & Bausserman LL, 1970; Poland A. et al., 1976], AhR activation by endogenous (bilirubin and biliverdin [Phelan D. et al., 1988]), pseudoendogenous (products of tryptophan biotransformation by intestinal microflora [Murray IA & Perdew GH, 2020]) and the same environmental (polycyclic aromatic hydrocarbons, halogenated biphenyls, polyphenols, indoles, flavonoids [Busbee PB et al., 2013]) agonists have important physiological effects, including regulation of immune [Quintana FJ & Sherr DH, 2013; Yang X. et al., 2020] and endocrine [Andric SA et al., 2000; Li L-A. et al., 2005; Ye L. et al., 2011; Trego ML et al., 2018] responses.

It is important that the AhRs are also, or rather primarily, expressed in the neurons of hippocampus and cerebral cortex [Eckers A et al, 2016; Kimura E & Tohyama C, 2017; Ojo ES et al, 2021]. Although AhR expression decreases from the embryonic period into adult life, several physiological functions remain in the adult brain, which include the regulation of synaptic plasticity, neurogenesis, neurotransmitter levels and blood-brain barrier functions [Wang X et al, 2011; Chen Y et al, 2017; Chen WC et al, 2019; Keshavarzi M et al, 2020].

AhR signaling is considered a promising drug and preventive target, especially in cases of cancer, inflammatory and autoimmune diseases. Binding of AhR to both xenobiotic and endogenous ligands leads to highly transcriptome-specific cell changes and changes in cellular functions [Esser C & Rannug A, 2015]. It is becoming increasingly clear that the physiological activity of the AhR is nuanced, involving a complex cooperative/competitive "interaction" and changing the AhR from a *toxic mediator to an important sensor of physiological homeostasis* [Murray IA & Perdew GH, 2020; Avilla MN, 2020; Kou Z & Dai W, 2021; Rejano-Gordillo CM et al., 2022].

In our opinion, among the given list of organic compounds of Naftussya bioactive water [Datsko OR et al., 2008], there is a high probability that at least one AhR agonist is present. In favor of such an assumption, the data show that AhR, due to the peculiarities of its site, can bind and be activated

or inhibited by very different structural compounds [Denison MS et al., 2002; Denison MS et al., 2011; Giani Tagliabue S et al., 2019].

The discovery of Wang Y et al. [2008] was a new stage in the research of the mechanisms of adaptogenic action of ginseng.

It is known that transcriptional activation of the CYP1A1 gene (coding for cytochrome P450 1A1) is mediated by the AhR. The authors have examined interaction of the ginsenoside Rg1 and Rb1 with the carcinogen activation pathway mediated by the AhR in HepG2 cells. The results showed that in HepG2 cells CYP1A1 mRNA expression was significantly increased in a concentration- and time- dependent manner by ginsenoside Rg1 and Rb1. Ginsenoside Rg1 and Rb1 activated the DNA-binding capacity of the AhR for the xenobiotic responsive element of CYP1A1. Rg1 and Rb1 were able to activate the ability of the AhR to bind to an oligonucleotide containing the xenobiotic-responsive element (XRE) of the Cyp1a1 promoter. These results indicate that Rg1 and Rb1's effects on CYP1A1 induction are mediated by the AhR. Since CYP1A1 and AhR play important roles in carcinogenesis, development, differentiation and many other essential physiological functions, these results suggest that the chemopreventive effect of Panax ginseng may be due, in part, to ginsenoside Rg1 and Rb1's ability to compete with aryl hydrocarbons for both the AhR and CYP1A1. Rg1 and Rb1 may thus be natural ligands and substrates of the AhR or have relationship with AhR pathway. These properties might be of help for future studies in P. ginseng and chemoprevention in chemical-induced cancer.

Later Hu Q et al. [2013] examined the ability of a series of ginsenosides extracted from ginseng to bind to and activate/inhibit the AhR and AhR signal transduction. The authors demonstrated the ability of selected ginsenosides to directly bind to and activate the guinea pig cytosolic AHR, and to stimulate/inhibit AHR-dependent luciferase gene expression in a recombinant guinea pig cell line. Comparative studies revealed significant species differences in the ability of ginsenosides to stimulate AhR-dependent gene expression in guinea pig, rat, mouse and human cell lines. The endogenous gene CYP1A1 could be inducted in all cell line. The authors concluded that the ability of these compounds to stimulate AhR signal transduction demonstrated that these *ginsenosides are a new class of naturally occurring AhR agonists*.

Incidentally, we cannot deny ourselves the pleasure of stating that as early as 1994, the Truskaveysian Scientific School, during a comparative study of the adaptogenic properties of ginseng tincture, the phytocomposition

"Balm Kryms'kyi" and Naftussya bioactive water, showed that a four-day treatment of female rats shortened the duration of Nembutal sleep from 159±8 min in control (tap water) to 131±8, 87±8, and 65±5 min respectively [Panasyuk YM et al., 1994; Alyeksyeyev ***OI*** et al., 1996]. This indirectly indicates the activation of microsomal hydroxylation, which is mediated by the cytochrome P450 and AhR complex.

2.2. Relationships between neuro-endocrine, electrocardiogram, and gastric mucosa injuries parameters in naïve and stressed rats

Summary

Introduction and aim. Despite the extensive and multidisciplinary research on stress during the last 80 years, a lot of basic and clinical research is needed to better understand the manifestations, central and peripheral molecular regulators of stress response. In the vast majority of publications on stress, the HPA-, HPG- and autonomous systems are the objects of research, while the place in the general adaptation syndrome of such important hormones as calcitonin and PTH has been studied only in a few publications. Another methodological shortcoming of most studies is that the subjects of analysis are limited to a *single* neuro-endocrine system. Therefore, we set ourselves the aim: to analyze relationships between some adaptation hormones, HRV, calcitonin, and PTH as well as electrocardiogram and damage to gastric mucosa in naïve and post stressed rats.

Material and methods. The experiment is at 38 rats Wistar line: 18 males and 20 females. Over the 10 days, one animal remained intact and 3 other rats were exposed to water-immersion and restraint stress (WIRS). The next day after stressing, the ECG was recorded, and right away the animals removed from the experiment by decapitation in order to remove the stomach, adrenal glands, and collect the blood in which was determined levels of main adaptation hormones such as corticosterone, aldosterone, testosterone, triiodothyronine, as well as parathyroid hormone and calcitonin. The stomach was cut along the greater curvature, and counted the amount of ulcers and their length was measured.

Results. First of all, by applying the WIRS model, we reproduced Selye's primary attributes of stress: an increase in adrenal mass, an increase

in corticosterone levels, damage to the gastric mucosa and myocardium, on the one hand, and Cannon's attributes: an increase in the level of circulating catecholamines and sympathetic tone and a reciprocal decrease in vagal tone – on the other hand side. We found that the severity of the gastric mucosa damage significantly correlates with changes in ECG parameters, in particular, depression of the T wave and S-T joint, which indicate myocardial dystrophy. Further, it was found that such a connection is caused by the damaging effect on both targets of increasing the level of parathyroid hormone, as well as the production of aldosterone and catecholamines by enlarged adrenal glands. In addition, an increase in the level of corticosterone and sympathetic tone with a simultaneous decrease in vagal tone as well as serum calcitonin and testosterone cause damage only to the gastric mucosa, but not to the myocardium. Such a constellation of neuro-endocrine reactions to stressors (cold, immobilization, hunger, etc.) determines the severity of damage to the gastric mucosa and myocardium by 73%.

Conclusion. The condition of the gastric mucosa and myocardium as essential targets of stressors is determined by the damaging and protective effects of adaptive hormones and the autonomic nervous system.

Introduction

The first scientific publication on *general adaption syndrome*, or as we know today *biologic stress* has been published in Nature in 1936 by the 29-year old Hans Selye [Selye H, 1936]. Szabo S et al. [2017] in the anniversary review "Stress" is 80 Years Old" conclude that despite the extensive and multidisciplinary research on stress during the last 80 years, a lot of basic and clinical research is needed to better understand the manifestations, central and peripheral molecular regulators of stress response, especially the modes of prevention/management of distress or its transformation into eustress and the treatment of stress-related diseases.

In the vast majority of publications on stress, the HPA-, HPG- and autonomous systems are the objects of research, while the place in the general adaptation syndrome of such important hormones as calcitonin and PTH has been studied only in a few publications. Another methodological shortcoming of most studies is that the subjects of analysis are limited to a *single* neuro-endocrine system.

Therefore, we set ourselves the goal: to analyze relationships between some adaptation hormones, HRV, calcitonin, and PTH as well as electrocardiogram and gastric mucosal damage in naïve and post stressed rats.

Material and methods are detailed in the previous subsection.

Adhering to the accepted algorithm, we recalculated the raw values of the parameters in Z-scores. This is all the more important in view of sexual dimorphism in endocrine parameters. In addition to drastically higher levels of testosterone (41.8±1.7 vs 3.53±0.24 nM/L), males have higher levels of calcitonin (36±6 vs 21±4 ng/L), but lower levels of parathyroid hormone (154±12 vs 185±3 ng/L), adrenals mass (44±5 vs 65±5 mg), corticosterone (340±45 vs 466±57 nM/L), and aldosterone (587±8 vs 639±24 pM/L).

First of all, by applying the WIRS model, we reproduced Selye's primary attributes of stress: an increase in adrenal mass, an increase in corticosterone level, damage to the gastric mucosa and myocardium, on the one hand, and Cannon's attributes: an increase in the level of circulating catecholamines and sympathetic tone and a reciprocal decrease in vagal tone – on the other hand side (Table 2.8).

Table 2.8. Ranking of post-stress changes

Variables	**Intact Rats (10)**	**Post Stress (28)**
1	2	3
AMo HRV as Sympathetic tone, %	48 6	+0.88 0.19*
Adrenals mass normalized by sex, Z	0	+0.51 0.12*
1/Mode HRV as Catecholamines, 1/msec	1/175 1/10	+0.47 0.16*
Parathyroid hormone normalized by sex, Z	0	+0.46 0.22*
Aldosterone normalized by sex, Z	0	+0.40 0.19*
Corticosterone normalized by sex, Z	0	+0.28 0.22
Calcitonin normalized by sex, Z	0	-0.09 0.16
MxDMn HRV as Vagal tone, msec	51 14	-0.59 0.07*

Table 2.8 (cont)

1	2	3
Testosterone normalized by sex, Z	0	-0.90 0.29*
Gastric Mucosal Damage, points	0	+1.19 0.20*
Gastric Ulcers Amount	0	+0.94 0.22*
Gastric Ulcers Length, mm	0	+0.93 0.19*
R wave ECG, μV	330 18	+0.90 0.33*
P wave ECG, μV	25 3	+0.80 0.25*
P-Q interval ECG, msec	55.6 0.8	-1.88 0.27*
T wave ECG, μV	131 3	-1.76 0.36*
Q-T interval ECG, msec	104.9 1.2	-1.07 0.21*
S-T joint ECG, μV	54 5	-0.79 0.30*

The moderate expression of the essential signs of stress is explained, firstly, by our deliberate use of mild stressor parameters (water temperature and duration of water immersion), and secondly, by pretreatment of 18 animals with a phytoadaptogen, which, in particular, prevented the post-stress increase in the level of corticosterone. The effects of the adaptogen are not the subject of this study and will be analyzed in the next article, already ready for printing.

We found (Tables 2.9-2.10 and Fig. 2.6) that the number and length of ulcers, as well as the severity of damage (taking into account also the appearance of only petechiae without ulcers) to the gastric mucosa significantly correlate with changes in ECG parameters, in particular, depression of the T wave and S-T joint, which indicate myocardial dystrophy [Zavodskaya IS et al., 1977; Berger EN, 1980; Zavodskaya IS & Moreva YeV, 1981; Markova OO et al., 1997], and only weakly with the amplitude of the R wave.

Table 2.9. Correlation Matrix for Gastric mucosa and EEG variables

Variables	T wave ECG	S-T joint ECG	R wave ECG
Gastric Ulcers Amount	**-0.650**	**-0.500**	*0.178*
Gastric Ulcers Length	**-0.611**	**-0.497**	0.241
Gastric Mucosal Damage	**-0.596**	**-0.493**	0.238

Note. According to the equation: $|r|=\{\exp[2t/(n-1.5)^{0.5}]-1\}/\{\exp[2t/(n-1.5)^{0.5}]+1\}$

for a sample of n=38 critical value |r| at $p<0.05$ ($t>2.02$) is **0.323,** at $p<0.01$ ($t>2.70$) is **0.420,** at $p<0.001$ ($t>3.55$) is **0.528**.

Table 2.10. Factor structure of Roots, which reflect post-stress damage to the gastric mucosa and myocardium

Left set	R
Gastric Ulcers Amount	**0.990**
Gastric Ulcers Length	**0.967**
Gastric Mucosa Injuries	**0.914**
Right set	R
T wave ECG	**-0.913**
S-T joint ECG	**-0.712**
R wave ECG	**0.282**

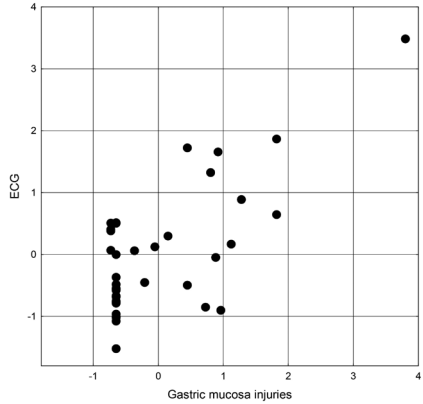

R=0.706; R^2=0.499; $\chi^2_{(12)}$=30.2; p=0.003; Λ Prime=0.400

Fig. 2.6. Scatterplot of canonical correlation between damage to gastric mucosa (X-line) and parameters of ECG (Y-line) at intact and stressed rats

Further, it was found that such a connection is caused by the damaging effect on both targets of increasing the level of parathyroid hormone, as well as the production of aldosterone and catecholamines by enlarged adrenal glands. In addition, an increase in the level of corticosterone and sympathetic tone with a simultaneous decrease in vagal tone as well as serum calcitonin and testosterone cause damage only to the gastric mucosa, but not to the myocardium (Table 2.11).

Table 2.11 Correlation Matrix for Neuro-endocrine and Gastric mucosa&EEG variables

Variables	GU Amount	GU Length	Gastric Injuries	T wave ECG	S-T joint
Parathyroid hormone	**0.584**	**0.621**	**0.516**	**-0.351**	**-0.342**
Adrenals Mass	0.236	**0.384**	**0.391**	*ns*	*-0.192*
Aldosterone	0.226	0.275	0.302	*ns*	*ns*
1/Mode HRV as Catecholamines	*0.188*	*ns*	*ns*	**-0.356**	-0.284
AMo HRV as Sympathetic tone	0.253	*0.214*	0.273	*ns*	*ns*
Corticosterone	*ns*	*0.206*	0.225	*ns*	*ns*
Calcitonin	-0.229	-0.283	-0.251	*ns*	*ns*
MxDMn HRV as Vagal tone	*ns*	-0.230	-0.283	*ns*	*ns*
Testosterone raw	*ns*	*-0,213*	*-0,204*	*ns*	*ns*
Testosterone normalized	*ns*	*-0,199*	*-0,218*	0,252	*0,190*

Interestingly, sex-normalized testosterone exerts a cardioprotective effect.

Such a constellation of neuro-endocrine reactions to stressors (cold, immobilization, hunger, etc.) determines the severity of damage to the gastric mucosa and myocardium by 73,5% (Table 2.12 and Fig. 2.7).

Table 2.12. Factor structure of Roots of neuro-endocrine parameters and parameters of ECG&gastric mucosa

Left set	R
1	2
Parathyroid hormone	**-0.694**
Adrenals mass	**-0.312**
AMo HRV as Sympathetic tone	**-0.303**

Table 2.12 (cont)

Aldosterone	**-0.266**
1/Mode HRV as Catecholamines	**-0.241**
Corticosterone	**-0.154**
MxDMn HRV as Vagal tone	**0.270**
Calcitonin	**0.258**
Testosterone normalized	**0,230**
Testosterone raw	**0.142**
Right set	**R**
Gastric Ulcers Length	**-0.969**
Gastric Ulcers Amount	**-0.967**
Damage to Gastric Mucosa	**-0.911**
T wave ECG	**0.719**
S-T joint ECG	**0.517**

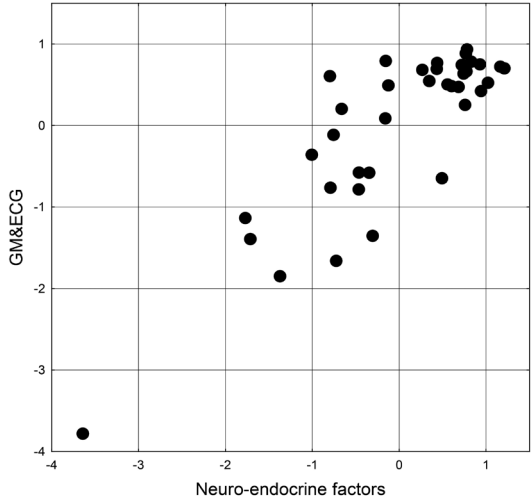

R=0.857; R^2=0.735; $\chi^2_{(50)}$=75; p=0.013; Λ Prime=0.075

Fig. 2.7. Scatterplot of canonical correlation between neuro-endocrine parameters (X-line) and parameters of ECG and gastric mucosa (Y-line) at intact and stressed rats

The maximum contribution (judging by the factor load on the causal neuro-endocrine root) to post-stress damage to the gastric mucosa and myocardium was precisely PTH, which was a surprise for us. After all, our search on PubMed and PMC resources revealed only one old article by Clementi G et al [1989] that PTH injected peripherally did not interfere with the development of experimental ulcers. Conversely, when PTH was administered in cerebral ventricle the development of ulcers was significantly inhibited. The gastric secretory volume and acid output were also reduced. The possibility was discussed that this antisecretory activity of PTH may be due to a direct effect at the CNS level. However, recently Castle C & Tietjens J [2021] stated that primary hyperparathyroidism is characterised by hypercalcaemia and peptic ulcer disease in 12% patients. The debate about whether primary hyperparathyroidism increases the risk of peptic ulcer disease remains controversial in the literature. It has been shown that hypercalcaemia by any mechanism will tend to increase gastric acid production due to the role calcium plays in regulating gastrin-secreting cells. The pathophysiological mechanism is not well established, but studies point to activation of stomach calcium-sensing receptors expressed on the basolateral membrane of gastrin cells resulting in gastrin secretion, which in turn stimulates gastric parietal cells leading to increased hydrochloric acid production, explaining the association between hypercalcaemia and peptic ulcer disease.

Calcitonin, whose functional antagonism with PTH is most pronounced in relation to bone tissue, also had the opposite effect on post-stress damage to the gastric mucosa, but not to the myocardium. In our study, the gastroprotective effect of Calcitonin turned out to be weaker than expected after analyzing the literature, which in this aspect is more numerous compared to that of PTH.

Back in 1985 Clementi G et al. [1985] found that eel-Calcitonin, iv injected, decreased gastric acid secretion and inhibited the development of stress-induced ulcers in rats. In isolated rat stomach the peptide at the concentrations of 1 nM to 1 μM did not modify acetylcholine, histamine or 5-hydroxytriptamine-induced contractions. These results suggest that this peripheral activity of (Asu1,7) eel-Calcitonin does not involve a direct interference with cholinergic, histaminergic or serotoninergic pathways at gastric level. At the same time Ohno H et al. [1985] found that el-Calcitonin, an analogue of natural eel-Calcitonin, inhibited the development of gastric ulcers induced by WIRS (as well as by pylorus ligation, aspirin and reserpine)

in rats. Similar antiulcer action was exerted by cimetidine and secretin. Moreover, once daily injections of el-Calcitonin (but not cimetidine and secretin) promoted the healing of acetic acid-induced chronic gastric ulcers not only in rats but in dogs. The healing effect persisted after the cessation of administrations. Guidobono F et al. [1991] later confirmed that e-Calcitonin has a high index of protection against ulcers induced by cold restraint stress or indomethacin, but not by ethanol.

Taché Y et al. [1988] studied the central nervous system action of Calcitonin to influence various experimental models of gastric ulcers and gastric function in rats. Intracisternal injection of salmon Calcitonin completely suppressed gastric ulcerations induced by exposure to cold restraint stress (as well as intracisternal injection of a stable thyrotropin-releasing hormone analogue, or peroral administration of aspirin). By contrast, intracisternal calcitonin enhanced gastric lesions elicited by peroral administration of 40% ethanol or 0.6 N HCl. Calcitonin action was dose-dependent (0.01-1 microgram) and central nervous system mediated in as much as intravenous Calcitonin, given at a dose 50-fold higher than that effective intracisternally, did not significantly modify gastric mucosal injuries elicited by aspirin or ethanol. Intracisternal injection of Calcitonin at 0.01 microgram inhibited gastric acid output by 90% in pylorus-ligated rats and suppressed gastric emptying of a liquid meal. Prostaglandin generation in the gastric mucosa was not modified by intracisternal injection of Calcitonin. These results demonstrate that intracisternal Calcitonin acts within the brain to potently prevent ulcer formation elicited by stress, thyrotropin-releasing hormone analogue, or aspirin, but is not cytoprotective against necrotizing agents. Calcitonin action is not related to modification of gastric prostaglandin generation but it may involve the inhibition of gastric secretory and motor function.

For the sake of historical justice, it should be noted that the gastroprotective effect (by pylorus ligation) of salmon Calcitonin was discovered back in 1983 in the USSR [Vasilenko VKh & Kochina EN, 1983], but remained invisible to the scientific community, probably because of the iron curtain.

After a rather long break, Calcitonin appeared as a member of its family calcitonin gene-related peptide (CGRP). CGRP is a predominant neurotransmitter from capsaicin-sensitive sensory nerves, which are widely distributed in the gastrointestinal system. The synthesis and release

of CGRP is regulated by the capsaicin receptor which is known as transient receptor potential vanilloid subfamily member 1 (TRPV1). CGRP is considered a marker of afferent fibers in the upper gastrointestinal tract being almost completely depleted following treatment with the selective neurotoxin capsaicin that targets these fibers via transient receptor potential vanilloid of type-1 [Evangelista S, 2009; Luo XJ et al., 2013].

Evangelista S & Renzi D [1997] investigated the role of endogenous and exogenous CGRP in WIRS-induced gastric ulcers in rats. Authors found that WIRS produced gastric ulcers which were inversely correlated to the decrease in CGRP-like immunoreactivity observed in the whole thickness of the corpus stomach but not in its mucosal layers. Systemic administration of CGRP (100 μg/kg s.c.) produced a significant decrease in lesion index of WIRS-ulcers and this protection was inhibited by functional ablation of afferent neurons induced by capsaicin pretreatment. These findings suggest that sensory endogenous CGRP plays a defensive role in WIRS-ulcers.

The use of CGRP knockout mice has let to characterize the endogenous role of CGRP showing that the local release of this neuropeptide favours ulcer healing. Decreased levels of gastric CGRP-like immunoreactivity were observed during WIRS-ulcers (as well as acetic acid-, cysteamine-, concentrated ethanol-ulcers). Restoration of CGRP was found in animals bearing ulcers in healing status and delayed healing in mice knockout to CGRP. CGRP was able to release somatostatin from gastric D cells but its main effects on the stomach homeostasis rely on local vasodilator action during increased acid-back diffusion [Evangelista S, 2009]. In addition to increase in gastric mucosal blood flow and inhibition of gastric acid secretion, the beneficial effects of CGRP on gastric mucosa include prevention of cellular apoptosis and oxidative injury. Therefore, the TRPV1/CGRP pathway represents a novel target for therapeutic intervention in human gastric mucosal injury [Luo XJ et al., 2013].

It is well known that the secretion of Calcitonin and PTH is controlled by calcium ions. In addition, the thyroid and parathyroid glands are dually innervated by sympathetic (cervical sympathetic trunk) and parasympathetic (superior laryngeal nerve) nerve fibers. Hotta H et al. [2017] found that the secretion of Calcitonin (as well as T3 and T4) increased during parasympathetic nerve fibers stimulation while decreased during sympathetic stimulation. PTH secretion increased during sympathetic stimulation, but was not affected by parasympathetic stimulation.

In our study, on the contrary, a weak, but still positive correlation was found between the level of Calcitonin and the HRV-marker of sympathetic tone (r=0.27) as well as catecholamines (r=0.21), but not vagal tone, in the absence of correlation with HRV parameters of PTH level (Table 2.13). However, the discrepancy may be due to different experimental approaches.

Table 2.13. Correlation matrix for neuro-endocrine factors

	Correlations							
Variable	Mode	AMo	DX	TES	COR	Ald	PTH	CT
Mode	1,00	-0,58	0,39	-0,26	0,18	0,31	0,05	-0,21
AMo	-0,58	1,00	-0,65	0,21	0,05	-0,27	-0,14	0,27
DX	0,39	-0,65	1,00	0,19	-0,25	0,04	-0,09	0,00
TEST	-0,26	0,21	0,19	1,00	-0,50	-0,55	-0,52	0,51
CORT	0,18	0,05	-0,25	-0,50	1,00	0,33	0,36	-0,37
Aldoster	0,31	-0,27	0,04	-0,55	0,33	1,00	0,51	-0,41
PTH	0,05	-0,14	-0,09	-0,52	0,36	0,51	1,00	-0,85
Calcitonin	-0,21	0,27	0,00	0,51	-0,37	-0,41	-0,85	1,00

It is time to move on to the analysis of the role of adrenergic and cholinergic factors in damage to the main targets of stressors.

Back in 1980, in monograph of Berger EN [1980], which reflected the results of research by employees of his laboratory (Khoma MA, Bolyarska VA, Bondarenko YuI, Rosolovskyi OP) during 1971-1977, it was stated that the administration of carbacholin (10 μg/kg) to rats 5 minutes before the administration of adrenaline (4 mg/kg), firstly, reduced mortality from pulmonary edema from 60% to 18%, secondly, reduced the index of ECG changes (on a 3-point scale) in surviving animals from 1.6±0.27 to 1.1±0.10. Interestingly, a lower dose of carbacholin (5 μg/kg) had no effect on both parameters, while a higher dose (20 μg/kg) drastically increased mortality to 88% (only one animal out of 8 survived). Reducing the dose of adrenaline to 1 mg/kg drastically reduced mortality (up to 10%) and, less significantly, dystrophic ECG changes (up to 1.4±0.21). Preventive administration of carbacholin (20 and 40 μg/kg) dose-independently reduced the severity of epinephrine myocardiodystrophy to 1.0±0.21 and 1.0±0.15 respectively. An even more noticeable cardioprotective effect of carbacholin was found when it was administered 40-45 minutes after the administration of adrenaline (0.5±0.16 and 0.6±0.24 after doses of 20 and 40 μg/kg, respectively).

Later, in the same laboratory under the leadership of Markova OO [1997], her colleagues (Koptyukh VV, Mysula IR, Khara MR, Denefil OV) discovered that the occurrence and development of adrenaline myocardiodystrophy significantly depend on the innate resistance of rats to hypoxic hypoxia. In particular, after a dose of adrenaline of 1 mg/kg, 85÷88% of highly resistant (HR) rats and only 56÷70% of low resistant (LR) survived. Increasing the dose to 1.5 mg/kg reduced HR survival to 82% but did not affect LR survival (72%). In animals that survived, after a day, changes in ECG parameters also depended on resistance to hypoxia: in LR, the Q-T interval was lengthened by 8%, but in HR it was shortened by 5%, the T wave decreased by 11%, but in HR by 9%, with the same lowering below the isoline of the S-T junction, which was accompanied by the appearance of 122 vs 62 necrosis in the field of view of the histological preparation of the myocardium. The HRV marker of sympathetic tone in LR rats increased by 8% (from 19.0% to 20.5%), while in HR rats, the initially 14% lower sympathetic tone (16.4%) decreased by another 7%. On the other hand, in HR rats, the initially 9% higher vagal tone (MxDMn= 12 msec vs 11 msec) increased by another 17%. The index of sympatho-vagal balance in LR rats increased from 1.73 by 19% (to 2.05) one day after administration of adrenaline, while being initially lower by 21% (1.37) in HR rats, it decreased by another 21% (up to 1.08). However, the HRV marker of circulating catecholamines (1/Mode) changed less significantly: in LR rats it increased by 2.6%, while in HR rats it decreased by 4.1%. As a result, the stress index, which includes all three HRV parameters, in LR rats increased from 74 by 22% (to 90), whereas the 20% lower stress index in LR rats decreased by another 24%: from 59 to 45.

Taken together, the presented data indicate that LR rats compared to HR are characterized by higher basal sympatho-adrenal activity and lower vagal tone, and exogenous epinephrine causes an increase in sympathetic tone and, to a lesser extent, circulating catecholamine levels and a decrease in vagal tone, i.e. acts similarly to stressors in our experiment. Instead, HR animals react to exogenous adrenaline in the opposite way: by increasing vagal tone and decreasing sympatho-adrenal activity.

Later, in the same laboratory, it was shown that the previously tested procedure (carbacholin 40 μg/kg before adrenalin 1 mg/kg) reduced the mortality of LR rats from 30% to 12%, while HR from 12% to 0%! At the same time, in LR rats, carbacholin reduced the basal level of stress

index from 57 to 36 and almost completely prevented its increase caused by adrenaline: 80 and 42 respectively. In HR rats, the lower basal level of stress index (35) carbacholin reduced even more (to 20) as well as minimized its adrenaline-induced increase from 60 to 35. Therefore, pharmacological enhancement of cholinergic effects significantly reduces the differences between LR and HR animals both at rest, and, especially, in the response of the autonomic nervous system to exogenous adrenaline as one of the main effectors of acute stress [Markova OO et al., 1997].

Another analytical approach was applied by Zavodskaya IS et al. [1977; 1981]. In these two monographs, long-term data of their laboratory were collected. It was shown that destructive changes in the myocardium of rats developed, firstly, after the introduction of adrenaline, norepinephrine, β-adrenoceptor agonist isadrin and indirect sympathomimetic ephedrine. Secondly, in rats and rabbits, after 0.4÷3-hour electrical stimulation of the reflexogenic zone of the aortic arch, which increases the secretion of both noradrenaline by axons of postganglionic sympathetic nerves and catecholamines (adrenaline, noradrenaline and dopamine) by cells of the medulla of the adrenal glands. It was found that prior administration of the postsynaptic alpha-adrenoblocker sympatholitin to rats completely prevented myocardial damage by exogenous adrenaline and significantly minimized the cardiotoxic effect of norepinephrine; blockade of β-adrenoceptors with dichloroisoproterenol minimized the cardiotoxic effect of their agonist isadrine. Sympatholitin also significantly minimized damage to the rat myocardium caused by electrical stimulation of the aortic arch (which increases the impulse of the cardiac branches of the sympathetic nerve): out of 16 pretreatment animals, 11 did not show destructive changes in the myocardium, 3 had mild dystrophic phenomena, and only 2 had foci of necrosis in the left ventricle, while out of 19 control animals, severe myocardial damage developed in 15. Postsynaptic β-adrenoblocker propranolol under similar conditions prevented the development of biochemical markers of myocardial dystrophy in rabbits: an increase in the content of lactate in the myocardium and a decrease in creatine phosphate and an increase in the activity of creatine kinase in the serum. In contrast, octadine, which blocks the release of norepinephrine by sympathetic terminals but does not block the effects of circulating catecholamines, minimized myocardial damage in rats after only 5 days of administration, whereas a single administration 40–50 min before

electrical stimulation of the aortic arch was ineffective. Benzohexonium, which blocks nerve transmission in both sympathetic and parasympathetic ganglia, acted similarly. When administered once 30 min before 3-hour electrical stimulation of the aortic arch, benzohexonium had only a very weak cardioprotective effect in rats, and moreover, when administered 30 min before adrenaline injection, it even increased myocardial damage. Instead, administration of a ganglioblocker 15 min before and one hour after electrical stimulation prevented morphological damage to the myocardium in rats, and dystrophic changes in the T wave and the S-T segment of the ECG in rabbits.

Paradoxically, after completion of electrical stimulation of the aortic arch, hypothalamus, or paws of animals, the damage to the myocardium caused by it was accompanied by a 2.5-3 times ***decrease*** in the content of norepinephrine in it, which was maintained for the next 2 days [Zavodskaya IS & Moreva YeV, 1981].

Similar to the development of myocardiodystrophy, already after 3 hours of electrical stimulation of rats, the content of norepinephrine in the gastric mucosa in 5 animals out of 11 fell below the sensitivity of the method, and in 6 it decreased by 67%; adrenaline content decreased in 10 animals, but less significantly. Similar results were obtained on another model of stress – 2-hour electrical stimulation of the negative emotiogenic zone of the hypothalamus of rabbits: the content of norepinephrine in the gastric mucosa of 6 out of 8 animals fell below the sensitivity of the method, and in the remaining two it decreased by 85% and 55%, respectively (epinephrine content, detectable before stress only in 3 rabbits, after 2 hours it disappeared even in them) [Zavodskaya IS & Moreva YeV, 1981].

In the laboratory of Berger EN [1980], a similar effect was detected in rats after a 2-hour immobilization-cold stress: the content of norepinephrine decreased on average from 0.56 to 0.13 μg/g, the content of adrenaline in 7 rats out of 12 was only 0.04 μg/g, and in the remaining 5 it fell below sensitivity level of the method, while in intact animals it was 0.14 μg/g.

Zavodskaya IS & Moreva YeV [1981] concluded that with extreme irritation of the reflexogenic zone or hypothalamus, a turbulent flow of sympathetic impulses is sent to the heart and stomach, which cause the release of norepinephrine from the tissue depot in unusual quantities. Such an increased release of norepinephrine from the depot is not compensated by its resynthesis and causes the subsequent depletion of its reserves.

However, the content of noradrenaline decreases in the myocardium and in the gastric mucosa (as well as in the liver, brain and aorta), also after the administration of toxic doses of noradrenaline itself as well as adrenaline or isadrin to animals. One of the mechanisms of such a phenomenon can be the inhibition of its own biosynthesis by an excess of catecholamines. However, later Meerson[28], confirming a decrease in the rat myocardium of norepinephrine one day after acute emotional and pain stress by 45% (as well as in the mucous membrane of the small intestine by 43%), revealed the ***activation*** of its biosynthesis in the atria by 33% in combination with a 40% decrease in its neuronal capture.

Berger EN [1980] provides data that 2 days after the administration of epinephrine at a dose of 3 mg/kg to rats, the content of acetylcholine in the heart decreased by a third, while the duration of its bradycardic effect did not significantly change, while a dose of 1 mg/kg probably did not affect the content of acetylcholine but continued its inhibitory effect by a third. At the same time, cholinesterase activity decreased by a quarter, and the intensity of acetylcholine bradycardia increased by 50-60% after both doses.

Markova OO [1997] later clarified that such protective cholinergic mechanisms differ in LR and HR rats. In particular, the basal content of acetylcholine in the atria of LR rats is one third higher (41.8 vs 30 nM/g), and one day after 1 mg/kg of adrenaline it was reduced by half (to 23.4 nM/g), while in HR rats it shows only a downward trend (to 28.2 nM/g). Thus, a cardiotoxic dose of adrenaline after a day eliminated the differences between HR and LR animals with respect to atrial acetylcholine. In the ventricles, the basal levels of acetylcholine did not differ significantly (5.5 vs 5.3 nM/g), but adrenaline reduced it in LR rats to 3.3 nM/g, without affecting its level in HR rats. The total cholinesterase activity of atrial tissues in intact LR rats was lower by 8% (156 vs 170 μM/g•h), and a day after the administration of adrenaline, the differences were completely eliminated (135 μM/g•h each). The same difference of 8% (108 vs 118 μM/g•h) was found for the basal activity of ventricular cholinesterase, but adrenaline reduced it in LR by 28% and in HR by 41%. The intensity of the negative chronotropic response to irritation n. vagus in HR rats significantly exceeded that in LR, and continued to increase after the administration of adrenaline, while it almost did not change in LR rats.

In another experiment by the Markova OO laboratory, it was shown that in rats that died shortly after an adrenaline dose of 2.5 mg/kg, the basal stress index was 129% of the average for the sample, due to

increased sympathetic tone to 119% and decreased vagal tone to 92% in the absence of deviations from the average Mode. In animals that survived, but were in a severe condition (adynamia, anorexia, etc.), the basal stress index was 88% of the average due, mainly, to reduced sympathetic tone to 91% in the absence of abnormalities in both vagal tone (101%) and a marker of circulating catecholamines (99%). At the same time, animals that satisfactorily tolerated the cardiotoxic effect of adrenaline were characterized by a slightly lower sympathetic tone (87%) in combination with increased vagal tone to 110% at the normal level of Mode, which gave a minimal level of the stress index (77%).

Therefore, our data are consistent with the data of Zavodskaya IS et al. [1977; 1981], that myocardial damage is caused by a stressor intensification of adrenergic effects on the heart due to an increase in the level of circulating catecholamines (the lion's share of which, as is well known, is adrenaline), which is evidenced by the presence of a negative correlation between by their HRV-marker and ECG-markers of myocardial dystrophy, but not sympathetic tone, the correlation of which with the latter is absent. In contrast to Berger EN [1980] and Markova OO et al. [1997], we did not find a cardioprotective effect of M-cholinergic influence, which is evidenced by the lack of correlation between vagal tone and ECG markers of myocardiodystrophy.

The reason for such discrepancies, in our opinion, is precisely the wide range of resistance to hypoxia in our sample. Having information and relying on previous experience [Meerson FZ, 1984; Popovych IL et al., 2010; Zukow W et al., 2022; Melnyk OI et al., 2023], in our experimental design, 2 LR (76 and 80 sec) and 2 HR (285 and 317 sec) rats were tentatively included in the intact group (n=10), and such the same percentage is observed for stressed animals: 21% LR (65÷78 sec) and 18% HR (227÷294 sec). The exact opposite directionality of responses of HRV parameters in LR and HR rats both to adrenaline injection and to stressors cancels out correlations between them and ECG parameters.

Now about another important target of catecholamines and acetylcholine – the gastric mucosa.

Several stress damage models were tested in the laboratory of Zavodskaya IS & Moreva YeV [1981]. It was shown that 3 days after one-hour electrical stimulation of the anterior hypothalamus, a positive reaction of feces to the presence of blood appeared in 4 out of 5 rabbits, and in the last one – on the 7th day. On the 10th day, an autopsy revealed

an average of 2.6 lesions of the gastric mucosa per animal. One day after electrocoagulation of the hypothalamus, destructive damage to the gastric mucosa developed in 8 rats out of 15; the total number of tissue defects was 25, i.e. 1.7 per animal. One day after 3-hour electrical stimulation of the front paws of immobilized rats, an average of 4.6 lesions were detected. Administration of norepinephrine at a dose of 2 mg/kg caused damage in all 17 rats in the form of hemorrhagic erosions in the amount of 12.7±3.3 per animal (range: 4÷27).

When clarifying the role of n. vagus, it was shown that vagotomy performed 8-25 days before one-hour electrical stimulation of the hypothalamus reduced the number of gastric mucosal lesions in 9 rabbits found the next day to 0.3 versus 2.0 in 7 rabbits that did not undergo vagotomy. In another experiment, the average number of damaged areas of the gastric mucosa one day after 3-hour electrical stimulation of the front paws of 17 immobilized rats subjected to vagotomy 2 weeks before this was 1.0 versus 3.4 in 17 animals with intact vagus nerves [Zavodskaya IS & Moreva YeV, 1981]. In Berger's laboratory, vagotomy prevented the formation of ulcers in 9 out of 10 rats subjected to immobilization-cold stress [Berger EN, 1980].

Because during subdiaphragmatic vagotomy, not only parasympathetic, but also sympathetic nerve fibers are crossed at the same time, researchers further resorted to pharmacological analysis of the mechanisms that support and disrupt the structural and functional integrity of the gastric mucosa.

In the laboratory of Zavodskaya IS [Zavodskaya IS & Moreva YeV, 1981], it was shown that the administration of benzohexonium to rabbits 30 minutes before the start of one-hour electrical stimulation of the hypothalamus and one hour after its completion, which achieved complete blocking of the transmission of excitation in parasympathetic and sympathetic ganglia, reduced the severity of damage to the gastric mucosa to 0.66 against 1.5 in the control. The gastroprotective effect of benzohexonium was also manifested in rats, reducing the number of damaged areas in the stomach by 5 times. However, administration of atropine sulfate at a dose of 1 mg/kg 10 min before electrification of rats, which completely eliminates the function of peripheral M-cholinergic receptors, did not protect the gastric mucosa from ulceration. On the other hand, administration of the postsynaptic α-adrenoblocker sympatholitin to rats one hour before electrical stimulation reduced the number of damaged areas of the gastric mucosa from 2.4 to 0.8; of β-blocker

dichloroisoproterenol – from 2.2 to 0.3; of the presynaptic sympatholytic guanethidine – from 3.3 to 2.2. The authors concluded that the efferent nerves through which impulses causing dystrophy are transmitted are adrenergic, but not cholinergic, and that the preventive effect of vagotomy is due to the crossing of precisely the sympathetic fibers in its composition.

However, there is evidence of the ineffectiveness of both α- and β-adrenergic blockers, and even the aggravation of stress ulceration by β-blockers and its attenuation by epinephrine [review: Berger EN, 1980]. In the laboratory of Berger EN, it was shown as early as 1977 that the blockade of both α- and β-adrenergic receptors with dihydroergotoxin, phentolamine or propranolol administered 30 minutes before immobilization-cold stress increased the number of ulcers. The presynaptic sympatholytic bretylium was ineffective; epinephrine (1 mg/kg) attenuated, while norepinephrine aggravated, gastric mucosal damage.

Later Esplugues J et al. [1982] showed that pretreatment with the β-adrenoceptor stimulant drugs, isoprenaline or salbutamol, significantly inhibited gastric ulcers induced by stress (as well as by pylorus ligation, exogenously perfused artificial gastric juice, various iatrogenic means such as histamine, polymyxin B, reserpine and indomethacin). Long-term treatment with salbutamol accelerated the healing of experimental chronic gastric ulcer. In anaesthetized rats, salbutamol produced a dose-related increase in mucosal blood flow which may contribute to its mode of action. Authors concluded that β-adrenoceptor agonists exert preventive and curative effects on gastric damage induced in the rat. This effect seems specific and mediated through β-adrenoceptor activation.

A number of authors, using a similar dose of atropine (0.8÷1.2 mg/kg), which was administered to rats 30 or 60 minutes before immobilization-cold or WIR stress, noted a decrease in the formation of ulcers [review: Berger EN, 1980]. Therefore, a comparative study of the gastroprotective effect of atropine at a dose of 1 mg/kg, administered 60 and 10 min before a 2-hour immobilization-cold stress, was conducted in Berger's laboratory [Berger EN, 1980]. It turned out that 10 minutes is still not enough to unfold the protective effect of blockade of peripheral M-cholinergic receptors against stressors.

In other studies of the Berger laboratory [Berger EN, 1980], it was shown that in rats exposed to stress, the content of acetylcholine in the gastric mucosa increased by 3.5 and 2.9 times in various experiments. This is caused by an increase in mediator release by vagal terminals in

combination with a halving of acetylcholinesterase activity. Administration of both carbacholin (10 μg/kg) and the acetylcholinesterase inhibitor ezerine immediately prior to stress increased the mean number of ulcers to 19 and 11, respectively, versus 3.5 in controls. Incidentally, let us recall the data of Zavodskaya IS & Moreva YeV [1981] that the introduction of the antipode of acetylcholine norepinephrine (2 mg/kg) also caused the appearance of hemorrhagic erosions in the amount of 12.7±3.3 per rat.

The ambiguity of adrenergic and cholinergic effects on the development or prevention of stress damage to the gastric mucosa is probably caused by the fact that RWIS-induced gastric mucosa damage is associated with the activation of both locus coeruleus, in which sympathoexcitatory neurones are located [Fan F et al., 2018], and ventrolateral periaqueductal gray, in which sympathoinhibitory neurones are located [Fan F et al., 2019], as well as nucleus raphe magnus, which contains both sympathoexcitatory and sympathoinhibitory neurones [Gao W et al., 2021].

It should also be taken into account that approximately 80% of catecholaminergic celiac ganglion neurons coexpress neuropeptide Y (NPY), and in the postganglionic sympathetic nerve fibers norepinephrine are colocalized with NPY [Romano TA et al., 1991; Kaestner CL et al., 2019].

NPY is one of the most abundantly expressed neuropeptides in the central and peripheral nervous systems and a key mediator in the responses to both acute and chronic stress. NPY occurs in the nucleus of the solitary tract and ventrolateral medulla, periaqueductal grey and locus coeruleus, hypothalamus (arcuate nucleus, paraventricular nucleus and other regions), septum, hippocampus, amygdala, basal ganglia, nucleus accumbens and cerebral cortex. Many experimental stressors induce NPY release and upregulate both NPY mRNA and its receptors' mRNA (Y_1, Y_2 and Y_5), which are responsible for the physiological actions of NPY in the periphery and brain. Acute stress upregulates NPY in the hypothalamic arcuate and paraventricular nuclei, where metabolic and stress-related signals are integrated and appropriate neuroendocrine and visceral responses are initiated. In the paraventricular nuclei, NPY activates the HPA axis and modulates the visceral stress responses mediated through corticotrophin-releasing hormone pathways [Forbes s et al., 2012; Holzer P et al., 2012].

NPY is involved in the emotional processing of stress. The amygdala, which is a key brain region coordinating behavioural stress responses, contains high levels of NPY and Y_1, Y_2, Y_4 and Y_5 receptors. Acute restraint

stress decreases NPY expression in the amygdala. Y_1 receptor expression in the amygdala is increased by acute restraint stress. NPY is not only a stress mediator in the central nervous system but also in the periphery. The stress-related implications of NPY impact on many physiological systems including the cardiovascular system, the gastrointestinal tract, the immune system, metabolism, and adaptation to stress [Forbes s et al., 2012; Holzer P et al., 2012].

It is appropriate to recall that the development of behaviorally induced (stressed by mild foot shock) acute gastric lesions in rats was studied by Kristt DA & Freimark SJ [1973]. Gastric lesions fell into two histologic classes: an acute ulcerative-hemorrhagic process with several different manifestations and a focal clear cell metaplasia of the gastric pit epithelium. The following explanation was tentatively offered to account for these findings: stress induces constriction of the blood vessels of the muscularis mucosa and results in focal mucosal infarction; the gastric pit metaplasia may reflect a response to a stress-induced impairment of the protective mucous coat.

Much later it was shown that that the sympathetic constriction of splanchnic resistance vessels is co-mediated by the sympathetic triad adenosine triphosphate (ATP), noradrenaline and NPY. In addition, NPY is able to potentiate the constrictor effect of noradrenaline and ATP. Both the vasoconstrictor response to NPY and its action to augment noradrenaline- and ATP-induced mesenteric vasoconstriction are mediated by post junctional Y_1 receptors [Holzer P et al., 2012].

At the same time, stress reduces vagal tone, which is accompanied by complete inhibition of gastric juice secretion. After the termination of the stressor, the vagal tone and gastric secretion are restored to the initial level, without exceeding it [Desiderato O & Testa M, 1976]. But even this is enough to damage the mucous membrane with gastric juice, which has lost its resistance to it due to ischemia. It is generally agreed that luminal acid and pepsin are required for ulceration to develop. Experimental evidence suggests that backdiffusion of acid is closely related to the formation of ulcers. In the absence of overt disruption of the gastric mucosal barrier, ischaemia appears to compromise the ability of the gastric mucosa to dispose of backdiffusing acid, which then results in a decrease in intramural pH and ulceration [Marrone GC & Silen W, 1984]. This idea was explained by the fact that the development of stress ulcers can be averted both by adrenolytics, which block adrenergic spasm of arterioles, and by cholinolytics, which block the post-stressor recovery of gastric secretion [Meerson FZ, 1981].

Incidentally, let us recall that in our rats, damage to the gastric mucosa was caused by an increase in sympathetic tone and, to a lesser extent, the level of circulating catecholamines, which is evidenced by a positive correlation between these parameters and is consistent with the cited authors. However, the negative correlation of the vagal tone with parameters of damage to the gastric mucosa indicates, contrary to the cited authors, its gastroprotective, but not gastroaltering effect under these conditions. However, this conclusion is consistent with the data of another group of authors.

Earlier experimental studies indicated that the integrity of vagal pathway was required to confer gastric protection against damaging agents. Several peptides located in the brainstem initially identified to influence vagal outflow to the stomach, as assessed by electrophysiological approach or by vagal dependent alterations of gastric secretory and motor function, were investigated for their influence in the vagal regulation of the resistance of the gastric mucosa to injury. Thyrotropin releasing hormone (TRH), or its stable TRH analog, RX-77368, injected at low doses into the cisterna magna or the dorsal motor nucleus (DMN) was the first peptide reported to protect the gastric mucosa against ethanol injury through stimulation of vagal cholinergic pathways, inducing the release of gastric prostaglandins/ nitric oxide (NO) and the recruitment of efferent function of capsaicin sensitive afferent fibers containing CGRP. Activation of endogenous TRH-TRH1 receptor signaling located in the brainstem plays a role in adaptive gastric protection against damaging agents. Since then, an expanding number of peptides, namely peptide YY, CGRP, adrenomedullin, amylin, glugacon-like peptide, opioid peptides acting on μ, δ1 or δ2 receptors, nocicpetin, nocistatin, ghrelin, leptin and TLQP-21, a peptide derived from VGF prohormone, have been reported to act in the brainstem to afford gastric protection against ethanol injury largely through similar peripheral effectors mechanisms than TRH. Therefore, gastric prostaglandins and CGRP/NO pathways represent a common final mechanism through which brain peptides confer vagally mediated gastroprotection against injury [Pescar BM, 2001; Taché Y, 2012].

Previous studies [review: Zhao DQ et al., 2020] have demonstrated that NO can inhibit gastric acid secretion and neutrophil adhesion, improve gastric mucosal blood circulation and eliminate oxygen free radicals, thereby protecting the gastric mucosa from injury. It was reported that the expression level of iNOS increased significantly in the gastric mucosa of RWIS rats, while that of eNOS reduced significantly, indicating that

the changes in iNOS and eNOS activities in the gastric mucosa are closely related to the incidence of gastric mucosal lesion (GML). NOS inhibitor can decrease the production of NO, thus exacerbating acute GML and inhibiting the healing process of chronic gastric ulcers, while NO precursor can obviously prevent the injury. It was showed that NO is involved in RWIS, and can promote the GML healing process. The mechanisms of NO in protecting gastric mucosa are as follows: (1) NO can reduce vascular permeability, inhibit platelet adhesion and aggregation in gastric mucosal vascular endothelium, and prevent thrombosis. (2) Under physiological conditions, gastric mucosal vascular endothelium synthesizes NO, which in turn regulates vascular smooth muscle tension and maintains gastric mucosa blood flow (GMBF). (3) In acute GML, NO increases GMBF by dilating the mucosal blood vessels, thus promoting gastric mucosal repair. In addition, the secretion of gastric acid can also be inhibited by NO. Upon the reaction of stimulus against gastric mucosa, enterochromaffin cells and mastocytes can release histamine to stimulate parietal cells for gastric acid production, thus aggravating the mucosal lesion. In addition, endogenous NO can inhibit the stimulation of histamine through parietal cells, thus reducing gastric acid secretion and protecting gastric mucosa. It has been found that, through *in vivo* and *in vitro* experiments, the NO donor FK409 and sodium nitroprusside can markedly suppress the gastrin-induced increase in histamine release and gastric acid secretion in rats, and NOS inhibitor further increases gastric acid secretion. Gastric mucous cells promote NO synthesis by expressing high-level NOS, and enhance the mucous barrier through the NO effects of promoting mucin synthesis and secretion. Based on the findings of previous experiments, RWIS-induced GMLs can weaken the synthesis and secretion of gastric mucus by reducing nNOS activity, while the NO donor can increase nNOS activity and mucus secretion.

More recently, on the example of nerve terminal innervating cerebral arteries at the base of the brain, has been shown that NO, which is not stored in vesicles, is colocalized and co-released with ACh, which is stored in the vesicles. NO is synthesized from L-arginine in the presence of NOS. The neuronal NO plays a major role in cerebral neurogenic vasodilation, which is mediated by activation of guanylate cyclase and cGMP synthesis in the smooth muscle cell. Electrical stimulation of a central cholinergic system originating in the nucleus basalis of Meynert and substantia innominata has been shown to contribute to the cortical vasodilator response via activation of muscarinic cholinergic receptors,

although nicotinic cholinergic receptors have been shown to consistently mediate vasodilator response in both cortical circulation and large arteries at the base of the brain. NE released from the sympathetic nerve, acting on presynaptic β_2-adrenoceptors located on the neighbouring parasympathetic nitrergic nerves, however, facilitates NO release with enhanced vasodilation. This axo-axonal interaction mediating NE transmission is supported by close apposition between sympathetic and parasympathetic nerve terminals, and has been shown in vivo at the base of the brain and the cortical cerebral circulation. This result reveals the physiological need for increased regional cerebral blood flow in 'fight-or-flight response' during acute stress. Furthermore, nicotinic ACh receptors on sympathetic nerve terminals mediate release of NE, leading to cerebral nitrergic vasodilation [Lee TJ et al., 2001; Lee TJ et al., 2011].

If we assume that similar processes take place with the participation of vagal efferents and blood vessels of the gastric mucosa, which is quite likely, then the gastroprotective effect of vagal innervation can be associated with the recruitment of gastric prostaglandins-CGRP-NO mechanisms.

Zhao DQ et al. [2020] give arguments, that the role of the vagal nerve is likely to be dual, as it can mediate both mucosal damaging and protective effects. RWIS-induced gastric dysfunction is mainly caused by the enhanced parasympathetic activity. In other words, there is a neural circuit ("medullary gastrointestinal center-gastrointestinal wall plexus loop") between the medulla oblongata and the gastrointestinal tract. Under RWIS, the information of gastrointestinal motility is transmitted as follows: Information → vagal afferent nerves → NTS → DMV/NA, while those of medullary efferents are disseminated as follows: DMV/NA → vagal efferent nerves → gastrointestinal wall plexuses, thereby causing gastric hyperkinesia, increasing gastric acid secretion and reducing gastric mucus secretion, and ultimately leads to GML and fecal impaction. However, in the case of electrical stimulation of NTS in normal rats, gastric motility may be inhibited, and a possible reason for this is that excitement of the NTS activates inhibitory neurons in the DMV, thus suppressing gastric motility through a non-cholinergic neural pathway. In addition, gastric motility was significantly inhibited when electrical or chemical stimulation induced neuronal excitation in the NA and DMV, indicating that excitation of the NA and DMV also exerts an inhibitory effect on gastric motility. This is probably due to the fact that the activity of the higher center (*e.g.*,

anterior hypothalamus) eliminates the inhibition of medullary visceral centers on the stomach during RWIS, thereby causing gastric hyperkinesia and increasing gastric acid secretion.

Despite the fact that the hypothalamic-pituitary-adrenocortical (HPA) axis is the cornerstone of the general adaptation syndrome and the famous triad [Selye H, 1936; Szabo S et al., 2017], the role of its hormones in the pathogenesis of stress injuries of the gastric mucosa and myocardium is still a matter of debate.

There are two opposite points of view regarding the influence of stress-induced activation of HPA system on the stomach. According to the widely held view, glucocorticoids released during stress are ulcerogenic hormones and, therefore, stress-induced activation of HPA system is harmful. Some studies have found that RWIS leads to the elevation of blood corticosterone and adrenocorticotropic hormone levels in rats, and their levels in plasma also gradually rise over a prolonged period of stress. This seems to indicate that the activity of the HPA axis is enhanced during RWIS. However, removing the pituitary glands and adrenal glands or administering phenoxybenzamine (adrenergic α-receptor blocker) has little impact on RWIS-induced GML, gastric hyperkinesia and RWIS-induced gastric acid secretion, but severing the subphrenic vagus nerves or consuming atropine can significantly alleviate and even cure RWIS-induced GML. This suggests that the HPA axis does not play a major role in RWIS-induced GML, and the peripheral nervous mechanism of RWIS-induced GML is mainly through the enhanced parasympathetic activity. Therefore, according to Zhao DQ et al. [2020], the nervous mechanism of RWIS-induced gastrointestinal dysfunction in rats is mainly the "enhanced activity of parasympathetic nervous system", rather than the traditional ideas of the "enhanced activity of sympathetic-adrenal medulla system" and "HPA axis".

Zhao DQ et al. [2020] have summarized the regulatory pathways of gastrointestinal function under normal physiological conditions, and the major nuclei involved. Several hypotheses have been put forward, and a preliminary consensus has been reached by scholars on the peripheral and central nervous mechanisms of RWIS-induced gastrointestinal dysfunction. It was shown that the sensory information from the gastrointestinal tract and other internal organs are transmitted to the NTS through visceral sensory fibers in the vagus nerve, integrated by NTS secondary neurons in the brain stem, and then conveyed to relevant nuclei, such as the DMV, *via*

neurotransmitters (*e.g.*, Glu). DMV regulates the gastric motility through parasympathetic nerves, and parasympathetic neurons control the gastric function *via* two different pathways. (1) The M receptor is activated to enhance gastric motility and secretion *via* the cholinergic excitatory pathway. And (2) Gastric function is inhibited mainly by releasing NO or vasopressin (VP) *via* activating the NANC pathway (Fig. 2.8).

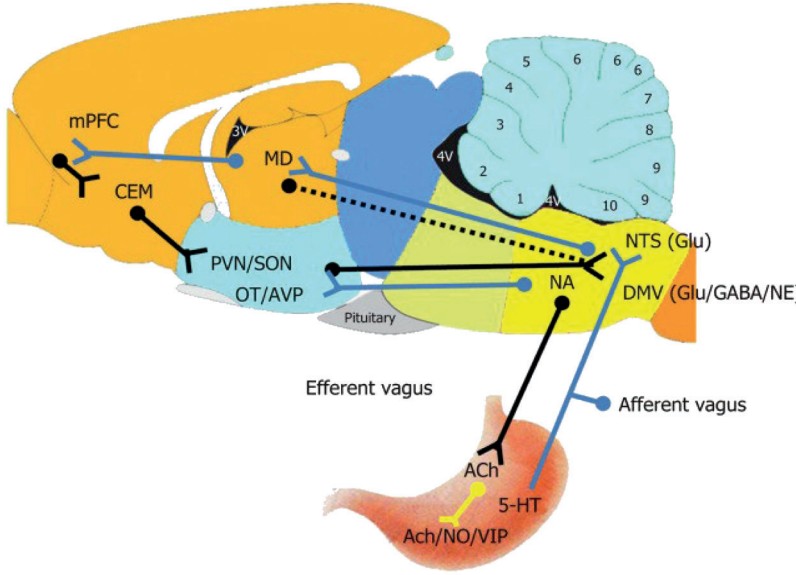

Fig. 2.8. Schematic diagram of the central nervous pathways of restraint water-immersion stress-regulated gastrointestinal function.
Solid line: The pathways that have been determined; Dashed line: The pathways that remain to be further verified; Blue line segment: Upward; Green line segment: Downward. mPFC: Medial prefrontal cortex; CEA: Central nucleus of the amygdala; MD: Mediodorsal nucleus of the thalamus; DMV: Dorsal motor nucleus of vagus; NA: Nucleus ambiguous; NTS: Nucleus of the solitary tract; VIP: Vasoactive intestinal peptide; 5-HT: 5-hydroxytryptamine; NO: Nitric oxide; ACh: Acetylcholine; NE: Norepinephrine; GABA: γ-aminiobutyric acid; Glu: Glutamate; PVN: Paraventricular nucleus; SON: Supraoptic nucleus; OT: Oxytocin; AVP: Arginine vasopressin [Zhao DQ et al., 2020].

With regard to the advanced central nervous mechanism of RWIS-induced gastrointestinal dysfunction, the potential advanced central nervous regulatory pathway of gastrointestinal function in rats under

RWIS is hypothesized based on the previous works. The MD receives the advanced neural activity information from the PFC (possibly IL) *via* the cortical-thalamic pathway, integrates such information with that from subcortical structures (*e.g*., the hypothalamus and medulla oblongata), and then feeds the integrated information back to the PFC *via* the thalamic-cortical pathway. At the same time, there is a two-way fiber connection between the IL and CEA, and the final integrated information from the PFC is directly or indirectly fed back to the medullary gastrointestinal center through the CEA, thereby inducing gastric dysfunction.

However, we cannot unconditionally agree with this in view of the concept of vagally mediated gastroprotection against injury [Pescar BM, 2001; Taché Y, 2012] and our own data in this regard.

In our study, we found only a minimal factor load on the neuro-endocrine canonical root from the side of corticosterone, which also indicates the insignificance of its causal influence on post-stress damage to the gastric mucosa and myocardium. This is only partially consistent with the old data of the Berger's laboratory [Berger EN, 1980] that the introduction of hydrocortisone (2 mg/200g) for 2 days before immobilization-cold stress increases the number of ulcers from 3.6±0.5 to 7.7±1.9, and the data of one of the latest studies [Kim MH et al., 2022] that phytoadaptogen (Banhasasim-tang) positively ameliorated in rats cold restraint stress-induced gastric hemorrhage with decrease in serum stress-related biomarkers such as ACTH and corticosterone (as well as epinephrine and dopamine). However, this is perfectly consistent with the dual role of corticosterone, similar to n. vagus, as both a gastroaltering [Selye H, 1936; Berger EN, 1980; Meerson FZ, 1981; Zavodskaya IS & Moreva YeV, 1981; Popovych IL, 2007; Fil V et al., 2021; Kim MH et al., 2022] and a gastroprotective [Zavodskaya IS & Moreva YeV, 1981; Filaretova LP et al., 1998; Filaretova LP, 2006; Filaretova LP et al., 2008; Filaretova LP & Makara G, 2014; Filaretova LP et al., 2014; Filaretova LP et al., 2021] factor.

It is interesting that the initiator and apologist of the last concept are two laboratories located in St. Petersburg. The results of their investigations are opposite to traditional view. Back in 1981, in the laboratory of Zavodskaya, it was shown that adrenalectomy worsens damage to the gastric mucosa of rats caused by electrocoagulation of the anterior or posterior hypothalamus. Thus, among 15 control rats, destructive damage to the gastric mucosa developed in 8, an average of 1.7 per animal, whereas among 15 previously (20-30 days) adrenalectomized

rats, 13 developed, an average of 3.0 per animal. Starting from 1998 in the laboratory of Filaretova, research in this direction was continued at a higher methodological level. To estimate the action of glucocorticoids released during stress on the gastric mucosa, the effects of glucocorticoid deficiency or occupation of glucocorticoid receptors by the antagonist RU-38486 on the formation of stress-induced gastric erosions were estimated. The reduction of stress-induced corticosterone release (induced by various experimental approaches) markedly potentiated a gastric erosion formation caused by stress and acute corticosterone replacement, mimicking stress-induced corticosterone response, prevented this erosion-potentiating effect. The administration of RU-38486 also caused a significant increase of vulnerability of gastric mucosa to stress action. Corticosterone replacement which mimics the corticosterone rise significantly reduced erosion areas of gastric mucosa in adrenalectomized rats. Thus, an acute stress-induced increase of glucocorticoids has a gastroprotective action against stress-induced gastric injury. Authors also showed that various ulcerogenic stimuli, similar to stress, induce an increase in glucocorticoid production that in turn helps the gastric mucosa to resist against a harmful action of ulcerogenic stimuli. Gastroprotective action of glucocorticoids may be mediated by multiple actions, including maintenance of glucose homeostasis, gastric mucosal blood flow, mucus production and attenuation of enhanced gastric motility and microvascular permeability. For maintenance of gastric mucosal integrity glucocorticoids may cooperate with prostaglandins. Furthermore, glucocorticoids exert a compensatory gastroprotective role in the case of impaired gastroprotective mechanisms provided by PGs, NO, and capsaicin-sensitive sensory neurons. The authors still admit that after single administration of glucocorticoids, there can arise gastroprotective and ulcerogenic effects. The initial gastroprotective effect that glucocorticoid hormones have, even after their single administration can be transformed into an ulcerogenic effect with a prolongation of the hormonal action, but not of the hormone dose.

Since Selye H [1953], mineralocorticoids have been considered glucocorticoid antagonists. In the laboratory of Berger EN [1980], administration of deoxycorticosterone acetate (DOCA, 1 mg/200g) for 4 days before immobilization-cold stress, as opposed to hydrocortisone, reduced the number of ulcers from 3.6±0.5 to 1.6±0.8. This is consistent with the data obtained in the same period, that aldosterone exhibited antiulcer actions in fasted rats stressed by the forced exertion technique,

but only when multiple subcutaneous injections were made. The antiulcer actions of aldosterone (and DOCA) were not mediated via an inhibitory effect on gastric secretion [Dajani EZ et al., 1979; Clavenna G et al., 1982]. Interestingly, the main object of these studies was carbenoxolone – a semisynthetic succinyl ester of glycyrrhizinic acid (licorice root substance) which has been used as an effective treatment for peptic ulceration since the 1960s [Sabbadin C et al., 2019]. Carbenoxolone given subcutaneously did not inhibit ulcer formation while intragastric administration of carbenoxolone significantly inhibited it [Dajani EZ et al., 1979]. Authors concluded that the beneficial antiulcerogenic action of carbenoxolone is due to a direct effect on gastric mucosa and is not related to an aldosterone-like component. Koo MW et al. [1986] shown that intragastric administration of carbenoxolone, given 30 min before restrain cold stress, exhibited similar actions as verapamil – significantly prevented stress-induced mucus depletion and gastric ulceration.

Stewart PM et al. [1990] have been evaluated the effect of the carbenoxolone on enzyme complex 11-β-hydroxysteroid dehydrogenase that consisting of 11-β-dehydrogenase and 11-oxoreductase responsible for the interconversion of cortisol to cortisone in man. It is known that inhibition of 11-β-dehydrogenase results in cortisol acting as a potent mineralocorticoid. Authors shown that carbenoxolone given to six volunteers in metabolic balance produced sodium retention with suppression of the renin-angiotensin-aldosterone system. Plasma potassium fell, although there was no kaliuresis. This was associated with inhibition of 11-β-dehydrogenase (as measured by a rise in the plasma half-life of [11-α-^{3}H]cortisol). Thus, the mineralocorticoid activity of carbenoxolone is mediated via cortisol by inhibition of 11-β-dehydrogenase. Carbenoxolone, however, also inhibited 11-oxoreductase activity (as measured by the generation of cortisol after oral cortisone acetate), and this may relate to its effect on renal potassium excretion.

Paradoxically, that medical use of carbenoxolone is limited just by side effects of a mineralcorticoid aldosterone-like property with hypokalemia, weight gain, hypertension, and retention of sodium, chloride, and water [Kawashima D et al., 2009].

Suleyman H et al. [2007] showed that nimesulide, a non-steroidal, anti-inflammatory drug, is gastro-protective in intact rats, but produces ulcerogenic effects in adrenalectomized rats. The objective of their study was to determine whether adrenal gland hormones are involved in the anti-ulcer

effects of nimesulide. The results revealed that nimesulide produces gastric ulceration in adrenalectomized rats, which is prevented by prednisolone and adrenaline, while DOCA did not cause any gastroprotective effect: the mean ulcer area was 17.2 mm^2 in the DOCA-treated nimesulide group and 18.0 mm^2 in control.

However, in our study, contrary to the cited ones, aldosterone was neither a gastroprotective nor a neutral factor, but on the contrary, judging by the factor load on the neuro-endocrine root, it exerted an ulcerogenic effect, even somewhat stronger than corticosterone. At the same time, the mass of the adrenal glands gave more factor load than each of their hormones separately. It would be tempting to explain this by an additional effect of medulla catecholamines.

Our conclusion about the ulcerogenic effect of aldosterone is supported by data of Pawlik MW et al. [2016] that the inhibition of angiotensin-converting enzyme or the blockade of angiotensin AT-1 receptors, that is, eliminating the effect of aldosterone, affords protection against acute gastric mucosal injury in rats.

Despite the expectations based on the classical position of Selye H [1976], that the administration of both glucocorticoids and mineralocorticoids to animals increases the cardiotoxic effect of catecholamines, in our study no correlation was found between the serum content of these hormones and ECG-markers of myocardial damage. We explain this situation by the peculiarities of the timing of post-stress corticosteronemia, beautifully illustrated by Meerson FZ [1981; 1984]. It was found that an hour after the start of a 6-hour emotional and painful stress, the level of corticosteroneemia exceeded the initial level by 280%, immediately after its end – by 250%, after another 2 hours – by 225%, and the next day (30 hours after the onset of stress) – by only 30%, which practically coincides with our data (+15%) and gives reason to assume that the dynamics of corticosteronemia were approximately the same during and after 4-hour WRIS in our experiment. And so, corticosterone (as well as aldosterone) is still involved in stress damage to the myocardium, as it has been shown in relation to the gastric mucosa.

Interestingly, 42 hours after the onset of emotional and painful stress, the level of corticosteronemia rose again to 180% of the initial level [Meerson FZ, 1981; 1984]. And in the experiments of the Berger's laboratory, the ECG was recorded exactly on the 2nd-3rd day after the injection of adrenaline (1.5 mg/kg). It was found that the previous (2 hours) administration of both hydrocortisone (2.5 mg/kg) and DOCA (2.5 mg/kg) did not significantly

affect ECG markers of myocardial dystrophy (1.4±0.14 and 1.5±0.14 respectively vs 1.3±0.10). This is consistent with our data on the lack of correlation of post-stress levels of both corticosterone and aldosterone with ECG markers of myocardiodystrophy. At the same time, it should be noted that a 5-fold increase in the dose of corticosteroids when administered for 2 days still significantly aggravated adrenaline myocardiodystrophy (ECG change index 1.7±0.14 for both corticosteroids). One of the mechanisms of such an aggravating effect should be considered a decrease in the content of acetylcholine in the heart by 30-33% [Berger EN, 1980].

Testosterone, judging by the results of the correlation analysis (Table 2.11), turned out to be a weak gastroprotective factor, as well as calcitonin, with which it is positively related, in contrast to negative relationships with gastroaltering factors such as PTH, aldosterone and corticosterone, but not catecholamines (Table 2.13).

Our conclusion contradicts the data of Zavodskaya IS & Moreva Ye V [1981] about twice the number of destructive damage to the gastric mucosa caused by electrical stimulation of the paws of immobilized rats in males (6±2 vs 3±1), whose testosterone level is an order of magnitude higher than in females. Castration of animals 12-19 days before stressor exposure did not cause destruction by itself, but increased their number in males to 13±4, and in females to 9±4, that is, it also minimized sexual dimorphism in the resistance of the gastric mucosa to stressors. However, administration of testosterone propionate to uncastrated males and diethylstilbestrol propionate to females also resulted in aggravation of gastric stress injuries. The introduction of chorionic gonadotropin, which stimulates the release of one's own sex hormones, also increased the number of post-stress destructions in uncastrated males and females. The researchers came to the conclusion that both depriving the body of sex hormones and saturating it with synthetic analogues lead to a decrease in the resistance of the gastric mucosa to the pathogenic influence of stressors.

We were not lucky enough to find more publications on the influence of testosterone on the development of stress-induced damage to the gastric mucosa, so we are forced to limit ourselves to the discussion of other models with the caveat that their pathogenesis is different from the stressor to one degree or another.

Rao SS & Saifi AQ [1987] in pylorus ligated male rats discovered that testosterone and cimetidine when used alone protected from ulceration while when used in combination the degree of protection was decreased.

Castration per se had no effect on ulcer index but potentiated cimetidine induced gastric ulcer protection.

László F et al. [1997] found that macroscopic mucosal damage and microvascular serum albumin leakage developed in the stomach of male rats 24 h after the administration of cysteamine. This mucosal injury was prevented by orchidectomy and by the pretreatment with the antiandrogen cyproterone. It was also shown that pretreatment with testosterone dose-dependently aggravated cysteamine-induced mucosal injury.

While Loginov AS et al. [1995] concluded that in gastric ulcer patients there were low concentrations of testosterone, hydrocortisone, estradiol, and progesterone.

Despite the fact that female sex hormones were not determined in our study, it is very appropriate to discuss their participation in the pathogenesis of gastric ulcer.

The female sex hormones (progesterone, estrogen and a combination of both) were found to have significant antiulcer activity in almost all the models (stress-, drug-, pylorus ligation induced). However, they did not affect the acidity or volume of gastric secretion in Shay's pyloric ligation model. As a results their antiulcer activity could not be explained by the effects on gastric acidity but by effects on other factors which may include enhanced mucus activity, or increase in parietal cells activity and maintenance of mucus integrity [Aguwa CN, 1984].

A more detailed study was conducted by Kurt D et al. [2007] To investigate the protective effects of estrogen and progesterone administrations on gastric mucosal barrier of rats applied ovariectomy, cold and immobility stress. It is shown that the levels of mucus and phospholipids were decreased in the rats applied ovariectomy and stress as compared to the control groups ($p<0.001$). The increase determined the mucus and phospholipids levels in estrogen and progesterone administered rats as compared to stress applied group ($p<0.001$). While the cold and immobility stress causes important damages in gastric mucosa, estrogen and progesterone administrations has protective effects in ovariectomized rats. Authors concluded that the estrogen and progesterone administration prevents the stress that caused decrease in the levels of mucus and phospholipids, thus females are more resistant to gastric ulcer rather than males due to their sex hormones. We were able to find only one study regarding the effect of testosterone on myocardial stress injury. Ribeiro Junior RF et al. [2018] showed that papillary muscle

contractility was preserved in the orchidectomized rats after myocardial infarction and was reduced when testosterone was replaced. Their results support the view that testosterone deficiency prevents myocardial infarction contractility dysfunction.

If the male is evaluated with a conditional one point, and the female with two, then it is possible to operate with the sex index, which was found in the factor structure of the neuro-endocrine canonical root. The sex index is most negatively correlated with the serum level of testosterone (r=-0.89), significantly stronger with calcitonin (r=-0.63) and on the verge of significance with sympathetic tone (r=-0.31). Instead, the sex index is positively correlated with the mass of the adrenal glands (r=0.80) and serum levels of corticoids such as aldosterone (r=0.63) and corticosterone (r=0.47), as well as PTH (r=0.61). This is explained by significantly higher levels of PTH (in our sample by 20%), corticosterone (by 37%) and, to a lesser extent, aldosterone (by 9%) in females than in males, as well as undoubtedly not recorded in this study estradiol and progesterone, instead drastically lower levels of testosterone and, to a lesser extent, calcitonin (by 40%) and sympathetic tone (by 20%).

The sex index determines the levels of registered neuro-endocrine parameters by 88% (Fig. 2.9).

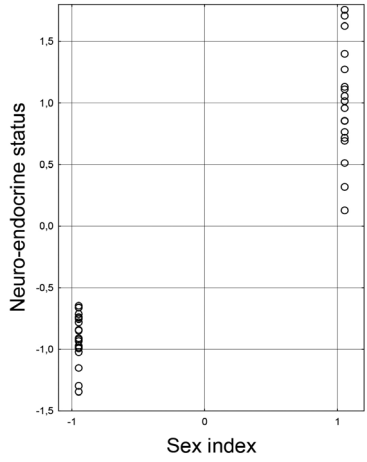

R=0.938; R^2=0.880; $\chi^2_{(7)}$=71; p<10^{-6}; Λ Prime=0.111

Fig. 2.9. Scatterplot of canonical correlation between Sex index (X-line) and neuro-endocrine parameters (Y-line) at intact and stressed rats

At the same time, the role of other sex-linked neuro-endocrine factors (gonadotropic hormones and their releasing factors, etc.) and, in particular, the recently discovered sexual dimorphism of a number of EEG parameters in humans is quite likely [Elsenbruch S & Enck P, 2017; Kozyavkina NV et al., 2021].

2.3. Metabolic and immune accompaniments of electrocardiographic and morphologic gastric mucosa parameters of damage in naïve and stressed rats

Summary

Introduction and aim. Earlier, by applying the water-immersion and restraint stress (WIRS) model, we found that the severity of the gastric mucosa damage significantly correlates with changes in ECG parameters, which indicate myocardial dystrophy. Further, it was found that such a connection is caused by the damaging effect on both targets of increasing the level of parathyroid hormone, as well as the production of aldosterone and catecholamines by enlarged adrenal glands. In addition, an increase in the level of corticosterone and sympathetic tone with a simultaneous decrease in vagal tone as well as serum calcitonin and testosterone cause damage only to the gastric mucosa, but not to the myocardium. Such a constellation of neuro-endocrine reactions to stressors determines the severity of damage to the gastric mucosa and myocardium by 73%. The purpose of this study is to find out metabolic and immune accompaniments of ECG and damage to gastric mucosa parameters.

Material and methods. The experiment is at 18 male and 20 female rats Wistar line. Over the 10 days, one animal remained intact and 3 other rats were exposed to WIRS. The next day after stressing, immune and metabolic parameters as well as ECG and gastric mucosa injuries was recorded.

Results. Serum levels of Phosphates, Catalase and α-LP Cholesterol as well as erythrocyte level of Potassium (as marker of Kalihistia) and Na,K-ATPase activity of the shadows of erythrocytes (as marker of membranes of myocardiocytes) are positively correlated with ECG markers of myocardial damage such as T wave amplitude and ST junction, and negatively correlated with visual markers of damage to the gastric

mucosa, i.e. reflect intactness (normality) of both targets of stressors – myocardium and gastric mucosa. Erythrocyte level of Sodium and serum levels of Potassium and Alkaline Phosphatase reflect the intactness of the gastric mucosa only. While serum level of Calcium reflects damage to the gastric mucosa. Taken together, the listed metabolic factors determine the morpho-functional state of the gastric mucosa and myocardium by 72% (R=0.851). Damage to the gastric mucosa and myocardium is more severe, the lower the bactericidal activity of blood neutrophils, and the greater the mass of the thymus. The spleen mass and the content of fibroblasts in the thymus are negatively correlated only with the severity of damage to the gastric mucosa, while the percentages of reticulocytes and lymphoblasts in the spleen are positively correlated with it. Finally, the higher the percentage of macrophages in the thymus, the deeper the damage to the myocardium. The canonical correlation between the listed immune parameters and markers of the two targets of stressors is very strong (R=0.809).

Conclusion. Water-immersion and restraint stress causes changes in the neuro-endocrine-immune complex, which lead to changes in the metabolome and damage to the gastric mucosa and myocardium.

Introduction

Earlier, by applying the water-immersion and restraint stress (WIRS) model, we found that the severity of the gastric mucosa damage significantly correlates with changes in ECG parameters, in particular, depression of the T wave and S-T joint, which indicate myocardial dystrophy. Further, it was found that such a connection is caused by the damaging effect on both targets of increasing the level of parathyroid hormone, as well as the production of aldosterone and catecholamines by enlarged adrenal glands. In addition, an increase in the level of corticosterone and sympathetic tone with a simultaneous decrease in vagal tone as well as serum calcitonin and testosterone cause damage only to the gastric mucosa, but not to the myocardium. Such a constellation of neuro-endocrine reactions to stressors determines the severity of damage to the gastric mucosa and myocardium by 73%.

As Dhabhar FS [1997; 2009; 2018] aptly pointed out, stress is known to suppress immune function and increase susceptibility to infections and cancer. Paradoxically, stress is also known to exacerbate asthma,

and allergic, autoimmune and inflammatory diseases, although such diseases should be ameliorated by immunosuppression. Moreover, the short-term fight-or-flight stress response is one of nature's fundamental defense mechanisms that enables the cardiovascular and musculoskeletal systems to promote survival, and it is unlikely that this response would suppress immune function at a time when it is most required for survival (e.g. in response to wounding and infection by a predator or aggressor). These observations suggest that stress may suppress immune function under some conditions while enhancing it under others. Author propose that it is important to study and, if possible, to clinically harness the immunoenhancing effects of the acute stress response, that evolution has finely sculpted as a survival mechanism, just as authors study its maladaptive ramifications (chronic stress) that evolution has yet to resolve. In view of the ubiquitous nature of stress and its significant effects on immunoprotection as well as immunopathology, it is important to further elucidate the mechanisms mediating stress-immune interactions and to meaningfully translate findings from bench to bedside.

It is well known that the immune system closely interacts with the nervous and endocrine systems through common mediators and receptors [Nance DM & Sanders VM, 2007; Kozyavkina OV, 2009; Thayer JF & Sternberg EM, 2010; Tracey Kj, 2010; Pavlov VA et al., 2018; Kulchynskyi AB et al., 2017; Kulchynskyi AB et al., 2017a; Popovych IL et al., 2017; Popovych IL et al., 2018; Melnyk OI et al., 2021] creating a triune neuro-endocrine-immune complex [Besedovsky H & Sorkin E, 1977; Besedovsky H & del Rey A, 1996; Popovych IL, 2011; Kozyavkina OV et al., 2015; Popovych IL et al., 2020; Popovych IL et al., 2022]. It is also known that stress effectors affect metabolism, and metabolites, in particular nitrogenous and electrolytes, in turn affect neurons, endocrinocytes, and immunocytes [Gozhenko AI et al., 2023, Korda MM et al., 2024]. Based on the above, we set ourselves a goal: to find out metabolic and immune accompaniments of electrocardiogram and gastric mucosa damage parameters at naïve and post stressed rats.

Material and methods are detailed in the previous subsection.

Results and discussion

As a result of the analysis of the metabolic accompaniment of post-stress injuries, the following was found (Table 2.14).

Table 2.14. Correlation Matrix for Neuro-endocrine and post stress Damage variables

Variables	**GU amount**	**GU length**	**GM damage**	**T wave**	**ST joint**
Phosphates of Serum	**-0.766**	**-0.759**	**-0.728**	**0.595**	**0.439**
Catalase of Serum	-0.245	*ns*	-0.313	0.285	*ns*
K of Erythrocytes	-0.324	-0.224	-0.260	**0.415**	0.280
α-LP Cholesterol	*ns*	-0.274	-0.283	*ns*	0.287
Na of Erythrocytes	**-0.342**	**-0.440**	**-0.450**	*ns*	*ns*
Na,K-ATPase of Erythr	*ns*	*ns*	*ns*	0.310	0.241
Alkaline Phosphatase	-0.306	**-0.412**	**-0.405**	*ns*	*ns*
K of Serum	*ns*	-0.276	-0.310	*ns*	*ns*
Ca of Serum	*ns*	0.300	0.274	*ns*	*ns*

Note. According to the equation: $|r|=\{\exp[2t/(n-1.5)^{0.5}]-1\}/\{\exp[2t/(n-1.5)^{0.5}]+1\}$

for a sample of n=38 critical value |r| at $p<0.05$ ($t>2.02$) is **0.323,** at $p<0.01$ ($t>2.70$) is **0.420,** at $p<0.001$ ($t>3.55$) is **0.528**.

Serum levels of Phosphates, Catalase and α-LP Cholesterol as well as erythrocyte level of Potassium (as marker of Kalihistia) and Na,K-ATPase activity of the shadows of erythrocytes (as marker of membranes of myocardiocytes) are positively correlated with ECG markers of myocardial damage such as T wave amplitude and ST junction, and negatively correlated with visual markers of damage to the gastric mucosa, i.e. reflect intactness (normality) of both targets of stressors – myocardium and gastric mucosa. Erythrocyte level of Sodium (as marker of Natrihistia) and serum levels of Potassium and Alkaline Phosphatase reflect the intactness of the gastric mucosa only. While serum level of Calcium reflects damage to the gastric mucosa. The canonical correlation between the listed metabolic parameters and state markers of the two targets of stressors is very strong (Table 2.15 and Fig. 2.10).

Table 2.15. Factor structure of Metabolic and Gastric mucosa&ECG Roots

Left set	**R**
Phosphates of Serum	**0.918**
Alkaline Phosphatase	**0.411**
Sodium of Erythrocytes	**0.407**
Potassium of Erythrocytes	**0.395**
Catalase of Serum	**0.362**
α-LP Cholesterol	**0.319**
Potassium of Serum	**0.311**
Calcium of Serum	**-0.270**
Na,K-ATPase of Erythrocytes	**-0.037**
Right set	**R**
Gastric Mucosa damage	**-0.961**
Gastric Ulcers amount	**-0.961**
Gastric Ulcers length	**-0.959**
ECG T wave	**0.752**
ECG ST joint	**0.585**

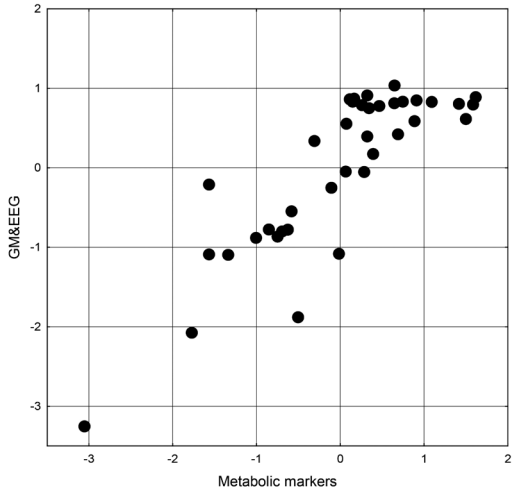

R=0.851; R^2=0.723; $\chi^2_{(45)}$=71; p=0,008; Λ Prime=0,090

Fig. 2.10. Scatterplot of canonical correlation between metabolic markers (X-line) and markers of state of gastric mucosa and myocardium (Y-line) at intact and stressed rats

In order to compare the results obtained by us with data from the literature, we consider it necessary to focus attention on the activity of alkaline phosphatase in view of its closest correlation with indicators of post-stressor damage to the gastric mucosa. Osteoblasts are considered the main source of this enzyme entering the blood; however, leukocytes and, especially, the epithelium of the gastrointestinal tract should not be neglected. The work of Stiel D et al. [1983] is of greatest interest. A day after the subcutaneous administration of cysteamine to rats, the authors noted the development of acute duodenal ulcers, which was accompanied by a significant decrease in the activity of enzymes involved in the secretion of bicarbonates by enterocytes – carbonic anhydrase and HCO3--activated ATPase, as well as – alkaline phosphatase, which, according to the authors, reflects the activity of the latter in the apical membranes of enterocytes. It is significant that the activity of other marker enzymes of neither the apical membrane nor intracellular organelles did not change, i.e., in this experimental ulcer model, there is no organelle pathology, but there is damage to the resistance of the duodenal mucosa, one of the markers of which is alkaline phosphatase, along with hypersecretion of acid by the stomach. Kuehl P et al. [1990] believe that the loss of the activity of this enzyme in human duodenal enterocytes may be an early marker of the development of metaplasia of the gastric mucosa or, at least, a morphological manifestation of epithelial cell damage. Vetvik K et al. [1991] found in patients with active duodenal ulcer an increase in the activity of alkaline phosphatase of the duodenal mucosa as a result of 4-week use of misoprostol – an analog of prostaglandin E1, known as a cytoprotector, compared to normal controls. The same group of authors [Vetvik K et al., 1994] in another study showed that the activity of alkaline phosphatase increases in the duodenal mucosa of the same patients due to the use of omeprazole, an inhibitor of gastric H^+,K^+-ATPase. Mizunashi K et al. [1993] in an in vitro study demonstrated that omeprazole also inhibits osteoresorption, which is known to be mediated by H^+-ATPase of osteoclasts, different from H^+,K^+-ATPase of parietal cells. In the same work, it was shown that omeprazole treatment of patients with gastric ulcer causes an increase in serum alkaline phosphatase activity associated with suppression of osteoresorption.

Therefore, the gastroprotective effect of omeprazole on osteoresorption is similar to that of calcitonin, which also has a gastroprotective ability, revealed in a number of experiments [see above], including ours. However,

according to Ward TL et al. [1993], the increase (under the influence of zeolite-A) of the activity of alkaline phosphatase in the serum of young pigs, associated with a decrease in the concentration of calcium and inorganic phosphorus in it (a marker of an increase in the level of calcitonin), does not protect animals from ulceration of the gastric mucosa.

Catalase showed both gastroprotective and cardioprotective effects. In the course of our project, the data on the antioxidant activity of adaptogens [Panossian A et al., 2021] are of particular interest. In particular, the efficacy of Kangfuxin liquid in WIRS-induced gastric ulcer at rats in the form of reduce the area of ulcers accompanied by improvement the pathological changes of ulcerated tissue: catalase (39%) as well as superoxide dismutase (58%) and malondialdehyde (54%) [Lu S et al., 2019].

The metabolome, in turn, is determined by the constellation of neuro-endocrine effectors of stress (Table 2.16). In particular, enzymes as markers of cytolysis, α-LP Cholesterol, Potassium of serum and Sodium of erythrocytes are upregulated by Testosterone and Calcitonin while are downregulated by Corticosterone, Aldosterone, PTH and, probably, judging by the negative correlation with the Sex index, female sex hormones such as Progesterone and Estradiol.

Superoxide dismutase, Diene conjugates, Calcium and Sodium of serum as well as Potassium of erythrocytes and Na,K-ATPase of the shadows of erythrocytes are downregulated by Testosterone, Calcitonin, Catecholamines and Sympathetic tone while are upregulated by Corticosterone, Aldosterone, PTH, Vagal tone and, probably, female sex hormones. Catalase and Malondialdehyde are downregulated by Corticosterone and PTH while upregulated by Calcitonin and Vagal tone. Phosphates are downregulated by PTH and Calcitonin.

Table 2.16. Correlation Matrix for Neuro-Endocrine and Metabolic variables

Variables	**Testo-ste-rone**	**Sex Index**	**Corti-coster**	**Aldos-terone**	**Adre-nal mas**	**PTH**	**Calci-tonin**	**1/ Mode**	**AMo**	**MxD Mn**
1	2	3	4	5	6	7	8	9	10	11
Alkaline Phosphatase	**0.788**	**-0.834**	**-0.512**	**-0.498**	**-0.647**	ns	**0.484**	ns	ns	ns
Acid Phosphatase	**0.547**	**-0.548**	**-0.421**	**-0.342**	ns	**-0.393**	**0.466**	ns	ns	ns

Table 2.16 (cont)

1	2	3	4	5	6	7	8	9	10	11
Asparagine Transam	ns	-0.321	ns	**-0.342**	ns	ns	0.286	ns	ns	ns
K of Serum	**0.544**	**-0.606**	**-0.377**	**-0.790**	**-0.606**	**-0.471**	**0.330**	0.296	0.233	*ns*
Na of Erythrocytes	ns	ns	-0.239	-0.269	-0.311	ns	ns	ns	ns	ns
α-LP Cholesterol	**0.473**	**-0.432**	**-0.328**	**-0.377**	ns	**-0.477**	0.292	ns	ns	0.234
SOD of Erythrocytes	**-0.516**	**0.626**	0.291	**0.484**	**0.351**	ns	**-0.487**	ns	ns	ns
Diene conjugates	-0.312	**0.384**	ns	ns	0.314	ns	ns	-0.304	**-0.348**	0.321
Ca of Serum	**-0.676**	**0.744**	**0.399**	**0.525**	**0.538**	**0.771**	**-0.774**	*ns*	-0.243	*ns*
Na of Serum	**-0.385**	**0.504**	*ns*	**0.644**	**0.359**	**0.418**	**-0.434**	**-0.343**	**-0.348**	*ns*
K of Erythrocytes	ns	ns	ns	ns	0.292	ns	ns	-0.244	**-0.322**	**0.375**
Na,K-ATPase of Ery	ns	ns	ns	ns	ns	ns	ns	-0.276	-0.227	**0.424**
Catalase of Erythroc	0.223	ns	**-0.380**	ns	ns	-0.264	0.257	ns	ns	ns
Catalase of Serum	ns	ns	-0.267	ns	ns	ns	-0.256	ns	ns	ns
Malon-dialdehyde	ns	-0.260	-0.280	-0.285	ns	-0.283	0.315	ns	ns	**0.490**
Phosphates of Serum	*ns*	*ns*	*ns*	*ns*	*ns*	**-0.510**	**-0.357**	*ns*	*ns*	*ns*

Keshavarzi Z et al. [2018] shown that the Glutathione (GSH) concentration significantly decreased after induction of gastric ischemia-reperfusion (IR) in male rats. Estradiol and combined estradiol and progesterone significantly increased GSH levels. The myeloperoxidase (MPO) concentration significantly increased after induction of gastric IR. Different treatments significantly reduced MPO levels. The gastric acid concentration significantly increased after induction of gastric IR. Treatment with estradiol, progesterone and combined estradiol and progesterone significantly reduced gastric acid levels. Superoxide dismutase (SOD)

concentration decreased after induction of gastric IR. The SOD levels were not significant. The authors concluded that female sexual steroids have a therapeutic effect on gastrointestinal ischemic disorders (which, as is known, are manifested by damage to the mucosa [Zhao DQ et al., 2020]) by reduction of MPO and gastric acid, and increasing gastric GSH & SOD levels following gastric IR.

As a result of the canonical correlation analysis between Neuro-Endocrine and Metabolic variables, two pairs of canonical roots were obtained. It was found that the hormonal constellation and Vagal tone determine the state of metabolism by 95% (Table 2.17 and Fig. 2.10).

Table 2.17. Factor structure of first pair of Neuro-Endocrine and Metabolic Roots

Left set	**R1**
Parathyroid hormone	**-0.831**
Aldosterone	**-0.510**
Sex Index (M=1;F=2)	**-0.416**
Corticosterone	**-0.350**
Adrenals mass	**-0.294**
Calcitonin	**0.457**
Testosterone	**0.369**
MxDMn HRV as Vagal tone	**0.286**
Right set	**R1**
Potassium of Serum	**0.798**
Phosphates of Serum	**0.792**
α-LP Cholesterol	**0.502**
Alkaline Phosphatase	**0.488**
Malondialdehyde	**0.356**
Acid Phosphatase	**0.292**
Potassium of Erythrocytes	**0.287**
Sodium of Erythrocytes	**0.275**
Calcium of Serum	**-0.804**
Superoxide dismutase of Erythrocytes	**-0.543**
Sodium of Serum	**-0.334**
Diene conjugates	**-0.156**

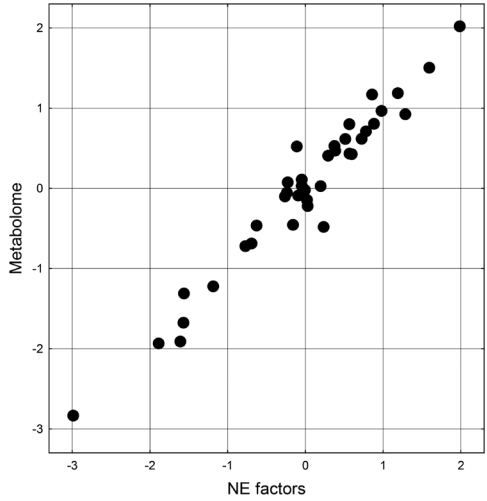

R=0.974; R^2=0.949; $\chi^2_{(130)}$=237; p<10^{-6}; Λ Prime<10^{-4}

Fig. 2.10. Scatterplot of canonical correlation between neuro-endocrine parameters (X-line) and parameters of metabolome (Y-line) at intact and stressed rats. First pair of Roots

The metabolic constellation of the second pair is determined by hormones and Sympathetic tone by 87% (Table 2.18 and Fig. 2.11).

Table 2.18. Factor structure of second pair of Neuro-Endocrine and Metabolic Roots

Left set	**R2**
1	2
Sex Index (M=1;F=2)	**-0.866**
Adrenals mass	**-0.613**
Aldosterone	**-0.546**
1/Mode HRV as Catecholamines	**-0.416**
Corticosterone	**-0.365**
Parathyroid hormone	**-0.302**
Testosterone	**0.739**
Calcitonin	**0.565**
AMo HRV as Sympathetic tone	**0.460**
Right set	**R2**

Table 2.18 (cont)

1	2
Potassium of Serum	**0.800**
Alkaline Phosphatase	**0.696**
Acid Phosphatase	**0.533**
α-LP Cholesterol	**0.490**
Asparagine Transaminase	**0.283**
Malondialdehyde	**0.226**
Catalase of Erythrocytes	**0.133**
Sodium of Serum	**-0.526**
Superoxide dismutase of Erythrocytes	**-0.523**
Calcium of Serum	**-0.500**
Phosphates of Serum	**-0.458**
Potassium of Erythrocytes	**-0.415**
Diene conjugates	**-0.343**
Catalase of Serum	**-0.136**
Na.K-ATPase of Erythrocytes	**-0.110**

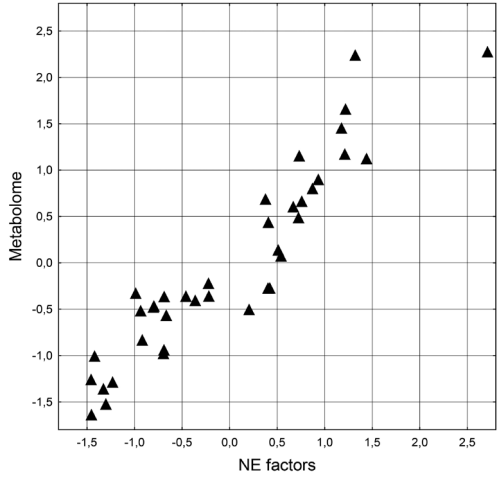

R=0.935; R^2=0.873; $\chi^2_{(108)}$=162; p=0.0006; Λ Prime=0.002

Fig. 2.11. Scatterplot of canonical correlation between neuro-endocrine parameters (X-line) and parameters of metabolome (Y-line) at intact and stressed rats. Second pair of Roots

Screening of correlations between immunity parameters and markers of morpho-functional state of the gastric mucosa and myocardium revealed the following (Table 2.19).

Table 2.19. Correlation Matrix for Immune and Gastric mucosa&ECG variables

Variables	**GU amount**	**GU length**	**GM damage**	**ST joint**	**T wave**
Killing Index of Neutrophils	**-0.392**	**-0.504**	**-0.429**	0.236	0.213
Spleen Mass	*ns*	-0.226	**-0.331**	*ns*	*ns*
Reticulocytes of Spleen	**0.335**	**0.388**	**0.427**	*ns*	*ns*
Lymphoblastes of Spleen	*ns*	0.213	0.251	*ns*	*ns*
Thymus Mass	0.276	0.263	*ns*	-0.237	*ns*
Fibroblastes of Thymus	-0.245	*ns*	*ns*	*ns*	*ns*
Macrophages of Thymus	*ns*	*ns*	*ns*	-0.208	*ns*

Damage to the gastric mucosa and myocardium is more severe, the lower the bactericidal activity of blood neutrophils (the completion of phagocytosis of *Staph. aureus*), and the greater the mass of the thymus. The spleen mass and the content of fibroblasts in the thymus are negatively correlated only with the severity of damage to the gastric mucosa, while the percentages of reticulocytes and lymphoblasts in the spleen are positively correlated with it. Finally, the higher the percentage of macrophages in the thymus, the lower the ST junction, that is, the deeper the damage to the myocardium. Taken together, the listed immune factors determine the morpho-functional state of the gastric mucosa and myocardium by 65% (Table 2.19 and Fig. 2.12).

Table 2.19. Factor structure of Immune and post stress Damage Roots

Left set	**R**
1	2
Killing Index of Neutrophils	**0.602**
Spleen Mass	**0.234**
Fibroblastes of Thymus	**0.217**
Macrophages of Thymus	**0.155**
Reticulocytes of Spleen	**-0.517**

Table 2.19 (cont)

1	2
Thymus mass	**-0.433**
Lymphoblastes of Spleen	**-0.323**
Right set	**R**
GU length	**-0.932**
GM damage	**-0.881**
GU amount	**-0.864**
ST joint ECG	**0.470**
T wave ECG	**0.398**

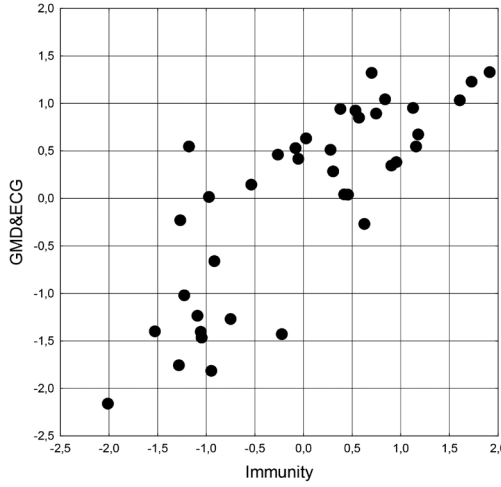

R=0.809; R^2=0.654; $\chi^2_{(40)}$=74; p=0.0008; Λ Prime=0.084

Fig. 2.12. Scatterplot of canonical correlation between immune parameters (X-line) and parameters of gastric mucosa&ECG damage (Y-line) at intact and stressed rats

From a formal/mathematical point of view, it appears that four immune factors are **protective (stress-limiting)**, while the other three are responsible for **enhance** of post-stress injuries. According to an alternative interpretation, both immune parameters and morpho-functional state of the gastric mucosa&myocardium parameters together are subject to the regulatory influence of neuro-endocrine factors of acute stress. In other

words, the detected immune parameters are only *companions*, but not *causal factors* of the morpho-functional state of the gastric mucosa&myocardium in naïve and stressed rats.

The solution to this problem is possible only by analyzing functional relationships supported by correlations (Tabl. 2.20).

Let's limit ourselves to the most illustrative example, such as the bactericidal activity of blood neutrophils. It is known that phagocytosis is not an isolated cell response. It usually occurs together with other cell responses, including formation of reactive oxygen species (ROS), secretion of pro-inflammatory mediators and production of cytokines [Uribe-Querol E & Rosales C, 2020]. The effect of ROS depends on the production site. Intracellular ROS suppressed IL-1β expression in these neutrophils, while extracellular ROS amplified IL-1β secretion. Production of extracellular H_2O_2 may thus affect cells of the surrounding tissue. Excessive neutrophil activity may cause tissue damage [Moghadam ZM et al., 2021].

Table 2.20. Correlation Matrix for Neuroendocrine, gastric mucosa&ECG and Immune variables

Variables	**Testo-stero-ne**	**Calci-tonin**	**Vagal tone**	**Sym-patho-tone**	**Cate-chola-mines**	**Corti-coste-rone**	**Aldo-stero-ne**	**PTH**	**Sex Index**	**Adre-nals mass**
1	2	3	4	5	6	7	8	9	10	11
Killing Ind Neutrophils	**0.430**	0.286	*0.204*	*ns*	*ns*	-0.291	-0.280	**-0.403**	**-0.509**	*ns*
Spleen Mass	**0.329**	*ns*	**0.459**	-0.274	*ns*	**-0.556**	-0.288	*ns*	**-0.339**	*ns*
Macrophages Thymus	**0.332**	0.244	*ns*	**0.415**	0.254	*ns*	*ns*	*-0.234*	-0.253	*ns*
Fibroblastes Thymus	*-0.201*	*ns*	**-0.411**	*ns*	*ns*	0.282	*ns*	*ns*	*0.220*	*ns*
Microbial Count Neutr	*ns*	0.315	*-0.219*	*0.221*	0.282	**-0.683**	*ns*	*-0.203*	-0.289	*ns*
Phagocytose Ind Neutr	**0.427**	**0.636**	*ns*	*ns*	*ns*	*ns*	-0.251	*ns*	*ns*	-0.283
B-Lympho-cytes Blood	**0.321**	0.237	*ns*	0.233	**0.515**	*ns*	-0.216	*-0.212*	-0.276	*ns*
Eosinophiles Spleen	*ns*	*ns*	*ns*	*ns*	*ns*	*ns*	**-0.440**	*ns*	*ns*	*ns*
Reticulocytes Spleen	**-0.413**	*-0.222*	*-0.224*	*ns*	*ns*	0.281	0.311	0.319	**0.325**	*ns*

Table 2.20 (cont)

1	2	3	4	5	6	7	8	9	10	11
Thymus Mass	-0.241	**-0.435**	*ns*	*ns*	*ns*	*ns*	*ns*	*ns*	*ns*	0.295
Lympho-blastes Spleen	*ns*	*-0.210*	*-0.214*	*ns*	0.262	*ns*	*ns*	*0.226*	*ns*	*ns*
Monocytes Blood	-0.246	**-0.380**	*ns*	*ns*	*ns*	*ns*	*ns*	*ns*	*ns*	*ns*
Bactericidity Monocyte	-0.306	-0.310	*ns*	*ns*	*ns*	*ns*	*ns*	*ns*	*ns*	**0.356**
NK-Lymphocyte Blood	*ns*	0.236	*ns*	*ns*	*0.226*	*ns*	*ns*	**-0.331**	*ns*	*ns*
Th T-Lymphoc Blood	*ns*	*ns*	*ns*	*ns*	*ns*	*0.234*	*ns*	*ns*	*ns*	*ns*
Tc T-Lymphoc Blood	*ns*	*ns*	*ns*	*ns*	0.249	*-0.215*	*ns*	*ns*	*ns*	*ns*
Gastric Ulcers Amount	*ns*	-0.229	*ns*	0.253	*0.188*	*ns*	0.226	**0.584**	*ns*	0.236
Gastric Ulcers Length	*-0.213*	-0.283	-0.230	*0.214*	*ns*	*0.206*	0.275	**0.621**	0.280	**0.384**
Gastric mucosa Damage	*-0.204*	-0.251	-0.283	0.273	*ns*	0.225	0.302	**0.516**	0.272	**0.391**
T wave ECG	*ns*	*ns*	*ns*	*ns*	**-0.356**	*ns*	*ns*	**-0.351**	*ns*	*ns*
S-T joint ECG	*ns*	*ns*	*ns*	*ns*	-0.284	*ns*	*ns*	**-0.342**	*ns*	*-0.192*

Note. Color highlighted Immune variables that **limited** or **enhanced** of post-stress injuries (see Table 2.19).

Back in 1992 Taché Y & Saperas E [1992] showed that IL-1β is one of the most potent centrally acting inhibitors of gastric acid secretion in rats. Sites of action have been located in the anterior/preoptic area and paraventricular nucleus of the hypothalamus where other biological

activities of IL-1 have also been described. IL-1β action is, so far, quite unique to this cytokine and its action is not reproduced by IL-2 or TNF-α. The IL-1 effect involves prostaglandin pathways and is unrelated to CRF. Similarly, systemic *injection* of IL-1 induces a long lasting inhibition of acid secretion through prostaglandin-dependent mechanisms. Several findings support the possibility that the effect of systemic IL-1 can be CNS-mediated and/or exerted at the periphery through local release of prostaglandin in the stomach. Exogenous IL-1 given into either the circulation or the cerebrospinal fluid also inhibits gastric injury induced by a variety of experimental models (stress, aspirin, ethanol). Such a protective effect is mediated through the inhibition of acid secretion and prostaglandin release, although other mechanisms may also contribute. Authors concluded: whether *endogenously* released IL-1β exerts a protective role in the gastric mucosa is still to be investigated.

In the same year, Uehara A et al. [1992] found that in rats the *central* administration of IL-1 dose-dependently suppressed the development of gastric mucosal lesions induced by WIRS. These results clearly demonstrated that IL-1 has potent antiulcer (and antisecretory) effects that are mediated by the *central nervous* system. Moreover, these findings suggest that there may exist an "immune-brain-gut" axis, which is involved in the regulation of gastric secretion and mucosal homeostasis, especially under certain pathophysiological conditions that activate the immune system to release various cytokines including IL-1.

Hence, we assume that the negative correlation of neutrophil bactericidality with markers of gastric mucosa injury and the positive correlation with T wave and ST joint ECG reflects not the direct effect of factors released by them, at least IL-1, on the gastric mucosa and myocardium, but the upregulating influence of IL-1 on the anterior/preoptic area and paraventricular nucleus of the hypothalamus with subsequent indirect ***upregulation*** of serum levels of Testosterone and Calcitonin and Vagal tone, while ***downregulation*** of Corticosterone, Aldosterone, PTH and, probably, judging by the negative correlation with the Sex index, female sex hormones such as Estradiol and Progesterone, which, in turn, have a ***limiting*** or ***enhancing*** effect on post-stress injuries of the gastric mucosa and myocardium.

At the same time, an alternative hypothesis can be put forward that the neuroendocrine response caused by acute stress factors (immobilization, cooling, starvation, etc.) modulates the production of IL-1 by blood

neutrophils (as well as thymic macrophages and blood B lymphocytes), which acts on the gastric mucosa and/or myocardium together with stress hormones and neurotransmitters. In particular, Testosterone, Calcitonin and Vagal tone have gastroprotective effect, while Sympathetic tone, Catecholamines, Corticosterone, Aldosterone, PTH and, probably, female sex hormones have gastro-and cardioaltering effects.

It should be noted that there is evidence of an adverse effect of both testosterone and interleukins on the gastric mucosa of rats.

The already mentioned Lu S et al. [2019] showed that the efficacy of Kangfuxin liquid in WIRS-induced gastric ulcer in rats in the form of reducing the area of ulcers accompanied by inhibition of inflammatory reactions: decrease in TNF-α (9%) and IL-6 (11%) levels.

Konturek PC et al. [2001] shown that caused by LPS injection the rise in plasma IL-1β and TNF-α levels resulted in a *delay* in ulcer healing associated with a significant decrease in gastric blood flow.

Machowska A et al. [2004] compared the effects of major male hormone, testosterone, and female hormone, progesterone, on the healing of gastric ulcers induced by acetic acid technique in male rats with intact or removed testicles (testectomy) and female rats with intact or removed ovaries (ovariectomy). The authors shown that the area of gastric ulcers in placebo-control rats decreased significantly at day 7 upon ulcer induction and this effect was significantly *accelerated* by testectomy or ovariectomy. In contrast, testosterone significantly *delayed* ulcer healing while producing a significant fall in the gastric blood flow determined at the margin of ulcer. Treatment with progesterone significantly accelerated ulcer healing and increased the gastric blood flow. Testosterone applied alone or supplemented in testectomized animals produced the significant increment in plasma IL-1β levels as compared to the respective levels of this cytokine in placebo-control animals. The authors concluded that: 1) major male (testosterone) and female (progesterone) sex hormones exhibit opposite effect on healing of preexisting ulcers in the stomach because testosterone markedly delayed while progesterone significantly accelerated this healing; 2) testosterone-induced delay in ulcer healing involves the fall in the gastric microcirculation at the margin of gastric ulcers and the excessive production and release of proinflammatory cytokine IL-1β; and 3) testectomy improves the gastric ulcer healing due to inhibition of gastric acid secretion and the rise in plasma gastrin, which exerts gastroprotective, trophic and ulcer healing action on the gastric mucosa.

Later Machowska A et al. [2008] studied the effects of depletion of testosterone on the healing of acetic acid-induced ulcers at rats. The authors shown that testosterone (0.01-10 mg/kg/day i. m.) dose-dependently *delayed* gastric ulcer healing. When applied in an optimal dose of 1 mg/kg/day, this hormone significantly raised gastric acid secretion and plasma IL-1β and TNF-α levels. Attenuation of plasma testosterone levels via bilateral orchidectomy inhibited gastric acid secretion and accelerated the healing of gastric ulcers, while increasing plasma gastrin levels and these effects were reversed by testosterone. The authors propose that testosterone delays ulcer healing via a fall in blood flow at the ulcer margin, a rise in plasma levels of IL-1β and TNF-α and, an increase in gastric acid secretion.

Wang M et al. [2012] have shown that male myocardium demonstrates greater loss in cardiac function in the presence of a given TNF level compared to female. In addition, estrogen has little influence on reducing TNF-caused myocardial dysfunction in female hearts, suggesting that male hormone – testosterone may be responsible for gender differences in TNF-mediated myocardial damage. Later the authors shown on isolated mouse hearts that TNF infusion significantly depressed left ventricular developed pressure, but not heart rate in males. Myocardial rate pressure product (RPP=LVDP•HR) was markedly decreased in male hearts compared to females in exposure to TNF, which was associated with higher levels of TNF-induced caspase-8&3. Importantly, depletion of endogenous testosterone by castration or blockade of androgen receptor by flutamide treatment abolished TNF-decreased RPP in male hearts. However, castration or flutamide treatment did not affect TNF production and myocardial expression of TNFR1 and TNFR2. The authors concluded that testosterone is critical to the gender difference in TNF-induced detrimental effects on myocardium.

However, a systematic review and meta-analysis shown that a lower total testosterone level was associated with a higher risk of cardiovascular disease mortality and all-cause mortality in males with chronic kidney disease CKD [Oh ES et al., 2022].

Regarding our research, the facts should be given that in a mouse model of ischemia-reperfusion injury, intraperitoneal treatment with CGRP significantly reduced gastric mucosal edema, hemorrhage, apoptosis, mucosal separation and inflammatory cell infiltration. It is known that after stimulation, capsaicin-sensitive sensory nerve fibers may release CGRP, and then CGRP increases the levels of prostacyclin and prostaglandin E2 in gastric mucosa, thereby

inhibiting the activation of neutrophils and degranulation of mastocytes, reducing the secretion of inflammatory mediators (*e.g.*, histamine), and alleviating gastrointestinal inflammation [Zhao DQ et al., 2020].

Interestingly, a similar mechanism underlies the carbon monoxide-induced gastroprotection against stress ulcerogenesis. The exposure of rats to 3.5 h of WIRS resulted in numerous hemorrhagic gastric lesions and significantly decreased the gastric blood flow, raised MDA content and significantly decreased the mucosal SOD and GSH contents compared with intact gastric mucosa, and these changes were exacerbated in rats with capsaicin denervation. The sensory nerve endings releasing CGRP can contribute, at least in part, to the CO-induced gastric hyperemia, the attenuation of gastric mucosal lipid peroxidation and prevention of oxidative stress and stress ulcerogenesis [Kwiecien S et al., 2016].

In conclusion, in order to create a complete picture, we consider it necessary to present our own illustration of the neuroendocrine-immune complex [Bes] created on the basis of the correlation matrix for neuroendocrine and immune variables (Table 8). Despite moderate pairwise correlations, the canonical correlation between neuroendocrine and immune variables turns out to be very strong (Tables 2.21 and 2.22, Figs. 2.13 and 2.14)

Table 2.21. Factor structure of first pair of Neuroendocrine and Immune Roots

Left set	**Root 1**
1	2
Corticosterone	**-0.753**
Parathyroid hormone	**-0.483**
Sex Index (M=1; F=2)	**-0.430**
Adrenals mass	**-0.300**
1/Mode HRV as Catecholamines	**-0.226**
AMo HRV as Sympathetic tone	**-0.193**
Aldosterone	**-0.165**
Testosterone	**0.273**
MxDMn HRV as Vagal tone	**0.330**
Calcitonin	**0.529**
Right set	**Root 1**
Fibroblastes of Thymus	**-0.372**
Theophylline-resistant T-Lymphocytes	**-0.257**
Thymus mass	**-0.247**
Lymphoblastes of Spleen	**-0.205**

Table 2.21 (cont)

1	2
Reticulocytes of Spleen	**-0.188**
Eosinophiles of Spleen	**0.229**
Killing Index of Neutrophils	**0.312**
Phagocytosis Index of Neutrophils	**0.383**
Spleen Mass	**0.469**
Microbial Count of Neutrophils	**0.636**

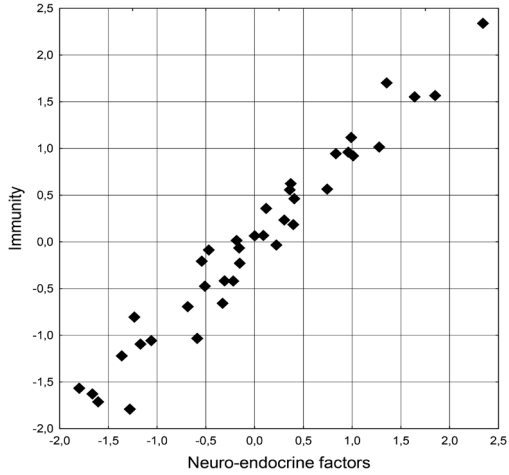

$R=0.976$; $R^2=0.952$; $\chi^2_{(160)}=284$; $p<10^{-6}$; Λ Prime$<10^{-5}$

Fig. 2.13. Scatterplot of canonical correlation between Neuroendocrine (X-line) and Immune (Y-line) parameters at intact and stressed rats. *First pair of Roots*

Table 2.22. Factor structure of second pair of Neuroendocrine and Immune Roots

Left set	**Root 2**
1	2
Parathyroid hormone	**0.549**
Sex Index (M=1; F=2)	**0.389**
1/Mode HRV as Catecholamines	**0.237**
Adrenals mass	**0.206**
Calcitonin	**-0.289**
Corticosterone	**-0.312**
Testosterone	**-0.370**

Table 2.22 (cont)

1	2
MxDMn HRV as Vagal tone	**-0.424**
Right set	**Root 2**
Thymus mass	**0.486**
Microbial Count of Neutrophils	**0.463**
Monocytes of Blood	**0.456**
Lymphoblastes of Spleen	**0.281**
Theophylline-susceptible T-Lymphocytes	**0.258**
Bactericidal Capacity of Monocytes	**0.221**
Macrophages of Thymus	**-0.179**
Theophylline-resistant T-Lymphocytes	**-0.242**
Phagocytosis Index of Neutrophils	**-0.250**
B-Lymphocytes of Blood	**-0.261**
Killing Index of Neutrophils	**-0.328**
NK-Lymphocytes of Blood	**-0.372**

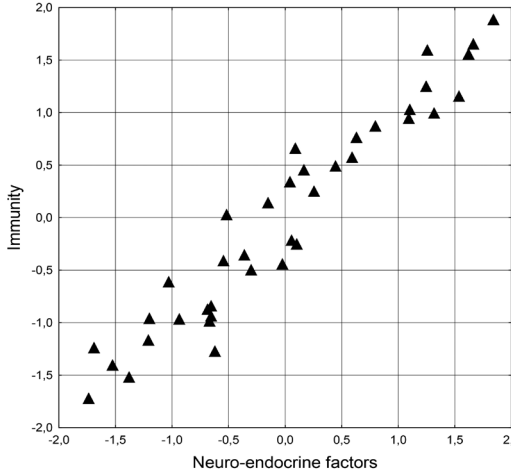

R=0.962; R^2=0.926; $\chi^2_{(135)}$=212; p<10^{-4}; Λ Prime<10^{-4}

Fig. 2.14. Scatterplot of canonical correlation between Neuroendocrine (X-line) and Immune (Y-line) parameters at intact and stressed rats. *Second pair of Roots*

The morpho-functional basis of the relationships between the three systems of the complex are: receptors for hormones, neurotransmitters, and neuropeptides in immune cells; receptors for immune cytokines in endocrine glands; receptors for immune cytokines in the nervous system; neuro-endocrine agents in lymphoid organs; immune cytokines in endocrine and nervous systems; endocrine effects on the immune system; neural effects on the immune system; immune mechanisms that can be affected by neuro-endocrine agents; effects of immune-derived products on endocrine mechanisms; effects of immune-derived products on the nervous system; metabolic effects of cytokines [Besedovsky HO & Del Rey A, 1996].

2.4. Sexual dimorphism in basal and post stress parameters of neuro-endocrine-immune complex, metabolome, electrocardiogram, and gastric mucosa at rats

Summary.

Introduction and aim. Previously, we found significant associations between sex index and a number of parameters of the neuro-endocrine-immune complex and metabolome. Therefore, the next goal was a detailed analysis of sexual dimorphism in these parameters in baseline and post stress situations.

Material and methods. The experiment conducted on the same 18 male and 20 female rats Wistar line. Over the 10 days, one animal remained intact and 3 other rats were exposed to (WIRS). The next day after stressing, endocrine, immune and metabolic parameters as well as ECG and gastric mucosa injuries was recorded.

Results. By the method of discriminant analysis was selected 23 variables (4 endocrine, 6 immune, 9 metabolic as well as 4 markers of damage in gastric mucosa and myocardium) whose constellation is characteristic for each group**.** The distance between the centroids of the major discriminant root of intact females and males as a measure of sexual dimorphism is 16.2 units. Acute stress increases it in control rats to 23.4 units, and in pretreated by phytoadaptogen – up to 29.4 units. Acute stress increases the severity of sexual dimorphism also in relation to variables, information about which is condensed in the minor root – from 0.99 to 2.29 units, while preventive use of phytoadaptogen limits it to 1.63 units.

Conclusion. In intact rats, significant sex differences were found for a number of endocrine, immune, and metabolic variables, which increase under the influence of acute stress per se, and to an even greater extent against the background of preventive use of a phytoadaptogen.

Introduction

Previously, we found significant associations between sex index and a number of parameters of the neuro-endocrine-immune complex and metabolome. Therefore, the next goal was a detailed analysis of sexual dimorphism in these parameters in baseline and post stress situations. To achieve this goal, the registered parameters were recalculated in Z-scores separately for males and females, both intact and subjected to acute stress against the background of drinking tap water or phytocomposition.

In intact females (Table 2.23), by definition, testosterone levels are an order of magnitude lower than in males. However, they have a greater adrenal mass than in males and, to an even greater extent, their mass index, given their somewhat lower body mass. This is accompanied by higher serum levels of adrenal-produced corticosterone and aldosterone. In addition, females have higher levels of parathyroid hormone, but lower levels of calcitonin. No significant sex differences were found for triiodothyronine levels, as well as markers of catecholamines and sympathetic and vagal tone (Fig. 2.15).

Table 2.23. Sexual dimorphism in endocrine and autonomic parameters in intact rats

Sex	**Males (5)**	**Females (5)**	**Males (5)**	**Females (5)**	**Parameters of Student's statistics**		
Variables	**Raw values**		**Z-scores**		**Cv**	**t**	**p**
1	2	3	4	5	6	7	8
Body mass, g	216±11	196±9	0.45±0.44	-0.45±0.44	0,108	1,52	**>0,1**
Adrenal glands mass, mg	44±4	65±5	-0.72±0.27	0.71±0.35	0,273	-3,26	**<0,02**
Adrenal mass index, mg/100g	21±3	33±3	-0.76±0.24	0.77±0.32	0,300	-3,78	**<0,02**
Corticosterone, nM/L	290±44	406±37	-0.55±0.42	0.55±0.35	0,302	-2,03	**>0,05**
Aldosterone, pM/L	587±8	639±33	-0.45±0.14	0.45±0.58	0,093	-1,51	**>0,1**
Testosterone, nM/L	41.8±1.4	3.53±0.24	0.94±0.07	-0.94±0.01	0,895	26,5	**<0,001**

Table 2.23 (cont)

1	2	3	4	5	6	7	8
Calcitonin, ng/L	32.3±3.2	24.7±0.3	0.61±0.51	-0.62±0.05	0,217	2,39	**<0,05**
Parathyroid hormone, µg/L	154±11	185±3	-0.65±0.48	0.65±0.11	0,141	-2,63	**<0,05**
Triiodothyronine, nM/L	3.06±0.52	3.73±0.26	-0.35±0.55	0.36±0.28	0,256	-1,14	>0,2
Mode as catecholamines, msec	178±18	172±12	-0.10±0.56	0.10±0.56	0,180	-0,28	>0,5
AMo as sympathetic tone, %	54±12	43±2	0.30±0.64	-0.30±0.10	0,392	0,91	>0,2
MxDMn as vagal tone, msec	63±38	39±7	0.27±0.64	-0.27±0,15	0,878	0,82	>0,2

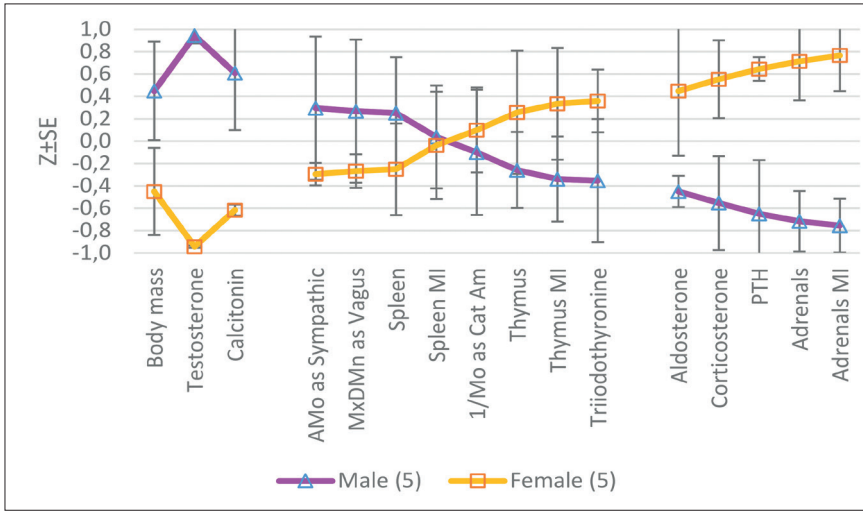

Fig. 2.15. Profile of mass of body, thymus, spleen, adrenal glands, and neuro-endocrine variables in intact rats

Against the background of the absence of differences in thymus mass, the thymocytogram revealed a higher percentage of lymphocytes and epithelial cells, but a lower percentage of lymphoblasts, macrophages, and reticulocytes, and as a result, a lower level of thymocytogram entropy (Table 2.24 and Fig. 2.16).

Table 2.24. Sexual dimorphism in thymus and thymocytogram parameters in intact rats

Sex	Males (5)	Females (5)	Males (5)	Females (5)	Parameters of Student's statistics		
Variables	**Raw values**		**Z-scores**		**Cv**	**t**	**p**
Thymus mass, mg	136±10	152±17	-0,26±0,34	0,26±0,55	0,210	-0,80	>0,2
Thymus mass index, mg/100g	64±8	79±11	-0,34±0,38	0,33±0,50	0,298	1,07	>0,2
Lymphocytes, %	63,8±1,6	67,8±1,7	-0,49±0,40	0,49±0,41	0,062	-1,72	**>0,1**
Lymphoblastes, %	8,80±1,74	6,20±0,58	0,42±0,57	-0,42±0,19	0,409	1,41	**>0,1**
Epitheliocytes, %	6,32±0,82	9,75±0,81	-0,69±0,33	0,69±0,32	0,310	-2,97	**<0,02**
Macrophages, %	6,38±0,76	4,40±0,24	0,63±0,48	-0,63±0,16	0,292	2,51	**<0,05**
Reticulocytes, %	5,68±1,02	2,65±0,55	0,65±0,43	-0,64±0,23	0,564	2,61	**<0,05**
Fibroblastes, %	4,86±1,02	5,80±0,86	-0,23±0,42	0,23±0,42	0,386	-0,70	>0,5
Basophiles, %	3,16±0,59	2,40±0,51	0,31±0,48	-0,31±0,42	0,441	0,98	>0,2
Hassal's corpuscles, %	1,00±0,00	1,00±0,00	0,00±0,00	0,00±0,00	0	-	-
Thymocytogram Entropy •10^3	622±14	570±24	0,52±0,28	-0,53±0,49	0,082	1,87	**>0,05**

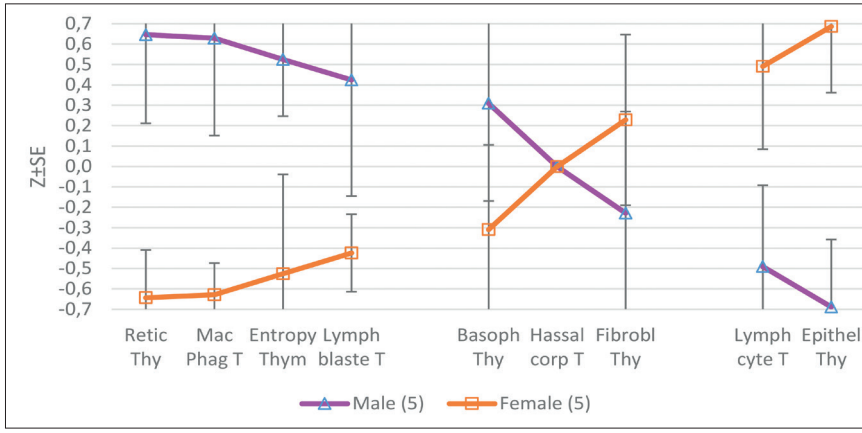

Fig. 2.16. Profile of Thymocytogram variables in intact rats

With the same spleen mass, the percentage of macrophages and reticulocytes was found to be higher in females, while males had a significantly higher percentage of eosinophils, and the remaining elements of the splenocytogram did not differ significantly (Table 2.25 and Fig. 2.17).

Table 2.25. Sexual dimorphism in spleen and splenocytogram parameters in intact rats

Sex	Males (5)	Females (5)	Males (5)	Females (5)	Parameters of Student's statistics		
Variables	**Raw values**		**Z-scores**		**Cv**	**t**	**p**
Spleen mass, mg	819±92	726±76	0,25±0,50	-0,25±0,41	0,239	0,78	>0,2
Spleen mass index, mg/100g	378±36	372±38	0,04±0,46	-0,04±0,48	0,208	0,11	>0,9
Lymphocytes, %	70,2±2,3	67,0±2,0	0,33±0,47	-0,33±0,42	0,071	1,06	>0,2
Lymphoblastes, %	7,50±1,43	9,40±1,40	-0,30±0,45	0,30±0,44	0,373	-0,95	>0,2
Plasmocytes, %	1,75±0,19	1,60±0,40	0,10±0,29	-0,12±0,60	0,398	0,34	>0,5
Microphages, %	11,3±0,66	13,2±1,53	-0,36±0,25	0,36±0,57	0,220	-1,17	>0,2
Rod shaped neutrophils, %	1,50±0,22	2,00±0,45	-0,32±0,28	0,32±0,57	0,452	-1,00	>0,2
Macrophages, %	2,00±0,32	3,00±0,45	-0,51±0,33	0,51±0,46	0,389	-1,83	**>0,1**
Reticulocytes, %	2,25±0,19	3,00±0,32	-0,55±0,28	0,55±0,47	0,259	-2,02	**>0,05**
Eosinophiles, %	3,50±1,02	0,80±0,20	0,64±0,49	-0,64±0,09	0,981	2,59	**<0,05**
Splenocytogram Entropy •10^3	521±31	546±20	-0,22±0,55	0,22±0,35	0,106	-0,68	>0,5

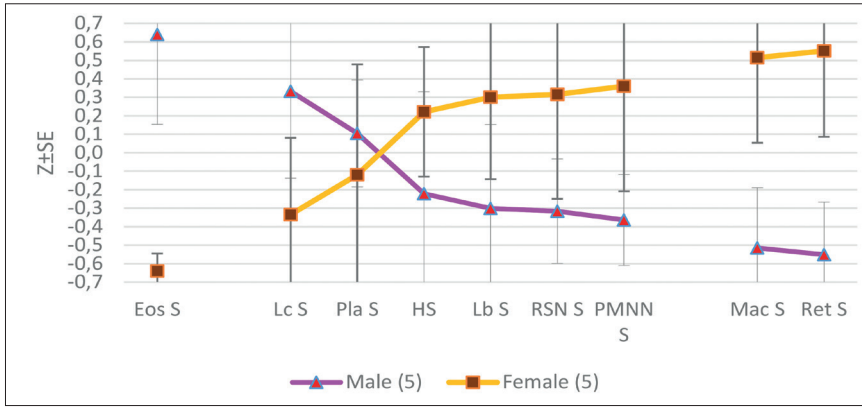

Fig. 2.17. Profile of Splenocytogram variables in intact rats

Regarding the absolute content of lymphocytes in the blood and the percentage of their populations, marginally significant sex differences were found only for B-Lymphocytes and plasma cells (Table 2.26 and Fig. 2.18).

Table 2.26. Sexual dimorphism in blood lymphocyte populations in intact rats

Sex	Males (5)	Females (5)	Males (5)	Females (5)	Parameters of Student's statistics		
Variables	**Raw values**		**Z-scores**		**Cv**	**t**	**p**
Pan Lymphocytes, 10^9/L	5,89±1,18	8,30±1,63	-0,37±0,36	0,37±0,50	0,458	-1,20	>0,2
TR T-helper Lymphocytes, %	30,0±0,3	29,4±0,4	0,36±0,38	-0,36±0,48	0,028	1,18	>0,2
TS T-cytolytic Lymphocytes, %	15,6±1,7	15,0±1,7	0,08±0,48	-0,08±0,47	0,235	0,25	>0,5
NK Lymphocytes, %	5,52±0,48	5,06±0,55	0,21±0,43	-0,21±0,49	0,212	0,63	>0,5
B-Lymphocytes, %	14,6±1,0	12,2±1,0	0,48±0,41	-0,48±0,41	0,187	1,66	**>0,1**
Plasmocytes, %	0,00±0,00	0,79±0,49	-0,47±0,00	0,47±0,58	2,109	-1,63	**>0,1**
0-Lymphocytes, %	34,3±2,6	37,6±1,9	-0,32±0,50	0,32±0,38	0,142	-1,02	>0,2
Immunocytogram Entropy •10^3	809±11	805±14	0,07±0,42	-0,07±0,53	0,033	0,21	>0,5

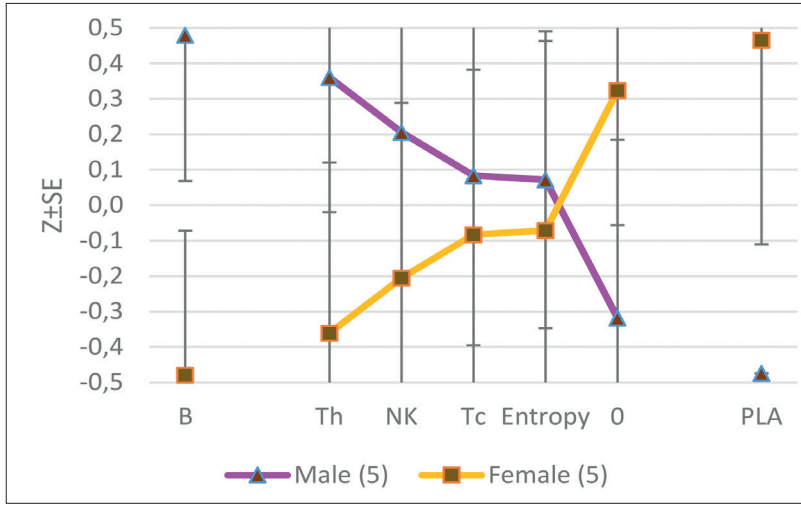

Fig. 2.18. Profile of Immunocytogram variables in intact rats

The blood leukocytogram revealed only a marginally significant difference between the percentage of rod-shaped neutrophils (Table 2.27 and Fig. 2.19).

Table 2.27. Sexual dimorphism in blood leukocyte populations in intact rats

Sex	Males (5)	Females (5)	Males (5)	Females (5)	Parameters of Student's statistics		
Variables	**Raw values**		**Z-scores**		**Cv**	**t**	**p**
Leukocytes, 10^9/L	11,23±2,23	16,30±3,41	-0,38±0,34	0,38±0,52	0,480	-1,22	>0,2
Pan lymphocytes, %	52,2±2,6	51,4±1,8	0,08±0,56	-0,08±0,37	0,091	0,25	>0,9
PMN neutrophils, %	34,8±1,4	34,6±1,8	0,03±0,41	-0,03±0,51	0,098	0,09	>0,9
Rod-shaped neutrophils, %	2,60±0,24	1,80±0,37	0,51±0,31	-0,51±0,47	0,359	1,79	**>0,1**
Eosinophiles, %	5,00±1,34	4,80±0,73	0,04±0,59	-0,04±0,32	0,466	0,13	>0,9
Monocytes, %	5,40±1,03	7,00±1,00	-0,35±0,45	0,35±0,43	0,371	-1,11	>0,2
Leukocytogram Entropy •10^3	679±34	686±8	-0,06±0,65	0,06±0,15	0,077	-0,19	>0,9

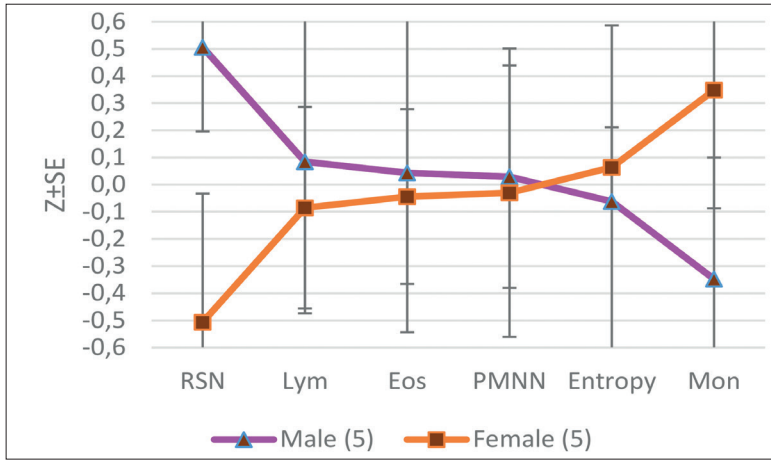

Fig. 2.19. Profile of Leukocytogram variables in intact rats

When comparing the parameters of phagocytosis, it was found (Table 2.28 and Fig. 2.20) that males have significantly higher activity of neutrophil phagocytosis, as well as, to a lesser extent, its intensity and completeness, however, due to the lower absolute content of neutrophils in the blood, their bactericidal capacity does not differ from that of females. On the other hand, at the same levels of activity and intensity of monocyte phagocytosis, their bactericidal capacity is greater in females due to their higher absolute content in the blood.

Table 2.28. Sexual dimorphism in parameters of phagocytic function of blood neutrophils and monocytes in intact rats

Sex	Males (5)	Females (5)	Males (5)	Females (5)	Parameters of Student's statistics		
Variables	Raw values		Z-scores		Cv	t	p
Pan neutrophils, 10^9/L	4,21±0,77	6,06±1,54	-0,34±0,28	0,34±0,56	0,536	-1,08	>0,2
Phagocytosis index neutr, %	59,6±1,8	50,8±1,4	0,77±0,31	-0,77±0,24	0,103	3,94	**<0,01**
Microbial count neutr, B/Ph	5,8±0,5	5,2±0,5	0,28±0,45	-0,28±0,45	0,196	0,87	>0,2
Killing index neutrophils, %	52,0±3,7	43,0±3,9	0,48±0,39	-0,48±0,42	0,196	1,67	**>0,1**
BC capacity neutroph, 10^9 B/L	7,70±1,78	7,38±2,35	0,04±0,41	-0,04±0,53	0,583	0,11	>0,9
Monocytes, 10^9/L	0,63±0,20	1,09±0,26	-0,42±0,37	0,42±0,45	0,610	-1,40	**>0,1**
Phagocytosis index monoc, %	5,7±0,7	6,0±0,9	-0,09±0,42	0,09±0,52	0,296	-0,26	>0,9
Microbial count monoc, B/Ph	4,5±0,3	4,4±0,4	0,07±0,42	-0,07±0,53	0,171	0,20	>0,9
Bactericidal cap mon, 10^6 B/L	144±32	273±57	-0,54±0,27	0,55±0,48	0,568	-1,98	**>0,05**

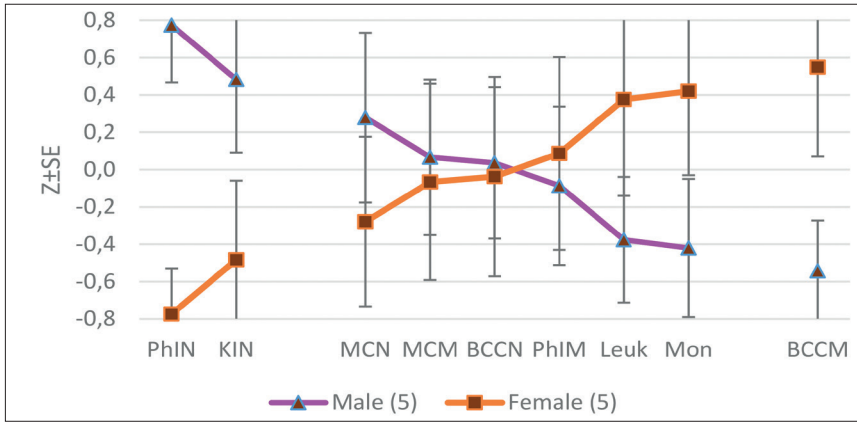

Fig. 2.20. Profile of Phagocytosis variables in intact rats

When comparing electrolyte metabolism parameters (Table 2.29 and Fig. 2.21), it was found that females have, to one degree or another, higher levels of calcium, phosphates, chloride, and sodium in serum, as well as sodium in erythrocytes as a marker of natriuresis, which is combined with a tendency to decrease the activity of Na,K-ATPase in erythrocyte shadows as markers of cell membranes. When comparing electrolyte metabolism parameters (Table

2.29 and Fig. 2.21), it was found that females have, to one degree or another, higher levels of calcium, phosphates, chloride, and sodium in serum, as well as sodium in erythrocytes as a marker of natrihistia, but lower of potassium in in serum, which is combined with a tendency to decrease the activity of Na,K-ATPase in erythrocyte shadows as markers of cell membranes.

In addition, females were found to have lower serum alkaline and acid phosphatases and aspartate aminotransferase activity, but higher erythrocyte superoxide dismutase activity.

Table 2.29. Sexual dimorphism in metabolic parameters in intact rats

Sex	**Males (5)**	**Females (5)**	**Males (5)**	**Females (5)**	**Parameters of Student's statistics**		
Variables	**Raw values**		**Z-scores**		**Cv**	**t**	**p**
1	2	3	4	5	6	7	8
Na,K-ATP-ase Erythr, M/L•h	0.83±0.11	0.71±0.05	0.32±0.57	-0.32±0.28	0,249	1,02	>0,2
Sodium of Erythrocyte, mM/L	19.1±3.2	25.2±3.0	-0.42±0.44	0.42±0.41	0,328	-1,41	**>0,1**
Potassium of Erythroc, mM/L	92±9	93±3	-0.03±0.64	0.03±0.20	0,159	-0,09	>0,9
Potassium of Serum, mM/L	4.34±0.10	3.85±0.38	0.38±0.16	-0.39±0.59	0,156	1,26	>0,2
Sodium of Serum, mM/L	131.6±0.5	133.9±0.6	-0.67±0.29	0.66±0.36	0,013	-2,91	**<0,02**
Chloride of Serum, mM/L	96.1±0.7	99.6±1.0	-0.68±0.26	0.68±0.39	0,027	-2,89	**=0,02**
Calciemia, mM/L	2.56±0.37	3.80±0.07	-0.72±0.43	0.72±0.08	0,272	-3,25	**<0,02**
Phosphatemia, mM/L	1.28±0.03	1.36±0.02	-0.55±0.42	0.53±0.36	0,051	-1,97	**>0,05**
$(Ca/K)^{0,5}$ ratio of Serum	0.59±0.08	1.03±0.10	-0.73±0.26	0.73±0.34	0,374	-3,39	**<0,01**
α-LP Cholesterol, mM/L	0.87±0.06	0.80±0.08	0.24±0.40	-0.24±0.51	0,177	0,75	>0,5
nonα-LP Cholesterol, mM/L	1.00±0.15	1.07±0.05	-0.15±0.62	0.15±0.23	0.229	-0,46	>0,5
Triglycerides, mM/L	1.08±0.02	1.06±0.03	0.19±0.35	-0.20±0.56	0,052	0,60	>0,5
Diene conjugates, E^{232}/mL	1.47±0.21	1.48±0.08	-0.01±0.63	0.02±0.23	0,231	-0,04	>0,9
Malondialdehyde, µM/L	69±11	58±4	0.31±0.60	-0.31±0.22	0,279	0,97	>0,2
Superoxide dismutase, U/mL	50.7±5.5	73.0±6.1	-0.66±0.33	0.66±0.36	0,275	-2,71	**<0,05**
Catalase of Erythroc, µM/L•h	230±7	225±34	0.05±0.14	-0.05±0.65	0,232	0,14	>0,9
Catalase of Serum, µM/L•h	147±15	139±21	0.11±0.40	-0.11±0.54	0,271	0,33	>0,9
Alaninami-notranspher, µKat/L	0.58±0.08	0.48±0.05	0.32±0.55	-0.32±0.32	0,288	1,02	>0,2

Table 2.29 (cont)

1	2	3	4	5	6	7	8
Aspartatami-notransph, μKat/L	0.25±0.03	0.17±0.02	0.56±0.45	-0.57±0.29	0,323	2,10	**>0,05**
Creatin Phosphokinase, IU/L	1.70±0.02	1.66±0.21	0.06±0.08	-0.06±0.67	0,184	0,18	>0,9
Acid Phosphatase, IU/L	36.0±2.4	27.8±0.9	0.72±0.41	-0.72±0.16	0,180	3,25	**<0,02**
Alkaline Phosphatase, IU/L	579±22	290±24	0.90±0.14	-0.90±0.15	0,367	8,85	**<10^{-3}**

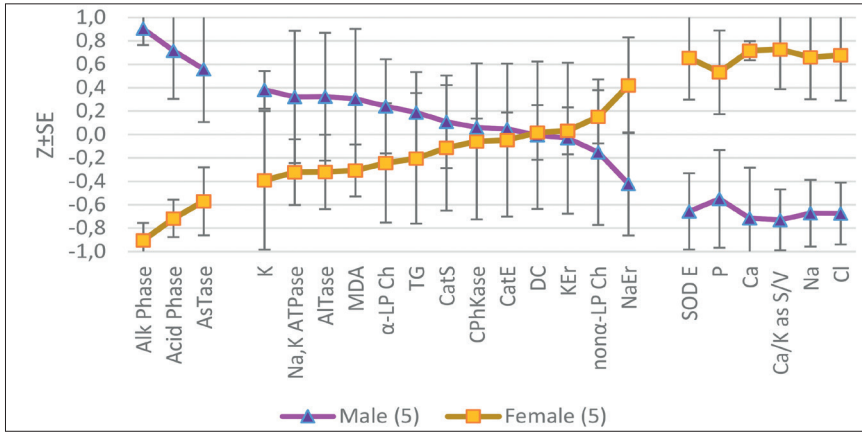

Fig. 2.21. Profile of Metabolic variables in intact rats

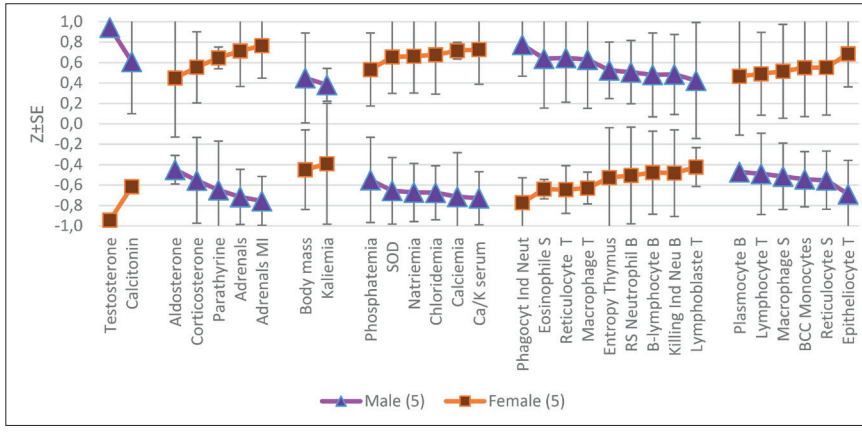

Fig. 2.22. Profile of endocrine, metabolic and immune parameters in intact rats

Figure 2.22 brings together endocrine, metabolic and immune parameters in intact rats for which significant or borderline sex differences were found, i.e. it visualizes sexual dimorphism.

Interestingly, control rats, loaded with tap water for a week, slightly increased body weight, and to a greater extent in males, so that the sex difference became clearer. This is probably due to a greater appetite stimulated by the loading procedure as a mild aversive stress []. The next day after a stronger, but still moderate, acute stress, it was found that the sex differences between the parameters of adrenals as well as PTH levels also increased. In addition, a slight difference between the levels of catecholamines appeared in favor of males (Table 2.30 and Fig. 2.23).

Table 2.30. Sexual dimorphism in endocrine and autonomic parameters in control stressed rats

Sex	**Males (5)**	**Females (5)**	**Males (5)**	**Females (5)**	**Parameters of Student's statistics**		
Variables	**Raw values**		**Z-scores**		**Cv**	**t**	**p**
Body mass, g	238±8	212±9	0.58±0.36	-0.58±0.39	0,099	2,21	**>0,05**
Adrenal glands mass, mg	47±1.5	76±3	-0.89±0.09	0.89±0.21	0,259	-7,85	**$<10^{-3}$**
Adrenal mass index, mg/100g	20.0±1.4	35.7±1.3	-0.90±0.16	0.90±0.15	0,313	-8,41	**$<10^{-3}$**
Corticosterone, nM/L	334±37	466±21	-0.69±0.40	0.70±0.23	0,236	-3,05	**<0,02**
Aldosterone, pM/L	580±23	695±43	-0,77±0.30	0.77±0.26	0,117	-3,86	**<0,01**
Testosterone, nM/L	38.1±3.6	3.28±0.24	0.91±0.19	-0.91±0.01	0,923	9,78	**$<10^{-3}$**
Calcitonin, ng/L	31.9±2.4	25.6±0.8	0.63±0.48	-0.63±0.16	0,174	2,51	**<0,05**
Parathyroid hormone, µg/L	151±11	205±6	-0.80±0.32	0.80±0.17	0,190	-4,38	**<0,01**
Triiodothyronine, nM/L	3.22±0.08	3.37±0.30	-0.16±0.16	0.16±0.60	0,141	-0,52	>0,5
Mode as catecholamines, msec	142±9	168±15	0.43±0.30	-0.44±0.51	0,188	1,46	**>0,1**
AMo as sympathetic tone, %	63±7	53±9	0.28±0.40	-0.28±0.50	0,302	0,87	>0,2
MxDMn as vagal tone, msec	28±8	31±12	-0.08±0.37	0.08±0.56	0,750	-0,23	>0,5

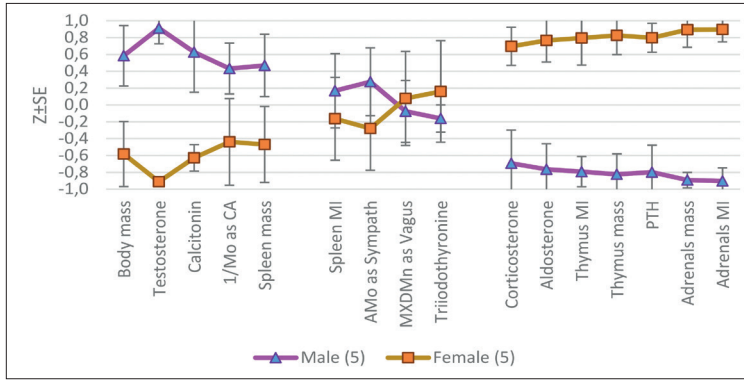

Fig. 2.23. Profile of body, thymus, spleen, adrenal glands mass, and neuro-endocrine variables in stressed rats

The expected post-stress decrease in thymus mass was more pronounced in males. This was accompanied by a somewhat more pronounced decrease in the percentage of lymphocytes in the thymocytogram. In contrast, in females, the percentage of lymphoblasts decreased and macrophages increased to a greater extent, so that sex differences increased in the former and decreased in the latter (Table 2.31 and Fig. 2.24).

Table 2.31. Sexual dimorphism in thymus and thymocytogram parameters in control stressed rats

Sex	**Males (5)**	**Females (5)**	**Males (5)**	**Females (5)**	**Parameters of Student's statistics**		
Variables	**Raw values**		**Z-scores**		**Cv**	**t**	**p**
Thymus mass, mg	117±6	159±6	-0.82±0.24	0.82±0.23	0,182	-4,94	**<0,01**
Thymus mass index, mg/100g	49±3	76±5	-0.79±0.18	0.79±0.32	0,264	-4,29	**<0,01**
Lymphocytes, %	60.3±2.3	66.6±3.2	-0.46±0.34	0.46±0.47	0,108	-1,51	**>0,1**
Lymphoblastes, %	7.75±0.66	5.80±0.49	0.61±0.41	-0.61±0.31	0,236	2,15	**>0,05**
Epitheliocytes, %	6.73±0.47	8.91±0.76	-0.62±0.27	0.62±0.43	0,224	-2,34	**<0,05**
Macrophages, %	8.25±1.16	5.80±0.49	0.54±0.51	-0.54±0.22	0,324	1,72	**>0,1**
Reticulocytes, %	5.77±0.83	2.89±0.87	0.61±0.35	-0.61±0.37	0,543	2,23	**>0,05**
Fibroblastes, %	6,75±0.37	6.00±0.84	0.26±0.26	-0.27±0.59	0,223	0,80	>0,5
Basophiles, %	2.50±0.39	2.60±0.87	-0.04±0.27	0.04±0.61	0,558	-0,10	>0,9
Hassal's corpuscles, %	2.00±0.32	1.40±0.24	0.44±0.47	-0.44±0.36	0,397	1,36	>0,2
Thymocytogram Entropy •10^3	670±22	588±42	0.50±0.26	-0.50±0.51	0,132	1,68	**>0,1**

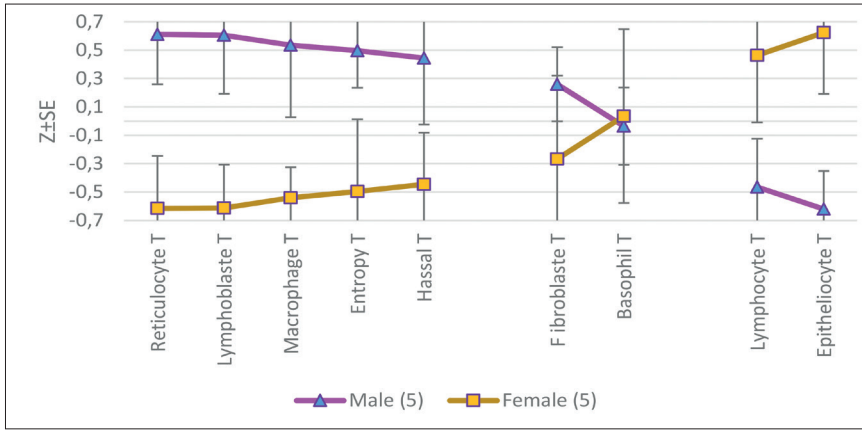

Fig. 2.24. Profile of Thymocytogram variables in stressed rats

The spleen mass decreased less significantly after stress than the thymus, but still somewhat more in males. This was accompanied by a decrease in the percentage of microphages in the splenocytogram of males, while there were no changes in females. On the other hand, stress eliminated the sex differences in the percentage of reticulocytes and even reversed those of macrophages: if in intact rats the percentage of reticulocytes in females significantly prevailed, and macrophages slightly, then after stress, due to the opposite changes, the differences in the former were eliminated, and in the latter there was a significant advantage of males. On the other hand, stress eliminated the advantage of males in the percentage of eosinophils in the same way (Table 2.32 and Fig. 2.25).

Table 2.32. Sexual dimorphism in spleen and splenocytogram parameters in control stressed rats

Sex	**Males (5)**	**Females (5)**	**Males (5)**	**Females (5)**	**Parameters of Student's statistics**		
Variables	**Raw values**		**Z-scores**		**Cv**	**t**	**p**
1	2	3	4	5	6	7	8
Spleen mass, mg	780±49	656±60	0.47±0.37	-0.47±0.35	0,184	1,61	**>0,1**
Spleen mass index, mg/100g	330±25	311±28	0.17±0.44	-0.16±0.49	0,178	0,50	>0,5
Lymphocytes, %	72.0±2.8	70.0±3.2	0.16±0.43	-0.16±0.50	0,090	0,44	>0,5

Table 2.32 (cont)

1	2	3	4	5	6	7	8
Lymphoblastes, %	6.50±0.92	7.00±1.58	-0.09±0.34	0.09±0.58	0,406	-0,26	>0,5
Plasmocytes, %	1.75±0.37	2.60±0.75	-0.32±0.28	0.32±0.56	0,608	-0,99	>0,2
Microphages, %	9.50±0.92	13.0±1.84	-0.49±0.26	0.49±0.51	0,319	-1,64	**>0,1**
Rod-shaped neutrophils, %	2.00±0.45	1.80±0.37	0.11±0.51	-0.11±0.43	0,461	0,31	>0,5
Macrophages, %	3.00±0.32	1.60±0.40	0.66±0.30	-0.66±0.38	0,461	2,58	**<0,05**
Reticulocytes, %	2.50±0.50	2.80±0.37	-0.16±0.53	0.16±0.40	0,356	-0,44	>0,5
Eosinophils, %	2.75±0.92	1.20±0.37	0.46±0.54	-0.46±0.22	0,853	1,38	>0,2
Splenocytogram Entropy •10^3	510±34	508±37	0.01±0.45	-0.01±0.49	0,149	0,02	>0,9

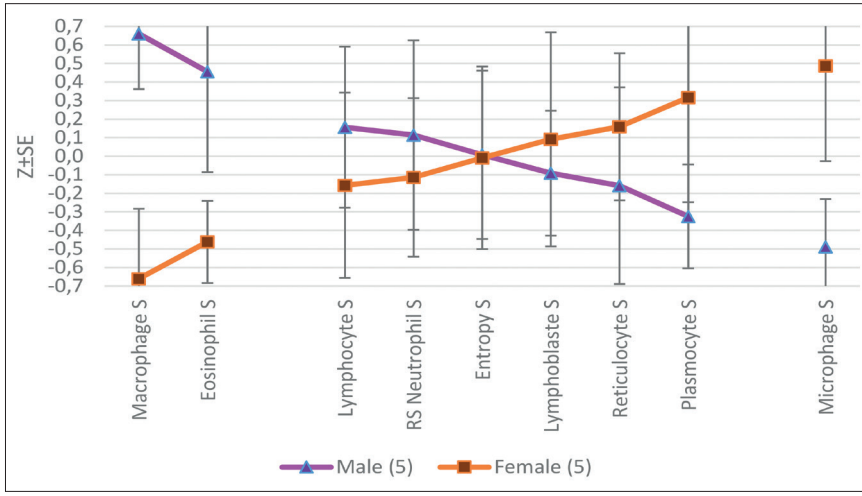

Fig. 2.25. Profile of Splenocytogram variables in stressed rats

The absence of significant sex differences in the content of lymphocytes in the blood and their populations in intact rats persisted after acute stress (Table 2.33 and Fig. 2.26). This is due to the same decrease in T-cytolytic and increase in NK lymphocytes for both sexes.

The slight single sex difference in the percentage of rod-shaped neutrophils in intact rats was completely eliminated by acute stress (Table 2.34 and Fig. 2.27).

Table 2.33. Sexual dimorphism in blood lymphocyte populations in control stressed rats

Sex	Males (5)	Females (5)	Males (5)	Females (5)	Parameters of Student's statistics		
Variables	**Raw values**		**Z-scores**		**Cv**	**t**	**p**
Pan Lymphocytes, 10^9/L	6.98±0.76	7.06±1.03	-0.02±0.40	0.02±0.54	0,270	0,07	>0,9
TR T-helper Lymphocytes, %	31.0±1.1	31.8±1.2	-0.16±0.45	0.16±0.48	0,080	-0,48	>0,5
TS T-cytolytic Lymphocytes, %	11.6±0.2	12.2±1.9	-0.11±0.09	0.11±0.66	0,239	-0,32	>0,5
NK Lymphocytes, %	6.68±0.38	5.68±0.54	0.45±0.34	-0.44±0.48	0,182	1,51	**>0,1**
B Lymphocytes, %	13.8±1.1	11.8±1.1	0.39±0.42	-0.39±0.44	0,198	1.30	>0,2
Plasmocytes, %	0.11±0.11	0.74±0.74	-0.27±0.09	0.28±0.64	2,752	-0,85	>0,5
0 Lymphocytes, %	36.8±0.5	37.8±3.3	-0.10±0.09	0.10±0.66	0,133	-0,29	>0,5
Immunocytogram Entropy •10^3	801±8	787±28	0.15±0.19	-0.15±0.63	0,055	0,46	>0,5

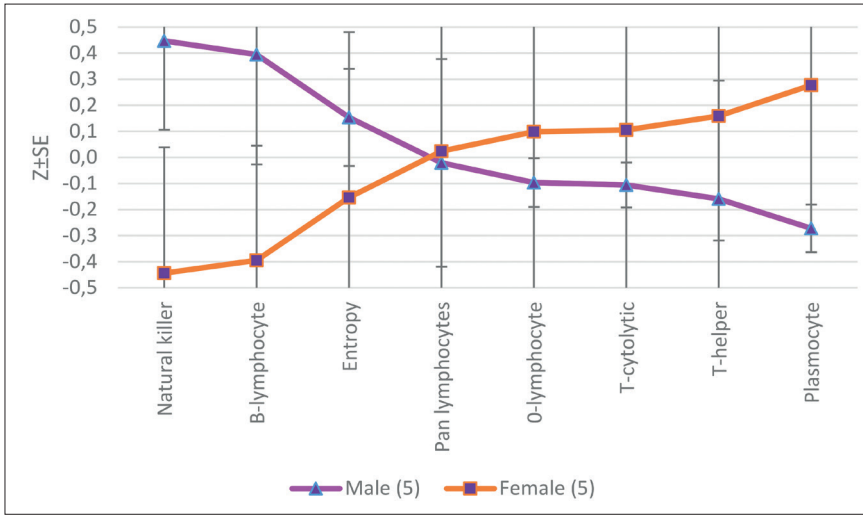

Fig. 2.26. Profile of Immunocytogram variables in stressed rats

Table 2.34. Sexual dimorphism in blood leukocyte populations in control stressed rats

Sex	Males (5)	Females (5)	Males (5)	Females (5)	Parameters of Student's statistics		
Variables	**Raw values**		**Z-scores**		**Cv**	**t**	**p**
Leukocytes, 10^9/L	14.9±1.7	15.2±2.2	-0.04±0.40	0.04±0.54	0,277	-0,12	>0,9
Pan lymphocytes, %	47.1±1.8	47.4±4.5	-0.02±0.24	0.02±0.62	0,153	-0,07	>0,9
PMN neutrophils, %	41.9±2.7	40.0±4.4	0.12±0.34	-0.12±0.57	0,190	0,36	>0,5
Rod-shaped neutrophils, %	2.60±0.68	2.80±0.37	-0.09±0.59	0.09±0.32	0,429	-0,26	>0,5
Eosinophils, %	2.76±0.82	3.40±0.87	-0.18±0.45	0.18±0.48	0,591	-0,53	>0,5
Monocytes, %	5.62±0.81	6.00±0.55	-0.13±0.55	0.13±0.37	0,253	-0,39	>0,5
Leukocytogram Entropy •10^3	658±15	671±11	-0.21±0.53	0.21±0.38	0,044	-0,64	>0,5

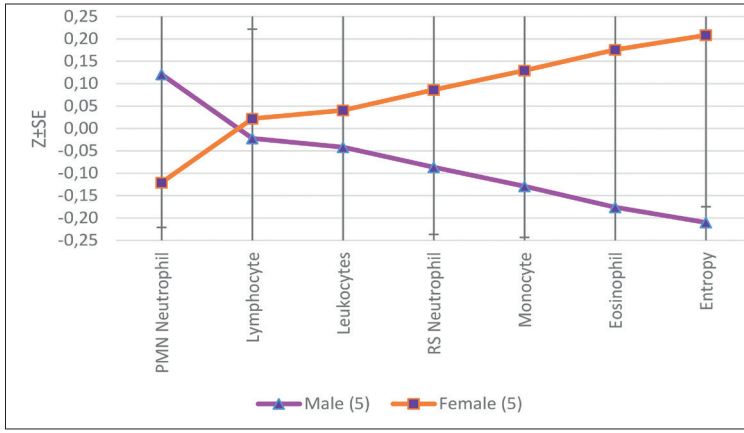

Fig. 2.27. Profile of Leukocytogram variables in stressed rats

The bactericidal capacity of neutrophils, the same in intact rats of both sexes, does not change after acute stress in females, and in males increases due to an increase, primarily, in their absolute content in the blood and, to a lesser extent, in the intensity of phagocytosis, which overlaps the post-stressor decrease in the completeness of phagocytosis in the absence of changes in its activity. On the other hand, the bactericidal capacity of monocytes, higher in intact females due to their absolute content in the blood, after acute stress increases in rats of both sexes, leveling the differences. In females, this is realized due to an increase in the intensity

and activity of phagocytosis, and in males due to, primarily, an increase in the absolute content of monocytes and, to a lesser extent, their activity (Table 2.35 and Fig. 2.28).

Table 2.35. Sexual dimorphism in parameters of phagocytic function of blood neutrophils and monocytes in control stressed rats

Sex	**Males (5)**	**Females (5)**	**Males (5)**	**Females (5)**	**Parameters of Student's statistics**		
Variables	**Raw values**		**Z-scores**		**Cv**	**t**	**p**
Pan neutrophils, 10^9/L	6.71±0.99	6.62±1.48	0.01±0.37	-0.02±0.56	0,399	0,04	>0,9
Phagocytosis index neutroph, %	58.4±2.6	51.0±1.8	0.60±0.43	-0.60±0.29	0,112	2,33	**<0,05**
Microbial count neutroph, B/Ph	6.2±0.5	5.2±0.2	0.53±0.52	-0.53±0.21	0,166	1,89	**>0,1**
Killing index neutrophils, %	46.6±4.3	42.8±4.5	0.20±0.45	-0.20±0.47	0,213	0,61	>0,5
BC capacity neutrophils, 10^9 B/L	11.3±2.2	7.26±1.4	0.46±0.50	-0.46±0.31	0,477	1,57	**>0,1**
Monocytes, 10^9/L	0.81±0.11	0.93±0.16	-0.20±0.37	0.20±0.54	0,339	0,61	>0,5
Phagocytosis index monocyt, %	6.2±0.7	6.8±1.3	-0.13±0.32	0.13±0.58	0,350	-0,40	>0,5
Microbial count monocyte, B/Ph	4.2±0.4	5.6±1.4	-0.31±0.17	0.31±0.61	0,456	-0,99	>0,2
Bactericidal capac mon, 10^6 B/L	207±39	460±237	-0.33±0.10	0.33±0.62	1,143	-1,05	>0,2

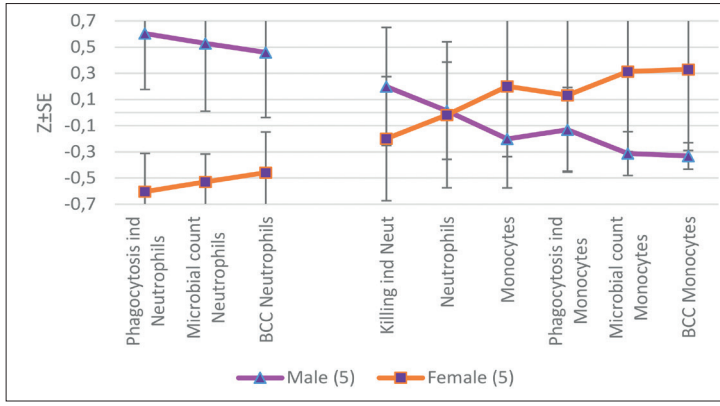

Fig. 2.28. Profile of Phagocytosis variables in stressed rats

The effects of acute stress on sex differences in metabolic parameters fit into seven patterns (Table 2.36 and Fig. 2.29). In particular, stress initiates a female preference for diene conjugates and increases it for SOD activity and serum calcium, while decreasing their preference for serum sodium and chloride, and reversing it for phosphate to a male preference. On the other hand, acute stress reduces the male preference for alkaline and acid phosphatase activity and eliminates it for aspartate aminotransferase, while initiating a male preference for alanine aminotransferase, α-LP cholesterol and serum potassium.

Table 2.36. Sexual dimorphism in metabolic parameters in control stressed rats

Sex	**Males (5)**	**Females (5)**	**Males (5)**	**Females (5)**	**Parameters of Student's statistics**		
Variables	**Raw values**		**Z-scores**		**Cv**	**t**	**p**
1	2	3	4	5	6	7	8
Na,K-ATP-ase Eryth, M/L•h	0.57±0.05	0.59±0.06	-0.13±0.45	0.12±0.49	0,193	-0,37	>0,5
Sodium of Erythrocyte, mM/L	33.7±3.4	27.5±2.8	0.42±0.46	-0.42±0.38	0,242	1,39	>0,2
Potassium of Erythroc, mM/L	80±6	81±2	-0.06±0.64	0.06±0.19	0,118	-0,18	>0,9
Potassium of Serum, mM/L	4.37±0.24	3.21±0.19	0.76±0.31	-0.76±0.25	0,202	3,77	**<0,01**
Sodium of Serum, mM/L	128.1±2.8	134.8±0.6	-0.61±0.50	0.61±0.11	0,042	-2,36	**<0,05**
Chloride of Serum, mM/L	91.9±3.5	101.1±1.0	-0.63±0.48	0.63±0.14	0,076	-2,52	**<0,05**
Calciemia, mM/L	2.50±0.37	4.06±0.09	-0.78±0.37	0.78±0.09	0,303	-4,14	**<0,01**
Phosphatemia, mM/L	1.32±0.05	1.19±0.06	0.47±0.38	-0.46±0.44	0,110	1,60	**>0,1**
$(Ca/K)^{0,5}$ ratio of Serum	0.59±0.12	1.28±0.08	-0.82±0.28	0.82±0.19	0,450	-4,82	**<0,01**
α-LP Cholesterol, mM/L	0.82±0.04	0.63±0.05	0.70±0.32	-0.69±0.33	0,187	3,03	**<0,02**
nonα-LP Cholesterol, mM/L	0.79±0.13	0.77±0.16	0.03±0.41	-0.03±0.53	0,388	0,09	>0,9
Triglycerides, mM/L	1.12±0.06	1.05±0.04	0.32±0.52	-0.32±0.36	0,106	1,01	>0,2
Diene conjugates, E^{232}/mL	1.32±0.10	1.70±0.13	-0.60±0.31	0.60±0.42	0,208	-2,31	**=0,05**
Malondialde-hyde, μM/L	58±7	54±4	0.16±0.57	-0.16±0.34	0,220	0,48	>0,5

Table 2.36 (cont)

1	2	3	4	5	6	7	8
Superoxide dismutase, U/mL	48.0±1.5	70.2±6.7	-0.71±0.10	0.71±0.43	0,263	-3,21	**<0,02**
Catalase of Erythroc, μM/L•h	216±19	188±20	0.32±0.44	-0.32±0.46	0,215	1,01	>0,2
Catalase of Serum, μM/L•h	121±16	111±20	0.13±0.41	-0.13±0.52	0,333	0,40	>0,5
Alaninami-notranspher, μKat/L	0.91±0.18	0.57±0.06	0.50±0.54	-0.50±0.18	0,458	1,74	**>0,1**
Aspartatami-notransph, μKat/L	0.29±0.08	0.25±0.03	0.16±0.63	-0.16±0.21	0,455	0,48	>0,5
Creatin Phosphokinase, IU/L	1.80±0.05	1.85±0.13	-0.09±0.20	0.09±0.49	0,114	-0,35	>0,5
Acid Phosphatase, IU/L	36.5±2.3	28.0±2.5	0.63±0.34	-0.63±0.36	0,210	2,54	**<0,05**
Alkaline Phosphatase, IU/L	494±30	264±32	0.84±0.22	-0.84±0.23	0,363	5,27	**$<10^{-3}$**

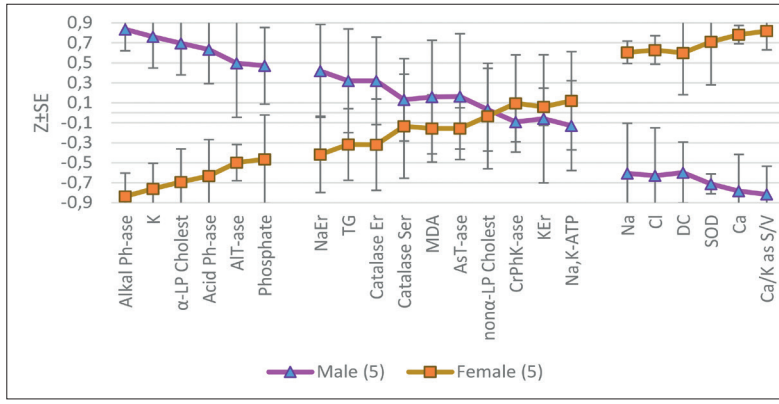

Fig. 2.29. Profile of Metabolic variables in stressed rats

A separate constellation is formed by indicators of stress damage to classical targets – gastric mucosa and myocardium. In intact rats, there are no sex differences in ST joint and T wave ECG voltage (see Table 2.24). Acute stress (S) caused their depression. It was found (Fig. 2.30) that the degree of depression of these markers of myocardial dystrophy in males is less, and concomitant damage to the gastric mucosa was limited to speckled erosions, while ulcers also occurred in females. Taken together, these differences indicate a higher stress tolerance of males.

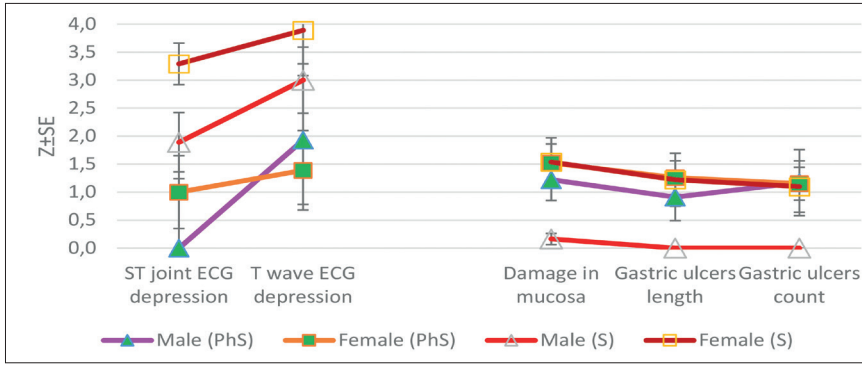

Fig. 2.30. Profile of post stress damage to myocardium and gastric mucosa in control and **pretreated** rats

The complete picture of sexual dimorphism in endocrine, metabolic, immune and damaged parameters in stressed rats is shown in Fig. 2.31. It turns out that in control stressed rats significant and borderline sex differences are recorded for 42 variables versus 30 variables in intact animals (see Fig. 2.22). In other words, acute stress expands sexual dimorphism.

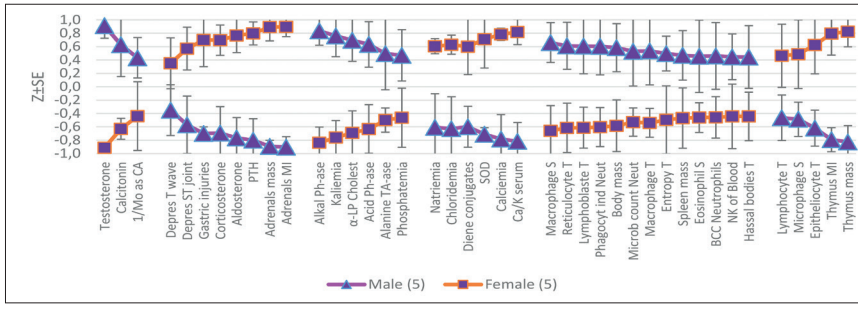

Fig. 2.31. Profile of endocrine, metabolic, immune and damaged parameters in stressed rats

Preventive use of the phytocomposition eliminated the difference in body weight by reducing its gain in males and increasing it in females. In contrast, the level of triiodothyronine increased slightly in males and decreased slightly in females, so that the sex differences became significant (Table 2.37 and Fig. 2.32).

Table 2.37. Sexual dimorphism in endocrine and autonomic parameters in pretreated stressed rats

Sex	Males (8)	Females (10)	Males (8)	Females (10)	Parameters of Student's statistics		
Variables	**Raw values**		**Z-scores**		**Cv**	**t**	**p**
Body mass, g	226±11	224±10	0.04±0.39	-0.04±0.35	0,123	0,16	>0,9
Adrenal glands mass, mg	48±2	70±3	-0.82±0.16	0.82±0.21	0,223	-6,20	$<10^{-3}$
Adrenal mass index, mg/100g	22±1	32±2	-0.76±0.11	0.75±0.28	0,257	-5,05	$<10^{-3}$
Corticosterone, nM/L	315±30	410±38	-0.45±0.24	0.45±0.36	0,292	-1,96	>0,05
Aldosterone, pM/L	591±14	677±22	-0.62±0.20	0.62±0.32	0,112	-3,28	<0,01
Testosterone, nM/L	37.3±1.8	3.09±0.26	0.96±0.08	-0.96±0.01	0,879	19,1	$<10^{-3}$
Calcitonin, ng/L	33.6±2.3	26.3±0.6	0.65±0.41	-0.65±0.11	0,195	3,06	<0,01
Parathyroid hormone, µg/L	168±14	198±6	-0.47±0.45	0.48±0.18	0,177	-1,94	>0,05
Triiodothyronine, nM/L	3.78±0.19	3.16±0.18	0.55±0.28	-0.55±0.31	0,164	2,42	<0,05
Mode as catecholamines, msec	154±11	170±5	0.35±0.47	-0.35±0.20	0,146	1,35	>0,1
AMo as sympathetic tone, %	78±7	62±5	0.45±0.39	-0.45±0.26	0,257	1,91	>0,05
MxDMn as vagal tone, msec	22±6	22±4	0.00±0.43	0.00±0.31	0,623	-0,02	>0,9

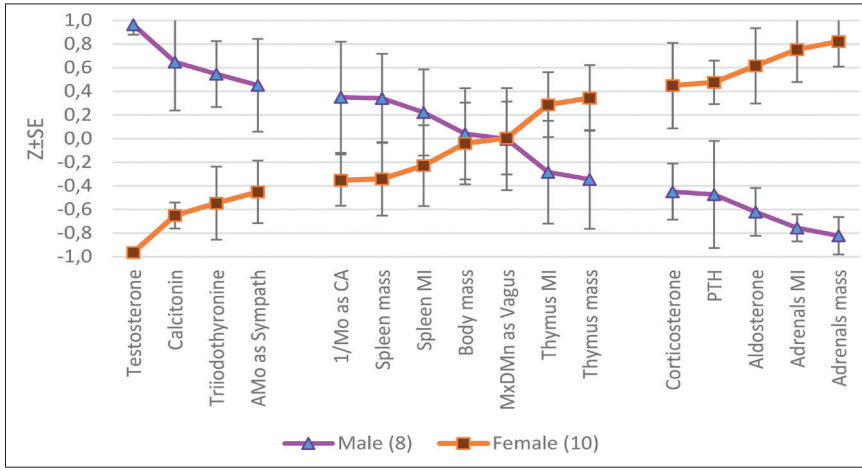

Fig. 2.32. Profile of body, thymus, spleen, adrenal glands mass, and neuro-endocrine variables in pretreated stressed rats

Preventive use of phytoadaptogen leveled post-stress sexual differences in thymus mass by increasing its involution in females. At the same time, in

males, the post-stress percentage in the thymocytogram of lymphoblasts, macrophages and reticulocytes decreased, but epithelial cells increased, while in females the changes had the opposite direction, so that there was a reversion of sexual dimorphism of both the elements of the thymocytogram and its entropy (Table 2.38 and Fig. 2.33).

Table 2.38. Sexual dimorphism in thymus and thymocytogram parameters in pretreated stressed rats

Sex	**Males (8)**	**Females (10)**	**Males (8)**	**Females (10)**	**Parameters of Student's statistics**		
Variables	**Raw values**		**Z-scores**		**Cv**	**t**	**p**
Thymus mass, mg	118±16	144±10	-0.35±0.42	0.34±0.28	0,286	-1,37	**>0,1**
Thymus mass index, mg/100g	54±9	66±6	-0.28±0.44	0.29±0.27	0,336	-1,11	>0,2
Lymphocytes, %	67.0±1.2	65.2±1.0	0.30±0.35	-0.30±0.35	0.045	-1,12	>0,2
Lymphoblastes, %	5.50±0.37	6.60±0.37	-0.49±0.28	0.49±0.33	0,186	-2,10	**>0,05**
Epitheliocytes, %	8.73±1.02	7.02±0.49	0.42±0.42	-0.42±0.24	0,257	1,51	**>0,1**
Macrophages, %	6.00±0.50	6.50±0.40	-0.22±0.36	0.22±0.35	0,186	-0,78	>0,2
Reticulocytes, %	3.61±0.37	3.78±0.27	-0.11±0.39	0.11±0.34	0,218	-0,38	>0,5
Fibroblastes, %	4.33±0.73	6.00±0.30	-0.55±0.41	0.55±0.20	0,292	-2,11	**>0,05**
Basophiles, %	3.00±0.95	3.40±0.54	-0.11±0.44	0.11±0.30	0,570	-0,37	>0,5
Hassal's corpuscles, %	1.83±0.14	1.50±0.17	0.36±0.27	-0.38±0.37	0,271	1,51	**>0,1**
Thymocytogram Entropy •10^3	588±19	616±13	-0.34±0.38	0.34±0.31	0.070	-1,25	>0,2

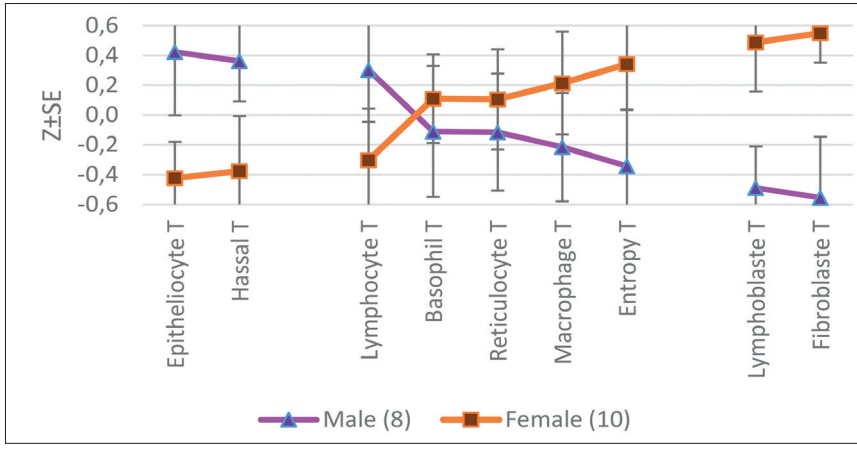

Fig. 2.33. Profile of Thymocytogram variables in pretreated stressed rats

The phytoadaptogen eliminated the post-stress advantage of males in terms of the percentage of macrophages in the splenocytogram, but increased it in terms of eosinophils (Table 2.39 and Fig. 2.34).

Table 2.39. Sexual dimorphism in spleen and splenocytogram parameters in pretreated stressed rats

Sex	Males (8)	Females (10)	Males (8)	Females (10)	Parameters of Student's statistics		
Variables	**Raw values**		**Z-scores**		**Cv**	**t**	**p**
Spleen mass, mg	689±45	608±37	0.34±0.38	-0.34±0.31	0,184	1,39	**>0,1**
Spleen mass index, mg/100g	309±25	278±24	0.22±0.36	-0.23±0.34	0,237	0,90	>0,2
Lymphocytes, %	68.2±1.6	67.1±2.6	0.09±0.22	-0.09±0.42	0,091	0,35	>0,5
Lymphoblastes, %	8.83±1.25	8.90±1.03	-0.01±0.37	0.01±0.36	0,325	-0,04	>0,9
Plasmocytes, %	2.50±0.58	2.00±0.39	0.20±0.40	-0.20±0.32	0,547	0,71	>0,2
Microphages, %	10.5±0.9	12.6±1.3	-0.32±0.23	0.32±0.39	0,285	-1,33	>0,2
Rod-shaped neutrophils, %	1.50±0.19	1.80±0.20	-0.28±0.30	0.28±0.37	0,328	-1,08	>0,2
Macrophages, %	2.33±0.29	2.40±0.37	-0.04±0.27	0.03±0.41	0,385	-0,14	>0,9
Reticulocytes, %	2.83±0.27	3.40±0.22	-0.42±0.33	0.41±0.32	0,219	-1,64	**>0,1**
Eosinophils, %	3.33±0.18	1.80±0.25	0.77±0.16	-0.78±0.25	0,386	4,96	**$<10^{-3}$**
Splenocytogram Entropy $\cdot 10^3$	54±17	551±28	0.02±0.22	-0.02±0.43	0,120	0,10	>0,5

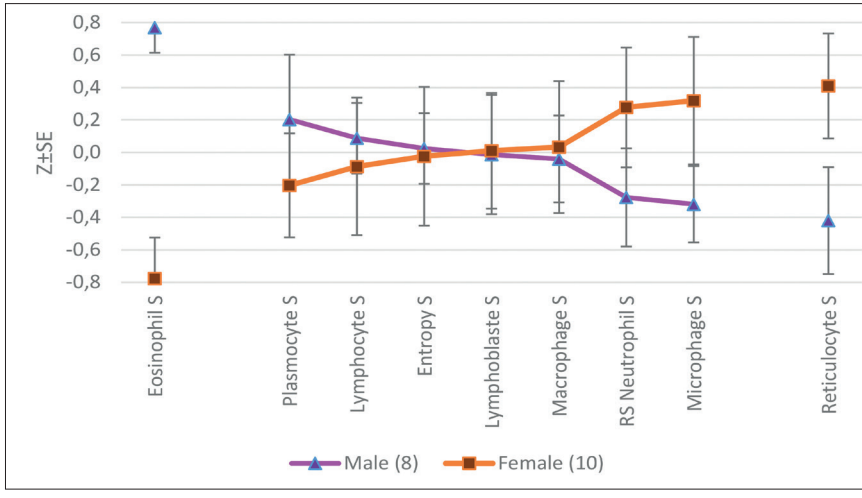

Fig. 2.34. Profile of Splenocytogram variables in pretreated stressed rats

Preventive use of phytoadaptogen did not affect the post-stress content of lymphocytes and their populations in the blood (Table 2.40 and Fig. 2.35).

Table 2.40. Sexual dimorphism in blood lymphocyte populations in pretreated stressed rats

Sex	**Males (8)**	**Females (10)**	**Males (8)**	**Females (10)**	**Parameters of Student's statistics**		
Variables	**Raw values**		**Z-scores**		**Cv**	**t**	**p**
Pan Lymphocytes, 10^9/L	6.86±0.54	7.08±0.58	-0.07±0.34	0.07±0.37	0,226	-0,18	>0,9
TR T-helper Lymphocytes, %	32.3±1.1	30.3±0.9	0.34±0.37	-0.34±0.31	0,091	1,41	**>0,1**
TS T-cytolytic Lymphocytes, %	12.8±1.1	14.0±0.9	-0.22±0.38	0.22±0.33	0,211	-0,88	>0,5
NK Lymphocytes, %	6.46±0.52	6.42±0.43	0.01±0.40	-0.02±0.33	0,202	0,06	>0,9
B-Lymphocytes, %	11.9±0.6	11.8±0.8	0.02±0.29	-0.02±0.40	0,160	0,08	>0,9
Plasmocytes, %	0.86±0.37	0.65±0.47	0.09±0.30	-0.08±0.39	1,609	0,35	>0,5
0-Lymphocytes, %	35.8±2.2	36.8±1.7	-0.09±0.41	0.09±0.32	0,149	-0,36	>0,5
Immunocytogram Entropy •10^3	807±16	806±12	0.02±0.41	-0.02±0.33	0,047	0,06	>0,9

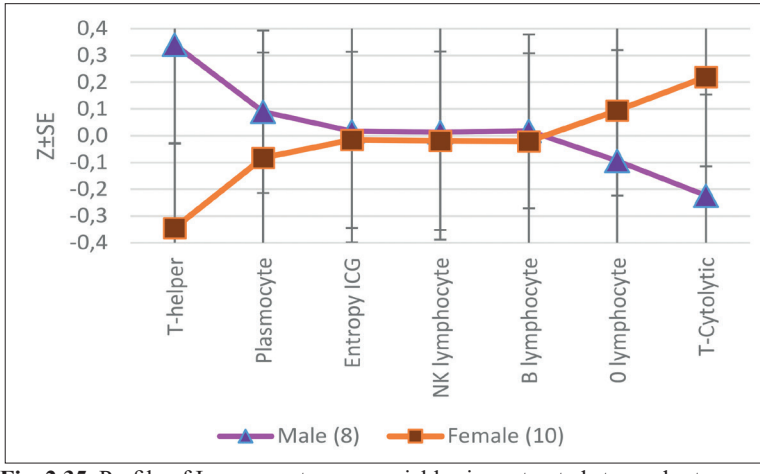

Fig. 2.35. Profile of Immunocytogram variables in pretreated stressed rats

No effect of the phytocomposition on the post-stress level of blood leukocytes and their populations was also found (Table 2.41 and Fig. 2.36).

Table 2.41. Sexual dimorphism in blood leukocyte populations in pretreated stressed rats

Sex	Males (8)	Females (10)	Males (8)	Females (10)	Parameters of Student's statistics		
Variables	**Raw values**		**Z-scores**		**Cv**	**t**	**p**
Leukocytes, 10^9/L	14.0±1.0	14.4±1.1	-0.08±0.35	0.08±0.37	0,205	-0,30	>0,5
Pan lymphocytes, %	49.1±1.1	49.0±1.3	0.01±0.33	-0.01±0.37	0,070	0,05	>0,9
PMN neutrophils, %	40.2±1.3	39.6±1.3	0.07±0.34	-0.08±0.37	0,092	0,31	>0,5
Rod-shaped neutrophils, %	2.94±0.33	2.50±0.27	0.26±0.39	-0.26±0.32	0,312	1,02	>0,2
Eosinophiles, %	2.84±0.47	3.20±0.29	-0.18±0.45	0.17±0.28	0,344	-0,66	>0,5
Monocytes, %	4.55±0.34	5.40±0.56	-0.30±0.24	0.29±0.39	0,286	-1,29	>0,2
Leukocytogram Entropy •10^3	654±15	663±9	-0.13±0.45	0.13±0.29	0,050	-0,50	>0,5

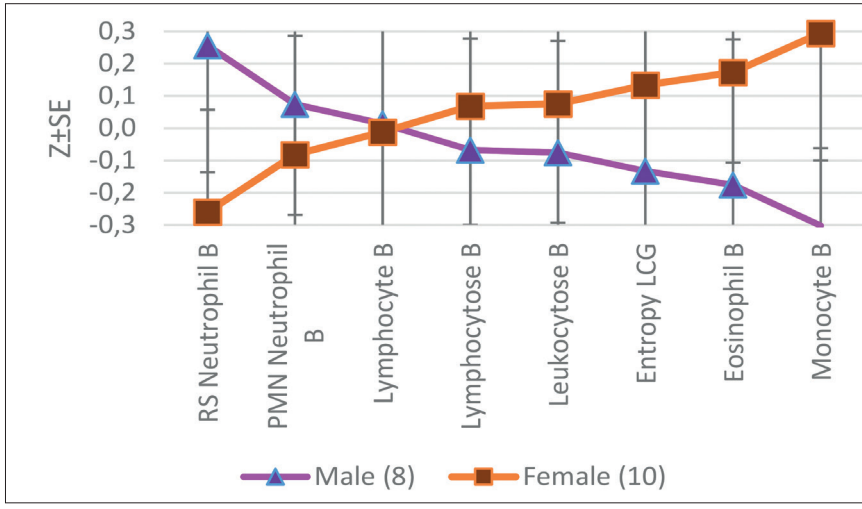

Fig. 2.36. Profile of Leukocytogram variables in pretreated stressed rats

Preventive use of phytoadaptogen eliminated sex differences in the activity of neutrophil phagocytosis, but instead initiated them in terms of its completion, so that the advantage of males in terms of bactericidal capacity of neutrophils increased (Table 2.42 and Fig. 2.37).

Table 2.42. Sexual dimorphism in parameters of phagocytic function of blood neutrophils and monocytes in pretreated stressed rats

Sex	Males (8)	Females (10)	Males (8)	Females (10)	Parameters of Student's statistics		
Variables	**Raw values**		**Z-scores**		**Cv**	**t**	**p**
Pan neutrophils, 10^9/L	5.99±0.42	6.07±0.51	-0.03±0.32	0.03±0.39	0,219	-0,12	>0,9
Phagocytosis index neutr, %	55.5±2.2	53.2±1.8	0.21±0.39	-0.21±0.33	0,101	0,82	>0,5
Microbial count neutr, B/Ph	6.4±0.3	6.0±0.4	0.22±0.31	-0.23±0.37	0,157	0,92	>0,5
Killing index neutrophils, %	48.0±3.3	35.7±1.0	0.70±0.38	-0.70±0.12	0,211	3,55	**<0,01**
BC capacity neutroph, 10^9 B/L	10.2±1.1	6.80±0.66	0.58±0.37	-0.58±0.23	0,342	2,70	**<0,02**
Monocytes, 10^9/L	0.64±0.08	0.76±0.08	-0.25±0.34	0.26±0.35	0,322	-1,05	>0,2
Phagocytosis index monoc, %	5.3±0.6	6.5±0.5	-0.37±0.36	0.36±0.32	0,292	-1,52	**>0,1**
Microbial count monoc, B/Ph	4.0±0.5	5.1±0.9	-0.25±0.23	0.25±0.41	0,487	-1,07	>0,2
Bactericidal cap mon, 10^6 B/L	155±50	271±68	-0.32±0.28	0.32±0.37	0,857	-1,37	**>0,1**

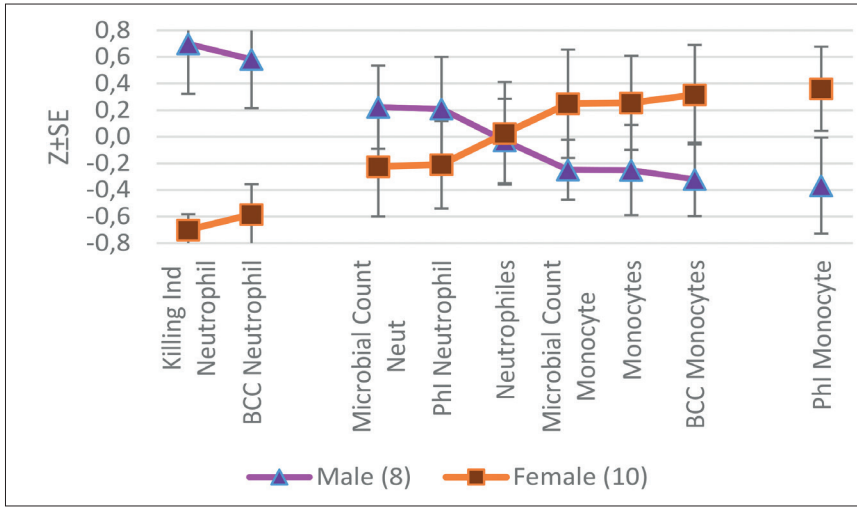

Fig. 2.37. Profile of Phagocytosis variables in pretreated stressed rats

Preventive use of phytoadaptogen significantly affects post stress sex differences in metabolic parameters (Table 2.43 and Fig. 2.30). In particular, phytoadaptogen reduces the male preference for **α-LP cholesterol** and serum potassium, eliminates it for alanine aminotransferase and phosphatemia, while initiates a male preference for aspartate aminotransferase, nonα-LP cholesterol and malondialdehyde as well as increases it for alkaline and acid phosphatase activity. On the other hand, phytoadaptogen initiates a female preference for Na,K-ATP-ase activity and potassium erythrocytes level, while decreasing their preference for serum calcium and superoxide dismutase activity.

Table 2.43. Sexual dimorphism in metabolic parameters in pretreated stressed rats

Sex	**Males (8)**	**Females (10)**	**Males (8)**	**Females (10)**	**Parameters of Student's statistics**		
Variables	**Raw values**		**Z-scores**		**Cv**	**t**	**p**
1	2	3	4	5	6	7	8
Na,K-ATP-ase Eryth, M/L•h	0.62±0.03	0.76±0.06	-0.43±0.17	0.43±0.39	0,231	-2,01	**>0,05**
Sodium of Erythrocyte, mM/L	26.2±2.0	22.9±3.9	0.17±0.21	-0.17±0.42	0,381	0,71	>0,2
Potassium of Erythroc, mM/L	72±3	86±2	-0.75±0.28	0.75±0.19	0,118	-3,88	**<0,01**
Potassium of Serum, mM/L	4.29±0.17	3.42±0.21	0.62±0.24	-0.61±0.30	0,184	3,17	**<0,01**
Sodium of Serum, mM/L	130.7±1.1	134.2±1.4	-0.44±0.27	0.44±0.36	0,030	-1,97	**>0,05**
Chloride of Serum, mM/L	94.9±1.5	100.6±2.1	-0.48±0.24	0.47±0.35	0,062	-2,23	**<0,05**
Calciemia, mM/L	2.67±0.33	3.81±0.08	-0.69±0.39	0.69±0.09	0,255	-3,42	**<0,01**
Phosphatemia, mM/L	1.17±0.08	1.21±0.06	-0.11±0.42	0.11±0.31	0,162	-0,42	>0,5
$(Ca/K)^{0,5}$ ratio of Serum	0.62±0.07	1.16±0.07	-0.75±0.19	0.76±0.25	0,401	-4,83	**$<10^{-3}$**
α-LP Cholesterol, mM/L	0.81±0.04	0.72±0.03	0.42±0.38	-0.42±0.28	0,145	1,77	**>0,05**
nonα-LP Cholesterol, mM/L	0.95±0.19	0.74±0.08	0.37±0.40	-0.37±0.29	0,342	1,43	**>0,1**
Triglycerides, mM/L	1.09±0.01	1.05±0.03	0.27±0.07	-0.28±0.44	0,069	1,26	.0,2
Diene conjugates, E^{232}/mL	1.31±0.10	1.63±0.11	-0.47±0.31	0.47±0.32	0,228	-2,13	**<0,05**
Malondialdehyde, μM/L	56.4±2.5	52.2±1.3	0.38±0.45	-0.38±0.23	0,102	1,50	**>0,1**
Superoxide dismutase, U/mL	53.8±3.8	67.0±3.7	-0.54±0.29	0.54±0.30	0,200	-2,49	**<0,02**

Table 2.43 (cont)

1	2	3	4	5	6	7	8
Catalase of Erythroc, μM/L•h	280±26	234±22	0.34±0.35	-0.34±0.33	0,262	1,37	**>0,1**
Catalase of Serum, μM/L•h	138±15	145±18	-0.08±0.31	0.08±0.39	0,327	-0,30	>0,5
Alaninamino-transpher, μKat/L	0.72±0.14	0.64±0.05	0.16±0.51	-0.15±0.21	0,374	0,52	>0,5
Aspartatamino-transph, μKat/L	0.32±0.04	0.24±0.02	0.42±0.45	-0.43±0.18	0,304	1,75	**>0,05**
Creatin Phosphokinase, IU/L	1.89±0.04	1.82±0.11	0.15±0.12	-0.15±0.44	0,132	0,63	>0,5
Acid Phosphatase, IU/L	43.4±2.1	32.4±2.9	0.61±0.22	-0.61±0.32	0,239	3,08	**<0,01**
Alkaline Phosphatase, IU/L	586±42	264±29	0.85±0.21	-0.85±0.15	0,446	6,27	**$<10^{-3}$**

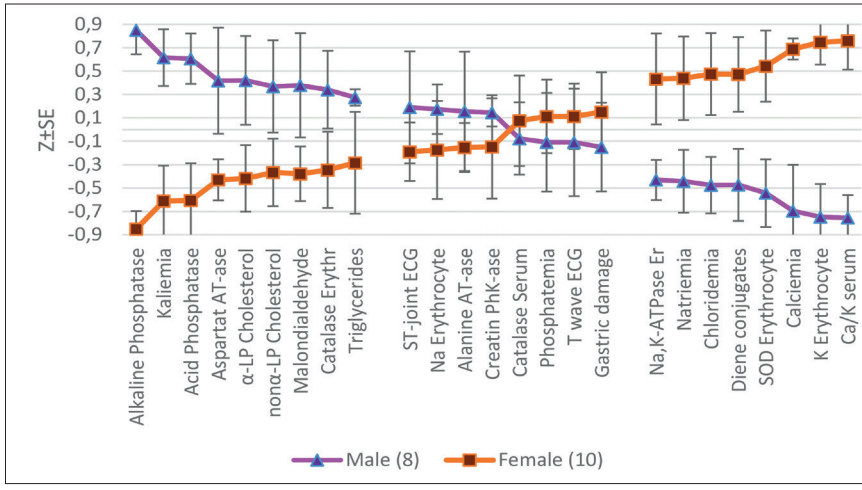

Fig. 2.38. Profile of Metabolic variables in pretreated stressed rats

In addition, phytoadaptogen eliminates sex difference in post stress damage to myocardium and gastric mucosa (see Fig. 2.30).

Fig. 2.38 shows that in in pretreated stressed rats significant and borderline sex differences are recorded for 35 variables versus 42 variables in control stressed rats and 30 variables in intact animals. In other words, phytoadaptogen reduces post stress sexual dimorphism.

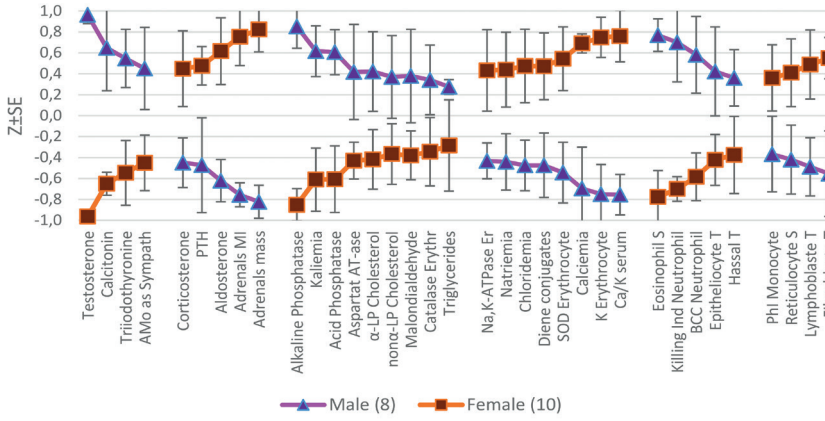

Fig. 2.38. Profile of endocrine, metabolic, and immune parameters in pretreated stressed rats

In order to identify exactly those parameters whose constellation is characteristic for each group, the available informational field was subjected to discriminant analysis by the method of forward stepwise. To include in the model (Tables 2.44 and 2.45), the program has selected 23 variables (4 **endocrine**, 6 **immune,** 9 **metabolic**, as well as 4 markers of damage in **gastric mucosa** and **myocardium**).

Table 2.44. Discriminant Function Analysis Summary

Step 23, N of vars in model: 23; Grouping: 6 grps; Wilks' Λ: 10^{-5}; approx. $F_{(115)}=4.5$; $p<10^{-6}$.

In each column, the top row is the average, the bottom is the standard error.

	Intact, control and main female and male groups (n)						Parameters of Wilks' Statistics				
Variables currently in the model	F PhC Str (10)	F CW Str (5)	F Intact (5)	M CW Str (5)	M Intact (5)	M PhC Str (8)	Wilks' Λ •10³	Partial Λ	F-remove (5.1)	p-value	Tolerancy
1	2	3	4	5	6	7	8	9	10	11	12
Testosterone, nM/L	3.09 0.26	3.28 0.27	3.53 0.24	38.1 4.1	41.8 1.7	37.3 1.8	0,018	0,457	2,38	0,114	0,273
Adrenals mass, mg	70.1 2.8	75.6 3.3	65.0 5.2	47.2 1.5	43.7 4.6	48.4 2.1	0,015	0,536	1,73	0,214	0,299

Table 2.44 (cont)

1	2	3	4	5	6	7	8	9	10	11	12
Calcitonin, ng/L	26.3 0.6	25.6 0.8	24.7 0.3	31.9 2.4	32.3 3.2	33.6 2.3	0,038	0,219	7,13	0,004	0,007
Parathyroid hormone, µg/L	198 6	205 6	185 3	151 11	154 11	168 14	0,021	0,386	3,18	0,056	0,001
Macrophages of Thymus, %	6.50 0.40	5.80 0.49	4.40 0.24	8.25 1.34	6.38 0.75	6.00 0.50	0,058	0,143	11,9	0,001	0,066
Reticulocytes of Thymus, %	3.78 0.27	2.89 0.87	2.65 0.55	5.77 0.95	5.68 1.02	3.61 0.37	0,013	0,650	1,08	0,429	0,167
Epitheliocytes of Thymus, %	7.02 0.49	8.91 0.76	9.75 0.81	6.73 0.54	6.32 0.82	8.73 1.02	0,019	0,446	2,48	0,104	0,388
Hassal's corpuscles of Thymus, %	1.50 0.17	1.40 0.24	1.00 0.00	2.00 0.37	1.00 0.00	1.83 0.14	0,016	0,501	1,99	0,166	0,229
Macrophages of Spleen, %	2.40 0.37	1.60 0.40	3.00 0.45	3.00 0.37	2.00 0.37	2,33 0.29	0,026	0,318	4,30	0,024	0,287
PMN Neutrophils of Blood, %	39.6 1.4	40.0 4.4	34.6 1.8	41.9 2.7	34.8 1.4	40.2 1.3	0,017	0,490	2,08	0,152	0,296
Damage to Gastric Mucosa, points	0.37 0.08	0.38 0.11	0	0.04 0.02	0	0.30 0.09	0,054	0,152	11,2	0,001	0,010
Gastric Ulcers Amount	2.1 0.5	2.0 0.8	0	0	0	2.1 1.1	0,022	0,371	3,39	0,048	0,018
ST joint ECG, µV	38 10	2 6	55 3	24 8	53 10	54 19	0,052	0,158	10,7	0,001	0,040
T wave ECG, µV	103 14	52 12	131 3	69 10	130 6	92 23	0,064	0,129	13,5	10^{-4}	0,019
Na,K-ATP-ase of Erythrocytes, M/L•h	0.76 0.06	0.59 0.06	0.71 0.05	0.57 0.05	0.83 0.11	0.62 0.03	0,037	0,222	7,02	0,005	0,015
Sodium of Erythro-cytes, mM/L	22.9 3.9	27.5 3.3	25.2 3.0	33.7 3.4	19.1 3.2	26.2 2.4	0,055	0,150	11,3	0,001	0,010
Aspartate Aminotra-nspherase, nKat/L	241 15	252 25	175 20	291 90	253 31	319 42	0,026	0,322	4,21	0,025	0,123

Table 2.44 (cont)

1	2	3	4	5	6	7	8	9	10	11	12
Alkaline Phosphata-se, IU/L	264 29	264 32	290 24	494 30	579 26	586 42	0,067	0,123	14,3	10^{-4}	0,040
Acid Phosphatase, IU/L	32.4 2.9	28.0 2.5	27.8 0.9	36.5 2.3	36.0 2.7	43.4 2.1	0,015	0,536	1,73	0,215	0,280
Calciemia, mM/L	3.81 0.08	4.06 0.09	3.80 0.07	2.50 0.37	2.56 0.37	2.67 0.33	0,031	0,266	5,51	0,011	0,002
Phosphatemia, mM/L	1.21 0.06	1.19 0.06	1.36 0.02	1.32 0.05	1.28 0.03	1.17 0.08	0,017	0,484	2,13	0,145	0,005
Superoxide dismuta-se, U/ mL Erythroc.	67.0 3.7	70.2 6.7	73.0 6.1	48.0 1.5	50.7 5.5	53.8 3.8	0,031	0,267	5,49	0,011	0,166
Diene conjugates, E^{232}/mL	1.63 0.11	1.70 0.13	1.48 0.08	1.32 0.10	1.47 0.21	1.31 0.10	0,013	0,616	1,25	0,358	0,365

Table 2.45 Summary of Stepwise Analysis for Variables ranked by criterion Λ

Variables currently in the model	**F to enter**	**p-level**	**Λ**	**F-value**	**p-level**
1	2	3	4	5	6
Testosterone, nM/L	25,8	10^{-6}	0,199	25,8	10^{-6}
Gastric Mucosa Injury, points	4,62	0,003	0,114	12,2	10^{-6}
Sodium of Erythrocytes, mM/L	4,02	0,007	0,068	9,12	10^{-6}
ST joint ECG, μV	4,36	0,004	0,039	8,06	10^{-6}
Alkaline Phosphatase, IU/L	3,17	0,022	0,025	7,19	10^{-6}
Adrenals mass, mg	3,69	0,011	0,015	6,85	10^{-6}
Epitheliocytes of Thymus, %	2,50	0,057	0,010	6,35	10^{-6}
T wave ECG, μV	2,35	0,070	0,007	5,99	10^{-6}
Superoxide dismutase, U/mL Erythrocytes	2,52	0,057	0,004	5,78	10^{-6}
Gastric Ulcers Amount	1,81	0,150	0,003	5,47	10^{-6}

Table 2.45 (cont)

1	2	3	4	5	6
Macrophages of Thymus, %	1,85	0,145	0,002	5,24	10^{-6}
Na,K-ATP-ase of Erythrocytes, M/L•h	2,61	0,055	0,0010	5,23	10^{-6}
Aspartate Aminotranspherase, μKat/L	2,01	0,121	0,0009	5,13	10^{-6}
Macrophages of Spleen, %	1,72	0,178	0,0006	4,99	10^{-6}
Calciemia, mM/L	1,33	0,297	0,0005	4,78	10^{-6}
Calcitonin, ng/L	1,45	0,257	0,0003	4,63	10^{-6}
Phosphatemia, mM/L	3,68	0,021	0,0002	4,97	10^{-6}
PMN Neutrophils of Blood, %	1,70	0,196	0,0001	4,91	10^{-6}
Parathyroid hormone, μg/L	2,14	0,121	0,0001	4,98	10^{-6}
Hassal's corpuscles of Thymus, %	2,02	0,143	0,0000	5,04	10^{-6}
Acid Phosphatase, IU/L	1,52	0,256	0,0000	4,98	10^{-6}
Diene conjugates, E^{232}/mL	1,08	0,424	0,0000	4,79	10^{-6}
Reticulocytes of Thymus, %	1,07	0,429	0,0000	4,62	10^{-6}

The rest of the registered variables were left out of the model, although some of them carry discriminant (recognizable) information.

Than the 23-dimensional space of discriminant variables transforms into 5-dimensional space of a canonical roots. The canonical correlation coefficient is for Root 1 0.997 (Wilks' $\Lambda=10^{-5}$; $\chi^2_{(115)}=263$; $p<10^{-6}$), root contains 89.0% of discriminative opportunities; for Root 2 0.972 (Wilks' $\Lambda=0.002$; $\chi^2_{(88)}=144$; $p=10^{-4}$), 7.7% of discriminative opportunities; for Root 3 – 0.883 (Wilks' $\Lambda=0.029$; $\chi^2_{(63)}=80$; $p=0.076$), and only 1.6% of discriminative opportunities, therefore this and the rest of the roots will be ignored in the future.

Table 2.46 presents standardized (normalized) and raw (actual) coefficients for discriminant variables as well as constants. Calculating the values of discriminant roots for each rat by raw coefficients and constants allows visualization of each animal in the information space of roots.

Table 2.46. Standardized and Raw Coefficients and Constants for Canonical Variables

Coefficients	Standardized		Raw	
Variables	Root 1	Root 2	Root 1	Root 2
Testosterone, nM/L	-0,684	-0,924	-0,085	-0,115
Gastric Mucosa Injury, points	4,523	8,095	22,12	39,57
Sodium of Erythrocytes, mM/L	7,793	4,039	0,901	0,467
ST joint ECG, μV	-4,442	0,360	-0,136	0,011
Alkaline Phosphatase, IU/L	-4,130	1,997	-0,044	0,021
Adrenals mass, mg	-0,588	-0,265	-0,078	-0,035
Epitheliocytes of Thymus, %	-0,795	0,006	-0,433	0,004
T wave ECG, μV	5,967	2,076	0,143	0,050
Superoxide dismutase, U/mL Erythrocytes	1,917	0,676	0,166	0,059
Gastric Ulcers Amount	-0,606	-5,785	-0,337	-3,212
Macrophages of Thymus, %	3,138	1,674	2,093	1,116
Na,K-ATP-ase of Erythrocytes, M/L•h	6,095	2,618	38,53	16,55
Aspartat Aminotranspherase, μKat/L	2,334	0,083	0,025	0,001
Macrophages of Spleen, %	-1,388	0,391	-1,501	0,423
Calciemia, mM/L	17,14	-11,34	27,78	-18,39
Calcitonin, ng/L	10,34	2,608	127,8	32,23
Phosphatemia, mM/L	0,052	8,961	0,319	54,76
PMN Neutrophils of Blood, %	0,946	-0,716	0,179	-0,136
Parathyroid hormone, μg/L	-9,673	17,12	-42,77	75,67
Hassal's corpuscles of Thymus, %	0,148	1,493	0,317	3,197
Acid Phosphatase, IU/L	-1,152	-0,025	-0,175	-0,004
Diene conjugates, E^{232}/mL	0,898	0,316	2,841	0,999
Reticulocytes of Thymus, %	-0,696	-1,243	-0,469	-0,838
		Constants	-153,1	-193,5
		Eigenvalues	195,3	16,81
		Cumulative Proportions	0,890	0,967

It can be seen (Fig. 2.39) that the distance between the centroids of the major discriminant root of intact females and males as a measure of sexual dimorphism is 16.2 units (2.8 + 13.4).

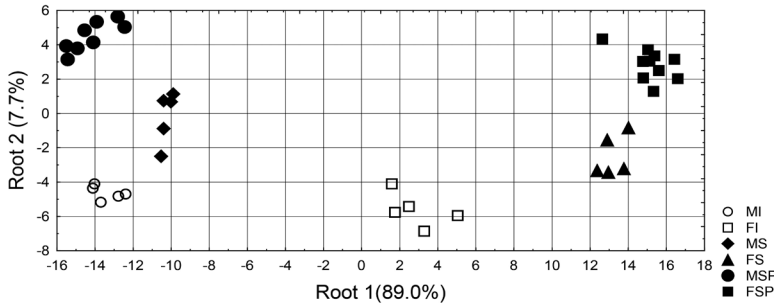

Fig. 2.39. Scattering of individual values of the first and second discriminant roots of males and females rats: intact (I), control stressed (S) and pretreated with Phytoadaptogen (SPh)

Acute stress increases it in control rats to 23.4 units (13.2 + 10.2), and in pretreated with phytoadaptogen up to 29.4 units (15.2 + 14.2). Acute stress increases the severity of sexual dimorphism also in relation to variables, information about which is condensed in the minor root – from 0.99 (-4.63 + 5.62) to 2.29 (-0.17 + 2.46) units, while preventive use of phytoadaptogen limits it to 1.63 (4.48 – 2.85) units.

The apparent clear demarcation of clusters is documented by calculating Mahalanobis distances (Table 2.47).

Table 2.47. Squared Mahalanobis Distances between clusters (above the diagonal), F-values (df=23.1) and p-levels (under the diagonal)

Clusters	Male Intact (5)	Female Intact (5)	M CW Stress (5)	F CW Stress (5)	M PhC Stress (8)	F PhC Stress (10)
Male Intact (5)	0	280	52.4	743	95.5	875
Female Intact (5)	9.5 0.0004	0	229	146	397	232
M CW Stress (5)	1.8 0.172	7.8 0.0009	0	577	60.0	670
F CW Stress (5)	25.2 10^{-5}	4.9 0.006	19.6	0	811	58.4
M PhC Stress (8)	4.0 0.014	16.6 10^{-4}	2.5	33.9	0	873
F PhC Stress (10)	39.6 10^{-6}	10.5 0.0003	30.3 10^{-5}	2.6 0.056	52.7 10^{-6}	0

The same discriminant parameters can be used to retrospective identify the belonging of one or another animal to one or another cluster. This purpose of discriminant analysis is realized with the help of classifying functions (Table 2.50).

The accuracy of classification (retrospective recognition) is **100%**.

Table 2.50. Coefficients and Constants for Classification Functions

Clusters	Male Intact (5)	Female Intact (5)	M CW Stress (5)	F CW Stress (5)	M PhC Stress (8)	F PhC Stress (10)
Variables	p=0.132	p=0.132	p=0.132	p=0.132	p=0.210	p=0.263
Testosterone, nM/L	-40,87	-42,51	-41,45	-43,18	-41,99	-44,25
Damage to Gastric Mucosa, points	12516	12832	12729	13172	12854	13437
Sodium of Erythrocytes, mM/L	166,1	179,9	171,8	190,1	168,9	195,5
ST joint ECG, μV	-20,56	-22,69	-20,84	-23,94	-20,23	-24,34
Alkaline Phosphatase, IU/L	-0,735	-1,438	-0,811	-1,847	-0,474	-1,835
Adrenals mass, mg	-6,655	-7,829	-7,059	-8,103	-6,571	-9,221
Epitheliocytes of Thymus, %	-31,33	-36,62	-32,28	-40,45	-29,04	-43,31
T wave ECG, μV	35,94	38,09	36,35	39,52	36,11	40,34
Superoxide dismutase, U/mL	33,91	36,58	34,56	38,20	34,23	39,10
Gastric Ulcers Amount	-935,4	-938,6	-949,6	-955,4	-966,9	-968,6
Macrophages of Thymus, %	450,4	482,2	462,9	507,1	457,6	518,6
Na,K-ATP-ase, M/L•h	6275	6873	6500	7269	6355	7510
Aspartat Aminotranspher, μKat/L	3814	4210	3895	4473	3788	4541
Macrophages of Spleen, %	-142,3	-165,3	-144,6	-183,1	-137,1	-181,2
Calciemia, mM/L	-2066	-1616	-2025	-1372	-2274	-1407
Calcitonin, ng/L	33605	35583	33996	36981	33745	37454
Phosphatemia, mM/L	22023	22001	22099	22119	22549	22416
PMN Neutrophils of Blood, %	-17,73	-14,82	-17,24	-12,96	-19,14	-13,58
Parathyroid hormone, μg/L	20960	20237	20986	19993	21739	20278
Hassal's corpuscles of Thymus, %	639,2	642,5	655,5	653,6	668,2	672,9
Acid Phosphatase, IU/L	-20,79	-23,28	-21,21	-24,98	-20,32	-25,72
Diene conjugates, E^{232}/mL	720,8	766,9	730,9	802,1	730,2	808,6
Reticulocytes of Thymus, %	-165,9	-173,4	-172,3	-180,3	-173,4	-186,0
Constants	-42891	-45118	-43752	-47248	-44559	-48651

Discussion

Sexual dimorphism across animals and human in nervous, endocrine and immune systems as well as metabolism has been the subject of a number of studies, but each of them was limited to one system [Ashton N & Balment RJ, 1991; Herbison AE & Spratt DP, 1995; Gaillard RC & Spinedi E, 1998; Reznikov AG et al., 2000; 2001; 2004; Spratt DP & Herbison AE, 2001; Yanes LL et al., 2006; Marassi MP et al., 2007; Nunn CL et al., 2009; Shepherd R et al., 2011; Bjelobaba I et al., 2015; Foo et al., 2017; Kelly CD et al., 2018; Jaillon S et al., 2019; Joseph-Bravo P et al., 2020; Song E et al., 2021; Alexander S et al., 2023; Zhang YY et al., 2024]. The advantage of this study, in our opinion, is the **simultaneous** comparison of parameters of the autonomic, endocrine and immune systems, which closely interact with each other within the framework of the triune neuro-endocrine-immune complex, as well as with parameters of metabolism [Popovych IL, 2007; Bilas VR et al., 2020; Popovych IL et al., 2020; 2022; Kozyavkina NV et al., 2021; Gozhenko AI et al., 2023; Korda MM et al., 2024].

The results of this study confirm, complement, and refine the results of a previous study conducted in our laboratory with a similar design on 20 intact rats and 90 rats exposed to chronic aversive stress [Popovych et al., 2018; 2020]. The most significant sex differences were found to be related to the morpho-functional parameters of the adrenal glands. In particular, females have higher androgenic, glucocorticoid, and mineralocorticoid activity, estimated according to the thickness of the reticular zone of the adrenal cortex and daily excretion in the urine of 17-ketosteroids, the thickness of the fascicular corticoadrenal zone, and the plasma level of corticosterone as well as of the thickness of glomerular zone of the adrenal cortex and plasma and urine sodium and potassium. However, females have higher parathyroid and calcitonin activities, as measured by plasma and urinary levels of calcium and phosphate. In addition, females have a smaller amount of HRV mode as an inverse measure of heart rhythm, which is subject to the so-called humoral regulation channel (circulating catecholamines, glucocorticoids, electrolytes, etc.), whereas HRV-markers of sympathetic and vagal tone are not significant. Instead, the plasma triiodothyronine level was 85±15% of the male level, and the lower plasma testosterone level requires no comment. Among the reported immune rates, 12 were significantly higher in females. First of all, this is the proportion in the thymocytogram of lymphocytes and lymphoblastes, the natural

killer cells and B-lymphocytes in the blood immunocytogram, as well as of fibroblasts, macrophages and microphages in the splenocytogram. In addition, females have a higher intensity of phagocytosis by monocytes of Staph. aureus, blood leukocytosis, RBTL on PhHA, as well as entropy of splenocytogram and immunocytogram. Instead, 10 indicators of immunity in females are significantly lower. This is, first of all, the phagocytosis activity of neutrophils and, to a lesser extent, monocytes, as well as thymocytogram entropy and its proportion of epitheliocytes, endothelial cells and macrophages, content of lymphocytes and lymphoblastes in the splenocytogram and 0-lymphocytes in immunocytogram as well as the completeness of phagocytosis by neutrophils of blood.

An important addition to the experimental data are our results of clinical observation, in which HRV and EEG were recorded almost simultaneously with the determination of the levels of adaptation hormones [Kozyavkina NV et al., 2021]. This sample is characterized (Mean±SE) by testosteronemia 3,5±0,4 nM/L vs 13,5±0,8 nM/L, and by calcitoninemia 5,7±0,4 ng/L vs 10,5±0,9 ng/L in women and men respectively. But there was no sexual dimorphism in the levels of other determined hormones: Cortisol 304±14 and 298±16 nM/L, Aldosterone 226±5 and 226±4 pM/L, Triiodothyronine 2,19±0,12 and 2,01±0,11 nM/L in women and men respectively. It was found that the Z-score (Mean±SE) for testosterone is -0,72±0,06 in women vs +0,72±0,11 in men, that is, sexual dimorphism is 1,44. The expression of sexual dimorphism of calcitoninemia is almost half as low: 0,83.

Screening of HRV and EEG parameters revealed that regardless of age, women differ significantly from men, except for drastically lower levels of testosterone and calcitonin by definition, lower levels of HRV-markers of sympathetic tone (but not heart rate), reactive anxiety, and beta-rhythm asymmetry. On the other hand, trait anxiety, levels of HRV-markers of vagal tone, variability and amplitude of the beta-rhythm, and its PSD in 12 loci (maximum differences in T6, F3, and T3 loci), amplitude of the theta-rhythm and its PSD in 16 loci (maximum differences in F3, C3, and T3 loci), PSD of the alpha-rhythm in T3, T6, F7, and T4 loci as well as entropy of PSD in F7 and F8 loci are significantly higher in women than in men. It is also worth noting the much greater variability (SE) of neuro-endocrine (but not anxiety) parameters in women compared to men (Fig. 2.40).

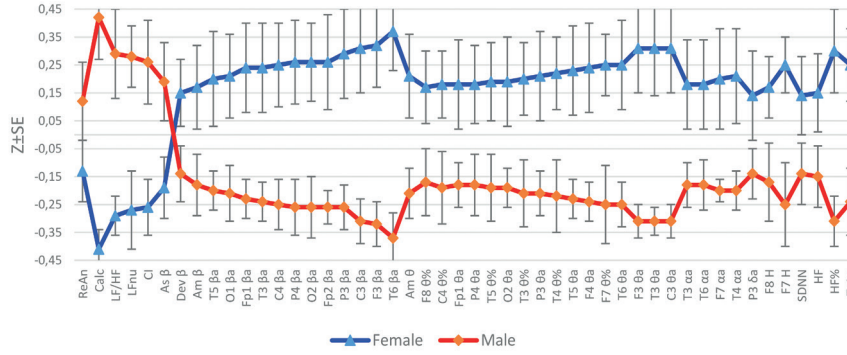

Fig. 2.40. Profiles of psycho-neuro-endocrine parameters (Z±SE) that differ in men and women. Testosterone (-0,72±0,06 vs +0,72±0,11) is not shown, so as not to coarsen the scale [Kozyavkina NV et al., 2021]

Thus, in intact rats, significant sex differences were found for a number of endocrine, immune, and metabolic variables, which increase under the influence of acute stress per se, and to an even greater extent against the background of preventive use of a phytoadaptogen. Sexual dimorphism should be taken into account in both experimental and clinical studies of new drugs and methods of treatment or prevention.

2.5. Reversion by Phytoadaptogen the adverse effects of Naftussya bioactive water on dynamic muscle performance in healthy rats

Summary.

Introduction and aim. Muscular performance is considered one of the attributes of health and non-specific resistance. Phytoadaptogens occupy an important place in the arsenal of means of increasing non-specific resistance and stress resistance. Many years of research of the Truskavetsian Scientific School of Balneology have demonstrated the adaptogenic properties of the main therapeutic factor of the resort, Naftussya bioactive water, as well as ozokerite and mineral baths. However, in contrast to the beneficial effect of the latter on stress resistance and the neuro-endocrine-immune complex, the effect on the physical performance is ambiguous. The **purpose** of this

subdivision is to test the ability of phytocomposition to prevent the adverse actotropic effect of Naftussya bioactive water at rats.

Material and methods. The experiment have been carried out at 42 female rats. Rats of the control group for 7 days loaded through a tube with tap daily water (2 mL once), while the animals of the other groups received according to a similar scheme daily water with the addition of 0,1 mL of Balm; bioactive Naftussya water per se or with the addition of 0,1 mL of Balm. The day after completion the course of water loads in the animal determined the urinary excretion of 17-ketosteroids, assessed the mineralocorticoid activity (MCA) by the urine K/Na ratio as well as the state of neutrophil phagocytosis by the number of absorbed latex particles.

Results. It was found that the weekly use of Naftyssya bioactive water reduces the duration of swimming of rats to exhaustion by 30% compared to the daily water control. Addition of phytoadaptogen to Naftyssya softens its negative actotropic effect by up to -9%, and adding Balsam to daily water prolongs the maximum duration of swimming compared to the control by 11%. A positive correlation of the swimming test with 17-KS excretion and water diuresis was revealed, but a negative correlation with MCA, spontaneous diuresis and neutrophils phagocytosis.

Conclusion. Phytoadaptogen reverses the adverse effects of Naftussya bioactive water on dynamic muscle performance in healthy rats by mitigating the decrease in the excretion of 17-ketosteroids and increased mineralocorticoid activity.

Introduction

Muscular performance is considered one of the attributes of health and non-specific resistance [Gozhenko AI, 2010; Fil VM et al., 2021; Zukow W et al., 2022]. Phytoadaptogens (ginseng, eleuterococcus, schizandra, aloe, etc.) occupy an important place in the arsenal of means of increasing non-specific resistance and stress resistance [Alyeksyeyev OI et al., 1996; Flyunt IS et al., 2002; Kostyuk PG et al., 2006; Flyunt IS et al., 2008; Panossian AG et al., 2021]. It is significant that the first informative test for the comparative evaluation of the effectiveness of phytoadaptogens was the swimming test [Brekhman II, 1968].

The experimental and clinical research of the Truskavetsian Scientific School of Balneology have demonstrated the adaptogenic properties of the main therapeutic factor of the resort, Naftussya bioactive water, as well as ozokerite and mineral baths, which together make up a standard balneotherapeutic complex. However, in contrast to the beneficial effect of the latter on stress resistance and the neuro-endocrine-immune complex, the effect on the physical performance of both rats and resort patients is ambiguous [Ruzhylo SV & Tserkovnyuk AV, 2003; Ruzhylo SV et al., 2003; Ruzhylo SV et al., 2003a; Zukow W et al., 2020; Zukow W et al., 2021; Zukow W et al., 2022].

It has recently been confirmed that weekly use of Naftussya bioactive water caused ambiguous changes in the fitness and the secretion of steroids associated with amines and phenols present in the composition of water [Zukow W et al., 2022].

The purpose of this study is to test the ability of phytocomposition "Balm Truskavets" to prevent the adverse actotropic effect of Naftussya bioactive water at rats.

Material and methods

It is known data by Datsko OR et al [2008] about organic compounds (in mg/L) water Naftussya obtained by Solid Phase Extraction method and mass-spectroscopy by using as Sorbents Tenacle GC 60/80 and Polysorb-2. Paraffins 4,10 and 4,20; monoolefins 1,67 and 1,75; dienes and monocycloolefins 0,84 and 0,85; alkylbenzene 1,55 and 1,54; alkenylbenzene 0,47 and 0,46; esters of aromatic acids 1,32 and 1,33; alkylphenols 1,14 and 1,14; polyaromatic hydrocarbons 0,077 and 0,059; oxygene-containing connections (acids) 1,12 and 1,14; sulfur-containing connections 0,30 and 0,31; alkylnaphthalenes 0,53 and 0,53; unidentified polyaromatic hydrocarbons 0,19 and 0,19; connections required subsquent identification 0,48 and 0,50 correspondingly.

Usually, due to the high cost of such analyses, the Truskavetsian Hydrogeological Operating Station conducts a simplified analysis. In the Naftussya water used in this study, the content of gross organic carbon (Corg) determined by the method of dry combustion of the sample [ГОСТ 26449, 1985] was 15,5 mg/L, organic nitrogen (Norg) determined by the Kjeldahl method [Lurye YY, 1973] – 0,52 mg/L, bitumen

(chromatographic separation in a thin layer of aluminum oxide and their subsequent luminescence measurement [Kiryukhin VK et al., 1976]) – 1,38 mg/L, carboxylic (fatty) acids (chloroform extraction method) – 50 μeqv/L, phenols (extraction-photometric method **APHA** [Lurye YY, 1973; Ivassivka SV et al., 1994]) – 0,15 mg/L.

The experimentt have been carried out at 42 female Wistar rats weighing 180-220 g. The rats of the control group for 7 days loaded through a tube with tap daily water (2 mL once), while the animals of the other groups received according to a similar scheme daily water with the addition of 0,1 mL of Balm; bioactive Naftussya water per se or with the addition of 0,1 mL of Balm.

The day after completion the course of water loads the animal were placed in individual chambers with perforated bottom for collecting for 10 hours urine, in which determined the concentration of 17-ketosteroids (by color reaction with m-dinitrobenzene). Then the animals were loaded with distilled water (6 mL) through a tube and placed in individual Plexiglas machines to collect two-hour urine, in which the concentration of potassium and sodium was determined (by flaming photometry) in order to assess mineralocorticoid activity (MCA) by the K/Na ratio. In a drop of blood from the tail vein, the state of neutrophil phagocytosis was determined by the number of absorbed latex particles, according to the instructions for the set. The next day, dynamic muscle fitness tested (by the time of swimming to exhaustion in the water t^0 26^0C).

Results and discussion

It was found that the weekly use of Naftussya bioactive water reduces the duration of swimming of rats to exhaustion by 30% compared to the daily water control. Addition of phytoadaptogen to Naftussya softens its negative actotropic effect by up to -9%, and adding Balsam to daily water prolongs the maximum duration of swimming compared to the control by 11% (Table 2.51).

In order to identify the parameters characteristic of actotropic effects, a discriminant analysis was performed. All registered parameters are included in the discriminant model, with the exception of one, obviously due to duplication/redundancy of information (Tables 2.51 and 2.52).

Table 2.51. Discriminant Function Analysis Summary for Variables

Step 5, N of vars in model: 5; Grouping: 4 grps; Wilks' Λ: 0,0250; approx. $F_{(16)}$=17,6; $p<10^{-6}$

Variables currently in the model	**Clusters of Entropy (n)**				**Parameters of Wilk's Statistics**				
	N (5)	**NB (8)**	**DW (20)**	**B (9)**	**Wilks' Λ**	**Parti-al Λ**	**F-remove (3,34)**	**p-level**	**Tole-rancy**
Swimming test, min	130 4	169 2	186 1	207 2	0,140	0,179	52,1	10^{-6}	0,600
Phagocytosis, bits/phagocyte	58.2 1.0	38.1 2.0	38.1 1.1	36.4 1.1	0,037	0,684	5,25	0,004	0,803
Ku/Nau as Mineralo-corticoid activity	2.95 0.08	2.23 0.09	1.99 0.05	1.99 0.05	0,033	0,749	3,80	0,019	0,761
Diuresis stimulated, mL/2h	4.52 0.12	5.07 0.06	5.23 0.03	5.42 0.15	0,028	0,887	1,45	0,246	0,679
Diuresis spontaneous, mL/10h	5.61 0.58	5.62 0.19	5.37 0.12	5.21 0.19	0,028	0,899	1,27	0,300	0,774
Variable currently not in model	**N (5)**	**NB (8)**	**DW (20)**	**B (9)**	Wilks' Λ	Parti-al Λ	F to enter	p-level	Tole-rancy
17-Ketosteroids, nM/10h	63.0 2.6	77.7 2.0	83.0 1.1	84.1 1.4	0,024	0,952	0,56	0,647	0,039

Notes. In each column, the first line is the average, the second – SE for variables

Table 2.52. Summary of Stepwise Analysis for physiological. The variables are ranked by criterion Lambda

Variables currently in the model	**F to enter**	**p-level**	**Λ**	**F-value**	**p-level**
Swimming test, min	181	10^{-6}	0,065	181	10^{-6}
Phagocytosis, bits/phagocyte	7,34	0,001	0,041	48,6	10^{-6}
Ku/Nau as Mineralocorticoid activity	3,88	0,017	0,031	30,9	10^{-6}
Diuresis stimulated, mL/2h	1,35	0,275	0,028	22,3	10^{-6}
Diuresis spontaneous, mL/10h	1,27	0,300	0,025	17,6	10^{-6}

The identifying information contained in the 5 discriminant variables is condensed into three roots. The major root contains 95,8% of discriminatory opportunities (r^*=0,975; Wilks' Λ=0,025; $\chi^2_{(15)}$=135; $p<10^{-6}$), while minor root – 3,4% only (r^*=0,637; Wilks' Λ=0,508; $\chi^2_{(8)}$=25; p=0,002), and the third is not worth paying attention to (0,8%; p=0,126).

Calculating the values of discriminant roots for each rat by the raw coefficients and the constant (Table 2.53) allows visualization of each animal in the information space of roots.

Judging by the structural coefficient, the major discriminant root reflects, first of all, the swimming test. The extreme left localization (centroid: -9,7) of the members of the Naftussya cluster (Fig. 2.41) reflects the duration of swimming, which is the minimum for the sample. This is accompanied by the minimal levels of water-load-stimulated diuresis and 17-ketosteroids excretion and maximally elevated levels of spontaneous diuresis and mineralocorticoid activity as well as intensity of phagocytosis. Rats of the Balm cluster are located at the opposite pole of the root axis (centroid: +4,7). This reflects their maximal/minimal levels mentioned parameters.

Table 2.53. Standardized, Structural and Raw Coefficients and Constants for Canonical Variables

Coefficients	**Standardized**		**Structural**		**Raw**	
Variables currently in the model	**Root 1**	**Root 2**	**Root 1**	**Root 2**	**Root 1**	**Root 2**
Swimming test, min	1,150	-0,521	**0,859**	-0,143	0,187	-0,085
Diuresis stimulated, mL/2h	-0,340	0,295	**0,235**	0,120	-1,298	1,127
Ku/Nau as Mineralocorticoid activity	-0,393	-0,252	**-0,331**	-0,556	-1,882	-1,208
Phagocytosis, bits/phagocyte	0,070	-0,914	**-0,318**	-0,833	0,016	-0,204
Diuresis spontaneous, mL/10h	0,328	-0,080	**-0,047**	0,139	0,500	-0,122
				Constants	-26,45	20,96
				Eigenvalues	19,33	0,685
				Cumulative Proportions	0,958	0,992

Fig. 2.41 illustrates that the addition of a phytoadaptogen to Naftussya water brings the state of these rats as close as possible to such a control (centroids: -2,1 and +1,2 respectively).

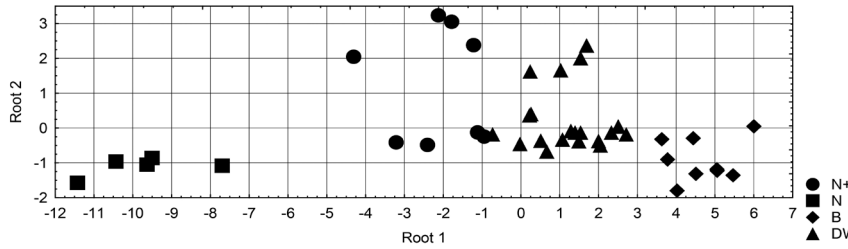

Fig. 2.41. Diagram of scattering of individual values of discriminant Roots of rats loaded by Daily Water (DW), Naftussya Bioactive Water (N), Balm (B) and Naftussya together with Balm (N+B)

All four clusters are quite clearly demarcated along the axis of even one root which is documented by calculating Mahalanobis distances (Table 2.54).

Table 2.54. Squared Mahalanobis Distances between groups (over diagonal), F-values and p-levels (under diagonal)

Groups	NB (8)	N (5)	B (9)	DW (20)
Naftussya + Balm		63,2	50,8	12,8
Naftussya	34,8 10^{-4}		208	121
Balm	38,5 10^{-4}	119 10^{-6}		13,9
Daily Water	13,1 10^{-3}	86,8 10^{-5}	15,5 10^{-3}	

Classification accuracy is 100% (Table 2.55).

Table 2.55. Classification matrix

	Rows: Observed classifications Columns: Predicted classifications				
Group	Percent Correct	N+B p=,19048	N p=,11905	B p=,21429	DW p=,47619
N+B	100	8	0	0	0
N	100	0	5	0	0
B	100	0	0	9	0
DW	100	0	0	0	20
Total	100	8	5	9	20

Of particular interest is the inverse relationship between the swimming test and the intensity of phagocytosis (Fig. 2.42).

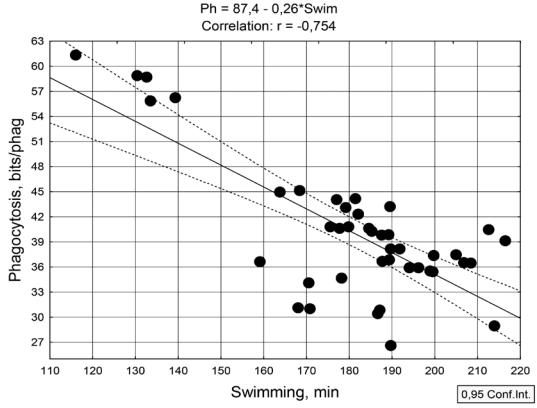

Fig. 2.42. Scatterplot of correlation between the swimming test (X-line) and intensity of phagocytosis (Y-line) in rats

This is consistent with recently published data on the combination of a decrease in the level of the cycle ergometric test with an increase in the intensity of phagocytosis of *Staphylococcus aureus* by neutrophils and monocytes of people who received Naftussya water and mineral baths [Zukow W et al., 2022a]. Phagocytosis, in turn, is upregulated by mineralocorticoids (Fig. 2.43) and downregulated by 17-Ketosteroids (Fig. 2.44).

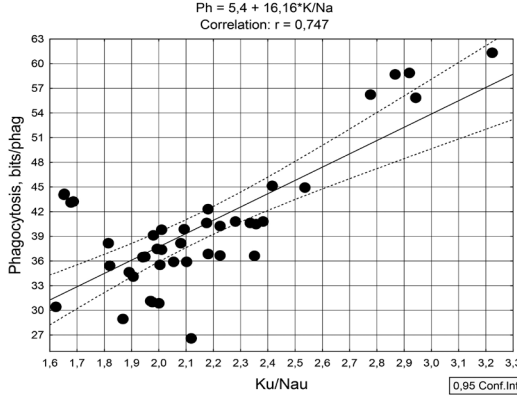

Fig. 2.43. Scatterplot of correlation between the mineralocorticoid activity (X-line) and intensity of phagocytosis (Y-line) in rats

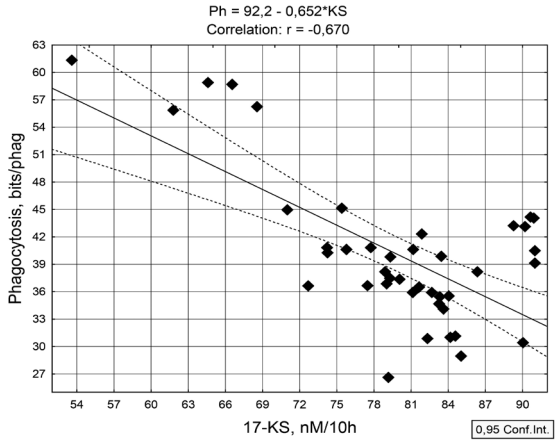

Fig. 2.44. Scatterplot of correlation between the urine excretion of 17-Ketosteroids (X-line) and intensity of phagocytosis (Y-line) in rats

It is well known that in females 17-ketosteroids are almost entirely metabolites of androgens secreted by the reticular zone of the adrenal cortex and the ovaries.

The long-known increase in spontaneous diuresis under the influence of Naftussya water [Chebanenko OI et al., 1997; Lukovych YuS et al., 2015] is due, among other factors, to a decrease in the level of antidiuretic hormone/arginine vasopressin in the blood. Hence, we assume that dynamic fitness is upregulated by reactivity of source of this hormone. This source are parvocellular neurons of the paraventricular nuclei of the hypothalamus. Some parvocellular neurons contain and secrete both arginine vasopressin (AVP) and corticotropin-releasing hormone (CRH) that in turn stimulates the secretion of ACTH. AVP alone has very little ACTH secretagogue activity but is apotent synergistic factor with CRH. AVP and CRH may act synergistically on other target tissue with AVP and CRH receptors in the CNS and perhaps the periphery [Chrousos GP, 2000], including, let's add, in skeletal muscles.

Previously, it was shown that the weekly use of Naftussya water increases the level of corticosterone in female rats to 619 nM/L vs 375 nM/L in daily water control, the thickness of the fascicular zone to 394 nM vs 386 nM, the glomerular zone to 192 nM vs 187 nM, the reticular zones

up to 45 nM vs 42 nM, however, testosterone plasma level decrease to 4,11 nM/L vs 5,98 nM/L [Popovych IL et al., 2022].

So, there are reasons to assume that in this experiment, Naftussya water stimulates the release of both mineralocorticoids and corticosterone into the blood, which, in turn, has a negative actotropic effect, as we have shown in humans.

Regarding the mechanism of stimulation by Naftussya water of mineralocorticoid and glucocorticoid, while suppression of androgenic functions of the adrenal cortex, there are two hypotheses. The first hypothesis allows for a direct activating effect of hydrophobic organic substances, in particular bitumen, on 21-hydroxylase of endocrinocyte microsomes with a subsequent increase in the biosynthesis of deoxycorticosterone and corticosterone, and a decrease in androgen secretion, apparently, due to a shift in the direction of use of pregnolol – a common precursor of all three steroids – towards deoxycorticosterone and corticosterone [Ivassivka SV, 1997; Popovych IL & Ivassivka SV, 2009].

An alternative hypothesis, much more substantiated, considers the endocrine and immune effects of Naphtussya water in the context of its modulating effect on the neuro-endocrine-immune complex [Popovych IL et al., 2022].

At least some of the listed organic substances (alkylbenzene, alkenylbenzene, alkylnaphthalenes, alkyl phenols, esters of aromatic acids, polyaromatic hydrocarbons) are, obviously, agonists of aryl hydrocarbon receptors (AhR), which are expressed by almost all types of cells of living organisms. The activation of AhR by endogenous and environmental factors has important physiologic effects, including the regulation of the endocrine and immune response [Esser C & Rannug A, 2015; Murray IA & Perdew GH, 2020].

We will say that one gets the impression that a decrease in fitness under the influence of balneofactors is compensated by their increase in phagocytosis, while the body "pays" for the increase in fitness by weakening it. This is consistent with the long-known principle of the "physiological price" of adaptation [Meerson FZ, 1991] as well as with the textbook fact of a decrease in athletes' resistance to a banal infection at the peak of cardiorespiratory fitness. Phytoadaptogen reverses the adverse effects of Naftussya bioactive water on dynamic muscle performance in healthy rats

by mitigating the decrease in the excretion of 17-ketosteroids and increased mineralocorticoid activity. This is probably due to its sympathotonic effect [Alyeksyeyev ***OI*** et al., 1996; Markova OO et al., 1997].

Conclusion

Phytoadaptogen reverses the adverse effects of Naftussya bioactive water on dynamic muscle performance in healthy rats by mitigating the decrease in the excretion of 17-ketosteroids and increased mineralocorticoid activity.

CLINICAL-PHYSIOLOGICAL OBSERVATIONS

Ethics approval

Tests in patients are carried out in accordance with positions of Helsinki Declaration 1975, revised and complemented in 2002, and directive of National Committee on ethics of scientific researches. During realization of tests from all participants the informed consent is got and used all measures for providing of anonymity of participants.

Chapter 3

RELATIONSHIPS BETWEEN THE NEURO-ENDOCRINE PARAMETERS AND VIRTUAL CHAKRAS ENERGY AND ASYMMETRY

Summary

Background. Earlier, we found a close correlation between EEG and gas-discharge image (GDI) parameters. The aim of this study is to analyze the relationship of EEG parameters with the energy and asymmetry of ***virtual*** Chakras, reconstructed on the basis of GDI parameters.

Material and Methods. We observed twice 31 women and 29 men aged 26-76 years with dysfunction of neuroendocrine-immune complex. In the morning in basal conditions at first registered GDI by the method of GDV by the device "GDV Chamber" ("Biotechprogress", SPb, RF). Than we registered EEG. Results processed by method of canonical analysis.

Results. The coefficients of canonical correlation between the EEG parameters and virtual Chakras Energy are in the interval 0,415÷0,564 and 0,358÷0,528 when registering without a filter and with a filter, respectively. Additional inclusion of HRV and endocrine parameters increases the strength of the canonical correlation to 0,768 and 0,772, respectively. The coefficients of canonical correlation between the EEG parameters and individual virtual Chakras Asymmetry are in the interval 0,284÷0,634 and 0,152÷0,458 when registering without a filter and with a filter, respectively. Integral coefficient of the canonical correlation is 0,820.

Conclusion. The above data, taken together with the previous ones, state that between parameters of neuroendocrine-immune complex and GDV in general and virtual Chakras in particular, exist strong canonical correlation suggesting suitability of the latter method.

Introduction

One of the areas of research of the Truskavetsian Scientific School is building bridges between the Western and Eastern paradigms of medicine. Adhering to this course, at the preparatory stage we chose *Chakras* as the object of study.

According to Ayurvedic medicine, Chakras are power centers, related to the endocrine glands and neural plexus as well as to some organs. Chase CR [2018] provides a table according to which the **first** Chakra is associated with adrenals, pelvic nerve plexus, spine, kidneys, bladder, large intestine; **second** Chakra with testes/ovaries, inferior mesenteric ganglion, ileum, organs of reproduction; third Chakra with [endocrine] pancreas, celiac plexus ganglion, liver, gall bladder, stomach, duodenum, pancreas, spleen; fourth Chakra with thymus, celiac plexus, heart, circulation, vagus nerve; fifth Chakra with thyroid and parathyroid glands, inferior cervical ganglion, lungs, bronchus, larynx, pharynx, large intestine, vagus nerve; sixth Chakra with pituitary and pineal glands, thalamus, hypothalamus, superior cervical ganglion, left brain, lower brain, ears/nose, left eye; **seventh** Chakra with pineal gland, right brain, upper brain, right eye. Korotkov KG [2007] put forward the concept that each Chakra is associated with a part of the finger. This approach is embodied in the "GDV Chakras" program, which allows us to quantify the state of ***virtual*** Chakras.

Earlier, we found a close correlation between EEG and gas-discharge image (GDI) parameters [Babelyuk VY et al., 2021]. The aim of this study is to analyze the relationship of EEG parameters with the energy and asymmetry of virtual Chakras, reconstructed on the basis of GDI parameters.

Material and methods

The object of observation were 60 volunteers: 31 women and 29 men aged 26-76 years with dysfunction of neuro-endocrine-immune complex and dysmetabolism.

In the morning we registered the GDI by the method of GDV by the device of "GDV Chamber" ("Biotechprogress", SPb, RF). The first base parameter of GDV is **Area** of GDI in Right, Frontal and Left projections registered both with and without polyethylene **filter**. The second base parameter is a **coefficient of Shape**. The third base parameter of GDI is **Entropy**. Program estimates also **Energy** and **Asymmetry** of virtual **Chakras** [Korotkov KG, 2001; 2007; 2014]. Than EEG recorded a hardware-software complex "NeuroCom Standard" (KhAI MEDICA,

Kharkiv) monopolar in 16 loci (Fp1, Fp2, F3, F4, F7, F8, C3, C4, T3, T4, P3, P4, T5, T6, O1, O2) by 10-20 international system, with the reference electrodes A and Ref on the earlobes. Two minutes after the eyes had been closed, 25 sec of artifact free EEG data were collected by computer. Among the options considered the average EEG amplitude (μV), average frequency (Hz), frequency deviation (Hz), index (%) as well as absolute (μV^2/Hz) and relative (%) power spectrum density (PSD) of basic rhythms: β (35÷13 Hz), α (13÷8 Hz), θ (8÷4 Hz) and δ (4÷0,5 Hz) in all loci, according to the instructions of the device. In addition, calculated coefficient of Asymmetry (As) and Laterality Index (LI) for PSD each Rhythm using formulas:

As, % = 100•(Max – Min)/Min; LI, % = Σ [200•(Right – Left)/(Right + Left)]/8.

We calculated also for each locus EEG Shannon's [1948] Entropy (h) of normalized PSD using Popovych's formulas [Popadynets OO et al., 2019; Gozhenko AI et al., 2021]:

$hEEG = – [PSD\alpha \bullet \log_2 PSD\alpha + PSD\beta \bullet \log_2 PSD\beta + PSD\theta \bullet \log_2 PSD\theta + PSD\delta \bullet \log_2 PSD\delta]/\log_2 4$.

Results and discussion

Screening (Table 3.1) revealed the closest link between relative PSD of β-rhythm in locus T5 and virtual Chakras 1 and 6 Energy registered with filter (Figs. 3.1 and 3.2).

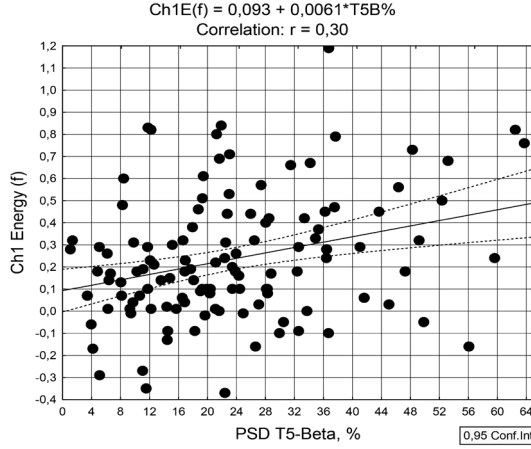

Fig. 3.1. Scatterplot of correlation between relative PSD of β-rhythm in locus T5 (X-line) and virtual Chakra 1 Energy (registration with filter) (Y-line)

The coefficients of canonical correlation between the EEG parameters and virtual Chakras Energy are in the interval 0,415÷0,564 and 0,358÷0,528 when registering without a filter and with a filter, respectively (Fig. 3.3).

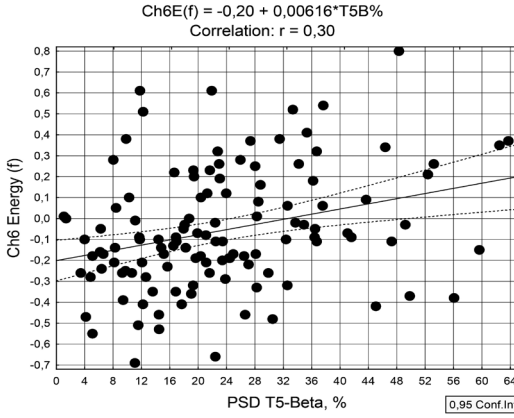

Fig. 3.2. Scatterplot of correlation between relative PSD of β-rhythm in locus T5 (X-line) and virtual Chakra 6 Energy (registration with filter) (Y-line)

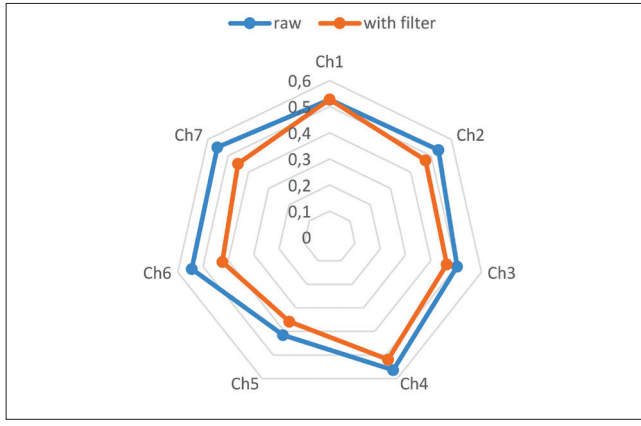

Fig. 3.3. Multiple correlation coefficients between EEG parameters and Energy of raw virtual Chakras and registered with filter

Table 3.1. Matrix of correlations between the virtual Chakras Energy and EEG parameters

Variable	Ch1E	Ch1Ef	Ch2E	Ch2Ef	Ch3E	Ch3Ef	Ch4E	Ch4Ef	Ch5E	Ch5Ef	Ch6E	Ch6Ef	Ch7E	Ch7Ef
DF	0,16	0,27	0,11	0,16	0,11	0,24	0,13	0,14	0,10	0,18	0,14	0,22	0,15	0,22
AF	0,24	0,22	0,24	0,22	0,17	0,16	0,19	0,21	0,14	0,12	0,19	0,14	0,19	0,19
LIA	0,17	0,19	0,23	0,21	0,21	0,17	0,20	0,17	0,23	0,16	0,28	0,17	0,24	0,20
FP1H	0,20	0,16	0,26	0,18	0,25	0,18	0,26	0,15	0,09	0,11	0,17	0,14	0,28	0,15
FP2H	0,18	0,12	0,21	0,14	0,22	0,12	0,24	0,15	0,09	0,12	0,19	0,14	0,17	0,10
FP2B%	0,21	0,26	0,16	0,19	0,17	0,19	0,17	0,20	0,10	0,21	0,20	0,24	0,15	0,17
F3H	0,21	0,19	0,19	0,16	0,23	0,15	0,25	0,14	0,18	0,23	0,24	0,22	0,17	0,16
F3B%	0,19	0,22	0,15	0,16	0,12	0,18	0,13	0,18	0,14	0,19	0,23	0,23	0,14	0,17
F3T%	0,25	0,22	0,24	0,20	0,22	0,20	0,35	0,25	0,17	0,17	0,19	0,19	0,25	0,18
F3A	-0,07	-0,21	-0,08	-0,15	-0,06	-0,18	-0,13	-0,22	-0,04	-0,11	-0,01	-0,08	-0,10	-0,13
F4H	0,25	0,19	0,29	0,23	0,28	0,21	0,28	0,18	0,15	0,18	0,24	0,22	0,28	0,25
F4T%	0,19	0,14	0,25	0,19	0,19	0,17	0,31	0,24	0,09	0,08	0,12	0,12	0,27	0,18
F7T%	0,22	0,13	0,28	0,18	0,24	0,10	0,33	0,23	0,06	0,01	0,11	0,07	0,28	0,15
F8H	0,15	0,18	0,22	0,23	0,20	0,18	0,22	0,19	0,12	0,14	0,18	0,19	0,27	0,22
F8T%	0,21	0,13	0,23	0,16	0,16	0,10	0,26	0,19	0,09	0,05	0,14	0,09	0,28	0,15
T3H	0,18	0,13	0,23	0,16	0,23	0,11	0,25	0,15	0,12	0,10	0,20	0,13	0,21	0,15
T4H	0,21	0,20	0,29	0,24	0,30	0,21	0,28	0,25	0,12	0,13	0,23	0,21	0,29	0,28
T4A	0,05	-0,06	0,06	0,02	0,08	-0,03	0,03	-0,08	0,11	0,01	0,17	0,09	0,07	0,05
T4D	-0,08	-0,17	-0,12	-0,20	-0,15	-0,24	-0,12	-0,19	-0,08	-0,14	-0,14	-0,17	-0,13	-0,21
C3T%	0,15	0,14	0,20	0,12	0,14	0,13	0,27	0,23	0,11	0,11	0,14	0,15	0,23	0,12
T5B%	0,25	0,30	0,15	0,20	0,21	0,24	0,17	0,22	0,23	0,29	0,27	0,30	0,14	0,20
T6H	0,13	0,15	0,19	0,17	0,18	0,14	0,25	0,22	0,09	0,16	0,16	0,21	0,21	0,16
T6B	0,22	0,22	0,26	0,28	0,25	0,27	0,20	0,18	0,24	0,17	0,29	0,21	0,26	0,29
P3A%	-0,08	-0,16	-0,06	-0,14	-0,06	-0,14	-0,18	-0,24	-0,13	-0,15	-0,10	-0,13	-0,06	-0,12
P4A	-0,02	-0,15	-0,03	-0,13	-0,03	-0,12	-0,14	-0,23	-0,02	-0,11	-0,00	-0,10	-0,04	-0,12
O2B%	0,19	0,28	0,15	0,18	0,20	0,27	0,18	0,20	0,20	0,27	0,27	0,29	0,14	0,18
O2D	-0,21	-0,17	-0,21	-0,15	-0,24	-0,15	-0,21	-0,15	-0,07	-0,12	-0,14	-0,13	-0,17	-0,15

As we can see, the registration with the use of the filter reduces the strength of the connections of the EEG parameters with the Energy of the Chakras, mostly the sixth and seventh, except for the first Chakra. This is in perfect agreement with the classical ideas about the relationship of the former to the nervous system [Chase CR, 2018], as well as with the concept of Korotkov KG [2001; 2007; 2014] that GDI, taken off without filter, characterizes the functional changes of organism, while taken with a filter characterizes organic changes.

Further, for canonical analysis, EEG parameters were combined with HRV parameters and hormones [Babelyuk VY et al., 2921a]. Interim results are shown in Tables 3.2 and 3.3 and Figures 3.4 and 3.5.

Table 3.2. Factor structure of EEG,HRV&Endocrine and virtual Chakras (without filter) Energy Roots

Left set *EEG, HRV&Hormones*	R
1	2
Entropy T4	**0.506**
Entropy F8	**0.436**
Entropy Fp1	**0.416**
Entropy F4	**0.408**
Entropy T6	**0.361**
Testosterone standard, Z	**0.356**
F8-θ PSD, %	**0.353**
Entropy Fp2	**0.318**
Laterality α, Hz	**0.305**
VLF, msec²	**0.302**
F4-θ PSD, %	**0.301**
T6-β PSD, μV²/Hz	**0.296**
F7-θ PSD, %	**0.295**
VLF+ULF, msec²	**0.287**
Entropy T3	**0.285**
C3-θ PSD, %	**0.250**
Total Power HRV, msec²	**0.233**
O2-β PSD, %	**0.196**
T4-α PSD, μV²/Hz	**0.181**
F3-θ PSD, %	**0.179**
Entropy F3	**0.155**
Frequency α, Hz	**0.134**
Heart Rate	**0.124**
Amplitude Mode HRV, %	**0.108**
Vegetative Balance Index	**0.089**
T5-β PSD, %	**0.083**
P3-α PSD, %	**0.081**
Testosterone, nM/L	**-0.315**
LFnu, %	**-0.229**

Table 3.2 (cont)

1	2
O2-δ PSD, μV²/Hz	**-0.215**
Right set Chakras Energy	**R**
7 E	**0.694**
2 E	**0.600**
4 E	**0.467**
3 E	**0.446**
6 E	**0.387**
1 E	**0.282**
5 E	**0.155**

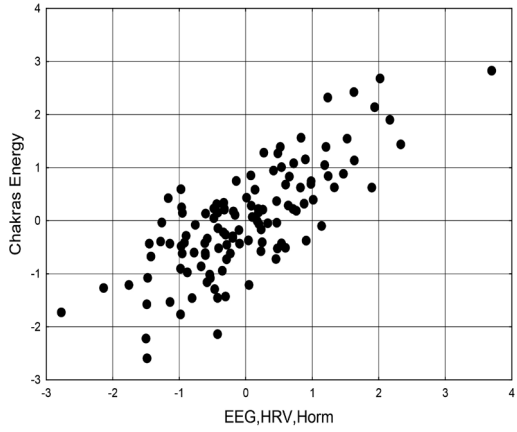

R=0,768; R^2=0,590; $\chi^2_{(245)}$=313; p=0,002; Λ Prime=0,039
Fig. 3.4. Scatterplot of canonical correlation between Neuro-endocrine parameters (X-line) and virtual Chakras Energy (registration without filter) (Y-line)

Table 3.3. Factor structure of EEG,HRV&Endocrine and virtual Chakras (with filter) Energy Roots

Left set EEG, HRV&Hormones	**R**
1	2
Entropy T4	**0,416**
HF/TP	**0,237**

Table 3.3 (cont)

1	2
Testosterone standard, Z	**0,235**
Frequency α, Hz	**0,216**
F3-θ PSD, %	**0,209**
T6-β PSD, μV²/Hz	**0,209**
Heart Rate	**0,192**
F3-β PSD, %	**0,168**
Laterality α, Hz	**0,159**
Fp2-β PSD, %	**0,127**
Frequency δ, Hz	**0,119**
T5-β PSD, %	**0,075**
O1-β PSD, %	**0,073**
O2-β PSD, %	**0,060**
Total Power HRV, msec²	**0,063**
VLF, msec²	**0,043**
Testosterone, nM/L	**-0,468**
P4-α PSD, μV²/Hz	**-0,196**
Amplitude Mode HRV, %	**-0,189**
T4-δ PSD, μV²/Hz	**-0,183**
P3-α PSD, %	**-0,159**
Vegetative Balance Index	**-0,145**
LFnu, %	**-0,143**
F3-α PSD, μV²/Hz	**-0,120**
Cortisol, nM/L	**-0,106**
Right set Chakras Energy	**R**
4 E f	**0,633**
7 E f	**0,586**
2 E f	**0,530**
1 E f	**0,296**
3 E f	**0,283**
6 E f	**0,208**
5 E f	**0,007**

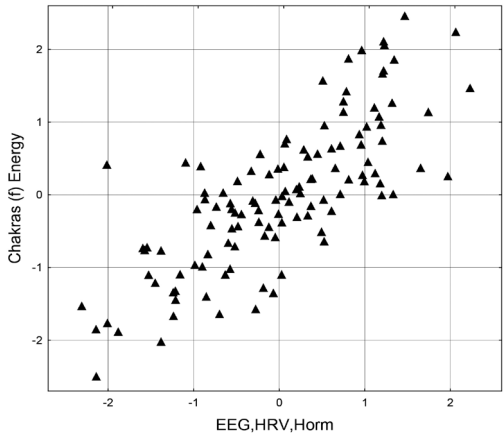

R=0,772; R^2=0,596; $\chi^2_{(210)}$=283; p=0,0006; Λ Prime=0,057

Fig. 3.5. Scatterplot of canonical correlation between Neuro-endocrine parameters (X-line) and virtual Chakras Energy (registration with filter) (Y-line)

In the end, it was found (Table 3.4) that the prominent places in the factor structure of the root of Chakra Energies are occupied by the seventh, second and fourth Chakras, which are responsible for: the pineal gland, right brain, upper brain, right eye; **testes/ovaries**; and heart, circulation, vagal nerve, respectively [Chase CR, 2018]. On the other hand, the factor structure of the neuro-endocrine root is represented primarily by Entropies and PSD **right**-handed (paired) loci, as well as **testosterone**.

Table 3.4. Factor structure of EEG,HRV&Endocrine and virtual Chakras Energy Roots

EEG, HRV&Hormones	**R**
1	2
Entropy T4	**-0,460**
Testosterone standard, Z	**-0,343**
F7-θ PSD, %	**-0,320**
Entropy F8	**-0,318**
F8-θ PSD, %	**-0,315**
T6-β PSD, μV²/Hz	**-0,298**

Table 3.4 (cont)

1	2
F4-θ PSD, %	**-0,283**
Laterality α, Hz	**-0,280**
Entropy F4	**-0,277**
Entropy T6	**-0,266**
C3-θ PSD, %	**-0,233**
Entropy T3	**-0,230**
F3-β PSD, %	**-0,226**
Frequency α, Hz	**-0,220**
Heart Rate	**-0,213**
Entropy Fp1	**-0,211**
HF/TP	**-0,189**
Entropy Fp2	**-0,172**
T4-α PSD, $\mu V^2/Hz$	**-0,165**
Fp2-β PSD, %	**-0,161**
F3-θ PSD, %	**-0,154**
Frequency δ, Hz	**-0,122**
O2-β PSD, %	**-0,111**
O1-β PSD, %	**-0,106**
VLF, $msec^2$	**-0,108**
Total Power HRV, $msec^2$	**-0,088**
T5-β PSD, %	**-0,078**
Entropy F3	**-0,055**
Testosterone, nM/L	**0,398**
T4-δ PSD, $\mu V^2/Hz$	**0,217**
O2-δ PSD, $\mu V^2/Hz$	**0,136**
LFnu, %	**0,124**
P4-α PSD, $\mu V^2/Hz$	**0,094**
Cortisol, nM/L	**0,053**
Amplitude Mode HRV, %	**0,017**
Chakras Energy	**R**
7 E	**-0,583**
7 E f	**-0,578**
2 E	**-0,531**

Table 3.4 (cont)

1	2
2 E f	**-0,522**
4 E f	**-0,544**
4 E	**-0,487**
3 E	**-0,333**
3 E f	**-0,286**
6 E	**-0,306**
6 E f	**-0,274**
1 E f	**-0,283**
1 E	**-0,259**
5 E	**-0,111**
5 E f	**-0,058**

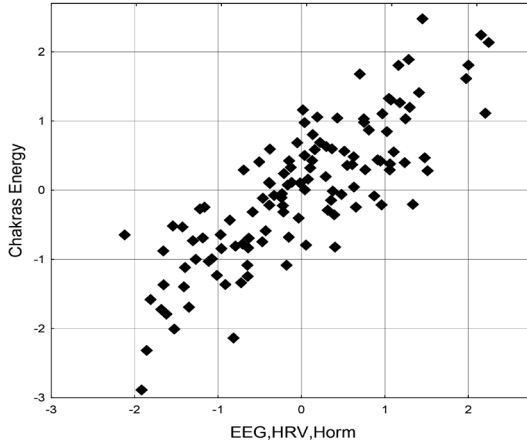

R=0,821; R^2=0,674; $\chi^2_{(490)}$=545; p=0,045; Λ Prime=0,003

Fig. 3.6. Scatterplot of canonical correlation between Neuro-endocrine parameters (X-line) and virtual Chakras Energy (Y-line)

Another basic characteristic of virtual Chakras is their Asymmetry. This is consistent with the position of the existence of morpho-functional asymmetry of many, if not all, paired organs or their halves, including the hemispheres of the brain [Miskovic V, 2010; Balle M et al., 2013; Barylyak LG et al., 2015; Kruhliy YuZ, 2010; 2012]. Screening revealed significant correlations (Figs 3.7 and 3.8).

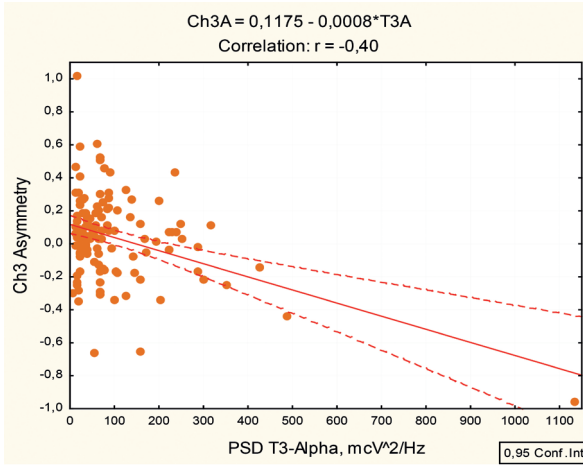

Fig. 3.7. Scatterplot of correlation between PSD of α-rhythm in locus T3 (X-line) and virtual Chakra 3 Asymmetry (Y-line)

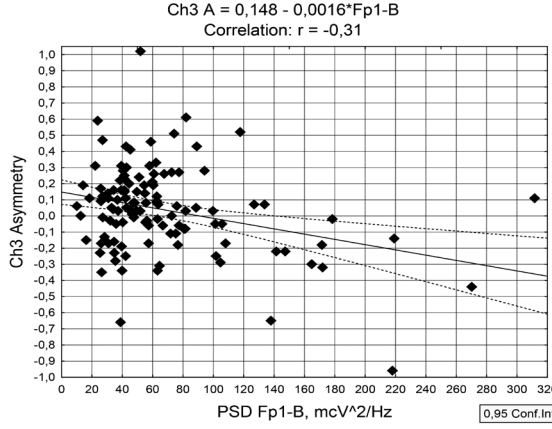

Fig. 3.8. Scatterplot of correlation between PSD of β-rhythm in locus Fp1 (X-line) and virtual Chakra 3 Asymmetry (Y-line)

Interestingly, the effect of the polyethylene filter on the strength of the bonds with the EEG parameters of the Asymmetry of the Chakras was much more noticeable compared to their Energy. This is especially true of the Asymmetry of the third and seventh Chakras, while the EEG connections of the sixth Chakra remain stable (Fig. 3.9).

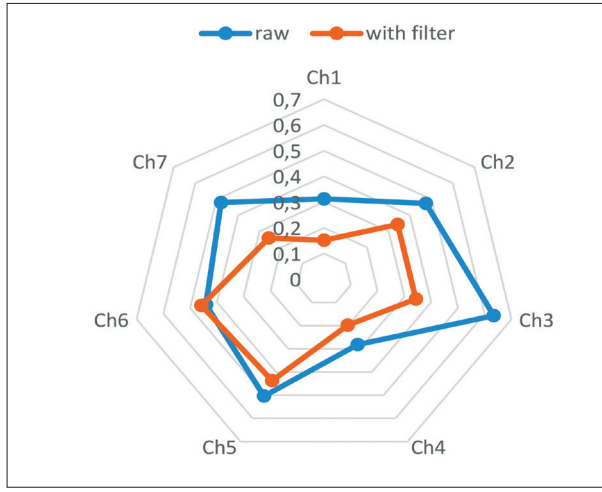

Fig. 3.9. Multiple correlation coefficients between EEG parameters and Asymmetry of raw virtual Chakras and registered with filter

In general, the canonical correlation between EEG parameters and the asymmetry of virtual chakras is stated as strong (Table 3.5 and Fig. 3.10).

Table 3.5. Factor structure of EEG and virtual Chakras Asymmetry Roots

Left set ***EEG, HRV&Hormones***	**R**
1	2
T5-θ PSD, μV²/Hz	**-0,488**
Fp1-θ PSD, μV²/Hz	**-0,471**
T4-α PSD, μV²/Hz	**-0,436**
Fp2-α PSD, μV²/Hz	**-0,432**
F7-α PSD, μV²/Hz	**-0,430**
C3-θ PSD, μV²/Hz	**-0,415**
T3-α PSD, μV²/Hz	**-0,407**
O1-θ PSD, μV²/Hz	**-0,404**
Index β, %	**-0,400**
P3-θ PSD, μV²/Hz	**-0,337**
F4-δ PSD, μV²/Hz	**-0,329**
T5-δ PSD, μV²/Hz	**-0,314**

Table 3.5 (cont)

1	2
T5-δ PSD, %	**-0,245**
O1-α PSD, μV²/Hz	**-0,313**
F7-θ PSD, μV²/Hz	**-0,291**
C4-δ PSD, μV²/Hz	**-0,289**
Fp2-θ PSD, μV²/Hz	**-0,275**
Fp1-β PSD, μV²/Hz	**-0,274**
T5-α PSD, μV²/Hz	**-0,245**
F3-α PSD, μV²/Hz	**-0,240**
C4-α PSD, μV²/Hz	**-0,212**
T6-β PSD, μV²/Hz	**-0,179**
Frequency β, Hz	**0,397**
Fp2-β PSD, %	**0,289**
Frequency θ, Hz	**0,282**
F3-β PSD, %	**0,278**
Laterality δ, %	**0,171**
P3-β PSD, %	**0,120**
O2-β PSD, %	**0,119**
Frequency δ, Hz	**0,091**
Right set Chakras Asymmetry	**R**
3 A	**0,519**
5 A f	**0,515**
2 A	**0,488**
6 A f	**0,421**
3 A f00	**0,375**
2 A f	**0,361**
7 A	**0,343**
7 A f	**0,260**
4 A	**-0,162**
1 A	**-0,147**
6 A	**-0,053**
5 A	**-0,048**
1 A f	**-0,037**

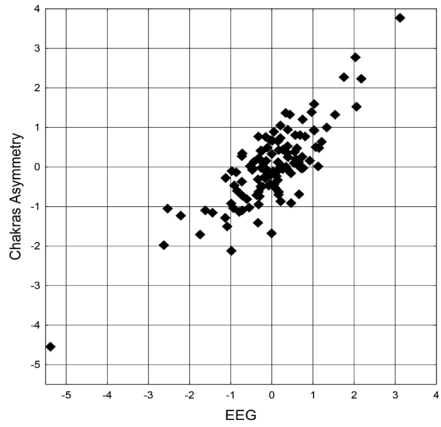

R=0,820; R^2=0,673; $\chi^2_{(468)}$=519; p=0,054; Λ Prime=0,004
Fig. 3.10. Scatterplot of canonical correlation between EEG parameters (X-line) and virtual Chakras Asymmetry(Y-line)

Conclusion

Thus, we have been shown that exist strong canonical correlation between neuro-endocrine and *virtual* Chakras parameters. The above data, taken together with the previous ones, state that between parameters of neuroendocrine-immune complex and GDV in general and virtual Chakras in particular, exist strong canonical correlation suggesting suitability of the latter method.

Chapter 4

RELATIONSHIPS BETWEEN LEVELS OF MAIN ADAPTATION HORMONES AND EEG&HRV PARAMETERS AT HUMAN WITH MALADAPTATION

Summary

Background. The immunoneuroendocrinology became the foundation of the Truskavetsian Scientific School of Balneology. The focus of research was on the relationships between EEG and HRV parameters, EEG&HRV and leukocytogram, phagocytosis, cellular and humoral immunity as well as between changes in these parameters under the influence of adaptogenic factors Truskavets' spa. The purpose of this study is relationships between serum levels of major adaptogene hormones and EEG&HRV parameters at human with dysadaptation.

Materials and Methods. The object of observation was 10 women 33-76 y and 10 men 37-67 y without a clinical diagnosis, but with the deviations from the norm in a number of parameters of the neuro-endocrine-immune complex as a manifestation of dysadaptation. Parameters of EEG and HRV as well as hormones levels before and after a one-week course of drinking of Naftussya bioactive water registered.

Results. Using the method of canonical correlation analysis, it was found that the level of triiodothyronine is determined by the constellation of 17 EEGs and 4 HRVs parameters by 87,5%. The rate of determination of the cortisol level by 14 EEGs and 3 HRVs parameters is 83,7%, and aldosterone by the other 14 EEGs and 3 HRVs parameters is 80,0%. Neuromodulation of testosterone and calcitonin levels is characterized by sexual dimorphism. With the same coefficients of determination (92,4%), the regression model for testosteroneemia in women included 15 EEGs parameters and no HRV parameters, instead testosteroneemia in men is modulated by other 11 EEGs parameters and one HRV parameter. The level of calcitonin in women is determined by 86,2% by the constellation of 9 EEGs and 2 HRVs parameters, while in men by 83,5% by the other 5 EEGs and 4 HRVs parameters.

Conclusion. The levels of the main adaptation hormones are accompanied by specific patterns of EEG and HRV parameters.

INTRODUCTION

According to the modern paradigm, three regulatory systems are involved in maintaining homeostasis: nervous, endocrine, and immune. It is the close and continuous functional interrelationship of the nervous, hormonal and immune systems, which is based on the existence of common and identical receptor structures, that determines the high adaptability of the organism [Besedovsky H & Sorkin E, 1977; Besedovsky H & del Rey A, 1996]. Interactions of the nervous and endocrine systems in this process are well studied and became the basis for the selection of an independent field of knowledge – neuroendocrinology [Akmayev PG, 1996; Chrousos GP, 1998; Reznikov OG et al., 2004; Baraboy VA & Reznikov OG, 2013; Reznikov OG, 2019]. Interactions between the neuroendocrine and immune systems are intensively studied and are considered the most intriguing field of modern research – immunoneuroendocrinology [Chrousos GP, 2000; Khaitov RM et al., 2005; Sternberg EM, 2006; Uchakin PN et al., 2007; Tracey KJ, 2007; Tracey KJ, 2010; Thayer JF & Sternberg EM, 2010; Popovych IL et al., 2014; Kozyavkina OV et al., 2015; Chavan SS et al., 2017; Chavan SS & Tracey KJ, 2017; Pavlov VA et al., 2018; Korneva EA, 2020; Popovych IL et al., 2020; Gozhenko **AI** et al., 2021; Popovych IL et al., 2022].

The immunoneuroendocrinology became the foundation of the Truskavetsian Scientific School of Balneology. Experimental and clinical-physiological research of this school, carried out in line with the concept of neuro-endocrine-immune complex [Popovych IL, 2009; Popovych IL, 2011], in 2015 was recognized by an expert as the main trend of the last decade in Ukrainian balneology [Portnychenko AG, 2015]. The focus of research was on the relationships between EEG and HRV parameters [Popovych IL et al., 2013; Popovych IL et al., 2014], EEG&HRV, on the one hand, and leukocytogram [Kulchynskyi AB et al., 2017], phagocytosis [Kulchynskyi AB et al., 2016], cellular and humoral immunity [Kulchynskyi AB et al., 2017a], on the other, as well as between changes in these parameters under the influence of adaptogenic factors Truskavets' spa, primarily bioactive Naftussya water [Kulchynskyi AB et al., 2017b; Kulchynskyi AB et al., 2017c; Popovych IL et al., 2017; Popovych IL et al., 2018]. A side effect of the obtained results was the addition and specification of the hypothesis of the immunological homunculus, according to which certain cortical structures exert a regulatory influence on certain links of immunity [Tracey KJ, 2007]. However, neuro-endocrine connections have been investigated only in an

experiment on rats, and without EEG recording [Popovych IL, 2011], and in humans, only a single fragmentary study of the acute effect of Naftussya bioactive water on EEG&HRV parameters, and blood levels of adaptation hormones has been conducted so far [Kozyavkina OV et al., 2015].

The purpose of this study is relationships between serum levels of major adaptation hormones and EEG&HRV parameters at human with maladaptation. Classical (main) hormones of adaptation usually include corticosteroid, sexual and thyroid [Garkavi LKh et al., 1990; Garkavi LKh et al., 1998; Garkavi LKh et al., 2000; Chrousos GP, 1998; Chrousos GP, 2000; Radchenko OM, 2004; Baraboy VA & Reznikov OG, 2013; Reznikov OG, 2019]. Our previous experience gave reason to supplement this list with calcitonin (as well as parathyroid hormone) [Popovych IL, 2011; Kozyavkina OV et al., 2015; Popovych IL et al., 2020].

MATERIAL AND RESEARCH METHODS

The object of observation were employees of the PrJSC "Truskavets' Spa": 10 women 33-76 years and 10 men 37-67 years. The volunteers were considered practically healthy (without a clinical diagnosis), but the initial testing revealed deviations from the norm in a number of parameters of the neuro-endocrine-immune complex as a manifestation of dysadaptation.

In the morning in basal condition we recorded simultaneosly electrocardiogram (ECG) and electroencephalogram (EEG). ECG recorded during 7 min in II lead to assess the parameters of heart rate variability (HRV) (hardware-software complex «CardioLab+HRV» produced by «KhAI-Medica», Kharkiv, Ukraine). For further analyses the following parameters HRV were selected. Baevskiy's parameters: heart rate (HR), the mode (Mo), the amplitude of mode (AMo), variation scope (MxDMn). Temporal parameters (Time Domain Methods): the standart deviation of all NN intervals (SDNN), the square root of the mean of the sum of the squares of differences between adjacent NN intervals (RMSSD), the percent of interval differences of successive NN intervals greater than 50 ms (pNN_{50}), triangular index (TNN). Spectral parameters (Frequency Domain Methods): power spectral density (PSD) bands of HRV: high-frequency (HF, range 0,40÷0,15 Hz), low-frequency (LF, range 0,15÷0,04 Hz), very low-frequency (VLF, range 0,040÷0,015 Hz) and ultralow-frequency (ULF, range 0,015÷0,003 Hz). Calculated classical indexes: LF/HF, LFnu=100%•LF/(LF+HF), Centralization Index (CI)=(VLF+LF)/HF), Baevskiy's Stress Index and

Activity of Regulatory Systems Index (BARSI) [Heart Rate Variability, 1996; Berntson GG et al., 1997; Baevskiy RM & Ivanov GG, 2001; Baevsky RM & Berseneva AP, 2008; Shaffer F & Ginsberg JP, 2017].

EEG recorded as previously described.

We calculated for HRV and each locus EEG the Entropy (h) of normalized PSD using Popovych's IL [Ruzhylo SV et al., 2015; Gozhenko **AI** et al., 2021] formulas based on classic Shannon's CE [1948] formula:

$hHRV=-[SPHF \bullet \log_2 SPHF+SPLF \bullet \log_2 SPLF+SPVLF \bullet \log_2 SPVLF+SPULF \bullet \log_2 SPULF]/\log_2 4$;

$hEEG=-[PSD\alpha \bullet \log_2 PSD\alpha+PSD\beta \bullet \log_2 PSD\beta+PSD\theta \bullet \log_2 PSD\theta+PSD\delta \bullet \log_2 PSD\delta]/\log_2 4$.

At last in portion of venous blood we determined serum levels of major hormones of adaptation: Cortisol, Testosterone, Aldosterone, Triiodothyronine and Calcitonin (by the ELISA with the use of analyzer "RT-2100C" and corresponding sets of reagents from "Алкор Био", XEMA Co., Ltd and DRG International Inc.). After the initial testing, seven days course of drinking of Naftussya bioactive water carried out. The next morning after completing the treatment, retesting was performed.

Results processed using the software package «Statistica 6.4».

RESULTS AND DISCUSSION

It is known that Naftussya **bioactive** water exhibits neurotropic, endocrinotropic, immunotropic, actotropic, cardiotropic, vasotropic [Ruzhylo SV et al., 2003; Kostyuk PG et al., 2006; Popovych IL, 2011; Popovych IL et al., 2014; Kozyavkina OV et al., 2015; Kulchynskyi AB et al., 2017; Popovych AI, 2019; Popovych IL et al., 2017; Popovych IL et al., 2018; Gozhenko **AI** et al., 2021; Popovych IL et al., 2022] activity (which, in fact, became the basis for its name), caused by the organic substances and autochthonous microbes present in its composition [Ivassivka SV et al., 1990; Ivassivka SV et al., 1994; Ivassivka SV, 1997; Popovych IL & Ivassivka SV, 2009; Popovych IL et al., 2018; Zukow W et al., 2020]. Therefore, there are grounds for assuming differences in neuro-endocrine relationships before and after balneotherapy, which will be the subject of the next study. Now let's consider the neuro-endocrine relationships regardless of the use of bioactive water.

According to the previously accepted algorithm, at the first stage, correlation coefficients were screened, then a regression model was built

from variables with statistically significant or borderline coefficients by stepwise exclusion of variables until the maximum Adjusted R^2 level was reached. At the final stage, in order to visualize the model, the procedure of canonical correlation analysis was carried out. It was found that the level of triiodothyronine positively correlates with 6 parameters of the alpha-rhythm (Fig. 4.1) and 3 – delta-rhythm of the EEG, as well as 3 HRV-markers of vagal tone (Fig. 4.2), on the other hand, it is negatively correlated with 6 parameters of the beta-rhythm and one – theta-rhythm, as well as with entropy in the O1 locus (Table 4.1).

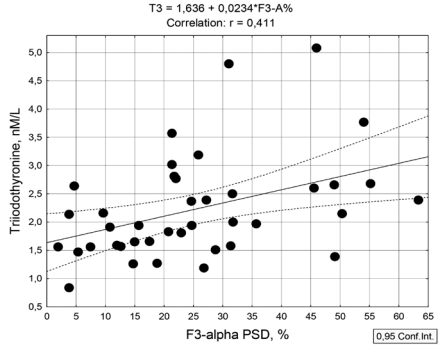

Fig. 4.1. Scatterplot of correlation between the PSD of α-rhythm in locus F3 (X-line) and Triiodothyronine serum level (Y-line)

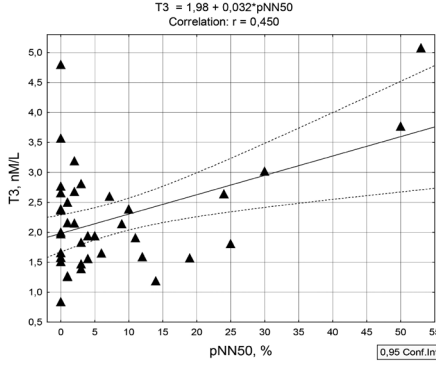

Fig. 4.2. Scatterplot of correlation between the pNN_{50} HRV (X-line) and Triiodothyronine serum level (Y-line)

Regarding the VLF band, there are opinions that it directly reflects both vagal and sympathetic tone [Akselrod S et al., 1981] or vagal tone

only [Taylor JA et al., 1998] as well as saliva testosterone level [Theorell T et al., 2007] while inversely – renin-angiotensin-aldosterone system activity [Akselrod S et al., 1981; Taylor JA et al., 1998]. Looking ahead, we note that in this study, was also found a direct correlation of the VLF band with the HF band (r=0,65) and serum testosterone in men (r=0,32), no correlation with LFnu (r=-0,16) as well as also inversely, but insignificantly, with aldosterone (r=-0,19).

Table 4.1. Regression Summary for Triiodothyronine
R=0,936; R^2=0,875; Adjusted R^2=0,730; $F_{(21,2)}$=6,0; p=0,0002; SE: 0,47 nM/L

N=40		Beta	St. Err. of Beta	B	St. Err. of B	$t_{(18)}$	p-level
Variables	r		Intercpt	-8,647	2,098	-4,12	0,001
F3-α PSD, %	**0,41**	1,149	0,393	0,065	0,022	2,93	0,009
O1-α PSD, %	**0,39**	-1,328	0,374	-0,055	0,016	-3,55	0,002
T4-α PSD, %	**0,35**	0,586	0,362	0,041	0,025	1,62	0,123
C3-α PSD, %	**0,35**	0,551	0,305	0,032	0,018	1,81	0,088
O2-α PSD, μV^2/Hz	**0,31**	0,961	0,305	0,0015	0,0005	3,15	0,006
T5-α PSD, %	**0,30**	-0,799	0,299	-0,042	0,016	-2,67	0,016
Frequency-δ, Hz	**0,45**	0,943	0,163	5,114	0,883	5,79	10^{-4}
C4-δ PSD, μV^2/Hz	**0,30**	0,207	0,139	0,0006	0,0004	1,49	0,155
F8-δ PSD, μV^2/Hz	**0,28**	-0,219	0,158	-0,0007	0,0005	-1,38	0,183
pNN_{50} HRV, %	**0,45**	-0,827	0,689	-0,059	0,049	-1,20	0,245
PSD HF band, $msec^2$	**0,44**	-1,722	0,550	-0,0027	0,0009	-3,13	0,006
RMSSD HRV, msec	**0,38**	2,928	0,671	0,150	0,034	4,36	10^{-3}
PSD VLF band, $msec^2$	**0,30**	0,455	0,196	0,0004	0,0002	2,32	0,032
O1 PSD Entropy	**-0,41**	0,455	0,264	3,140	1,824	1,72	0,102
T3-β PSD, %	**-0,34**	-0,317	0,189	-0,019	0,011	-1,68	0,111
Fp2-β PSD, %	**-0,31**	0,439	0,185	0,026	0,011	2,38	0,029
T4-β PSD, %	**-0,30**	-0,325	0,186	-0,023	0,013	-1,75	0,098
O2-β PSD, %	**-0,29**	-0,679	0,216	-0,054	0,017	-3,15	0,006
T6-β PSD, %	**-0,28**	0,254	0,168	0,016	0,010	1,51	0,147
Asymmetry-β, %	**-0,29**	0,500	0,147	0,032	0,009	3,41	0,003
O2-θ PSD, %	**-0,27**	-0,287	0,160	-0,056	0,031	-1,80	0,089

Judging by the coefficient of determination, the constellation of EEG and HRV parameters modulates the level of triiodothyronine by 87,5% (Table 4.1 and Fig. 3.3).

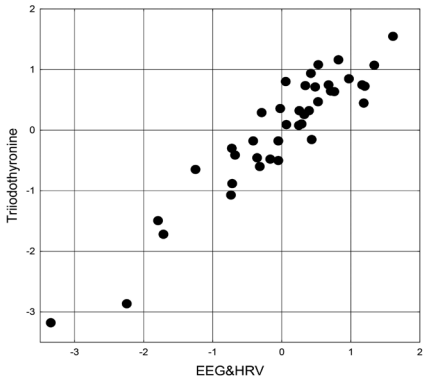

R=0,936; R^2=0,875; $\chi^2_{(21)}$=57; p<10^{-4}; Λ Prime=0,125

Fig. 4.3. Scatterplot of canonical correlation between the EEG&HRV parameters (X-line) and Triiodothyronine serum level (Y-line)

The serum cortisol level is upregulated by δ-rhythm generating neurons projecting to the right loci of the scalp (Fig. 4.4), and θ-rhythm generating neurons projecting to the left loci, as well as β-rhythm asymmetry and entropy of PSD in locus O1 (Table 4.2).

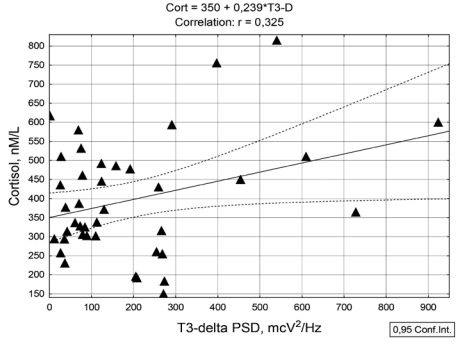

Fig. 4.4. Scatterplot of correlation between the PSD of δ-rhythm in locus T3 (X-line) and Cortisol serum level (Y-line)

Instead, entropy of PSD in other loci, β- and α-rhythm generating neurons projecting to F7 and T3 loci respectively as well as HRV-markers of vagal tone (Fig. 4.5) carry out downregulation.

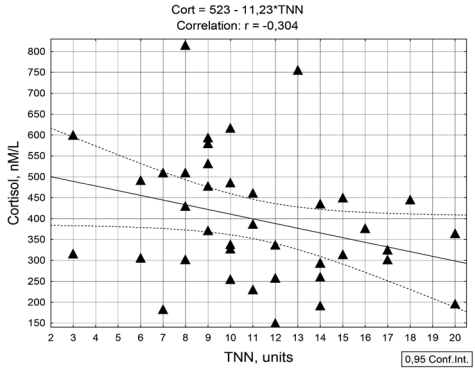

Fig. 4.5. Scatterplot of correlation between the Triangular index HRV (X-line) and Cortisol serum level (Y-line)

Table 4.2. Regression Summary for Cortisol

R=0,915; R^2=0,837; Adjusted R^2=0,712; $F_{(17,2)}$=6,7; p=0,00003; SE: 82 nM/L

N=40		Beta	St. Err. of Beta	B	St. Err. of B	$t_{(22)}$	p-level
Variables	r		Intercpt	311	276	1,13	0,272
T3-δ PSD, μV²/Hz	**0,32**	-1,077	0,315	-0,791	0,232	-3,42	0,002
T5-δ PSD, %	**0,30**	0,549	0,185	3,763	1,265	2,97	0,007
F7-δ PSD, %	**0,27**	-0,503	0,217	-3,631	1,566	-2,32	0,030
F7-δ PSD, μV²/Hz	**0,26**	0,546	0,223	0,369	0,151	2,45	0,023
T3-δ PSD, %	**0,26**	0,813	0,375	6,048	2,793	2,17	0,041
T6-θ PSD, μV2/Hz	**0,33**	0,229	0,162	0,623	0,440	1,41	0,171
F8-θ PSD, μV2/Hz	**0,25**	0,581	0,199	1,446	0,497	2,91	0,008
Asymmetry-β, %	**0,26**	0,664	0,187	7,054	1,989	3,55	0,002
O1 PSD Entropy	**0,35**	0,389	0,146	383,0	143,2	2,68	0,014
T4 PSD Entropy	**-0,27**	0,212	0,138	246,8	160,8	1,53	0,139
T3 PSD Entropy	**-0,26**	-0,963	0,189	-1118,7	219,8	-5,09	10^{-4}
F4 PSD Entropy	**-0,26**	0,487	0,198	404,5	164,2	2,46	0,022
F7-β PSD, μV²/Hz	**-0,25**	-0,646	0,151	-1,577	0,368	-4,28	10^{-3}
T3-α PSD, %	**-0,25**	0,627	0,244	6,427	2,498	2,57	0,017
TNN HRV, units	**-0,30**	-1,120	0,348	-41,34	12,83	-3,22	0,004
SDNN HRV, msec	**-0,28**	0,950	0,397	7,067	2,954	2,39	0,026
PSD VLF band, msec²	**-0,24**	-0,493	0,246	-0,081	0,040	-2,01	0,057

The integral effect of this constellation of EEG and HRV parameters determines the cortisol level by 83,7% (Fig. 4.6).

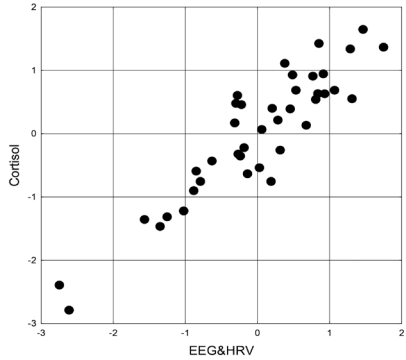

R=0,915; R^2=0,837; $\chi^2_{(17)}$=54; p<10^{-4}; Λ Prime=0,163

R=0,915; R^2=0,837; $\chi^2_{(17)}$=54; p<10^{-4}; Λ Prime=0,163

Fig. 4.6. Scatterplot of canonical correlation between the EEG&HRV parameters (X-line) and Cortisol serum level (Y-line)

The serum aldosterone level is upregulated by α-rhythm generating neurons projecting to the left (Fig. 4.7) and right loci, and θ-rhythm generating neurons projecting to the T3 locus while downregulated by δ-rhythm generating neurons projecting to the left loci.

It is interesting that the α-rhythm index is positively correlated with aldosteroneemia, while its frequency and laterality are negatively correlated, as are the θ-rhythm index and deviation.

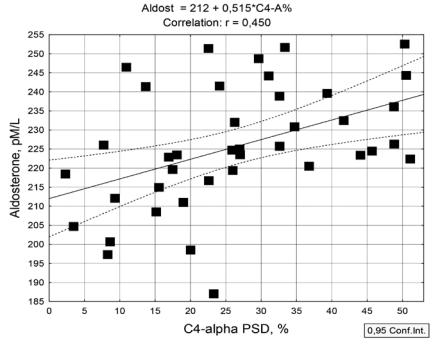

Fig. 4.7. Scatterplot of correlation between the PSD of α-rhythm in locus C4 (X-line) and Aldosterone serum level (Y-line)

The physiological interpretation of the HRV parameters included in the regression model is still ambiguous. LF power may be produced by both the vagal and sympathetic, and blood pressure regulation *via* baroreceptors [Shaffer F & Ginsberg JP, 2017], primarily by the vagal [Reyes del Paso GA et al., 2013] or by baroreflex activity alone [Goldstein DS et al., 2011]. In resting conditions, the LF band reflects baroreflex activity and not cardiac sympathetic innervation [Shaffer F & Ginsberg JP, 2017]. In this study, LF band correlates positively with vagal markers HF (r=0,66) and RMSSD (r=0,25), and the latter, in turn, negatively correlates with aldosteroneemia (r=-0,31), but was outside model. So, in this study, the LF band reflects vagal tone. Baevskiy's Activity of Regulatory Systems Index also reflects both sympathotonia and vagotonia. However, the ULF band continues to be terra incognita.

Table 4.3. Regression Summary for Aldosterone

R=0,894; R^2=0,800; Adjusted R^2=0,628; $F_{(18,2)}$=4,7; p=0,00054; SE: 9,8 pM/L

N=40		Beta	St. Err. of Beta	B	St. Err. of B	$t_{(21)}$	p-level
Variables	**r**		**Intercpt**	**267**	**37**	**7,27**	**10^{-6}**
C4-α PSD, %	**0,45**	0,492	0,311	0,563	0,356	1,58	0,128
P3-α PSD, %	**0,36**	2,217	0,691	1,935	0,603	3,21	0,004
T5-α PSD, %	**0,33**	-2,308	0,572	-2,155	0,534	-4,03	0,001
T3-α PSD, %	**0,30**	0,281	0,235	0,304	0,254	1,20	0,245
T4-α PSD, %	**0,28**	-0,700	0,290	-0,865	0,358	-2,42	0,025
T3-θ PSD, %	**0,29**	0,285	0,129	0,977	0,441	2,21	0,038
PSD ULF band, %	**0,30**	0,380	0,146	1,266	0,487	2,60	0,017
Index-α, %	**0,31**	0,505	0,271	0,270	0,145	1,86	0,077
Frequency-α, Hz	**-0,40**	-0,439	0,130	-8,651	2,558	-3,38	0,003
Laterality-α, %	**-0,27**	-0,195	0,125	-0,099	0,064	-1,56	0,134
C3-δ PSD, %	**-0,38**	-0,229	0,201	-0,166	0,146	-1,14	0,267
P3-δ PSD, %	**-0,34**	1,880	0,532	1,518	0,429	3,54	0,002
T5-δ PSD, %	**-0,30**	-1,480	0,389	-1,068	0,280	-3,81	0,001
PSD LF band, $msec^2$	**-0,32**	0,296	0,187	0,0045	0,0029	1,58	0,128
Activity RS Index, un.	**-0,26**	-0,266	0,156	-1,547	0,907	-1,71	0,103
Index-θ, %	**-0,29**	-0,248	0,126	-0,177	0,090	-1,97	0,063
Deviation-θ, Hz	**-0,26**	-0,244	0,144	-8,093	4,786	-1,69	0,106

Taken together, the listed EEG and HRV parameters determine the serum aldosterone level by 80,0% (Fig. 4.8).

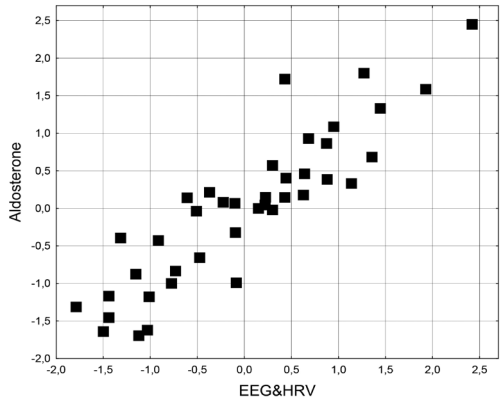

R=0,894; R^2=0,800; $\chi^2_{(18)}$=47; p-0,0002; Λ Prime=0,200

Fig. 4.8. Scatterplot of canonical correlation between the EEG&HRV parameters (X-line) and Aldosterone serum level (Y-line)

Unlike the first three hormones, the norms of which for the sexes, according to the kits instructions, are the same, testosteroneemia by definition shows sexual dimorphism. Therefore, the analysis of relationships was conducted separately for women and men.

It was found that the level of testosterone in women is upregulated by β- and θ-rhythm generating neurons (Fig. 4.9) while downregulated by δ-rhythm generating neurons (Fig. 4.10).

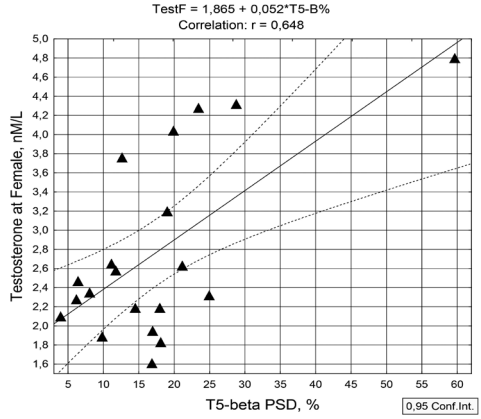

Fig. 4.9. Scatterplot of correlation between the PSD of β-rhythm in locus T5 (X-line) and Testosterone serum level (Y-line) at Female

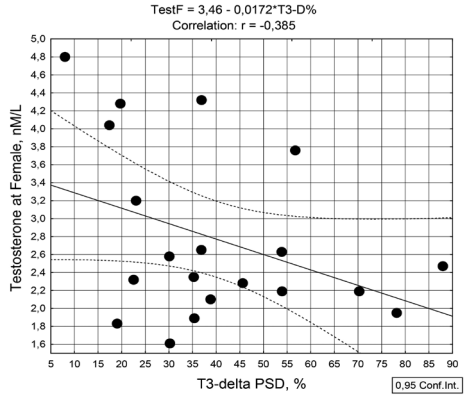

Fig. 4.10. Scatterplot of correlation between the PSD of δ-rhythm in locus T3 (X-line) and Testosterone serum level (Y-line) at Female

Taken together, the listed EEG parameters determine the serum testosterone level by 92,4% (Table 4 and Fig. 4.11).

Table 4.4. Regression Summary for Testosterone at women

R=0,961; R^2=0,924; Adjusted R^2=0,637; $F_{(15,4)}$=3,2; p=0,029; SE: 0,57 nM/L

N=20		Beta	St. Err. of Beta	B	St. Err. of B	$t_{(4)}$	p-level
Variables	**r**		**Intercpt**	**0,255**	**1,188**	**0,21**	**0,840**
T5-β PSD, %	**0,65**	0,953	0,499	0,076	0,040	1,91	0,129
F7-β PSD, %	**0,50**	2,368	0,742	0,164	0,051	3,19	0,033
O2-β PSD, %	**0,50**	-1,436	0,613	-0,1208	0,0516	-2,34	0,079
P4-β PSD, %	**0,49**	-3,292	1,186	-0,391	0,141	-2,78	0,050
P3-β PSD, %	**0,48**	1,393	0,561	0,174	0,070	2,48	0,068
T6-β PSD, %	**0,39**	0,708	0,324	0,054	0,025	2,19	0,094
O1-β PSD, %	**0,39**	1,669	0,754	0,1225	0,0554	2,21	0,091
T3-β PSD, %	**0,35**	-2,086	0,592	-0,164	0,047	-3,52	0,024
C3-θ PSD, %	**0,39**	0,310	0,233	0,069	0,052	1,33	0,254
Deviation-θ, Hz	**0,35**	0,970	0,343	1,937	0,686	2,82	0,048
T3-δ PSD, %	**-0,38**	-1,489	0,518	-0,066	0,023	-2,87	0,045
T3-δ PSD, μV²/Hz	**-0,35**	-1,199	0,561	-0,0048	0,0022	-2,14	0,099
O2-δ PSD, μV²/Hz	**-0,36**	-0,985	0,312	-0,0050	0,0016	-3,16	0,034
T5-δ PSD, μV²/Hz	**-0,35**	2,112	0,734	0,0095	0,0033	2,88	0,045
T6-δ PSD, %	**-0,31**	1,599	0,473	0,086	0,025	3,38	0,028

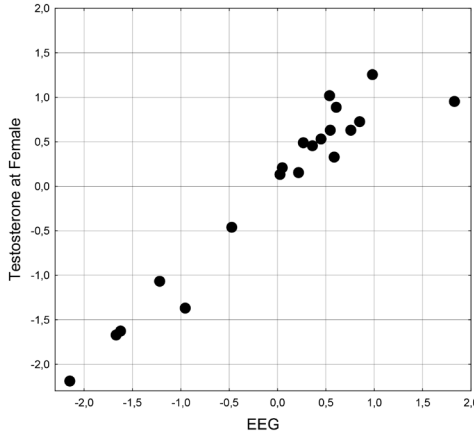

R=0,961; R^2=0,924; $\chi^2_{(15)}$=27; p=0,029; Λ Prime=0,076

Fig. 4.11. Scatterplot of canonical correlation between the EEG parameters (X-line) and Testosterone serum level (Y-line) at Female

Although the degree of neurogenic determination of testosterone level was exactly the same (92,4%) in men as well (Fig. 4.14), the structure of the regression model is completely different (Table 4.5). And this is quite natural, because the main source of testosterone in women is normally the reticular zone of the adrenal cortex.

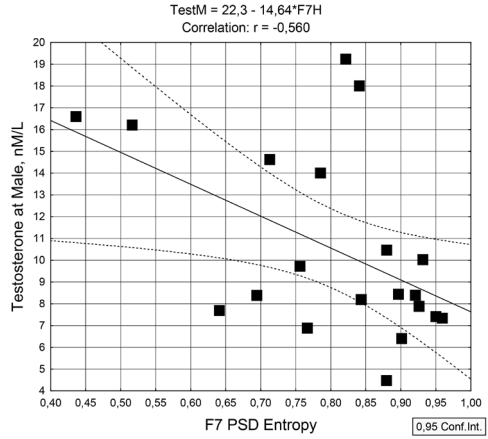

Fig. 4.12. Scatterplot of correlation between the Entropy of PSD in locus F7 (X-line) and Testosterone serum level (Y-line) at Male

With regard to EEG parameters, it was found that downregulation is carried out by entropy (Fig. 4.12) and θ-rhythm generating neurons projecting to the F7 locus (Table 4.5), while similar neurons projecting to the T4 locus, as well as scattered δ-rhythm generating neurons, carry out upregulation (Fig. 4.13).

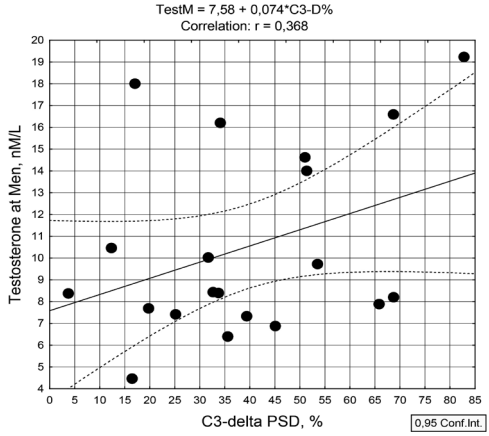

Fig. 4.13. Scatterplot of correlation between the PSD of δ-rhythm in locus C3 (X-line) and Testosterone serum level (Y-line) at Male

Additional upregulating factors are the deviation of the β-rhythm and the laterality of the α-rhythm, instead, the sympathetic tone exerts a downregulating effect. By the way, the level of testosterone in women is also negatively correlated with sympathetic tone, but not strongly enough to be included in the regression model (r=-0,29).

Table 4.5. Regression Summary for Testosterone at men

R=0,961; R^2=0,924; Adjusted R^2=0,771; $F_{(12,6)}$=6,1; p=0,019; SE: 2,09 nM/L

N=20		**Beta**	**St. Err. of Beta**	**B**	**St. Err. of B**	$t_{(6)}$	**p-level**
Variables	**r**		**Intercpt**	**2,51**	**8,69**	**0,29**	**0,782**
1	2	3	4	5	6	7	8
F7 PSD Entropy	**-0,56**	-0,639	0,195	-19,61	5,974	-3,28	0,017
Fp1 PSD Entropy	**-0,46**	0,833	0,359	26,84	11,57	2,32	0,059
C3 PSD Entropy	**-0,43**	0,420	0,239	14,10	8,02	1,76	0,129
F7-θ PSD, %	**-0,48**	-0,348	0,198	-0,414	0,234	-1,76	0,128

Table 4.6 (cont)

1	2	3	4	5	6	7	8
Amplitude Mode, %	**-0,47**	-0,787	0,217	-0,337	0,093	-3,63	0,011
C3-δ PSD, μV²/Hz	**0,43**	0,857	0,452	0,0130	0,0069	1,90	0,107
C4-δ PSD, μV²/Hz	**0,40**	-1,046	0,461	-0,0142	0,0063	-2,27	0,064
F7-δ PSD, %	**0,40**	-0,523	0,285	-0,108	0,059	-1,83	0,117
Fp1-δ PSD, μV²/Hz	**0,38**	0,729	0,348	0,0181	0,0086	2,09	0,081
T4-θ PSD, μV²/Hz	**0,40**	1,280	0,314	0,2172	0,0533	4,07	0,007
Deviation-β, Hz	**0,49**	0,602	0,169	4,158	1,168	3,56	0,012
Laterality-α, %	**0,40**	-0,534	0,202	-0,063	0,024	-2,64	0,039

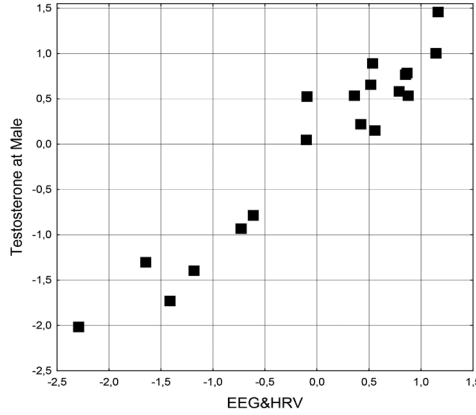

R=0,961; R^2=0,924; $\chi^2_{(12)}$=28; p=0,005; Λ Prime=0,076
Fig. 4.14. Scatterplot of canonical correlation between the EEG&HRV parameters (X-line) and Testosterone serum level (Y-line) at Male

The serum level of calcitonin also shows sexual dimorphism, although it is less pronounced compared to testosterone. According to the instructions for the DRG International Inc. kit, normal range in women 0,1÷10,0 ng/L, in men 0,2÷27,7 ng/L.

It was found that calcitoninemia in women is upregulated by β-rhythm generating neurons projecting to the T4 (Fig. 4.15) and Fp2 loci as well as δ-rhythm generating neurons projecting to the O2 and C3 loci. Instead, frequency of δ-rhythm, θ- and α-rhythm generating neurons projecting to F3, C3 and P3 (Fig. 4.16) loci respectively, as well as entropy of PSD in C3 locus, carry out downregulation (Table 4.6).

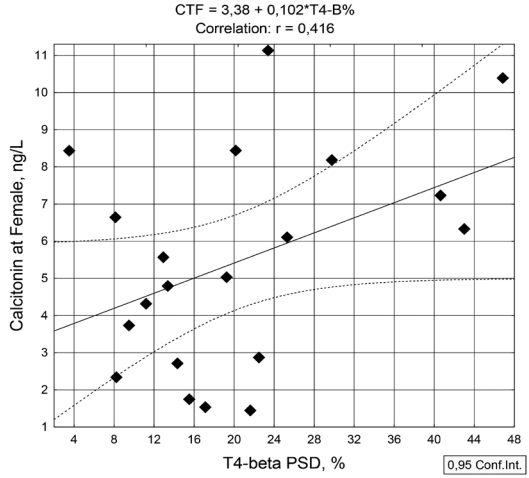

Fig. 4.15. Scatterplot of correlation between the PSD of β-rhythm in locus T4 (X-line) and Calcitonin serum level (Y-line) at Female

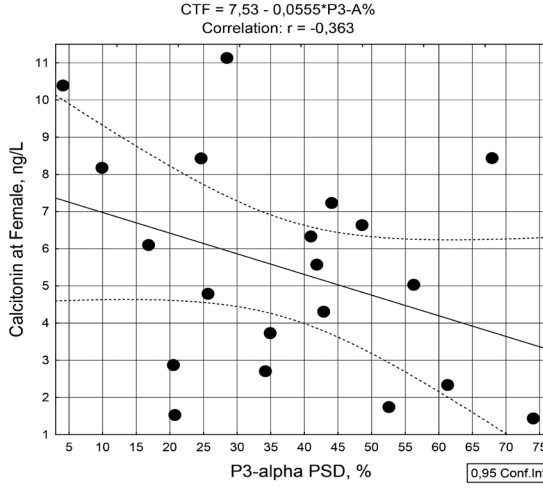

Fig. 4.16. Scatterplot of correlation between the PSD of α-rhythm in locus P3 (X-line) and Calcitonin serum level (Y-line) at Female

Additional upregulating factors are the HRV-markers of the sympathetic tone (Fig. 4.17).

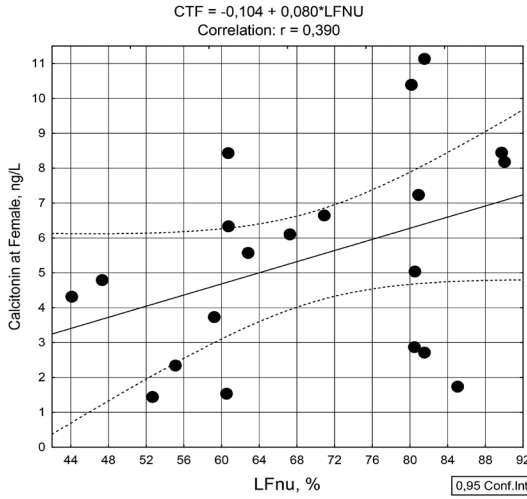

Fig. 4.17. Scatterplot of correlation between the LFnu HRV (X-line) and Calcitonin serum level (Y-line) at Female

Taken together, the listed EEG and HRV parameters determine the serum calcitonin level at women by 86,2% (Table 6 and Fig. 4.18).

Table 4.6. Regression Summary for Calcitonin at women

R=0,928; R^2=0,862; Adjusted R^2=0,672; $F_{(11,8)}$=4,5; p=0,021; SE: 1,67 ng/L

N=20		**Beta**	**St. Err. of Beta**	**B**	**St. Err. of B**	**$t_{(8)}$**	**p-level**
Variables	**r**		**Intercpt**	**70,8**	**19,3**	**3,66**	**0,006**
T4-β PSD, %	**0,42**	-1,754	0,528	-0,428	0,129	-3,32	0,011
Fp2-β PSD, %	**0,37**	0,397	0,240	0,112	0,068	1,65	0,137
LFnu HRV, %	**0,39**	0,796	0,400	0,163	0,082	1,99	0,081
LF/HF Ratio HRV	**0,37**	1,130	0,439	1,353	0,526	2,57	0,033
O2-δ PSD, %	**0,38**	-2,011	0,662	-0,269	0,089	-3,04	0,016
C3-δ PSD, %	**0,32**	-1,436	0,654	-0,180	0,082	-2,20	0,059
Frequency-δ, Hz	**-0,38**	-0,599	0,181	-11,36	3,43	-3,31	0,011
P3-α PSD, %	**-0,36**	-2,361	0,675	-0,361	0,103	-3,50	0,008
F3-θ PSD, %	**-0,34**	1,199	0,493	0,741	0,304	2,43	0,041
C3-θ PSD, %	**-0,35**	-1,940	0,536	-1,318	0,364	-3,62	0,007
C3 PSD Entropy	**-0,32**	-1,806	0,579	-33,37	10,69	-3,12	0,014

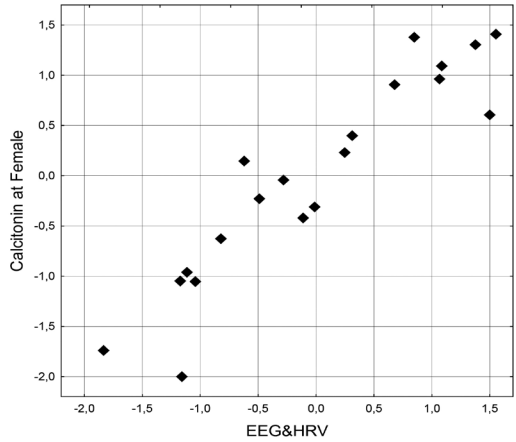

R=0,928; R^2=0,862; $\chi^2_{(11)}$=25; p=0,010; Λ Prime=0,138

Fig. 4.18. Scatterplot of canonical correlation between the EEG&HRV parameters (X-line) and Calcitonin serum level (Y-line) at Female

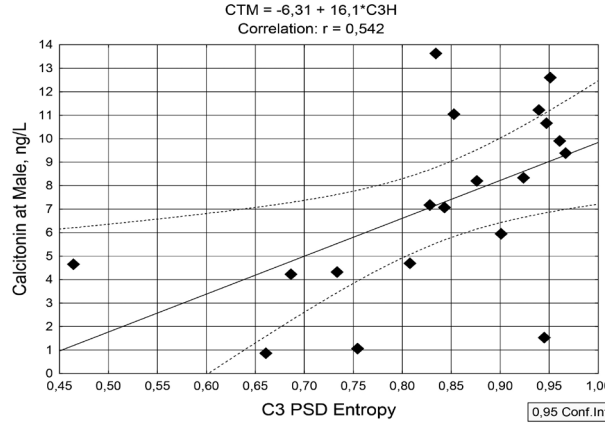

Fig. 4.19. Scatterplot of correlation between the Entropy of PSD in locus C3 (X-line) and Calcitonin serum level (Y-line) at Male

In men, the upregulation of the calcitonin level is carried out by EEG entropy (Fig. 4.19) and θ-rhythm generating neurons projecting to the F8 and F4 loci, as well as, apparently, circulating catecholamines, the markers of which are primarily the parameter inverted to Mode HRV, as well as other Baevskiy's RM HRV parameters.

Recall that in women, unlike men, θ-rhythm-generating neurons (although with a different localization) negatively regulate the level of calcitonin. An even more striking contrast is shown by β-rhythm generating neurons projecting to the T4 locus: upregulation at women versus downregulation at men (Fig. 4.20). Here it is appropriate to note the opposite of cortisol-testosterone correlations: -0,42 at women versus +0,36 at men.

Taken together, the listed EEG and HRV parameters determine the serum calcitonin level at men by 83,5% (Table 7 and Fig. 4.21).

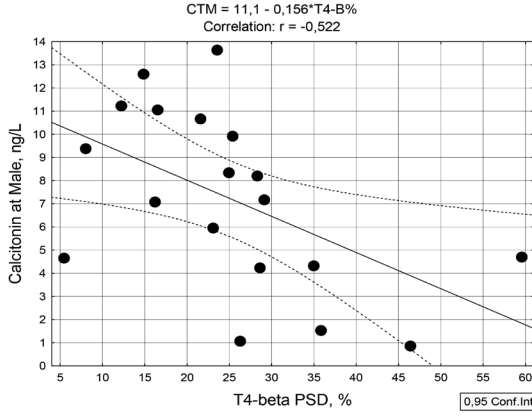

Fig. 4.20. Scatterplot of correlation between the PSD of β-rhythm in locus T4 (X-line) and Calcitonin serum level (Y-line) at Male

Table 4.7. Regression Summary for Calcitonin at men

R=0,914; R^2=0,835; Adjusted R^2=0,670; $F_{(9,9)}$=5,1; p=0,012; SE: 2,22 ng/L

N=19		Beta	St. Err. of Beta	B	St. Err. of B	$t_{(9)}$	p-level
Variables	**r**		**Intercpt**	**-92,3**	**51,9**	**-1,78**	**0,109**
C3 PSD Entropy	**0,54**	0,943	0,235	28,07	7,00	4,01	0,003
C4 PSD Entropy	**0,38**	-0,819	0,271	-18,79	6,23	-3,02	0,015
HR, beats/min	**0,47**	2,113	0,996	0,840	0,396	2,12	0,063
1/Mode HRV, msec^{-1}	**0,44**	1,324	0,971	0,041	0,030	1,36	0,206
Activity RS Index, un.	**0,43**	1,167	0,377	1,993	0,644	3,09	0,013
Stress Index HRV, un.	**0,35**	-0,650	0,305	-0,0215	0,0101	-2,13	0,062
F8-θ PSD, %	**0,40**	0,330	0,177	0,387	0,207	1,87	0,095
F4-θ PSD, μV^2/Hz	**0,35**	-0,903	0,309	-0,169	0,058	-2,92	0,017
T4-β PSD, %	**-0,52**	-0,272	0,180	-0,034	0,022	-1,52	0,164

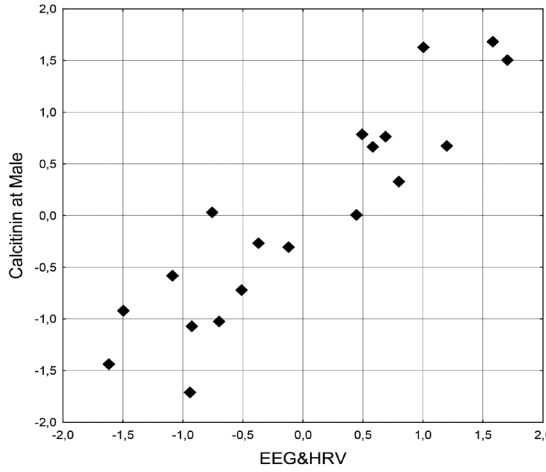

R=0,914; R^2=0,835; $\chi^2_{(9)}$=22,5; p=0,007; Λ Prime=0,165

Fig. 4.21. Scatterplot of canonical correlation between the EEG&HRV parameters (X-line) and Calcitonin serum level (Y-line) at Male

Conclusion

Serum levels of the main adaptation hormones are accompanied by specific patterns of EEG and HRV parameters.

Chapter 5

IMMEDIATE EFFECTS OF UKRAINIAN PHYTOCOMPOSITION "BALM TRUSKAVETS" ON BIOPHOTONICS (GDV), EEG AND HRV PARAMETERS IN HUMANS WITH MALADAPTATION

Summary

Background. Previous experimental and clinical-physiological studies have shown that the Ukrainian phytocomposition "Balm Kryms'kyi" has adaptogenic properties, which are manifested in its vegetative, endocrine, immunotropic, coagulotropic, actotropic and metabolic effects. However, the neurotropic effects of the phytocomposition remain unclear, which is the purpose of this study.

Materials and methods. The object of observation were 12 women (44±13 years) and 62 men (44±12 years) with dysfunction of neuro-endocrine-immune complex. HRV and EEG as well as GDV parameters were recorded in the morning in basal conditions. Then the members of the main group used 5 ml of phytocomposition "Balm Truskavets'" (is analogous to the previous "Balm Kryms'kyi") dissolved in 45 ml of tap water, instead in the control group used 50 ml of the latter. After 1,5 hours, the test was repeated.

Results. Discriminant analysis revealed 26 EEG, 6 HRV and 7 GDV parameters characteristic of the initial state and after consumption of phytocomposition or tap water. The use of balm causes the normalizing decrease of increased sympathotonic markers and the increase of decreased vagotonic markers. Physiologically favorable vegetotropic effects of the balm are accompanied by a further increase in the initially increased activity of β-rhythm-generating cortical and subcortical structures as well as activation of θ-rhythm-generating and inhibition of α- and δ-rhythm-generating nuclei whose initial activity was within normal limits. Neurotropic effects are accompanied by a decrease in fractality and entropy and an increase in the area of GDI, as well as the energy of the first, fourth, fifth and seventh virtual Chakras.

Conclusion. Ukrainian phytocomposition "Balm Truskavets'" causes favorable immediate neurotropic and biophysic changes at patients with dysfunction of neuro-endocrine-immune complex.

INTRODUCTION

Previous experimental and clinical-physiological studies have shown that the Ukrainian phytocomposition "Balm Kryms'kyi" [Pat. 10271 Ukraine, 1996] has adaptogenic properties, which are manifested in its vegetative, endocrine, immunotropic, coagulotropic, actotropic and metabolic effects [Panasyuk YM et al., 1994; Alyeksyeyev ***OI*** et al., 1996; Markova OO et al., 1997; Flyunt IS et al., 2002; Hrinchenko BV et al., 2006; Kostyuk PG et al., 2006; Flyunt IS et al., 2008; Hrinchenko BV, 2008]. However, the neurotropic properties of the phytocomposition remain unclear, which is the purpose of this study.

MATERIAL AND METHODS

The object of observation were 12 women (44±13 years) and 62 men (44±12 years) with dysfunction of neuro-endocrine-immune complex, employees of the clinical sanatoria "Kryshtalevyĭ Palats" and "Moldova" (Truskavets', Ukraine). Every of morning before work, carried out initial tests of 6 persons, then the two of them (basic group) used 5 ml of phytocomposition "Balm Truskavets'", pre-diluted in 45 ml of boiled tap water. The other 4 individuals (control group) used 50 ml of the same water at room temperature (CW).

In the morning on an empty stomach we registered kirlianogram by the method of GDV by the device of "GDV Chamber" ("Biotechprogress", SPb, RF).

To assess the parameters of HRV recorded during 7 min electrocardiogram in II lead (software and hardware complex «CardioLab+HRV», KhAI-MEDICA, Kharkiv). After 8-13 minutes, the EEG recorded a hardware-software complex "NeuroCom Standard" (KhAI MEDICA, Kharkiv).

HRV reference values were taken from the instructions for the "CardioLab+HRV" device, GDV and EEG references were taken from the database of Truskavetsian Scientific School of Balneology.

RESULTS AND DISCUSSION

In order to identify among the registered parameters those whose constellation is three states of persons: initial and after the use of a solution of phytocomposition or control water – differ significantly from each other, discriminant analysis was used. The forward stepwise program

included 39 variables in the discriminant model (Tables 1 and 2). Among them, 2 relate to **delta-rhythm**, 4 – **theta-rhythm**, 9 – **alpha-rhythm**, 10 – **beta-rhythm**, 1 – **entropy** of EEG, and the other 6 – HRV, including 2 **sympathetic** and 3 **vagal** markers as well as **entropy** of HRV bands. However, we are most interested in the 7 parameters of **biophotonics**, which confirms their relationship with the parameters of EEG and HRV.

Table 5.1. Discriminant Function Analysis Summary for GDV, EEGs and HRVs Variables as well as their Reference levels and Coefficients of Variability

Step 39, N of vars in model: 39; Grouping: 3 gr; Wilks' Λ: 0,199; appr. $F_{(78)}$=3,4; $p<10^{-6}$

Variables currently in the model (n=148)	Groups (n)			Parameters of Wilks' Statistics					
	After Balm (20)	Base-line (74)	After CW (54)	Wilks' Λ	Par-tial Λ	F-re-move (2,1)	p-level	Tole-rancy	Refe-rence Cv/SD
1	2	3	4	5	6	7	8	9	10
Area GDI Right, kpixels	29,41 0,68	27,04 0,56	27,02 0,65	0,206	0,968	1,75	0,178	0,060	27,02 0,151
Shape Coefficient GDI Right	14,2 0,5	16,9 0,8	16,9 0,8	0,215	0,925	4,35	0,015	0,054	17,2 0,331
Shape Coefficient GDI Frontal	19,1 1,2	22,1 1,3	23,3 1,5	0,217	0,920	4,63	0,012	0,065	23,4 0,395
Chakra 1 Energy	0,35 0,06	0,23 0,04	0,16 0,06	0,213	0,938	3,56	0,032	0,156	0,20 **0,34**
Chakra 2 Asymmetry	0,20 0,07	-0,02 0,05	0,21 0,06	0,201	0,989	0,58	0,561	0,431	0,22 **0,38**
Chakra 5 Energy	0,27 0,07	0,11 0,03	0,13 0,04	0,215	0,925	4,33	0,016	0,316	0,12 **0,23**
Chakra 7 Energy	0,13 0,06	0,03 0,03	-0,01 0,04	0,203	0,980	1,07	0,346	0,192	0,04 **0,26**
ULF/TP HRV, %	2,3 0,7	6,8 0,8	10,4 1,2	0,230	0,867	8,24	10^{-3}	0,337	4,6 0,674
LF/HF HRV	3,45 0,85	4,04 0,33	5,21 0,41	0,201	0,990	0,53	0,593	0,288	2,80 0,714
HF HRV PSD, msec²	468 174	291 61	145 15	0,200	0,996	0,20	0,818	0,064	452 0,768
RMSSD HRV, msec	26,4 4,2	23,5 1,5	19,2 1,0	0,214	0,929	4,08	0,020	0,091	37,0 0,459
pNN_{50} HRV, %	8,3 3,7	5,4 1,2	2,6 0,4	0,205	0,973	1,48	0,233	0,037	9,0 0,858

Table 5.1 (cont)

1	2	3	4	5	6	7	8	9	10
P4-δ PSD, %	14,3 1,7	20,2 1,3	19,4 1,6	0,223	0,892	6,45	0,002	0,186	27,1 0,671
P4-δ PSD, μV²/Hz	47 8	79 9	95 11	0,229	0,871	7,92	0,001	0,152	107 0,886
Asymmetry-θ, %	28,6 3,7	23,0 2,1	18,1 1,8	0,204	0,975	1,37	0,258	0,467	23,0 0,699
O1-θ PSD, %	9,0 1,3	6,6 0,5	6,0 0,5	0,204	0,977	1,28	0,283	0,182	6,7 0,636
O1-θ PSD, μV²/Hz	24 4	36 5	38 5	0,203	0,983	0,91	0,405	0,227	36 1,213
O2-θ PSD, %	7,1 1,0	5,2 0,3	5,0 0,4	0,202593	0,984	0,89	0,412	0,491	6,0 0,603
Fp1-α PSD, %	27,1 2,5	37,7 2,3	39,7 2,7	0,206	0,966	1,91	0,153	0,089	37,2 0,501
F3-α PSD, %	24,2 2,2	35,7 2,2	41,4 2,3	0,206	0,966	1,89	0,156	0,038	34,5 0,547
F3-α PSD, μV²/Hz	85 11	156 20	183 24	0,220	0,904	5,69	0,004	0,057	146 1,071
T3-α PSD, %	24,0 2,0	31,6 1,9	36,2 2,0	0,205	0,972	1,54	0,219	0,064	30,7 0,546
T3-α PSD, μV²/Hz	62 8	104 13	119 15	0,205	0,970	1,66	0,196	0,107	97 0,988
C3-α PSD, %	26,4 2,2	35,4 2,1	42,4 2,3	0,214	0,932	3,89	0,023	0,043	35,3 0,510
T6-α PSD, %	23,5 2,7	33,6 2,4	37,3 2,9	0,207	0,962	2,09	0,128	0,095	32,2 0,623
O2-α PSD, %	38,6 4,4	45,5 3,0	50,1 3,5	0,203	0,982	0,98	0,377	0,071	44,6 0,532
O2-α PSD, μV²/Hz	229 84	463 79	697 128	0,225	0,884	7,03	0,001	0,104	410 1,627
Frequency-β, %	17,2 0,8	19,6 0,5	20,0 0,5	0,215	0,929	4,11	0,019	0,570	19,0 0,200
Asymmetry-β, %	21,7 4,3	23,9 2,1	17,6 2,8	0,211	0,945	3,11	0,049	0,610	20,1 0,699
F3-β PSD, μV2/Hz	108 10	83 7	69 6	0,208	0,960	2,22	0,113	0,128	78 0,667
T4-β PSD, %	42,5 4,3	36,7 2,1	30,6 2,3	0,212	0,938	3,55	0,032	0,088	27,9 0,591

Table 5.1 (cont)

1	2	3	4	5	6	7	8	9	10
C4-β PSD, %	38,9 3,2	30,9 1,8	25,8 2,1	0,210	0,951	2,76	0,068	0,098	26,3 0,493
C4-β PSD, μV²/Hz	122 12	89 7	71 5	0,228	0,874	7,69	0,001	0,072	84 0,671
T4-β PSD, μV²/Hz	99 10	88 10	64 4	0,232	0,859	8,81	10^{-3}	0,177	72 0,745
T6-β PSD, %	49 5	40 2	26 3	0,214	0,931	3,96	0,022	0,098	30 0,646
P3-β PSD, %	41,6 3,7	30,2 1,8	26,8 2,1	0,209	0,951	2,73	0,070	0,100	25,0 0,549
O1-β PSD, %	42,3 4,7	36,1 2,5	31,1 2,9	0,205	0,973	1,48	0,233	0,106	26,7 0,656
Entropy PSD HRV	0,728 0,025	0,766 0,012	0,785 0,013	0,205	0,970	1,63	0,201	0,273	0,825 0,114
Entropy EEG PSD in O1	0,798 0,036	0,718 0,021	0,709 0,023	0,207	0,961	2,17	0,119	0,190	0,738 0,245

Note. For groups the average values and standard errors are specified; for the norm – the average values and coefficients of variation (Cv) or standard deviations (**SD**).

Table 5.2. Summary of Stepwise Analysis for GDV, EEGs and HRVs Variables. The variables are ranked by criterion Lambda

Variables currently in the model	**F to enter**	**p-level**	**Λ**	**F-va-lue**	**p-level**
1	2	3	4	5	6
ULF/TP, %	10,8	10^{-4}	0,871	10,8	10^{-4}
F3-α PSD, %	8,05	0,0005	0,783	9,36	10^{-6}
P4-δ PSD, %	9,22	0,0002	0,694	9,56	10^{-6}
C4-β PSD, μV²/Hz	5,79	0,0038	0,641	8,83	10^{-6}
Chakra 2 Asymmetry	4,52	0,0125	0,603	8,12	10^{-6}
T4-β PSD, μV²/Hz	4,87	0,0090	0,564	7,75	10^{-6}
Fp1-α PSD, %	3,71	0,0270	0,535	7,29	10^{-6}
P4-δ PSD, μV²/Hz	3,22	0,0431	0,511	6,88	10^{-6}
LF/HF	3,01	0,0527	0,490	6,53	10^{-6}

Table 5.2 (cont)

1	2	3	4	5	6
Asymmetry-β, %	3,27	0,0409	0,467	6,30	10^{-6}
O2-θ PSD, %	3,12	0,0474	0,447	6,09	10^{-6}
Frequency-β, %	2,56	0,0810	0,430	5,86	10^{-6}
O1-θ PSD, μV²/Hz	1,72	0,1830	0,419	5,57	10^{-6}
C3-α PSD, %	1,77	0,1738	0,408	5,33	10^{-6}
Chakra 5 Energy	1,64	0,1970	0,398	5,10	10^{-6}
T6-α PSD, %	2,16	0,1196	0,385	4,96	10^{-6}
C4-β PSD, %	2,72	0,0698	0,370	4,89	10^{-6}
P3-β PSD, %	2,33	0,1016	0,357	4,79	10^{-6}
Entropy HRV	2,73	0,0694	0,342	4,74	10^{-6}
HF HRV PSD, msec²	1,87	0,1587	0,332	4,63	10^{-6}
Chakra 1 Energy	1,83	0,1640	0,323	4,52	10^{-6}
T3-α PSD, μV²/Hz	1,64	0,1981	0,315	4,41	10^{-6}
F3-α PSD, μV²/Hz	1,75	0,179	0,306	4,32	10^{-6}
O2-α PSD, μV²/Hz	1,73	0,1816	0,297	4,24	10^{-6}
O2-α PSD, %	1,86	0,1607	0,289	4,17	10^{-6}
T6-β PSD, %	1,89	0,1560	0,280	4,11	10^{-6}
T4-β PSD, %	2,33	0,1018	0,269	4,09	10^{-6}
RMSSD HRV, msec	1,15	0,3192	0,264	3,99	10^{-6}
pNN_{50} HRV, %	1,37	0,2589	0,258	3,91	10^{-6}
F3-β PSD, μV2/Hz	1,19	0,3067	0,253	3,82	10^{-6}
Asymmetry-θ, %	1,28	0,2808	0,247	3,75	10^{-6}
Shape Coef GDI Right	1,46	0,2373	0,241	3,69	10^{-6}
Shape Coe GDI Frontal	2,92	0,0578	0,229	3,73	10^{-6}
O1-β PSD, %	1,42	0,2449	0,224	3,67	10^{-6}
Area GDI Right, pixels	1,36	0,2617	0,218	3,62	10^{-6}
T3-α PSD, %	1,46	0,2372	0,213	3,57	10^{-6}
Entropy EEG O1	1,16	0,3180	0,208	3,51	10^{-6}
O1-θ PSD, %	1,32	0,2717	0,203	3,46	10^{-6}
Chakra 7 Energy	1,07	0,3457	0,199	3,40	10^{-6}

In addition, a number of other GDV, EEG and HRV parameters that were not included in the model are noteworthy (Table 3).

Table 5.3. Discriminant Function Analysis Summary for GDV, EEG and HRV Variables currently not in the model

Variables	Groups (n)			Parameters of Wilks' Statistics					
	After Balm (20)	Base-line (74)	After CW (54)	Wilks' Λ	Par-tial Λ	F to enter	p-level	Tole-rancy	Refe-rence Cv/SD
Entropy GDI Right	3,75 0,04	3,86 0,03	3,88 0,03	0,199	0,998	0,09	0,911	0,333	3,86 0,052
Chakra 3 Asymmetry	0,37 0,10	0,18 0,05	0,25 0,06	0,199	0,994	0,19	0,894	0,333	0,22 **0,38**
Chakra 4 Energy	0,51 0,03	0,39 0,04	0,34 0,06	0,196	0,982	0,97	0,382	0,277	0,40 **0,28**
LFnu, %	64,7 4,8	72,9 1,9	79,5 1,5	0,198	0,993	0,38	0,683	0,165	61,8 0,247
HF/TP, %	20,9 3,9	14,0 1,3	9,3 0,5	0,199	0,996	0,20	0,820	0,151	17,1 1,230
Frequency-δ, Hz	1,08 0,04	1,09 0,02	1,03 0,02	0,199	0,997	0,15	0,860	0,596	1,07 0,165
Deviation-θ, Hz	1,25 0,14	1,11 0,08	0,94 0,08	0,199	0,999	0,03	0,973	0,701	1,00 0,616
Amplitude-α, μV	13,9 1,9	17,8 1,5	20,9 2,1	0,197	0,988	0,63	0,536	0,030	17,7 0,703
Index α, %	34,1 6,2	42,9 4,0	47,7 4,4	0,197	0,988	0,65	0,526	0,193	48,4 0,558
Fp1-α PSD, $\mu V^2/Hz$	63 9	120 15	140 18	0,197	0,986	0,73	0,483	0,025	109 1,063
Fp2-α PSD, %	27,5 2,4	35,3 2,2	37,3 2,5	0,199	1,000	0,01	0,991	0,188	33,2 0,535
F4-α PSD, %	25,8 2,2	34,7 2,2	41,7 2,4	0,199	0,997	0,18	0,833	0,073	32,7 0,564
F4-β PSD, %	32,4 3,5	29,9 1,9	25,2 1,9	0,199	0,998	0,08	0,920	0,158	24,5 0,544
F7-α PSD, $\mu V^2/Hz$	97 3	56 8	63 9	0,198	0,994	0,30	0,744	0,149	59 1,410
T6-α PSD, $\mu V^2/Hz$	49 6	102 15	124 18	0,196	0,983	0,93	0,399	0,147	100 1,397
O1-α PSD, %	32,7 3,1	40,7 3,0	46,3 3,4	0,199	0,998	0,11	0,894	0,059	39,9 0,591
Entropy EEG PSD in O2	0,760 0,029	0,688 0,018	0,666 0,022	0,199	0,996	0,19	0,827	0,141	0,727 0,242

Next, the 39-dimensional space of discriminant variables transforms into 2-dimensional space of canonical roots. The canonical correlation coefficient is for Root 1 0,770 (Wilks' Λ=0,223; $\chi^2_{(68)}$=193; $p<10^{-6}$), for Root 2 0,673 (Wilks' Λ=0,547; $\chi^2_{(33)}$=78; $p<10^{-4}$). The major root contains 63,7% of discriminative opportunities, the minor – 36,3%.

Table 4 presents raw (actual) and standardized (normalized) coefficients for discriminant variables. The calculation of the discriminant root values for each person as the sum of the products of raw coefficients to the individual values of discriminant variables together with the constant enables the visualization of each person in the information space of the roots.

Table 5.4. Standardized and Raw Coefficients and Constants for Canonical GDV, EEGs and HRVs Variables

Coefficients	**Standardized**		**Raw**	
1	2	3	4	5
Variables	Root 1	Root 2	Root 1	Root 2
ULF/TP, %	0,650	-0,546	0,094	-0,079
F3-α PSD, %	0,656	0,808	0,038	0,047
P4-δ PSD, %	0,798	0,629	0,071	0,056
C4-β PSD, μV²/Hz	-1,492	-0,976	-0,030	-0,020
Ch2 Asymmetry	-0,079	-0,163	-0,286	-0,587
T4-β PSD, μV²/Hz	0,789	0,931	0,012	0,014
Fp1-α PSD, %	-0,124	0,331	-0,007	0,020
P4-δ PSD, μV²/Hz	-0,226	-0,239	-0,079	-0,084
LF/HF	-0,032	-0,283	-0,011	-0,093
Asymmetry-β, %	-0,124	-1,185	-0,002	-0,016
O2-θ PSD, %	0,413	0,109	0,108	0,029
Frequency-β, %	0,181	0,435	0,005	0,011
O1-θ PSD, μV²/Hz	-0,197	-2,245	-0,012	-0,132
C3-α PSD, %	0,819	-0,099	0,054	-0,007
Ch5 Energy	-0,779	-0,167	-0,049	-0,011
T6-α PSD, %	-0,416	-0,071	-4,057	-0,689
C4-β PSD, %	-0,320	-0,585	-1,789	-3,271
P3-β PSD, %	0,693	-0,007	0,035	-0,0004

Table 5.4 (cont)

1	2	3	4	5
Entropy HRV	0,523	-0,298	0,001	-0,0006
HF, msec^2	0,644	0,157	0,006	0,002
Ch1 Energy	-0,431	1,482	-0,003	0,009
T3-α PSD, μV^2/Hz	0,022	-1,540	0,00003	-0,0020
F3-α PSD, μV^2/Hz	-0,183	1,319	-0,007	0,053
O2-α PSD, μV^2/Hz	-0,550	-1,358	-0,026	-0,064
O2-α PSD, %	0,602	0,964	0,034	0,054
T6-β PSD, %	0,508	-0,522	2,933	-3,018
T4-β PSD, %	-0,483	0,346	-0,115	0,082
RMSSD, msec	-0,402	0,581	-0,033	0,048
pNN$_{50}$, %	-0,039	0,803	-0,158	3,243
F3-β PSD, μV2/Hz	-0,021	1,524	-0,005	0,373
Asymmetry-θ, %	-0,509	-1,172	-0,076	-0,175
Shape C Right	-0,884	-0,257	-0,0003	-0,00008
Shape C Frontal	-0,032	0,289	-0,002	0,018
O1-β PSD, %	0,367	-0,104	1,958	-0,552
Area GDI R, pixels	0,650	-0,546	0,094	-0,079
T3-α PSD, %	0,656	0,808	0,038	0,047
Entropy O1	0,798	0,629	0,071	0,056
O1-θ PSD, %	-1,492	-0,976	-0,030	-0,020
Ch7 Energy	-0,079	-0,163	-0,286	-0,587
		Constants	8,033	2,886
		Eigenvalues	1,457	0,829
		Cumulative Proportion	0,637	1

Table 5 presents the full structural coefficients. There are also average values (centroids) of Roots and Z-scores of Variables. We consider it expedient to include in the table also out-of-model variables in view of their recognizability.

Table 5.5. Factor Structure Matrix and Means of Roots and Variables

Variables, Z	Correlations Variables-Roots		After Balm (20)	Base-line (74)	After CW (54)
1	2	3	4	5	6
Root 1 (63,8%)	**R1**	**R2**	**-2,96**	+0,25	+0,76
ULF/TP, %	**0,281**	-0,200	**-0,73**	+0,70	+1,88
LF/HF	**0,128**	0,166	**+0,33**	+0,62	+1,20
LFnu, %			**+0,19**	+0,73	+1,16
F3-α PSD, %	**0,250**	-0,104	**-0,55**	+0,06	+0,36
C3-α PSD, %	**0,228**	-0,154	**-0,50**	0,00	+0,39
T6-α PSD, %	**0,177**	-0,048	**-0,43**	+0,07	+0,25
F3-α PSD, μV²/Hz	**0,155**	-0,045	**-0,39**	+0,06	+0,24
O2-α PSD, μV²/Hz	**0,146**	-0,121	**-0,27**	+0,08	+0,43
O2-α PSD, %	**0,113**	-0,065	**-0,25**	+0,04	+0,23
T3-α PSD, %			**-0,40**	+0,05	+0,33
Fp1-α PSD, μV²/Hz			**-0,39**	+0,10	+0,27
F4-α PSD, %			**-0,38**	+0,11	+0,49
O1-α PSD, %			**-0,31**	+0,03	+0,27
Amplitude-α, μV			**-0,31**	+0,01	+0,26
Frequency-β, Hz	**0,194**	-0,010	**-0,46**	+0,15	+0,27
T3-α PSD, μV²/Hz	**0,140**	-0,033	**-0,36**	+0,08	+0,22
Fp1-α PSD, %			**-0,54**	+0,08	+0,14
F7-α PSD, μV²/Hz			**-0,38**	-0,04	+0,05
T6-α PSD, μV²/Hz			**-0,36**	+0,02	+0,17
Fp2-α PSD, %			**-0,32**	+0,12	+0,23
Index α, %			**-0,53**	-0,20	-0,03
O1-θ PSD, μV²/Hz	**0,095**	0,005	**-0,26**	+0,02	+0,05
Shape C GDI Right	**0,136**	0,031	**-0,52**	-0,06	-0,05
Shape C GDI Frontal	**0,111**	-0,019	**-0,46**	-0,14	-0,01
Entropy GDI Right			**-0,50**	+0,06	+0,15
P4-δ PSD, μV²/Hz	**0,162**	-0,067	**-0,64**	-0,30	-0,13
P4-δ PSD, %	**0,133**	0,074	**-0,71**	-0,38	-0,43
Entropy HRV	**0,140**	-0,056	**-1,03**	-0,62	-0,43

Table 5.5 (cont)

1	2	3	4	5	6
C4-β PSD, μV²/Hz	**-0,262**	0,122	**+0,69**	+0,09	-0,23
F3-β PSD, μV²/Hz			**+0,56**	+0,08	-0,19
O2-θ PSD, %	**-0,200**	-0,015	**+0,30**	-0,23	-0,28
O1-θ PSD, %	**-0,185**	0,024	**+0,52**	-0,03	-0,17
Asymmetry-θ, %	**-0,153**	0,116	**+0,35**	0,00	-0,30
Deviation-θ, Hz			**+0,39**	+0,16	-0,10
Area GDI Right	**-0,170**	-0,023	**+0,59**	+0,01	0,00
Chakra 5 Energy	**-0,166**	-0,094	**+0,65**	-0,05	0,04
Chakra 7 Energy	**-0,145**	0,033	**+0,35**	-0,05	-0,20
Chakra 1 Energy	**-0,132**	0,046	**+0,43**	+0,08	-0,13
Chakra 4 Energy			**+0,40**	-0,02	-0,22
Entropy EEG O1	**-0,139**	-0,009	**+0,33**	-0,11	-0,16
Entropy EEG O2			**+0,19**	-0,22	-0,34
P3-β PSD, %	**-0,243**	0,048	**+1,21**	**+0,38**	+0,13
C4-β PSD, %	**-0,215**	0,120	**+0,97**	**+0,36**	-0,04
T6-β PSD, %	**-0,161**	0,064	**+0,98**	**+0,51**	+0,29
T4-β PSD, %	**-0,157**	0,135	**+0,89**	**+0,54**	+0,16
T4-β PSD, μV²/Hz	**-0,121**	0,120	**+0,51**	**+0,30**	-0,16
F4-β PSD, %			**+0,73**	**+0,41**	+0,05
O1-β PSD, %			**+0,94**	**+0,53**	+0,25
HF, msec²	**-0,164**	0,116	**+0,04**	**-0,46**	-0,88
RMSSD, msec	**-0,136**	0,152	**-0,63**	**-0,79**	-1,05
HF/TP, %			**+0,18**	**-0,15**	-0,37
pNN_{50}, %			**-0,06**	**-0,47**	-0,83
Root 2 (36,3%)	**R1**	**R2**	-0,45	**+0,88**	-1,04
Chakra 2 Asymmetry	-0,086	**-0,232**	+0,28	**-0,39**	+0,31
Chakra 3 Asymmetry			+0,40	**-0,10**	+0,07
Asymmetry-β, %	-0,036	**0,185**	+0,11	**+0,27**	-0,18
Frequency-δ, Hz			+0,02	**+0,13**	-0,25

We present existing views on the interpretation of HRV parameters. Well-known markers of Vagal tone are HF, RMSSD and pNN_{50}. LFnu

is admitted HRV marker of Sympathetic tone, LF/HF ratio reflects the sympathetic-vagal balance. It is speculated that absolute PSD LF band reflects mainly Sympathetic outflow or both Sympathetic and Vagal origin [HRV, 1996; Berntson GG et al., 1997; Baevskiy RM & Ivanov GG, 2001; Shaffer F & Ginsberg JP, 2017]. The interpretation of the other two bands remains the most controversial. VLF band (0,040÷0,0033 Hz) associated with oscillation blood levels of renin (0,04 Hz) and epinephrine (0,025 Hz), reflects thermoregulatory cycles, endothelial influences, cerebral ergotropic and metabolotropic outflows, activation of cerebral sympatho-adrenal system, sympathetic and vagal activity [Khayutin VM & Lukoshkova EV, 1999; Baevskiy RM & Ivanov GG, 2001; Kotelnikov SA et al., 2002; Khaspekova NB, 2003; Korkushko OV et al., 2009; Shaffer F & Ginsberg JP, 2017]. ULF band (<0,0033 Hz) associated with oscillation blood level of norepinephrine (0,0020 Hz) as well as 17-OCS (0,0019 Hz) [cit by: Kotelnikov SA et al., 2002]. Because in our device ULF band (range 0,015÷0,003 Hz) is integrated into the lower zone of VLF band, what has been said about the latter also applies to the former.

The above gives grounds to state in our contingent a sympathotonic shift of the autonomic balance due to both an increase in **sympathetic** tone and a decrease in **vagal** tone. There may be elevated levels of norepinephrine and glucocorticoids in the blood. This is accompanied by **increased** activity of beta-rhythm-generating cortical and subcortical structures that are designed on the right (paired) loci C4, T4, T6 and F4 as well as left loci P3 and O1. The right-hand shift of beta-rhythm symmetry is documented by a positive value of the asymmetry index. Interestingly, the symmetry of **Chakra 2** and, to a lesser extent, **Chakra 3** is shifted to the left.

It is traditionally believed that loci C3/C4 projected hippocampus, loci T3/T4 reflect the activity of the amygdala [Romodanov AP, 1993]. In practice, transcranial magnetic and direct current stimulation of the T3/T4 scalp position is used to reach the insular cortex, and F3/F4 loci – to activate the dorsolateral prefrontal cortex nuclei [review: Iseger TA et al., 2020]. The figures presented by Winkelmann T et al. [2017] and Yoo HJ et al. [2018] give us reason to assume that the loci C3/C4 projected precentral gyrus, T3/T4 – inferior temporal gyrus, F3/F4 – caudal anterior cingulate cortex or rostral middle frontal gyrus or superior frontal gyrus, P3/P4 – supramarginal gyrus, T5/T6 – caudal anterior cingulate cortex.

These cortical structures affect the activity of the vagus and sympathetic nuclei.

Figures 5.1 and 5.2 show that the use of balm causes a shift in the information field of the discriminant roots of the GDV, HRV and EEG parameters to the left and up. The shift to the left reflects, first of all, the normalizing decrease of increased sympathotonic markers and the increase of decreased vagotonic markers.

This is in line with the concept we put forward back in 1993 about ambivalence-equilibratory character of influence on organism of human of curative water Naftussya [Balanovskyi VP et al., 1993], which is now considered a generally accepted adaptogen [Alyeksyeyev ***OI*** et al., 1996; Flyunt IS et al., 2002; Ruzhylo SV et al., 2003; Popovych IL et al., 2005; Kostyuk PG et al., 2006; Flyunt IS et al., 2008; Hrinchenko BV, 2008; Popovych IL et al., 2014; Kozyavkina OV et al., 2015].

Physiologically favorable vegetotropic effects of the balm are accompanied by a further increase in the initially increased activity of **beta-rhythm**-generating cortical and subcortical structures as well as activation of **theta-rhythm**-generating and inhibition of **alpha**- and **delta**-rhythm-generating nuclei whose initial activity was within normal limits.

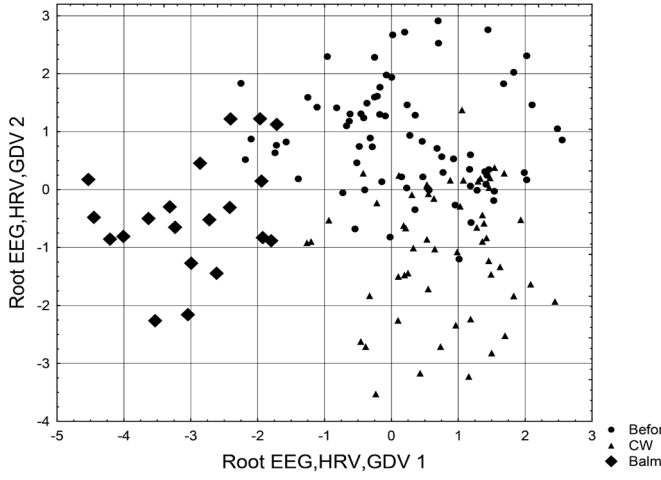

Fig. 5.1. Individual values of the first and second the GDV, EEG and HRV roots of the patients before **(Baseline)** and 1,5 hours after application of **Control Water** or **Balm**

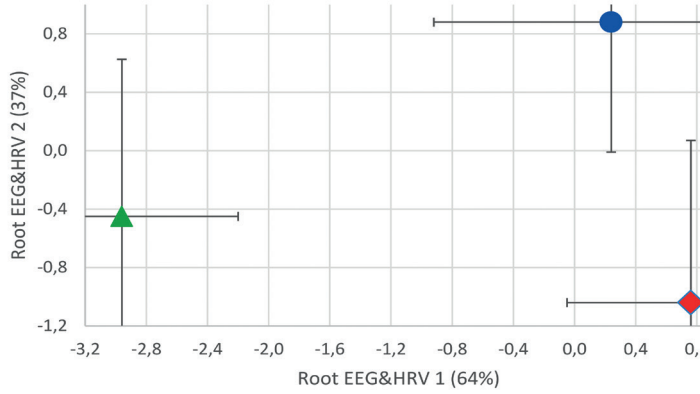

Fig. 5.2. Average (Mean±SD) of the first and second GDV, EEG and HRV roots of the patients **before** and 1,5 hours after application of **control water** or **balm**

The neurotropic effects of the balm are accompanied by significant changes in a number of GDV parameters. First of all, it is a decrease in the initially normal values of GDI fractality in the right and frontal projections and entropy in the right projection in combination with an increase in the GDI area in the right projection. It is important that the entropy of HRV decreases and the entropy of EEG in occipital loci increases. The physiological essence of entropy is discussed in detail in a recent monograph [Gozhenko **AI** et al., 2001].

The biophysical and informational/mathematical essence of these parameters is unquestionable for unbiased scientists. Chakra issues remain debatable, in our opinion, **for now**. It will be recalled that even until the mid-1960s, the "most advanced Soviet science" denied the existence of genes (???).

We found that after applying the balm, the energy of the ***virtual*** first, fourth, fifth and seventh chakras increases significantly. And now let's remember that **fourth** and **fifth** Chakras associated with vagus nerve [Chase CR, 2018], the tone of which increases; **first** Chakra is associated with adrenals, consistent with increased PSD of ULF band as a marker of circulating catecholamines and glucocorticoids; **seventh** Chakra associated with **right** (paired EEG loci!) and upper brain [Chase CR, 2018].

The previously identified effects of the balm on the parameters of immunity and hemodynamics [Alyeksyeyev ***OI*** et al., 1996; Markova OO et al., 2007; Flyunt IS et al., 2002; Popovych IL et al., 2005; Kostyuk PG et al., 2006; Flyunt IS et al., 2008] are consistent with the notion that **fourth** Chakra is associated with thymus, celiac and cardial plexus, heart, circulation [Chase CR, 2018]. It is appropriate to mention the research data of our laboratory on the relationship between the parameters of EEG&HRV and immunity, as well as their changes under the influence of adaptogenic factors of the Truskavets' spa [Kozyavkina OV et al., 2013; Kulchynskyi AB et al., 2016; Kulchynskyi AB et al., 2017; Kulchynskyi AB et al., 2017a; Kulchynskyi AB et al., 2017b; Popovych IL, 2009; Popovych IL, 2018; Popovych IL & Kozyavkina OV, 2012; Popovych IL et al., 2005; Popovych IL et al., 2013; Popovych IL et al., 2014; Popovych IL et al., 2014a; Popovych IL et al., 2017; Popovych IL et al., 2018; Popovych IL et al., 2020].

Based on the fact that the balm activates the **fifth** Chakra, we risk predicting its short-term thyrotropic effect, as shown for Naftussya bioactive water [Kozyavkina NV et al., 2013; Kozyavkina OV et al., 2015].

The cluster of individuals in the control group was shifted along the axis of the first root in the opposite direction, which reflects the sympathotonic shift of autonomous balance and opposite changes in EEG parameters. It is unlikely that the reason for such changes in neurodynamics is the use of 50 ml of tap water. The neurotropic effects of individuals' occupational activity within 1,5 hours between tests and/or the ultradian biorhythm of the autonomic nervous system and cortisol are more obvious. Their interpretation as **spontaneous rhythmic changes** (the term is borrowed by us from Hildebrandt G [1980]) is much more likely.

Interestingly, slight displacements along the axis of the second root were almost the same in both groups.

In general, all GDV&EEG&HRV clusters on the planes of two roots are quite clearly delineated, which is documented by calculating the Mahalanobis distances (Table 5.6).

The same discriminant parameters can be used to identify the belonging of one or another person to one or another cluster. This purpose of discriminant analysis is realized with the help of classifying (discriminant) functions (Table 5.7).

Table 5.6. Squared Mahalanobis Distances between EEG&HRV Clusters, **F-values** (df=39) and p-levels

Groups	Base-line (74)	After CW (54)	After Balm (20)
Baseline (74)	0	**4,80**	**12,48**
After CW (54)	**2,83 10^{-4}**	0	**15,07**
After Balm (20)	**3,72 10^{-6}**	**4,16 10^{-6}**	0

Table 5.7. Coefficients and Constants for Classification Functions

Clusters	Base-line (74)	After CW (54)	After Balm (20)
1	2	3	4
Variables	p=,500	p=,365	p=,135
ULF/TP, %	-3,715	-3,497	-3,898
F3-α PSD, %	-1,323	-1,338	-1,576
P4-δ PSD, %	2,082	2,017	1,769
C4-β PSD, $\mu V^2/Hz$	-0,059	-0,067	0,060
Ch2 Asymmetry	-82,42	-80,78	-81,02
T4-β PSD, $\mu V^2/Hz$	-0,005	-0,028	-0,065
Fp1-α PSD, %	0,467	0,372	0,488
P4-δ PSD, $\mu V^2/Hz$	0,182	0,217	0,215
LF/HF	4,406	4,551	4,624
Asymmetry-β, %	-0,176	-0,229	-0,177
O2-θ PSD, %	0,587	0,595	0,881
Frequency-β, %	-0,412	-0,523	-0,835
O1-θ PSD, $\mu V^2/Hz$	0,242	0,232	0,210
C3-α PSD, %	1,760	1,976	1,940
Ch5 Energy	-59,01	-52,98	-48,47
T6-α PSD, %	1,948	1,943	1,804

Table 5.7 (cont)

1	2	3	4
C4-β PSD, %	-0,381	-0,317	-0,551
P3-β PSD, %	4,229	4,191	4,409
Entropy HRV	429,2	427,8	443,2
HF PSD, msec^2	-0,013	-0,014	-0,015
Ch1 Energy	-95,01	-102,8	-98,87
T3-α PSD, μV^2/Hz	0,042	0,038	0,018
F3-α PSD, μV^2/Hz	-0,192	-0,216	-0,199
O2-α PSD, μV^2/Hz	0,024	0,028	0,028
O2-α PSD, %	-0,670	-0,729	-0,718
T6-β PSD, %	1,106	1,193	1,261
T4-β PSD, %	-0,541	-0,645	-0,721
RMSSD, msec	-0,689	-0,904	-0,657
pNN$_{50}$, %	3,469	3,726	3,449
F3-β PSD, μV2/Hz	0,070	0,101	0,078
Asymmetry-θ, %	0,487	0,443	0,471
Shape C Right	16,86	15,99	16,28
Shape C Frontal	8,862	9,298	9,383
O1-β PSD, %	-0,926	-0,853	-0,893
Area GDI R, kpixels	65,89	66,04	67,01
T3-α PSD, %	1,387	1,498	1,541
Entropy O1	187,2	193,3	181,5
O1-θ PSD, %	-4,974	-5,080	-4,653
Ch7 Energy	-199,2	-196,8	-205,3
Constants	-1463	-1466	-1500

In this case, we can retrospectively recognize members in the initial state with 8 errors, after using control water – with 8 errors, and after applying the balm – with 2 errors. Overall classification accuracy is 87,8% (Table 8).

Table 5.8. Classification Matrix for EEG&HRV Clusters
Rows: Observed classifications; Columns: Predicted classifications

	Clusters	Base-line	After CW	After Balm
Clusters	% Correct	p=,500	p=,365	p=,135
Baseline (74)	89,2	**66**	8	0
After CW (54)	85,2	8	**46**	0
After Balm (20)	90,0	2	0	**18**
Total	87,8	76	54	18

The digital data of Table 5.5 are visualized in Fig. 5.3.

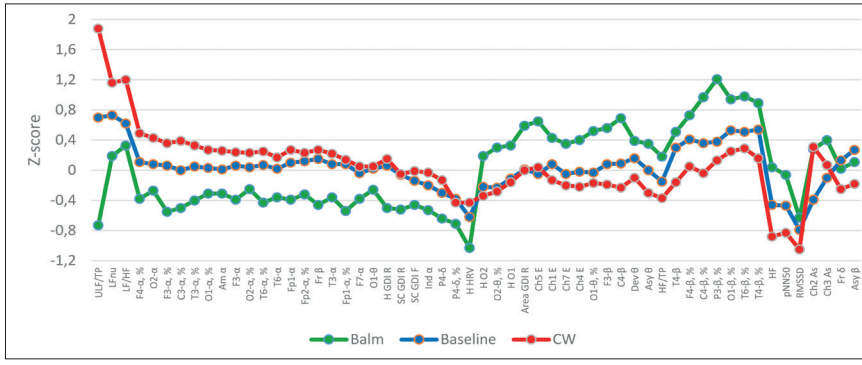

Fig. 5.3. Profiles of Z-scores of EEGs and HRVs variables in the **initial state** and 1,5 hours after drinking **control water** or **balm**

A clear divergence of profiles is visible, however, it is heterogeneous. Therefore, for more detailed analysis, the profiles were structured in 9 homogeneous patterns. This approach also makes it possible to model the essential (per se) neurotropic effects of the balm as algebraic sums of effects in the main and control groups.

It is clearly seen that, taking into account spontaneous rhythmic changes, the essential neurotropic effects of the balm are downregulatory in relation to 30 variables, and upregulatory in relation to the other 26 variables.

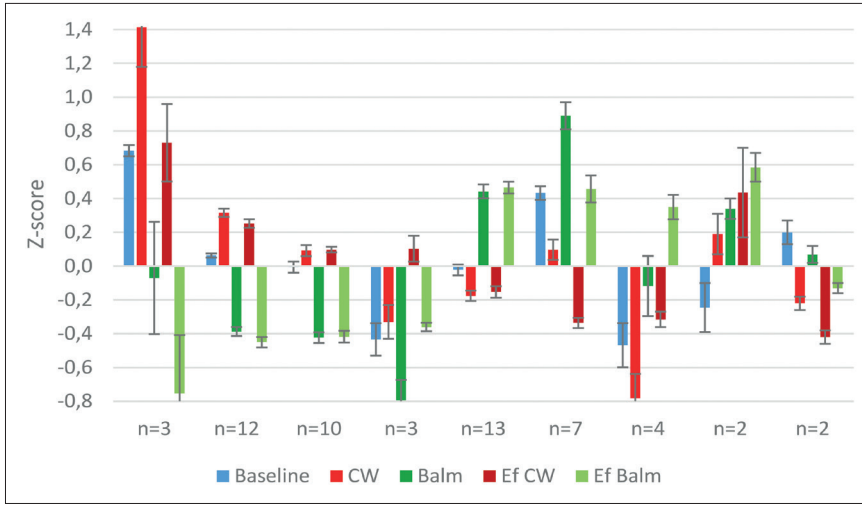

Fig. 5.4. Patterns of GDV, EEG and HRV (Mean±SE) parameters before and 1,5 hours after application of control water or balm and simulated effects per se. The members of the patterns are separated in Table 5.5 by spaces

Conclusion

Ukrainian phytocomposition "Balm Truskavets'" causes favorable immediate neurotropic and biophysic changes at patients with dysfunction of neuro-endocrine-immune complex. This provides grounds for further research into long-term effects.

Chapter 6

LONG-TERM EFFECTS OF THE UKRAINIAN PHYTOCOMPOSITION «BALM TRUSKAVETS'» ON PARAMETERS OF NEURO-ENDOCRINE-IMMUNE COMPLEX AND BIOPHOTONICS IN HUMANS WITH MALADAPTATION

Summary

Background. Earlier we showed that the Ukrainian phytocomposition "Balm Truskavets'" exerts immediate modulating effects on parameters of EEG and HRV as well as biophotonics. This provided the basis for studying long-term effects on parameters of neuro-endocrine-immune complex and biophotonics.

Materials and Methods. The object of observation were 16 women 46±15 ys and 24 men 50±11 ys. The volunteers were practically healthy, but the initial testing revealed deviations from the norm in a number of parameters of the neuro-endocrine-immune complex as a manifestation of maladaptation. The adaptation hormones levels, Popovych's leukocytary adaptation and strain indices, parameters of phagocytosis, biophotonics, acupuncture points, EEG and HRV, before and after a 9-day course of use of phytocomposition registered.

Results. A noticeable effect of the phytocomposition on 38 parameters was revealed, grouped into 6 clusters, of which 4 are enhancing and 2 are reducing. In particular, the reduced levels of the adaptation index and phagocytosis parameters increase significantly, instead, the increased levels of the strain index, testosterone, triiodothyronine, LF band HRV as well as two biophotonics parameters decrease, that is, there is a normalizing/ beneficial effect. At the same time, normal levels of HRV-markers of vagal tone decrease, and cortisol and circulating catecholamines as well as the activity of β- and α-rhythm generating neurons increase, but within the normal range. Finally, there is a further increase in the upper limit levels of activity of δ-rhythm generating neurons.

Conclusion. Ukrainian phytocomposition "Balm Truskavets'" exerts classical adaptogenic effects on parameters of neuro-endocrine-immune complex as well as biophotonics and acupuncture in humans with maladaptation.

INTRODUCTION

Earlier we showed that the Ukrainian phytocomposition "Balm Truskavets'" (ТУ У 15.8-24055046-005:2009, produced by private research-production enterprise «Ukrainian Balms», Mykolaïv, Ukraine; is analogous to the previous "Balm Kryms'kyi") exerts immediate (in 1,5 hours after use) modulating effects on parameters of EEG and HRV as well as biophotonics (GDV). This gives grounds for finding out the long-term (course) effects of the phytocomposition on these parameters. In a pilot study on 10 volunteers, we found that the use of the phytocomposition for 11 dais causes changes in EEGs parameters accompanied by a sympatho(adreno)mimetic effect. The modulating effects of the balm on the parameters of the central and autonomous nervous systems are combined with the changes in GDVs parameters [Fihura OA et al., 2022]. This study was conducted on a four times larger cohort and with a wider range of methods, that allow assessing the state of the neuro-endocrine-immune complex as a marker of adaptation.

MATERIAL AND RESEARCH METHODS

The object of observation was employees of the clinical sanatorium "Moldova" and PrJSC "Truskavets' Spa": 16 women 33-71 (M±SD: 46±15) years and 24 men 24-69 (50±11) years. The volunteers were considered practically healthy (without a clinical diagnosis), but the initial testing revealed deviations from the norm in a number of parameters of the neuro-endocrine-immune complex (details follow) as a manifestation of maladaptation.

In the morning in basal condition we registered kirlianogram by the method of GDV by the device of "GDV Chamber" ("Biotechprogress", SPb, RF). Than recorded simultaneosly electrocardiogram (ECG) and electroencephalogram (EEG). ECG recorded during 7 min in II lead to assess the parameters of HRV. Used hardware-software complex «CardioLab+HRV» produced by «KhAI-Medica» (Kharkiv, Ukraine). EEG recorded a hardware-software complex "NeuroCom Standard" (KhAI Medica, Kharkiv, Ukraine).

Electroconductivity (EC) recorded in follow points of acupuncture: Pg(ND), TR(X) and MC(AVL) at Right and Left side. Used complex "Medissa". For each pair, the Laterality Index was calculated.

In portion of capillary blood counted up Leukocytogram (LCG) (Eosinophils, Stub and Segmentonucleary Neutrophils, Lymphocytes

and Monocytes) and calculated its Adaptation Index as well as Strain Index by Popovych IL [Kostyuk PG et al., 2006; Gozhenko **AI** et al., 2021; Popovych IL et al., 2022]. We remind that the algorithm of quantization of the Popovych's indexes is based on the proposed Garkavi LKh et al. [1990] ranges of relative content in the leukocytogram of lymphocytes, which determines the type of General Adaptation Reaction of Organism as well as other components of leukocytogram and total leukocyte levels indicating harmonic or disharmonious character of GARO (Table 6.1).

Table 6.1. Quantification of General Adaptation Reaction of Organism, first version [Gozhenko **AI** et al., 2021]

Leukocyto-gram Lymphocy-tes level, %	**G**eneral **A**daptation **R**eaction of **O**rganism	Eosinophils and Stub Neutrophils: 1÷6 %; Monocytes: 4÷7 %; Leukocytes: 4÷8 G/l	Eosinophils and Stub Neutrophils: <1; >6; Monocytes: <4; >7; Leukocytes: <4; >8 G/l
<21	Stress	**1,22**	**0,02**
21÷27	Training	**1,46**	**0,74**
28÷33	Quiet Activation	**1,95**	**0,98**
34÷43,5	Heightened Activation	**1,70**	**0,50**
≥44	Overactivation	**0,26**	

Strain Index-1 = $[(Eo/3,5\text{-}1)^2 + (SN/3,5\text{-}1)^2 + (Mon/5,5\text{-}1)^2 + (Leu/6\text{-}1)^2]/4$.

Parameters of phagocytic function of neutrophils estimated as described by Kovbasnyuk MM [Kulchynskyi AB et al., 2016; Popovych IL et al., 2018]. The objects of phagocytosis served daily cultures of Staphylococcus aureus (ATCC N 25423 F49) as typical specimen for Gram-positive Bacteria and Escherichia coli (O55 K59) as typical representative of Gram-negative Bacteria. Take into account the following parameters of Phagocytosis: activity (percentage of neutrophils, in which found microbes – Hamburger's Phagocytic Index PhI), intensity (number of microbes absorbed one phagocytes – Microbial Count MC or Right's Index) and completeness (percentage of dead microbes – Killing Index KI). On the basis of the registered partial parameters of phagocytosis, taking into account the content of neutrophils (N) in 1 L of blood, the integral parameter – the bactericidal capacity of neutrophils – was calculated by the equation:

BCCN (10^9 Bact/L) = N (10^9/L)•PhI (%)•MC (Bact/Phag)•KI (%)•10^{-4}.

At last in portion of venous blood we determined serum levels of major hormones of adaptation: Cortisol, Testosterone, Aldosterone, Triiodothyronine and Calcitonin by the ELISA with the use of analyzer "RT-2100C" (ChPR) and corresponding sets of reagents from "Алкор Био", XEMA Co, Ltd and DRG International Inc.

After the initial testing patients used 5 ml of Phytocomposition, pre-diluted in 45 ml of boiled tap water, half an hour before meals three times a day for 9 days. The next morning after completing the treatment, retesting was performed.

Reference values are taken from the database of our laboratory (EEG, GDV, Immunity) or instructions (HRV, ELISA).

Results processed using the software package «Statistica 6.4».

RESULTS AND DISCUSSION

According to the algorithm of Truskavetsian Scientific School, at the preparatory stage of data analysis the registered parameters were normalized, which allowed their correct comparison. Further, profiles of normalized parameters were created, the levels of which differ significantly before and after Balm treatment, as well as several parameters which according to the following discriminant analysis were still **recognizable**, despite the **insignificant** value of Student's t criterion (Fig. 6.1).

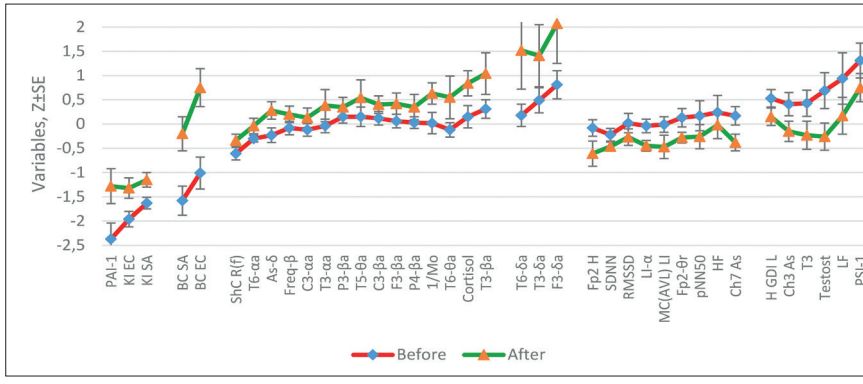

Fig. 6.1. Profiles of variables whose normalized levels (Z±SE) are changing under the influence of the Phytocomposition

Another approach to quantifying effects is to calculate the direct differences between the final and initial parameters levels of each patient (Fig. 6.2).

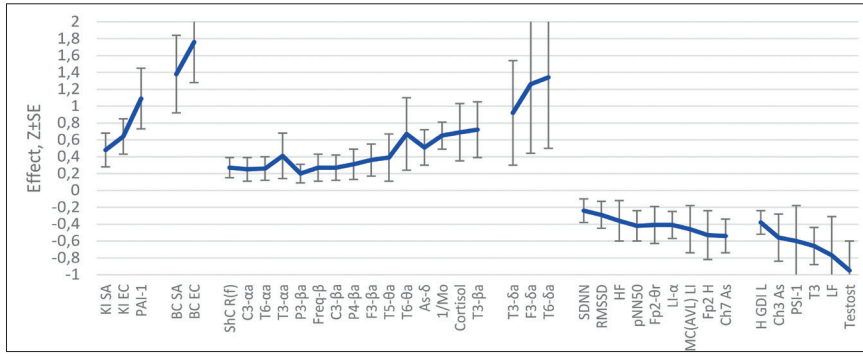

Fig. 6.2. The effects of the Phytocomposition as direct differences of normalized variables (Z±SE)

Next, 38 parameters were grouped into 6 clusters, of which 4 are enhancing and 2 are reducing (Fig. 6.3 and Table 6.8).

In particular, the **reduced** levels of the Popovych's adaptation index and killing indices vs both E. coli and Staph. aureus **increase** significantly, still remaining low (cluster B--/A-).

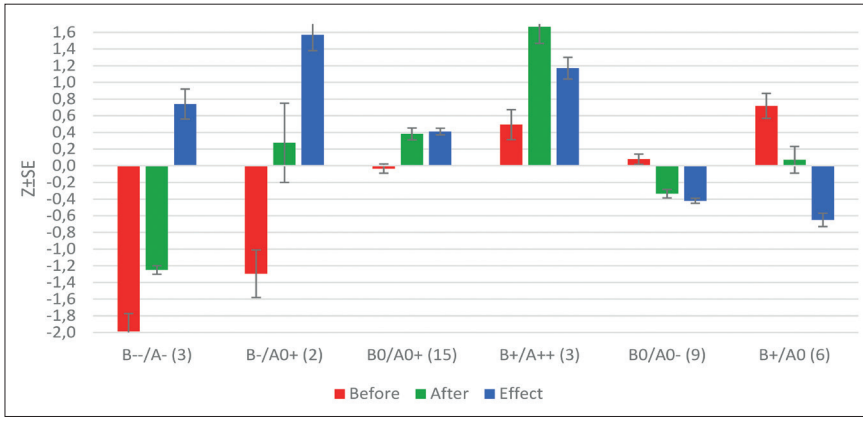

Fig. 6.3. The clusters of normalized (Z±SE) parameters before (B) and after (A) intake of the Phytocomposition as well as its effects as direct differences (A-B). The number of variables in the cluster is indicated in parentheses

At the same time, BCCN in relation to gram-positive microbes is completely normalized, and in relation to gram-negative microbes it even reaches the upper zone of the normal range due to the additional slight increase of other elements of this integral parameter of phagocytosis (cluster B-/A0+).

Instead, the **increased** levels of the Popovych's strain index, serum testosterone and triiodothyronine, LF band of HRV, Entropy of Gas Discharge Image in Left projection (H GDI L) as well as right-sided (positive sign of symmetry index) asymmetry of the virtual third Chakra **decrease** (cluster B+/A0).

That is, there is a **normalizing** (ambivalence-equilibratory) effect as one of the attributes of adaptogens [Balanovskyi VP et al., 1993; Alyeksyeyev ***OI*** et al.,1996; Kostyuk PG et al., 2006] according to the good old "law of initial level".

At the same time, **normal** levels of four HRV-markers of vagal tone as well as PSD of θ-rhythm and Entropy in Fp2 locus **also decrease,** albeit slightly. This is accompanied by left lateralization (negative sign of symmetry/lateralization indices) of initially symmetrical (quasi-zero symmetry/lateralization indices) EEG α-rhythm, electrical conductivity of acupuncture points MC(AVL) and virtual seventh Chakra (cluster B0/A0-).

On the other hand, **normal** levels of cortisol and circulating catecholamines (1/Mo as marker) as well as activity of β- and α-rhythm generating neurons **also increase**, albeit slightly. This is accompanied by a rightward shift in the symmetry of δ-rhythm and an increase in Shape Coefficient of GDI in Right projection (SC GDI R) (cluster B0/A0+).

Finally, there is a further increase in the upper limit levels of activity of δ-rhythm generating neurons (cluster B+/A++).

The described changes in parameters of EEG, HRV, hormones and bioelectrophotonics are negatively/positively correlated with the changes in parameters of phagocytosis [Babelyuk VY et al., 2021; Gozhenko **AI** et al., 2021; Kulchynskyi AB et al., 2016; Popovych IL et al., 2018] (as well as of immunity [Kulchynskyi AB et al., 2017; Kulchynskyi AB et al., 2017a; Popovych IL et al., 2017; Babelyuk VYe et al., 2020; Babelyuk VYe et al., 2021; Babelyuk VYe et al., 2021a; Gozhenko **AI** et al., 2021]), so effects of the Phytocomposition are physiologically favorable and therefore adaptogenic.

The previously selected variables were further subjected to discriminant analysis with the aim not so much to discover which of them are formally characteristic, but to visualize the integral state of each volunteer. The forward stepwise program included only 24 variables in the discriminant model, including those subject to non-significant (t<2,02) effects according to the Student criterion (Tables 6.2 and 6.3), while other variables were outside the model, despite significant (*) changes (Tables 6.4-6.6). On the face of it, the Wilks' and Student's statistics do not match completely.

Table 6.2. Discriminant Function Analysis Summary
Step 24, N of vars in model: 24; Grouping: 2 grps; Wilks' Λ: 0,2860;
approx. $F_{(24)}$=5,7; $p<10^{-6}$

Variables currently in the model	State (n) and Means±SE			Parameters of Wilks' Statistics					
	Before (40)	After (40)	*Effect (40)*	Wilks' Λ	Partial Λ	F-remove (1,55)	p-level	Tolerancy	Refer Cv/SD
1	2	3	4	5	6	7	8	9	10
Frequency-β, Hz	17,6 0,6	18,8 0,7	*+1,2* *0,7*	0,398	0,719	21,50	0,000	0,498	17,9 0,244
C3-β PSD, μV²/Hz	102 9	121 13	*+19* *10*	0,382	0,748	18,53	0,000	0,041	93,5 0,733
F3-β PSD, μV²/Hz	82 7	101 12	*+19* *10*	0,353	0,809	12,96	0,001	0,040	79 0,682
P3-β PSD, μV²/Hz	103 8	115 12	*+12* *7*	0,315	0,908	5,55	0,022	0,061	93 0,665
P4-β PSD, μV²/Hz	91 6	108 14	*+17* *10*	0,302	0,946	3,16	0,081	0,058	89 0,611
T3-β PSD, μV²/Hz	94 10	135 24	*+40* *18**	0,292	0,979	1,18	0,281	0,143	77 0,726
Laterality-α, %	-3 5	-17 4	*-14* *5**	0,341	0,839	10,56	0,002	0,430	-1 **34**
T6-α PSD, μV²/Hz	69 10	108 24	*+39* *20*	0,324	0,882	7,34	0,009	0,111	114 1,302
C3-α PSD, μV²/Hz	142 21	183 34	*+42* *24*	0,298	0,959	2,33	0,132	0,129	162 1,039
Asymmetry-δ, %	36,3 3,7	48,7 4,4	*+12,4* *5,0**	0,297	0,963	2,13	0,150	0,603	41,8 0,580

Table 6.2 (cont)

1	2	3	4	5	6	7	8	9	10
T6-δ PSD, μV²/Hz	89 19	198 66	*+109* *69*	0,310	0,922	4,67	0,035	0,257	74 1,110
F3-δ PSD, μV²/Hz	175 27	296 89	*+121* *78*	0,302	0,948	3,00	0,089	0,292	98 0,981
T5-θ PSD, μV²/Hz	33 5	43 9	*+10* *7*	0,315	0,908	5,60	0,022	0,131	29 0,906
T6-θ PSD, μV²/Hz	21 3	34 9	*+13* *9*	0,290	0,987	0,75	0,390	0,215	23 0,869
SDNN HRV, msec	49,6 4,0	42,6 2,8	*-7,1* *4,0*	0,300	0,954	2,64	0,110	0,570	56,1 0,529
Testosterone normalized, Z	0,69 0,37	-0,26 0,28	*-0,95* *0,35**	0,331	0,865	8,59	0,005	0,671	0 **1**
Chakra 7 Asymmetry	0,08 0,05	-0,05 0,04	*-0,13* *0,05**	0,310	0,922	4,68	0,035	0,518	0,04 **0,24**
Chakra 3 Asymmetry	0,15 0,06	0,02 0,05	*-0,13* *0,06**	0,294	0,973	1,53	0,222	0,590	0,06 **0,23**
Entropy GDI Left	3,83 0,03	3,77 0,03	*-0,05* *0,02**	0,298	0,959	2,38	0,129	0,561	3,75 0,038
Bactericidity vs E. coli, 10^9 Bacteria/L	89 3	106 4	*+17* *5**	0,286	1,000	0,00	0,980	0,174	99 0,100
Killing Index vs Escherichia. coli, %	43,4 1,5	49,5 2,0	*+6,0* *2,0**	0,317	0,902	5,96	0,018	0,115	62,0 0,156
Bactericidity vs St. aureus, 10^9 Bact/L	89 3	104 4	*+15* *5**	0,294	0,972	1,57	0,215	0,179	106 0,100
Killing Index vs Sta-phyloc. aureus, %	45,3 1,0	49,3 1,3	*+4,0* *1,6**	0,286	0,999	0,04	0,843	0,200	58,9 0,142
Popovych's Adapta-tion Index-1, units	1,13 0,08	1,39 0,09	*+0,27* *0,09**	0,419	0,682	25,66	0,000	0,546	1,705 0,245

Notes. In each column, the first line is the average, the second – SE. In norm column – the average and Cv or ***SD***. The "*Effect*" and "*Norm*" columns are not the result of discriminant analysis

Table 6.3. Summary of stepwise analysis of discriminant variables ranked by criterion Λ

Variables currently in the model	F to enter	p-level	Λ	F-value	p-value
Bactericidity vs E. coli, 10^9 Bacteria/L	11,6	0,001	0,870	11,6	0,001
Popovych's Adaptation Index-1, units	6,06	0,016	0,807	9,22	0,0003
T6-θ PSD, $\mu V^2/Hz$	7,74	0,007	0,732	9,27	10^{-4}
Laterality-α, %	4,53	0,037	0,690	8,41	10^{-4}
Killing Index vs E. coli, %	7,09	0,010	0,630	8,69	10^{-5}
Frequency-β, Hz	8,19	0,006	0,567	9,31	10^{-6}
SDNN HRV, msec	5,74	0,019	0,525	9,31	10^{-6}
Testosterone normalized by sex&age, Z	3,37	0,071	0,501	8,84	10^{-6}
Bactericidity vs Staph. aur, 10^9 Bacteria/L	3,46	0,067	0,477	8,52	10^{-6}
Chakra 7 Asymmetry	1,99	0,163	0,464	7,97	10^{-6}
Killing Index vs Staph. aureus, %	1,58	0,213	0,453	7,45	10^{-6}
Asymmetry-δ, %	2,04	0,158	0,440	7,10	10^{-6}
F3-δ PSD, $\mu V^2/Hz$	1,53	0,221	0,430	6,73	10^{-6}
T6-α PSD, $\mu V^2/Hz$	1,16	0,285	0,423	6,34	10^{-6}
T5-θ PSD, $\mu V^2/Hz$	1,67	0,201	0,412	6,09	10^{-6}
T6-δ PSD, $\mu V^2/Hz$	1,25	0,267	0,404	5,81	10^{-6}
C3-β PSD, $\mu V^2/Hz$	1,10	0,298	0,397	5,58	10^{-6}
F3-β PSD, $\mu V^2/Hz$	9,40	0,003	0,344	6,47	10^{-6}
C3-α PSD, $\mu V^2/Hz$	3,19	0,079	0,326	6,52	10^{-6}
P3-β PSD, $\mu V^2/Hz$	1,46	0,232	0,319	6,31	10^{-6}
P4-β PSD, $\mu V^2/Hz$	1,76	0,189	0,309	6,17	10^{-6}
Entropy of Gas Discharge Image Left	2,06	0,157	0,298	6,09	10^{-6}
Chakra 3 Asymmetry	1,20	0,279	0,292	5,90	10^{-6}
T3-β PSD, $\mu V^2/Hz$	1,18	0,281	0,286	5,72	10^{-6}

Table 6.4. EEG variables currently not in the discriminant model

	State (n) and Means±SE			Parameters of Wilks' Statistics					
Variables	**Before (40)**	**After (40)**	***Effect (40)***	Wilks' Λ	Par-tial Λ	F to enter	p-le-vel	Tole-rancy	Refer Cv/**SD**
Fp2 PSD Entropy	0,823 0,020	0,769 0,029	*-0,054* *0,033*	0,285	0,995	0,26	0,614	0,549	0,835 0,135
Fp2-θ PSD, %	10,7 1,2	8,2 0,6	*-2,5* *1,4*	0,284	0,994	0,35	0,556	0,631	9,9 0,620
T3-α PSD, μV²/Hz	86 12	122 29	*+36* *23*	0,286	0,999	0,08	0,780	0,088	89,5 0,972
T3-δ PSD, μV²/Hz	129 23	213 58	*+83* *56*	0,285	0,998	0,11	0,740	0,143	86 1,055

Table 6.5. HRV variables currently not in the discriminant model

Variables	State (n) and Means±SE			Parameters of Wilks' Statistics					
	Before (40)	**After (40)**	***Effect (40)***	Wilks' Λ	Par-tial Λ00000	F to enter	p-level	Tole-rancy	Refer Cv/**SD**
Mode HRV, msec	871 23	811 23	*-65* *17**	0,285	0,998	0,11	0,738	0,515	874 0,115
RMSSD HRV, msec	29,4 3,1	24,8 2,5	*-4,6* *2,1**	0,286	0,999	0,04	0,851	0,220	29,7 0,482
pNN_{50} HRV, %	10,7 2,5	6,9 1,9	*-3,8* *1,6**	0,286	1,000	0,01	0,927	0,336	9,0 0,846
HF PSD, $msec^2$	500 122	378 93	*-122* *77*	0,286	1,000	0,00	0,952	0,414	363 0,750
LF PSD, $msec^2$	890 152	664 107	*-226* *122*	0,283	0,991	0,48	0,493	0,220	640 0,466

Table 6.6. Endocrine, Immune and Biophysics variables currently not in the discriminant model

Variables	State (n) and Means±SE			Parameters of Wilks' Statistics					
	Before (40)	After (40)	*Effect (40)*	Wilks' Λ	Par-tial Λ	F to enter	p-level	Tole-rancy	Refer Cv/**SD**
Triiodothyronine, nM/L	2,41 0,14	2,09 0,15	*-0,33* *0,11**	0,283	0,991	0,49	0,489	0,631	2,20 0,227
Cortisol, nM/L	386 26	464 29	*+78* *38**	0,286	1,000	0,00	0,987	0,496	370 0,303
Popovych's Strain Index-1	0,170 0,019	0,138 0,016	*-0,033* *0,023*	0,286	1,000	0,02	0,880	0,482	0,097 0,559
Shape Coefficient GDI Right (f), un.	13,28 0,22	13,71 0,22	*+0,43* *0,20**	0,284	0,991	0,47	0,498	0,600	14,3 0,114
MC(AVL) EC Laterality, %	-0,03 0,31	-0,88 0,46	*-0,85* *0,54*	0,285	0,997	0,15	0,697	0,747	0,04 **1,91**

On the basis of the raw coefficients and constant (Table 6.7), the individual values of the canonical discriminant roots were calculated with the following visualization in Fig. 6.4.

Table 6.7. Standardized and raw coefficients and constant for discriminant variables

	Coefficients	
Variables	**Standar-dized**	**Raw**
1	2	3
Bactericidity vs E. coli, 10^9 Bac/L	0,009	0,0004
Popovych's Adaptation Ind-1, un.	-0,903	-1,695
T6-θ PSD, μV²/Hz	-0,296	-0,007
Laterality-α, %	0,724	0,027
Killing Index vs E. coli, %	-1,091	-0,096
Frequency-β, Hz	-0,889	-0,211
SDNN HRV, msec	0,336	0,015
Testosterone normalized, Z	0,531	0,282
Bactericidity vs St. aur, 10^9 Bac/L	-0,466	-0,021
Chakra 7 Asymmetry	0,461	1,944
Killing Index vs Staph. aureus, %	0,071	0,001
Asymmetry-δ, %	-0,294	-0,011
F3-δ PSD, μV²/Hz	0,498	0,001
T6-α PSD, μV²/Hz	-1,220	-0,010

Table 6.7 (cont)

1	2	3
T5-θ PSD, μV²/Hz	0,995	0,020
T6-δ PSD, μV²/Hz	-0,653	-0,002
C3-β PSD, μV²/Hz	-2,945	-0,042
F3-β PSD, μV²/Hz	2,584	0,042
C3-α PSD, μV²/Hz	0,665	0,004
P3-β PSD, μV²/Hz	1,455	0,022
P4-β PSD, μV²/Hz	-1,148	-0,017
Entropy GDI Left	0,322	2,294
Chakra 3 Asymmetry	0,253	0,893
T3-β PSD, μV²/Hz	-0,455	-0,004
Constant		3,410
Eigenvalue		2,496
Squared Mahalanobis Distance=9,73; $F_{(25)}$=5,7; $p<10^{-6}$		
Canonical R=0,845; Wilks' Λ=0,2860; $\chi^2_{(24)}$=83; $p<10^{-6}$		

As you can see, the level of the root after the course of using the Phytocomposition in all volunteers, without exception, is lower than the initial level to one degree or another. This reflects both increasing levels of variables represented in the root inversely and decreasing levels of variables that are positively correlated with the root (Table 6.8).

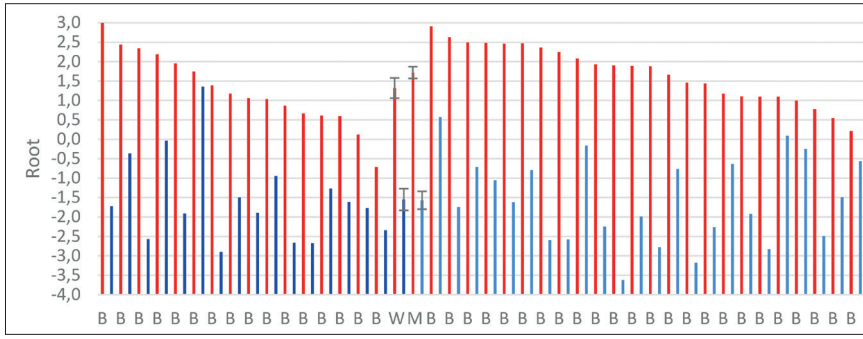

Fig. 6.4. Individual and average (M±SE) values of discriminant Root at **Women** and **Men** before **(B)** and **after** course of intake of the Phytocomposition

No sexual dimorphism was found either in the initial or final variables (Fig. 6.5), as well as in the effects of the phytocomposition. At the same time, there are significant differences in the individual effects of the phytocomposition in both women and men (Fig. 6.6).

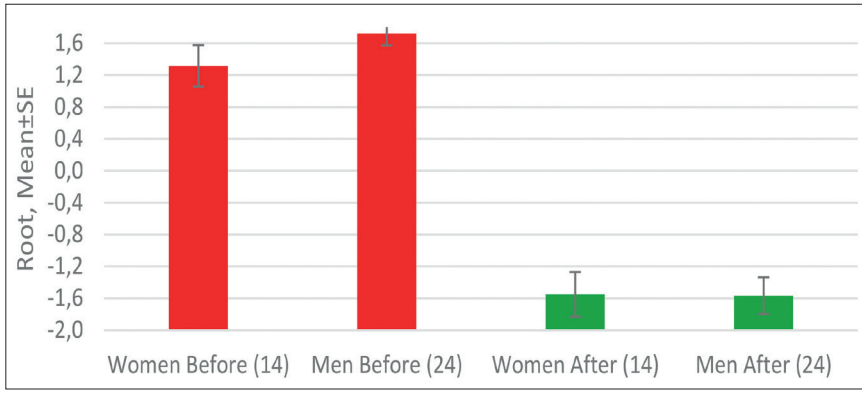

Fig. 6.5. Average (M±SE) values of discriminant Root at Women and Men **before** and **after** course of use of the Phytocomposition

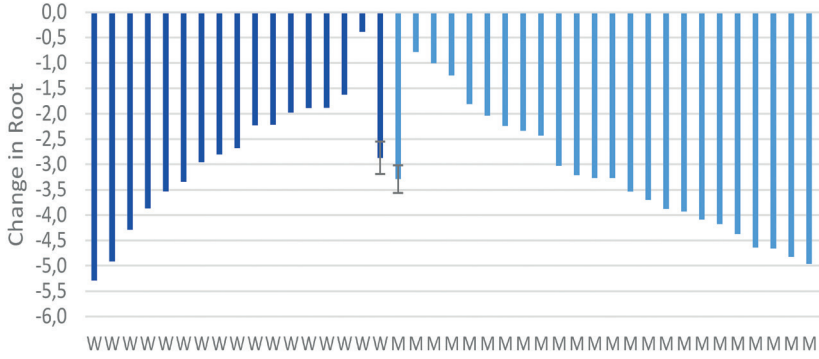

Fig. 6.6. Individual and average (M±SE) changes in discriminant Root at **Women** and **Men** caused by intake of Phytocomposition

Table 6.8. Clusters of effects as differences between levels (Z±SE) after and before treatment

Clusters and Variables	Structu-ralcoeffi-cient	Before (40)	After (40)	*Effect (30)*
1	2	3	4	5
B--/A- (3)		**-1,99±0,21**	**-1,25±0,05**	**+0,74±0,18**
Popovych's Adaptation Index-1	-0,160	-2,37±0,33	-1,28±0,36	+1,09±0,36
Killing Index vs E. coli	-0,171	-1,96±0,16	-1,32±0,21	+0,64±0,21
Killing Index vs Staph. aureus	-0,176	-1,63±0,12	-1,15±0,15	+0,48±0,20
B-/A0+ (2)		**-1,30±0,29**	**+0,28±0,48**	**+1,57±0,19**
Bactericidity vs E. coli	-0,244	-1,01±0,33	+0,75±0,39	+1,76±0,48
Bactericidity vs Staph. aureus	-0,215	-1,58±0,30	-0,20±0,35	+1,38±0,46
B0/A0+ (15)		**-0,03±0,05**	**+0,38±0,07**	**+0,41±0,04**
Asymmetry-δ	-0,147	-0,23±0,15	+0,28±0,18	+0,51±0,21
1/Mode HRV		+0,02±0,22	+0,63±0,22	+0,65±0,16
Cortisol		+0,15±0,23	+0,84±0,26	+0,69±0,34
T6-θ PSDa	-0,103	-0,12±0,15	+0,55±0,44	+0,67±0,43
T5-θ PSDa	-0,066	+0,15±0,20	+0,54±0,37	+0,39±0,28
T3-α PSDa		-0,04±0,14	+0,38±0,33	+0,41±0,27
T6-α PSDa	-0,106	-0,30±0,07	-0,04±0,16	+0,26±0,14
C3-α PSDa	-0,074	-0,12±0,13	+0,13±0,20	+0,25±0,14
T3-β PSDa	-0,111	+0,31±0,19	+1,04±0,43	+0,72±0,33
F3-β PSDa	-0,101	+0,06±0,14	+0,42±0,22	+0,36±0,19
Frequency-β	-0,091	-0,08±0,14	+0,20±0,17	+0,27±0,16
C3-β PSDa	-0,085	+0,12±0,14	+0,40±0,18	+0,27±0,15
P4-β PSDa	-0,078	+0,03±0,12	+0,35±0,26	+0,31±0,18
P3-β PSDa	-0,061	+0,15±0,13	+0,35±0,20	+0,20±0,11
Shape Coefficient GDI Right (f)		-0,61±0,13	-0,34±0,13	+0,27±0,12
B+/A++ (3)		**+0,49±0,18**	**+1,67±0,20**	**+1,17±0,13**
T6-δ PSDa	-0,114	+0,18±0,23	+1,52±0,80	+1,34±0,84
F3-δ PSDa	-0,093	+0,81±0,29	+2,07±0,93	+1,26±0,82
T3-δ PSDa		+0,49±0,26	+1,41±0,64	+0,92±0,62
B0/A0- (9)		**+0,04±0,06**	**-0,36±0,05**	**-0,40±0,03**

Table 6.8 (cont)

1	2	3	4	5
Laterality-α	0,167	-0,04±0,14	-0,45±0,11	-0,41±0,16
MC(AVL) EC Laterality		-0,01±0,16	-0,47±0,24	-0,46±0,28
Chakra 7 Asymmetry	0,132	+0,17±0,19	-0,38±0,17	-0,54±0,20
Fp2 PSD Entropy		-0,08±0,17	-0,61±0,26	-0,53±0,29
Fp2-θ PSDa		+0,13±0,14	-0,28±0,11	-0,41±0,22
SDNN HRV	0,104	-0,22±0,13	-0,46±0,09	-0,24±0,14
pNN_{50} HRV		+0,17±0,31	-0,26±0,25	-0,42±0,18
HF HRV PSD		+0,34±0,35	-0,02±0,28	-0,36±0,24
RMSSD HRV		+0,02±0,20	-0,27±0,17	-0,29±0,16
B+/A0 (6)		**+0,72±0,15**	**+0,07±0,16**	**-0,65±0,08**
Testosterone	0,131	+0,75±0,36	-0,32±0,28	-1,07±0,34
Triiodothyronine		+0,43±0,27	-0,23±0,29	-0,66±0,22
LF HRV PSD		+0,94±0,53	+0,17±0,38	-0,77±0,46
Chakra 3 Asymmetry	0,110	+0,41±0,24	-0,15±0,21	-0,56±0,28
Entropy GDI Left	0,093	+0,53±0,18	+0,15±0,18	-0,38±0,14
Popovych's Strain Index-1		+1,35±0,36	+0,75±0,29	-0,60±0,42

The accuracy of the retrospective classification of phytocomposition effects by calculating individual classification functions based on its coefficients and constants (Table 6.9) is 95% (Table 6.10).

Table 6.9. Coefficients and constants of classification functions

State	Before	After
1	2	3
Variables	0,500	0,500
Bactericidity vs E. coli, 10^9 Bact/L	-0,631	-0,632
Popovych's Adaptation Index-1, un.	6,974	12,26
T6-θ PSD, $\mu V^2/Hz$	0,162	0,184
Laterality-α, %	-0,131	-0,215
Killing Index vs E. coli, %	1,555	1,856
Frequency-β, Hz	-0,093	0,564

Table 6.9 (cont)

1	2	3
SDNN HRV, msec	0,108	0,060
Testosterone normalized, Z	1,579	0,697
Bactericidity vs St. aur, 10^9 Bac/L	0,699	0,766
Chakra 7 Asymmetry	7,788	1,722
Killing Index vs Staph. aureus, %	0,410	0,380
Asymmetry-δ, %	0,591	0,626
F3-δ PSD, $\mu V^2/Hz$	0,050	0,046
T6-α PSD, $\mu V^2/Hz$	0,178	0,210
T5-θ PSD, $\mu V^2/Hz$	0,060	-0,003
T6-δ PSD, $\mu V^2/Hz$	-0,068	-0,061
C3-β PSD, $\mu V^2/Hz$	0,097	0,227
F3-β PSD, $\mu V^2/Hz$	0,075	-0,056
C3-α PSD, $\mu V^2/Hz$	0,042	0,031
P3-β PSD, $\mu V^2/Hz$	0,434	0,364
P4-β PSD, $\mu V^2/Hz$	-0,818	-0,766
Entropy GDI Left	324,3	317,2
Chakra 3 Asymmetry	13,60	10,82
T3-β PSD, $\mu V^2/Hz$	-0,070	-0,058
Constants	-687,6	-698,3

Table 6.10. Classification Matrix

	Rows: Observed classifications Columns: Predicted classifications		
Group	Percent Correct	Before p=,50	After p=,50
Before	97,5	39	1
After	92,5	3	37
Total	95,0	42	38

Therefore, the phytocomposition «Balm Truskavets'» increases the resistance of the observed cohort to **bacterial** infection, i.e. corresponds to one of the attributes of adaptogens: the ability to cause a state of non-specifically increased resistance of the body to the influence of adverse environmental factors of a physical, chemical and **biological nature** [Kostyuk PG et al., 2006; Panossian AG et al., 2021]. An even stronger proof of the adaptogenic ability of the phytocomposition is an increase in the Popovych's leukocytary **adaptation** index, which reflects the quantitative assessment of qualitative changes in the body's general adaptive reactions, namely, a decrease in the share of pathological and premorbid (disharmonious) reactions and an increase in the share of normal (harmonious) reactions [Garkavi LKh et al., 1990; Flyunt IS et al., 2002; Kostyuk PG et al., 2006].

To what substances does this phytocomposition owe its adaptogenicity? The most investigated medicinal herbs for their adaptogenic activity are Eleutherococcus senticosus, Panax ginseng, Withania somnifera, Schisandra chinensis, Rhaponticum carthamoides, Lepidium meyenii, and Rhodiola spp. Salidroside, ginsenosides, andrographolide, methyl jasmonate, cucurbitacin R, dichotosin, and dichotosininare are phytochemicals that have shown a considerable adaptogenic activity. Phytochemicals that have been demonstrated adaptogenic properties mainly belong to phytoecdysteroids, flavonoids, phenolic acids, et al. Phytoecdysteroids – a large class of steroid compounds. Their structures are composed by 27–29 C-atoms, with a four-ring steroid skeleton and contain polyhydroxyl groups (4-7 hydroxyl groups). Flavonoids are substances with a phenolic structure, and over 8000 flavonoids are known. Flavonoids are divided into the subclasses flavonols, flavones, flavanones, catechins, and their glycosides. Phenolic acids: Protocatechuic, Benzoic, Hydroxyphenylacetic, Hydroxybenzoic, Salicylic, Gentisic, Elagic, Chlorogenic, Vanillic, Coumaric, Synapic, Caffeic, Ferulic, Gallic, Syringic [Todorova V et al., 2021; Esmaealzadeh N et al., 2022]. Sergeeva I et al. [2021] give a different classification of phenols. In accordance with the pathways of biosynthesis in plants, phenolic compounds are subdivided into eight groups: compounds of the C6 series, or simple phenols; compounds of the C6-C1 series, or phenolic acids (derivatives of benzoic acid); C6-C2 compounds, or phenolic alcohols and phenylacetic acids; compounds of the C6-C3 series, or hydroxycinnamic acids, phenylpropenes, and coumarins; compounds of the C6-C4 series,

or flavonoids or isoflavonoids, as well as lignins and polymeric phenolic compounds—lignin, tannins, and melanins. An important property of phenolic compounds is the ability to oxidize; they are especially easily oxidized in an alkaline environment. Phenolic compounds with two phenolic rings include: flavonoids, catechins, leukoanthocyanins, flavones, and anthocyanidins. Flavonoids differ in the degree of oxidation: the most reduced of them are catechins, the most oxidized are flavonols.

Currently, we do not have data on the chemical composition of the "Balm Truskavets'". In the composition of its predecessor and analogue "Balm Kryms'kyi", polyphenols were detected in the amount of 4 mg/L compared to 7 mg/L in ginseng tincture (produced by "Lubnykhimfarm", Ukraine) [Alyeksyeyev ***OI*** et al., 1996]. It is interesting that polyphenols in amounts of 0,039÷0,28 mg/L were also found in the composition of bioactive Naftussya water [Ivassivka SV et al., 1994; Ivassivka SV et al., 1999; Fihura OA et al., 2022; Zukow W et al., 2022], the adaptogenic properties of which have long been known.

The adrenomimetic effect of both «Balm Kryms'kyi» and ginseng tincture on the isolated heart of a frog [Alyeksyeyev ***OI*** et al., 1996], due to inhibition of catechol-o-methyltransferase activity [Lupandin AV, 1989], is associated with polyphenols.

However, we are inclined to the neurogenic mechanism of the adreno-sympathomimetic effect of the phytocomposition revealed in this study. This is consistent with literature data on the direct neurotropic effect of phytoadaptogens in vitro and in vivo [Asea A et al., 2013; Panossian A et al., 2018; Panossian A et al., 2019; Panossian A et al., 2020], as well as our data on changes in EEG parameters.

The figures presented by Winkelmann T et al. [2017] give us reason to assume that the loci C3/C4 projected precentral gyrus, T3/T4 – inferior temporal gyrus, F3/F4 – caudal anterior cingulate cortex or rostral middle frontal gyrus, P3/P4 – supramarginal gyrus, T5/T6 – transverse temporal cortex. The **thickness** of these cortical structures is positively correlated with the HF HRV as marker of vagal tone. However, according to our data, an increase in **electrical activity**, or more precisely PSD, of neurons that project to the listed loci is accompanied by a moderate, within the normal range, decrease in vagal tone, as well as serum levels of testosterone and triiodothyronine in combination with a moderate increase in the levels of cortisol and circulating catecholamines. This is consistent with the concept

that adaptogens are **eustress** inducers that prevent the development of **distress** under the influence of pathogenic factors [Garkavi LKh et al., 1990; Flyunt IS et al., 2002; Kostyuk PG et al., 2006; Kozyavkina OV et al., 2015; Panossian AG et al., 2021]. With regard to the mechanism of the neurotropic action of phytochemicals, in particular polyphenols, we suggest the mediating role of aryl hydrocarbon receptors of neurons [Kimura E & Tohyama C, 2017; Keshavarzi M et al., 2020; Ojo ES & Tischkau SA, 2021]. The possibility of irritation by phytochemicals of the chemoreceptor terminals of the afferent vagal fibers in the intestine with subsequent influence on the activity of CNS neurons should not be rejected [Chavan SS et al., 2017].

In conclusion, we will discuss the place and role of biophotonics and acupuncture parameters in the adaptogenic effects of the phytocomposition. Previously, it was shown in our laboratory that GDV parameters significantly correlate with parameters of the neuro-endocrine-immune complex [Babelyuk VY et al., 2017; Babelyuk VY et al., 2020; Babelyuk VY et al., 2021; Babelyuk VY et al., 2021a; Babelyuk VY et al., 2022] and acupuncture points [Babelyuk VY et al., 2021] and respond to the influence of another adaptogen – Naftussya bioactive water [Gozhenko AI et al., 2016]. Unidirectional changes in the symmetry of the third and seventh Chakras, electrical conductivity of acupuncture points MC(AVL) (represent the immune system) and EEG alpha-rhythm as well as opposite changes in the delta-rhythm were found in this study. According to Ayurveda **third** Chakra associated with **celiac plexus ganglion** and **spleen** as well as [endocrine] pancreas, liver, gall bladder, stomach, duodenum, pancreas; **seventh** Chakra – with **right** (paired EEG loci) and upper brain as well as pineal gland [Chase CR, 2018]. Therefore, these parameters of biophotonics and acupuncture logically fit into the structure of the anti-inflammatory cholinergic reflex [Chavan SS et al., 2017].

Conclusion

Ukrainian phytocomposition “Balm Truskavets’” exerts classical adaptogenic effects on parameters of neuro-endocrine-immune complex as well as biophotonics and acupuncture in humans with maladaptation.

Chapter 7

AMELIORATION BY PHYTOADAPTOGENE OF EFFECTS OF BALNEOFACTORS OF TRUSKAVETS' SPA ON PATIENTS WITH POST-RADIATION ENCEPHALOPATHY

Summary

Background. We have previously explored effects of Ukrainian phytocomposition "Balm Truskavets'" on parameters of neuro-endocrine-immune complex and biophotonics in humans with maladaptation. It is known that in patients with post-radiation encephalopathy the reaction to some stimuli is significantly changed, therefore it needs correction. The purpose of this study is to test the ability of this phytocomposition to amelioration the effects of standard balneotherapeutic complex in patients with post-radiation encephalopathy.

Material and methods. The research was carried out through a retrospective analysis of the database of the Truskavetsian Scientific School of Balneology, which remained unpublished. The object of observation in 1997 were 19 men and 3 women with urate urolithiasis and chronic pyelonephritis who were exposed to pathogenic factors of the accident at the Chornobylian nuclear power plant during the liquidation of its consequences in 1986-87. The survey was conducted twice: on admission and after two weeks of rehabilitation in sanatorium "Perlyna Prykarpattya" (Truskavets' Spa). 11 patients received standard balneotherapy while the other 11 patients additionally received the phytocomposition "Balm Truskavets'". According to the protocol, blood pressure, routine hematological and biochemical blood parameters were determined. In addition, physical working capacity (PWC_{150}) as well as EEG, HRV and immunity parameters were determined.

Results. Standard balneotherapy increases the decreased level of T-helper lymphocytes, but further decreases the level of B-lymphocytes, glomerular filtration rate and PWC_{150}, in combination with increased normal levels of blood creatinine and urea, as well as decreased levels of diastolic BP and heart rate. This is accompanied by a further increase in the sympathetic tone and the leveling of the increased of ULF band HRV

as marker of level in the serum of catecholamines and glucocorticoids. Additional use of phytocomposition limits the adverse effects of standard balneotherapy by modulating EEG and HRV parameters.

Conclusion. Phytocomposition «Balm Truskavets'» by modulating the parameters of the nervous system limits the adverse effects of standard balneotherapy at the Truskavets' Spa in patients with post-radiation encephalopathy.

INTRODUCTION

Many years of experimental and clinical research of the Truskavetsian Scientific School of Balneology have demonstrated the adaptogenic properties of the main therapeutic factor of the spa, Naftussya bioactive water, as well as ozokerite and mineral baths, which together make up a standard balneotherapeutic complex. However, in contrast to the beneficial effect of the latter on stress resistance and the neuro-endocrine-immune complex, the effect on the physical performance of both rats and resort patients is ambiguous [Hrinchenko BV, 1998; Hrinchenko BV et al., 1999; Flyunt IS et al., 2002; Tserkovnyuk AV et al., 2002; Ruzhylo SV et al., 2003; Ruzhylo SV et al., 2003a; Ruzhylo SV et al., 2003b; Kostyuk PG et al., 2006], which prompted the additional use of aerobic training [Tserkovnyuk AV et al., 2001; Tserkovnyuk AV et al., 2002a; Ruzhylo SV et al., 2003b] and/or phytoadaptogens, both well-known (ginseng, Bittner's balsam), and the Ukrainian phytocomposition «Balm Kryms'kyi» [Flyunt IS et al., 2002; Flyunt IS et al., 2008; Hrinchenko BV, 1998; Hrinchenko BV et al., 1999], the adaptogenic properties of which first discovered by representatives of the Truskavetsian Scientific School of Balneology [Panasyuk YM et al., 1994].

We have previously explored effects of phytocomposition "Balm Truskavets'", which is analogous to the "Balm Kryms'kyi", on parameters of neuro-endocrine-immune complex and biophotonics in humans with maladaptation.

It is known that in patients with post-radiation encephalopathy the reaction to some stimuli is significantly changed [Romodanov AP, 1993; Alyeksyeyev ***OI*** et al., 1996; Kostyuk PG et al., 2006], therefore it needs correction.

The purpose of this study is to test the ability of this phytocomposition to amelioration the effects of standard balneotherapeutic complex in patients with post-radiation encephalopathy.

MATERIAL AND RESEARCH METHODS

The research was carried out through a retrospective analysis of the database of the Truskavetsian Scientific School of Balneology, which remained unpublished.

The object of observation in 1997 were 19 men (age 26÷61 years) and 3 women (38, 40 and 47 years) with urate urolithiasis and chronic pyelonephritis who were exposed to pathogenic factors of the accident at the Chornobylian nuclear power plant during the liquidation of its consequences in 1986-87. According to the documents, the total effective radiation dose was 10÷25 cGy, which is most typical for this contingent [Romodanov AP, 1993; Alyeksyeyev ***OI*** et al., 1996]. The survey was conducted twice: on admission and after two weeks of rehabilitation in sanatorium "Perlyna Prykarpattya" of the Ministry of Internal Affairs (Truskavets' Spa). 11 patients received standard balneotherapy: bioactive Naftussya water by 3 mL/kg for 1 hour before meals three times a day; baths with mineral water (Cl^--SO_4^{2-}-Na^+-Mg^{2+} containing salt concentration 25 g/L; t^0 36-37^{0}C during 8-10 min); application of Ozokerite on the lumbar region (t^0 45^{0}C, exposure 30 min, every other day, 5 procedures); therapeutic physical exercises (motion mode II). The other 11 patients additionally received the Ukrainian phytocomposition "Balm Truskavets'" (5 ml, pre-diluted in 45 ml of boiled tap water, half an hour before meals three times a day).

According to the protocol, routine hematological (hemoglobin, erythrocytes, reticulocytes, hematocrit, erythrocyte sedimentation rate) and biochemical blood parameters: albumins, alpha-1, alpha-2, beta- and gamma-globulins, urea, uric acid, creatinine, glucose, sialic acids, alkaline phosphatase, pseudocholinesterase, amylase, alanine and aspartic transaminases, medium-weight molecules, lipids in general, high-, low-, and very-low-density lipoprotein cholesterol, diene conjugates, malondialdehyde, catalase, and erythrocyte superoxide dismutase were determined. The analyzes were carried out according to the instructions. The analyzers "Pointe-180" ("Scientific", USA) and "Reflotron" (Boehringer Mannheim, BRD) were used with appropriate sets.

For estimation of physical working capacity (PWC) a bicycle ergometer "Tunturi" (Finland) was used. The power of the first load was 0,5 W/kg at a pedaling frequency of 60-75 rpm. The power of the second load (after 3 min), according to the recommendations for a gentle version of the PWC test, taking into account the age of the subjects [Belotserkovskiy ZB, 1986], was selected so that the heart rate (HR) at the end of the load was close to that calculated by the formula:

HR = (220 – Age)•0,87.

Calculated submaximal PWC_{150} with the mechanical power in Watt per kilogram body weight (W/kg) as indicator of cardiorespiratory fitness.

Systolic and diastolic blood pressure as well as heart rate was measured by tonometer "Omron M4-I" (Netherlands) in a sitting position. Then recorded electrocardiogram in II lead to assess the parameters of HRV (software and hardware complex «CardioLab+HRV»). EEG recorded a hardware-software complex "NeuroCom Standard".

The parameters of immunity were determined as described in the manual [Perederiy VG et al., 1995]. Determined the relative content of the population of T-lymphocytes in a test of spontaneous rosette formation with erythrocytes of sheep, their theophylline-resistant and theophylline-sensitive subpopulations (by the test of sensitivity of rosette formation to theophylline), B-lymphocytes by the test of complementary rosette formation with erythrocytes of sheep.

The reference values are taken from the database of the Truskavetsian Scientific School of Balneology.

Statistical processing performed using a software package "Microsoft Excell" and "Statistica 6.4 StatSoft Inc".

RESULTS AND DISCUSSION

Previously, statistically significant deviation from the norm of 18 EEG parameters (increase in 8 and decrease in 10) have been revealed in this cohort of patients, which were not affected by balneotherapy and were interpreted as a manifestation of post-radiation encephalopathy. Such an EEG state was accompanied by a pronounced sympathotonic shift of the autonomic balance [Ruzhylo SV et al., 2022].

In this study, it was found that autonomic dysfunction, as well as some normal (but not abnormal) EEG parameters were sensitive to balneofactors, but the severity and even the directionality of nervous system reactions differed in patients who received standard balneotherapy or balneotherapy supplemented with Balm. This also applies to a number of other registered parameters.

And now in more detail. At the first stage of the analysis, only those parameters that were significantly changed in at least one group of patients were selected. Then, according to the algorithm of the Truskavetsian Scientific School of Balneology, the actual values were normalized, that is, recalculated into Z-scores. The effects of standard balneotherapy were assessed by the difference between final and initial Z-scores. The

difference between the Z-scores after the combined (ST+B) and standard (ST) balneotherapy makes it possible to evaluate the partial (per se) effects of the Balm (B) (please see Table 7.16). Finally, 6 clusters were formed from 22 parameters (Fig. 7.1).

The first cluster reflects the enhancing effect of ST on normal heart rate and already increased sympathetic tone. This is consistent with the data of a previous clinical study [Popovych AI, 2019] and an experiment on rats [Ruzhylo SV et al., 2021]. Additional use of the Balm reduces sympathetic tone to normal, and heart rate to the lower normal range, i.e. the phytocomposition has a sympathoinhibitory/vagotonic effect.

The second cluster reflects the normalizing effect of ST on reduced blood pressure diastolic (but not systolic), which is probably related to its sympathomimetic effect. Naturally, the Balm limits this effect of ST. However, Balm reduces the normal level of Entropy of PSD in both right temporal loci, while ST does not affect these EEG parameters. On the other hand, ST reduces the degree of reduction in the level of T-helper lymphocytes, while the Balm does not affect this parameter of immunity. It turned out quite unexpectedly that after ST, the normal level of urea increases and the upper limit level of creatinine increases even more. This is combined with a deepening of the lower boundary level of glomerular filtration rate (fourth cluster). Additional use of the Balm normalizes the creatinine level, lowers the urea level to the lower normal range and limits the decrease in glomerular filtration rate.

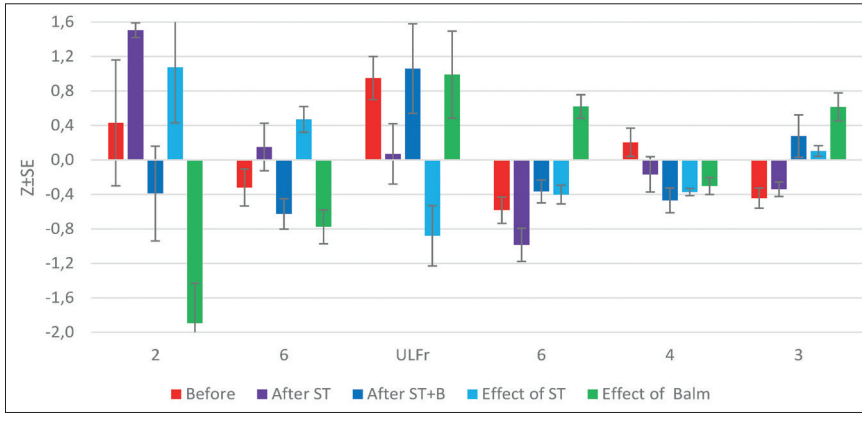

Fig. 7.1. Clusters of normalized parameters before and after standard (ST) and combined (ST+B) balneotherapy; the effects of standard balneotherapy and Balm were also calculated. Below is the number of parameters combined into a cluster

The third cluster contains only one parameter, the increased level of which is completely normalized due to ST, while the Balm completely counteracts this effect. It is speculated that ULF band HRV associated with oscillation blood level of norepinephrine (0,002 Hz) as well as 17-OCS (0,0019 Hz) [cit. by: Kotelnikov SA et al., 2002]. This assumption is consistent with literature data that such a cohort of patients had elevated serum levels of both catecholamines and glucocorticoids [Kostyuk PG et al., 2006], as well as with the previously registered drastically increased Baevskiy's stress index in these patients: 688±134 units versus reference level 132±11 units [Ruzhylo SV et al., 2022].

Such hypothetical changes in ergotropic hormones are accompanied by a further decrease in the lower limit level of PWC_{150}, which is reversed by phytoadaptogen. This is in excellent agreement with the data of our experiment on rats.

Changes in PWC_{150} are accompanied by unidirectional changes in other parameters combined in the fourth (and also sixth) cluster, instead, by opposite changes in some other parameters. Let's dwell on these connections in more detail.

Among the EEG parameters, a significant negative correlation of changes in PWC_{150} and PSD Fp2-θ (Fig. 2), F8-θ (r=-0,50), T5-θ (r=-0,28), Entropy of PSD in T6 locus (r=-0,50), instead, a positive correlation with changes in PSD O1-δ (Fig. 7.3) and O2-δ (r=0,40).

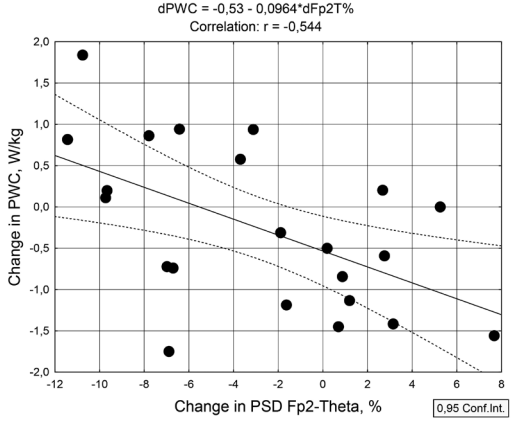

Fig. 7.2. Scatterplot of correlation between the changes in PSD of theta-rhythm in Fp2 locus (X-line) and PWC_{150} (Y-line)

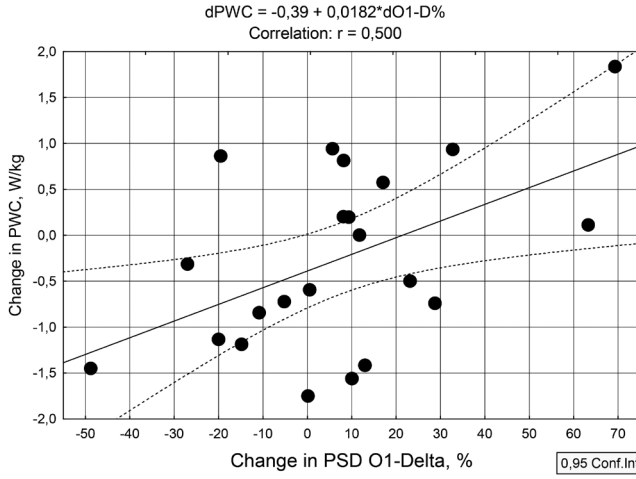

Fig. 7.3. Scatterplot of correlation between the changes in PSD of delta-rhythm in O1 locus (X-line) and PWC_{150} (Y-line)

It is interesting that when building a regression model by stepwise exclusion until reaching the maximum value of Adjusted R^2, some parameters were left out of the model, instead, the ULF band was included in it despite the insignificant relationship (Table 7.1). Taken together, changes in the three parameters of the nervous system determine changes in PWC_{150} by 51,5% (Fig. 7.4).

Table 7.1. Regression Summary for change in PWC_{150}
R=0,718; R^2=0,515; Adjusted R^2=0,434; $F_{(3,2)}$=6,4; p=0,004; SE: 0,74 W/kg

N=22		Beta	St. Err. of Beta	B	St. Err. of B	$t_{(18)}$	p-level
Change in Variables	r		Intercpt	-0,596	0,184	-3,24	0,005
Fp2-θ PSD, %	**-0,54**	-0,551	0,170	-0,098	0,030	-3,24	0,005
O2-δ PSD, %	**0,40**	0,359	0,168	0,016	0,008	2,13	0,047
ULF PSD, %	**0,19**	0,362	0,170	0,054	0,025	2,14	0,046

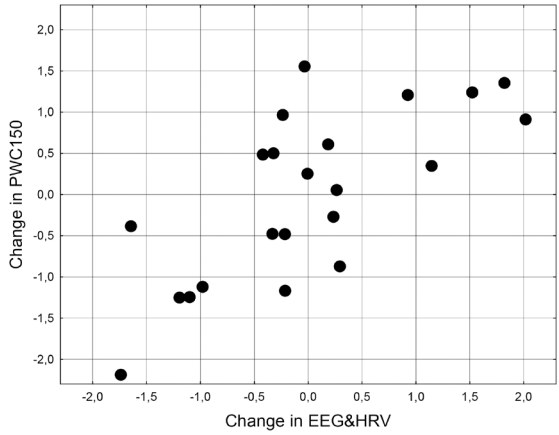

R=0,718; R^2=0,515; $\chi^2_{(3)}$=14; p=0,004; Λ Prime=0,485

Fig. 7.4. Scatterplot of canonical correlation between the changes in EEG&HRV parameters (X-line) and PWC_{150} (Y-line)

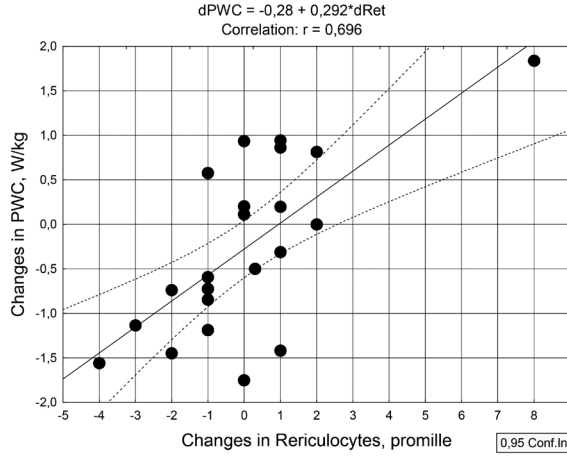

Fig. 7.5. Scatterplot of correlation between the changes in blood Reticulocytes level (X-line) and PWC_{150} (Y-line)

In addition, a strong positive correlation was found between changes in PWC_{150} and the content of reticulocytes in the blood (Fig. 7.5), but not erythrocytes (r=0,20) and hemoglobin (r=0,13), as well as malondialdehyde (r=0,28) and the level of glomerular filtration (r=0,25).

Instead, the correlation with changes in serum urea is negative (Fig. 7.6).

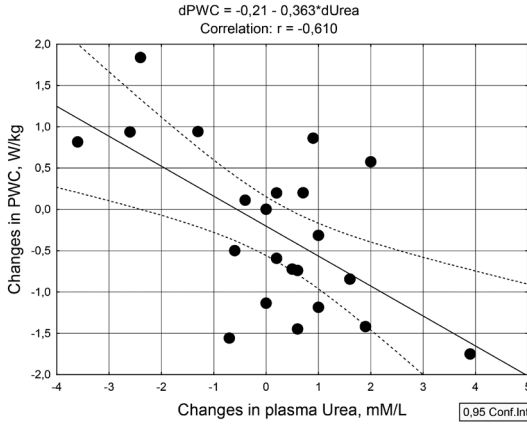

Fig. 7.6. Scatterplot of correlation between the changes in serum Urea level (X-line) and PWC_{150} (Y-line)

Taken together, changes in these parameters determine changes in PWC150 by 67,8% (Table 7.2 and Fig. 7.7).

With regard to immunity parameters, an inverse relationship with the relative level of T-helper Lymphocytes (Fig. 7.8) was found, instead, a direct relationship with the level of B-Lymphocytes.

Taken together, changes in immune parameters determine changes in PWC150 by 36,7% (Table 7.3 and Fig. 7.9).

Finally, a strong negative correlation of changes in PWC150 and diastolic (but non systolic) blood pressure was found (Fig. 7.10).

Table 7.2. Regression Summary for change in PWC_{150}
R=0,823; R^2=0,678; Adjusted R^2=0,624; $F_{(3,2)}$=12,6; p=0,0001; SE: 0,60 W/kg

N=22		**Beta**	**St. Err. of Beta**	**B**	**St. Err. of B**	**$t_{(18)}$**	**p-level**
Change in Variables	**r**		**Intercpt**	**-0,242**	**0,129**	**-1,87**	**0,078**
Reticulocytes, ‰	**0,70**	0,634	0,153	0,266	0,064	4,13	0,001
Malondyaldehid, µM/L	**0,28**	-0,255	0,163	-0,007	0,004	-1,57	0,135
Urea, mM/L	**-0,61**	-0,505	0,154	-0,300	0,092	-3,27	0,004

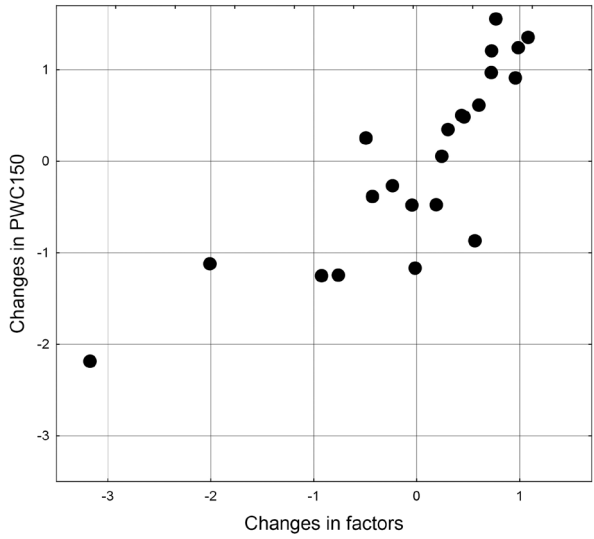

R=0,823; R^2=0,678; $\chi^2_{(3)}$=21; p=0,0001; Λ Prime=0,322

Fig. 7.7. Scatterplot of canonical correlation between the changes in factors (X-line) and PWC_{150} (Y-line)

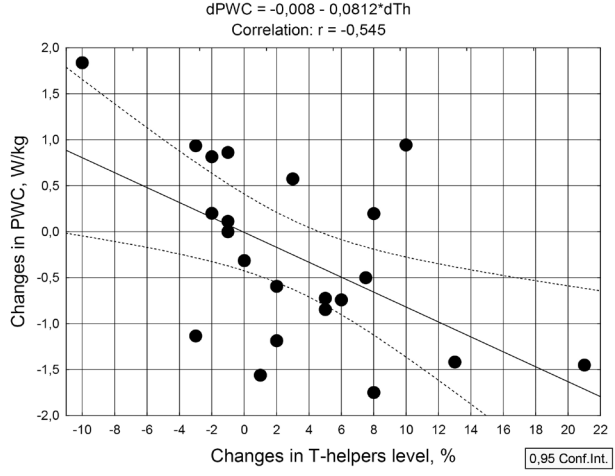

Fig. 7.8. Scatterplot of correlation between the changes in T-helper Lymphocytes level (X-line) and PWC_{150} (Y-line)

Table 7.3. Regression Summary for change in PWC_{150}
R=0,606; R^2=0,367; Adjusted R^2=0,300; $F_{(2,2)}$=5,5; p=0,013; SE: 0,82 W/kg

N=22		Beta	St. Err. of Beta	B	St. Err. of B	$t_{(19)}$	p-level
Change in Variables	r000000		Intercpt	-0,012	0,195	-0,06	0,952
T-helper Lymphocytes, %	**-0,55**	-0,507	0,184	-0,075	0,027	-2,75	0,013
B-Lymphocytes, %	**0,34**	0,267	0,184	0,046	0,032	1,44	0,165

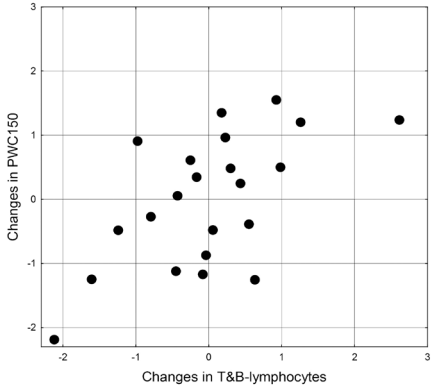

R=0,606; R^2=0,367; $\chi^2_{(2)}$=8,7; p=0,013; Λ Prime=0,633

Fig. 7.9. Scatterplot of canonical correlation between the changes in immune parameters (X-line) and PWC_{150} (Y-line)

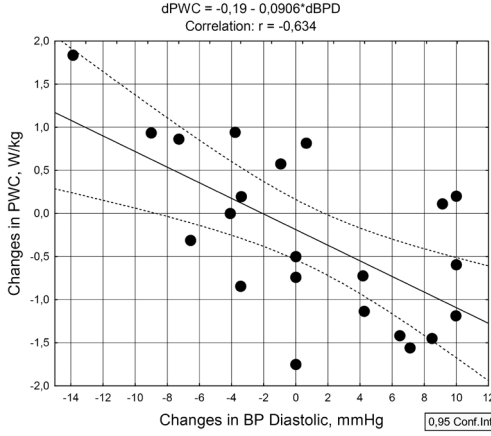

Fig. 7.10. Scatterplot of correlation between the changes in Blood Pressure Diastolic level (X-line) and PWC_{150} (Y-line)

However, despite the significant correlation coefficient, the last parameter was outside the integral regression model (Table 7.4).

Table 7.4. Regression Summary for change in PWC_{150}
R=0,880; R^2=0,774; Adjusted R^2=0,683; $F_{(6,2)}$=8,6; p=0,0004; SE: 0,55 W/kg

N=22		Beta	St. Err. of Beta	B	St. Err. of B	$t_{(15)}$	p-level
Change in Variables	r		Intercpt	-0,280	0,152	-1,84	0,085
Reticulocytes, ‰	**0,70**	0,248	0,167	0,104	0,070	1,49	0,158
B-Lymphocytes, %	**0,34**	0,190	0,145	0,033	0,025	1,31	0,211
ULF PSD, %	**0,19**	0,162	0,133	0,024	0,020	1,22	0,241
T-helper Lymphocytes, %	**-0,55**	-0,242	0,143	-0,036	0,021	-1,70	0,111
Urea, mM/L	**-0,61**	-0,269	0,143	-0,160	0,085	-1,88	0,080
Fp2-θ PSD, %	**-0,54**	-0,385	0,157	-0,068	0,028	-2,45	0,027

Judging by the coefficient R2, changes in PWC150 are determined by changes in the parameters included in the regression model by 77,4% (Fig. 7.11).

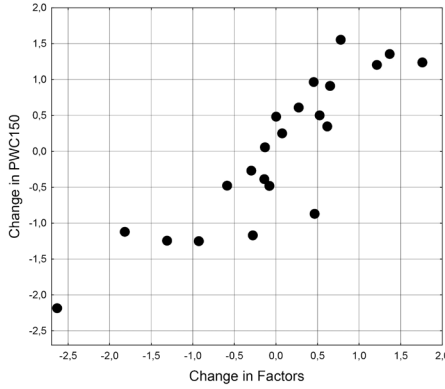

R=0,880; R^2=0,774; $\chi^2_{(6)}$=25; p=0,0003; Λ Prime=0,226
Fig. 7.11. Scatterplot of canonical correlation between the changes in factors (X-line) and PWC_{150} (Y-line)

Since PWC is calculated based on HR response to exercise, its relationship with HRV&EEG parameters is quite natural. It is also possible to understand the physiological mechanism of the direct connection between PWC150 and the content of reticulocytes in the blood, even in the absence of connections with the content of erythrocytes and hemoglobin. Instead, the physiological mechanisms of direct connections between PWC and the content of immunocytes and metabolites in the blood seem to be problematic. Given the well-known functional relationships between HRV&EEG parameters and immunity, it was appropriate to analyze them in this cohort.

It was found that changes in the levels of both T-helper (Table 7.5 and Fig. 7.12) and B-Lymphocytes (Table 7.6 and Fig. 7.13) as well as reticulocytes close to them in terms of genesis (Table 7.7 and Fig. 7.14) are determined by changes in neural parameters, that is, their connections with PWC_{150} are formal (mathematical), but not causal.

Table 7.5. Regression Summary for change in T-helpers
R=0,564; R^2=0,318; Adjusted R^2=0,247; $F_{(2,2)}$=4,4; p=0,026; SE: 5,7%

N=22		Beta	St. Err. of Beta	B	St. Err. of B	$t_{(19)}$	p-level
Change in Variables	**r**		**Intercpt**	**4,937**	**1,366**	**3,61**	**0,002**
F8-θ PSD, %	**0,50**	0,383	0,206	0,392	0,211	1,86	0,079
O2-δ PSD, %	**-0,44**	-0,290	0,206	-0,088	0,062	-1,41	0,176

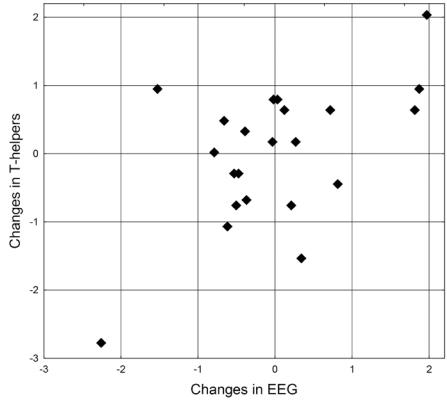

R=0,564; R^2=0,318; $\chi^2_{(2)}$=7,3; p=0,026; Λ Prime=0,682
Fig. 7.12. Scatterplot of canonical correlation between the changes in EEG (X-line) and T-helpers (Y-line)

Table 7.6. Regression Summary for change in B-lymphocytes
R=0,455; R^2=0,207; Adjusted R^2=0,123; $F_{(2,2)}$=2,5; p=0,111; SE: 5,3%

N=22		Beta	St. Err. of Beta	B	St. Err. of B	$t_{(19)}$	p-level
Change in Variables	**r**		**Intercpt**	**0,496**	**1,192**	**0,42**	**0,682**
ULF PSD, %	**0,33**	0,404	0,210	0,351	0,183	1,92	0,070
T6 PSD Entropy	**0,23**	0,323	0,210	7,746	5,040	1,54	0,141

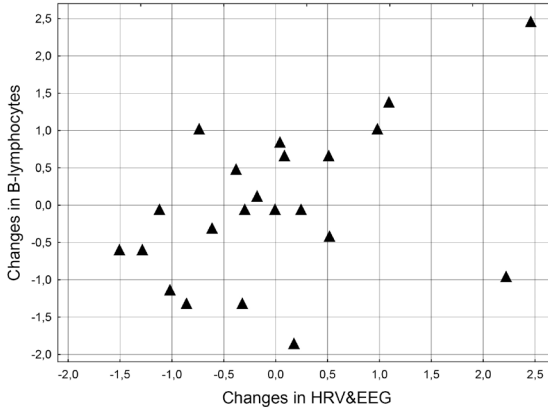

R=0,455; R^2=0,207; $\chi^2_{(2)}$=4,4; p=0,111; Λ Prime=0,793
Fig. 7.13. Scatterplot of canonical correlation between the changes in HRV&EEG (X-line) and B-lymphocytes (Y-line)

Table 7.7. Regression Summary for change in Reticulocytes
R=0,676; R^2=0,457; Adjusted R^2=0,329; $F_{(4,2)}$=3,6; p=0,027; SE: 1,9 ‰

N=22		Beta	St. Err. of Beta	B	St. Err. of B	$t_{(17)}$	p-level
Change in Variables	**r**		**Intercpt**	**-0,703**	**0,467**	**-1,51**	**0,150**
Fp2-θ PSD, %	**-0,48**	-0,241	0,210	-0,102	0,088	-1,15	0,267
T5-θ PSD, %	**-0,46**	-0,303	0,203	-0,097	0,065	-1,49	0,154
T4 PSD Entropy	**-0,24**	-0,226	0,182	-2,395	1,923	-1,25	0,230
O1-δ PSD, %	**0,49**	0,304	0,194	0,026	0,017	1,57	0,135

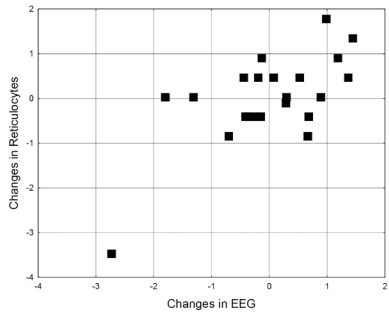

R=0,676; R^2=0,457; $\chi^2_{(4)}$=11; p=0,027; Λ Prime=0,543

Fig. 7.14. Scatterplot of canonical correlation between the changes in EEG (X-line) and Reticulocytes (Y-line)

Changes in diastolic blood pressure (Table 7.8 and Fig. 7.15) and associated glomerular filtration rate (Table 7.9 and Fig. 7.16) are also expected to be subject to neural determination.

Table 7.8. Regression Summary for change in BP diastolic
R=0,608; R^2=0,370; Adjusted R^2=0,265; $F_{(3,2)}$=3,5; p=0,036; SE: 5,9 mmHg

N=22		Beta	St. Err. of Beta	B	St. Err. of B	$t_{(18)}$	p-level
Change in Variables	**r**		**Intercpt**	**2,239**	**1,427**	**1,57**	**0,134**
F8-0 PSD, %	**0,48**	0,326	0,202	0,348	0,216	1,61	0,125
T5-0 PSD, %	**0,36**	0,381	0,214	0,358	0,201	1,78	0,092
ULF PSD, %	**-0,23**	-0,327	0,206	-0,344	0,216	-1,59	0,130

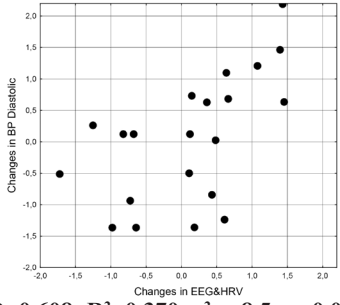

R=0,608; R^2=0,370; $\chi^2_{(3)}$=8,5; p=0,036; Λ Prime=0,630

Fig. 7.15. Scatterplot of canonical correlation between the changes in EEG&HRV (X-line) and BP diastolic (Y-line)

Table 7.9. Regression Summary for change in Glomerular Filtration
R=0,551; R^2=0,304; Adjusted R^2=0,230; $F_{(2,2)}$=4,1; p=0,032; SE: 15 mL/min

N=22		Beta	St. Err. of Beta	B	St. Err. of B	$t_{(19)}$	p-level
Change in Variables	**r**		**Intercpt**	**-4,415**	**3,502**	**-1,26**	**0,223**
T4 PSD Entropy	**-0,47**	-0,498	0,192	-39,59	15,27	-2,59	0,018
T5-θ PSD, %	**-0,24**	-0,281	0,192	-0,674	0,461	-1,46	0,160

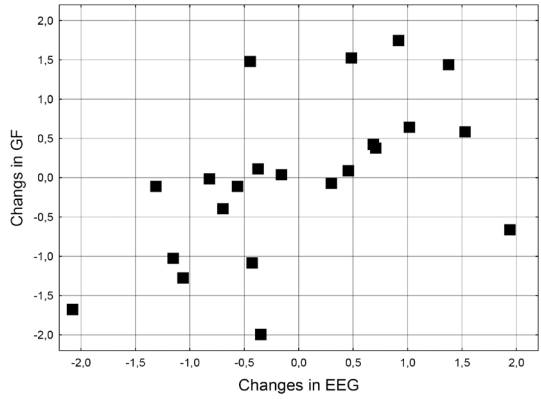

R=0,551; R^2=0,304; $\chi^2_{(2)}$=6,9; p=0,032; Λ Prime=0,696
Fig. 7.16. Scatterplot of canonical correlation between the changes in EEG (X-line) and Glomerular Filtration (Y-line)

Table 7.10. Regression Summary for change in serum Urea
R=0,655; R^2=0,429; Adjusted R^2=0,205; $F_{(6,2)}$=1,9; p=0,151; SE: 1,5 mM/L

N=22		Beta	St. Err. of Beta	B	St. Err. of B	$t_{(15)}$	p-level
Change in Variables	**r**		**Intercpt**	**0,595**	**0,378**	**1,57**	**0,136**
O1-δ PSD, %	**-0,41**	-0,606	0,322	-0,037	0,020	-1,88	0,080
LF PSD, %	**0,32**	0,347	0,220	0,033	0,021	1,58	0,135
T4 PSD Entropy	**0,30**	0,679	0,321	5,077	2,402	2,11	0,052
Frequency-β, Hz	**0,28**	-0,350	0,289	-0,108	0,089	-1,21	0,245
T6 PSD Entropy	**0,26**	-0,593	0,385	-4,130	2,681	-1,54	0,144
Fp2-θ PSD, %	**0,25**	0,468	0,261	0,139	0,078	1,80	0,093

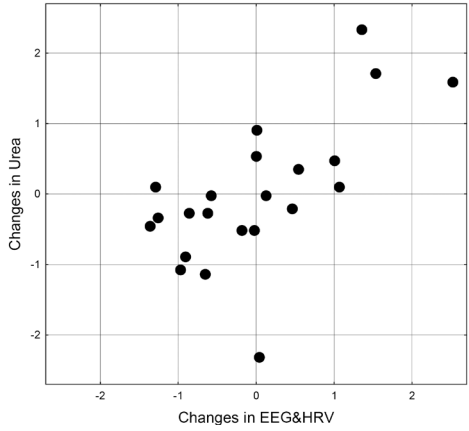

R=0,655; R^2=0,429; $\chi^2_{(6)}$=9,5; p=0,146; Λ Prime=0,571

Fig. 7.17. Scatterplot of canonical correlation between the changes in EEG (X-line) and Glomerular Filtration (Y-line)

It is interesting that the multiple urea-neural correlation turned out to be maximal in this series and at the same time statistically insignificant (Table 7.10 and Fig. 7.17).

Finally, a canonical correlation analysis was performed between changes in EEG&HRV parameters, taken as factors, and metabolic and hemato-immune parameters, taken as responses. It was found that changes in nervous regulation caused by balneofactors determine changes in diastolic pressure, glomerular filtration, serum concentration of urea, malondialdehyde, as well as the content of T-helpers, B-lymphocytes and reticulocytes in the blood by 98.6% (Table 7.11 and Fig. 7.18).

Table 7.11. Factor structure of Canonical Roots

EEG&HRV	**R**
1	2
T6 PSD Entropy	**-0,638**
F8-θ PSD, %	**-0,627**
Fp2-θ PSD, %	**-0,603**
T5-θ PSD, %	**-0,484**
T4 PSD Entropy	**-0,362**
LF PSD, %	**-0,038**

Table 7.11 (cont)

1	2
O1-δ PSD, %	**0,348**
O2-δ PSD, %	**0,229**
ULF PSD, %	**0,069**
Frequency-β, Hz	**0,067**
Other	**R**
BP Diastolic, mmHg	**-0,698**
Urea, mM/L	**-0,416**
T-helpers, %	**-0,449**
B-Lymphocytes, %	**-0,145**
Reticulocytes, ‰	**0,640**
Glom Filtration, mL/min	**0,564**
Malondyaldehid, μM/L	**0,311**

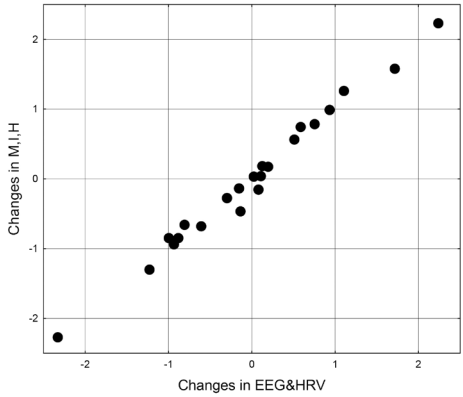

R=0,993; R^2=0,986; $\chi^2_{(70)}$=101; p=0,009; Λ Prime=0,0002
Fig. 7.18. Scatterplot of canonical correlation between the changes in EEG&HRV (X-line) and metabolic, immune and other (Y-line) parameters

The results of a discriminant analysis testify in favor of the alternativeness of primary targets, according to which the characteristic effects of balneofactors are both neurotropic and immunotropic. In addition, the forward stepwise program also included PWC and bilirubin level in the discriminant model (Tables 7.12 and 7.13).

Table 7.12. Summary of the analysis of discriminant functions.

Step 10, N of vars in model: 10; Grouping: 3 grps; Wilks' Λ: 0,2094; approx. $F_{(21)}$=3,8; $p<10^{-4}$

Variables currently in the model	Groups (n) and Means±SE			Parameters of Wilks' Statistics					
	Before Standard therapy (22)	After Standard Therapy + Balm (11)	After Standard therapy (11)	Wilks' Λ	Par-tial Λ	F-remove (2,32)	p-level	Tolerancy	Norm Cv
F8-θ PSD, %	10,1 0,8	6,3 0,9	8,2 1,2	0,258	0,813	3,68	0,036	0,606	9,8 0,492
Fp2-θ PSD, %	10,7 1,1	7,6 1,7	8,2 1,3	0,249	0,842	2,99	0,064	0,612	9,9 0,620
T6 PSD Entropy	0,778 0,025	0,697 0,057	0,772 0,044	0,228	0,919	1,41	0,259	0,549	0,825 0,149
LF PSD, %	38,8 1,8	29,1 3,9	42,6 3,9	0,276	0,757	5,13	0,012	0,871	27,2 0,381
Heart Rate, beats/min-	65,9 2,2	60,8 2,7	79,9 2,2	0,280	0,747	5,42	0,009	0,572	68,5 0,118
B-Lympho-cytes, %	19,0 1,0	19,8 1,3	17,7 0,8	0,238	0,879	2,21	0,127	0,738	21,5 0,196
T-helper Lympho-cytes, %	25,6 1,5	28,4 1,5	29,1 2,0	0,260	0,804	3,90	0,030	0,656	33,2 0,196
Bilirubin, μM/L	9,66 0,89	10,12 0,68	8,81 0,89	0,269	0,779	4,53	0,018	0,544	11,7 0,355
Reticulo-cytes, ‰	5,09 0,35	5,82 0,64	4,48 0,37	0,2304262	0,9085783	1,60993	0,2156739	0,5838795	6,9 0,403
Physical Working Capacity, W/kg	2,28 0,16	2,56 0,17	1,47 0,11	0,2399976	0,8723431	2,341408	0,1124597	0,4348455	2,67 0,333

Table 7.13. Summary of stepwise analysis of discriminant variables ranked by criterion Λ

Variables currently in the model	F to enter	p-level	Λ	F-value	p-level
Heart Rate, beats/min-	12,7	10^{-4}	0,618	12,7	10^{-4}
LF PSD, %	4,77	0,014	0,499	8,32	10^{-5}
F8-θ PSD, %	4,54	0,017	0,404	7,44	10^{-5}
T-helper Lymphocytes, %	2,11	0,136	0,364	6,24	10^{-5}
Bilirubin, μM/L	1,96	0,155	0,329	5,50	10^{-4}
Fp2-θ PSD, %	2,24	0,121	0,293	5,09	10^{-5}
T6 PSD Entropy	1,29	0,288	0,273	4,58	10^{-5}
B-Lymphocytes, %	1,35	0,272	0,253	4,21	10^{-4}
Physical Working Capacity, W/kg	1,58	0,221	0,230	3,97	10^{-4}
Reticulocytes, ‰	1,61	0,216	0,209	3,79	10^{-4}

Other variables were left out of the discriminant model, apparently due to duplication/redundancy of separating information (Table 7.14).

Table 7.14. Variables currently not in the model

Variables	Groups (n) and Means±SE			Parameters of Wilks' Statistics					
	Before Standard therapy (22)	After Standard Therapy + Balm (11)	After Standard therapy (11)	Wilks' Λ	Partial Λ	F to enter	p-level	Tolerancy	Norm Cv
1	2	3	4	5	6	7	8	9	10
Frequency-β, Hz	20,9 0,9	17,5 1,0	19,8 1,4	0,207	0,990	0,16	0,855	0,775	17,9 0,244
T4 PSD Entropy	0,826 0,025	0,770 0,052	0,839 0,030	0,208	0,993	0,11	0,894	0,868	0,844 0,137
T5-θ PSD, %	8,3 0,7	5,8 0,7	6,6 0,9	0,207	0,989	0,17	0,843	0,477	9,7 0,471
O1-δ PSD, %	20,3 3,0	34,4 8,4	20,5 3,7	0,208	0,994	0,10	0,908	0,674	23,5 0,655

Table 7.14 (cont)

1	2	3	4	5	6	7	8	9	10
O2-δ PSD, %	15,0 2,3	27,9 8,6	18,4 3,1	0,207	0,989	0,17	0,843	0,133	22,8 0,720
ULF PSD, %	7,7 0,8	8,2 1,8	4,5 1,1	0,207	0,990	0,16	0,851	0,848	4,8 0,735
Blood Pressure Diastolic, mmHg	76,7 1,6	75,1 1,1	80,0 1,8	0,207	0,987	0,21	0,815	0,007	78,7 0,054
Glomerular Filt-ration, mL/min	95,6 4,0	103,5 6,6	83,8 3,9	0,209	0,996	0,06	0,939	0,502	127 0,200
Creatinine, µM/L	83,5 2,3	80,6 3,7	91,0 4,1	0,198	0,944	0,92	0,409	0,618	78,3 0,167
Urea, mM/L	5,60 0,29	4,95 0,44	6,57 0,46	0,207	0,989	0,17	0,843	0,501	5,57 0,281
Malon-dyaldehid, µM/L	74,8 5,6	78,2 7,0	67,5 7,5	0,201	0,958	0,68	0,514	0,564	77,5 0,339
Gamma-globulins, g/L	11,13 0,97	13,15 0,54	11,49 1,44	0,203	0,970	0,49	0,616	0,481	13,88 0,348

The identifying information contained in the 10 discriminant variables is condensed into two roots. The major root contains 69,7% of discriminatory opportunities ($r^*=0,796$; Wilks' $\Lambda=0,209$; $\chi^2_{(20)}=57$; $p<10^{-4}$), while minor root 30,3% ($r^*=0,655$; Wilks' $\Lambda=0,571$; $\chi^2_{(9)}=20$; $p=0,015$).

Table 7.15. Standardized and raw coefficients and constants for discriminant variables

Coefficients	**Standardized**		**Raw**	
1	2	3	4	5
Variables	Root 1	Root 2	Root 1	Root 2
Heart Rate, beats/min-	0,647	0,644	0,069	0,069
LF PSD, %	0,620	-0,285	0,057	-0,026
F8-θ PSD, %	0,038	-0,847	0,010	-0,229

Table 7.15 (cont)

1	2	3	4	5
T-helper Lymphocytes, %	-0,120	0,822	-0,019	0,129
Bilirubin, μM/L	-0,794	0,125	-0,227	0,036
Fp2-θ PSD, %	-0,380	-0,623	-0,083	-0,136
T6 PSD Entropy	0,369	0,379	2,563	2,636
B-Lymphocytes, %	-0,488	0,177	-0,115	0,042
Physical Working Capacity, W/kg	-0,584	0,426	-0,032	0,023
Reticulocytes, ‰	-0,199	0,554	-0,118	0,329
		Constants	0,378	-10,97
		Eigenvalues	1,728	0,751
		Cumulative Proportion	0,697	1

Calculating the values of discriminant roots for each patient by coefficients and constants given in Table 7.15 allows visualization of each patient in the information space of roots (Figs. 7.12-7.14).

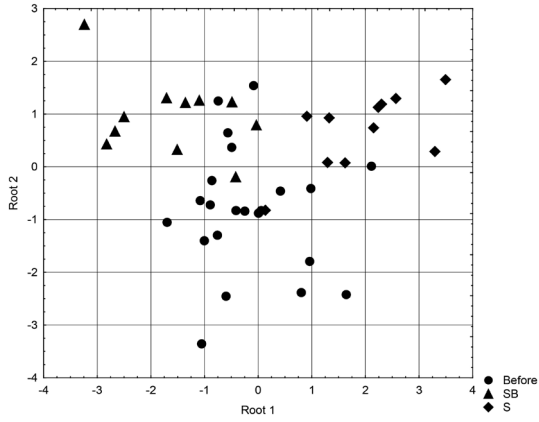

Fig. 7.12. Scattering of individual values of the first and second discriminant roots of patients before **(circles)** and after the course of standard balneotherapy **(rhombuses)** and in combination with Balm «Truskavets'» **(triangles)**

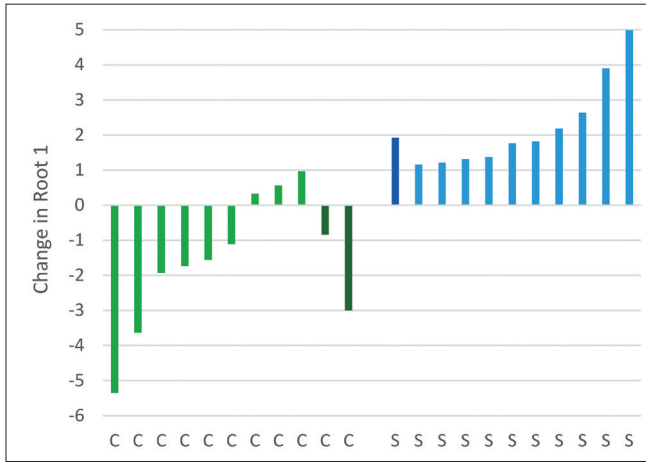

Fig. 7.13. Changes in individual values of the first discriminant root of patients after the course of **standard balneotherapy** and in **combination** with Balm «Truskavets'». Women are highlighted in shades of colors

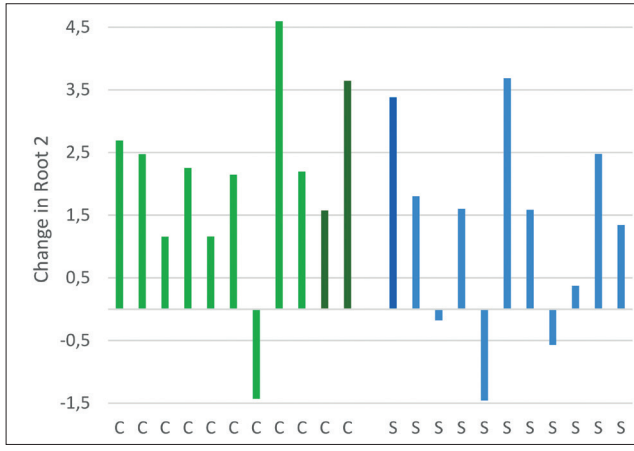

Fig. 7.14. Changes in individual values of the second discriminant root of patients after the course of **standard balneotherapy** and in **combination** with Balm «Truskavets'». Women are highlighted in shades of colors

The separation of patients who received two schemes of balneotherapy is more clearly manifested by the centroids of the discriminant roots (Fig. 7.15).

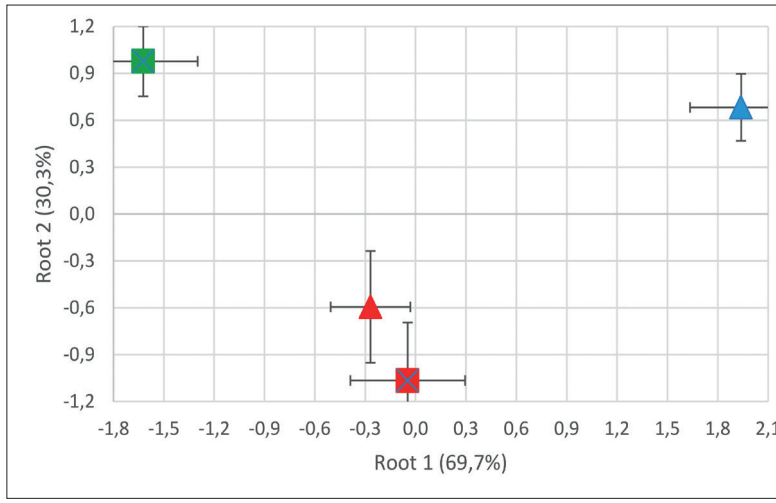

Fig. 7.15. Scattering of average values (M±SE) of the first and second discriminant roots of patients **before** and after the course of standard balneotherapy **(triangles)** and in combination with Balm «Truskavets'» **(squares)**

The shift along the axis of the first root of the centroid of the control group to the right relative to its initial localization reflects both an increase in the parameters that are positively correlated with the root, and a decrease in the parameters associated with it inversely. Instead, the opposite shift of the centroid of patients who received combined phytobalneotherapy reflects its opposite effects on these parameters (as well as on those not included in the model, but presented in Table 7.16 and Fig. 7.1).

An additional, but less tangible, delimitation of groups occurs along the axis of the second root. The top position of the main group of patients reflects, more deeply than in the control group, a decrease in EEG parameters inversely related to the root (as well as not included in the model, but included in the fifth cluster – Fig. 7.1).

In addition, it is worth noting three parameters of the sixth cluster (Fig. 7.1), which deviate in opposite directions relative to the initial levels, but are not visualized in the information field of the roots, since they were not included in the model.

Table 7.16. Correlations between variables and roots, centroids of clusters and Z-scores of clusters. Clusters are separated by spaces

Variables	Correlations Variables-Roots		After Standard ther +Balm (11	Before Standard therapy (22)	After Standard therapy (11)	Efect of Balm (11)	Effect of The-rapy (11)
Root 1 (69,7 %)	**Root 1**	**Root 2**	**-1,62**	**-0,16**	**+1,94**	**-3,56**	**+2,10**
Heart Rate	**0,587**	0,177	**-0,94±0,33**	**-0,30±0,28**	**+1,42±0,29**	**-2,36**	**+1,72**
LF PSDr	**0,330**	-0,222	**+0,16±0,36**	**+1,16±0,19**	**+1,59±0,41**	**-1,43**	**+0,43**
T6 PSD Entropy	**0,130**	-0,204	**-1,04±0,46**	**-0,39±0,20**	**-0,43±0,36**	**-0,61**	**+0,04**
T4 PSD Entropy			**-0,77±0,46**	**-0,28±0,22**	**-0,16±0,27**	**-0,61**	**+0,12**
BP Diastolic			**-0,84±0,28**	**-0,49±0,33**	**+0,27±0,38**	**-1,11**	**+0,76**
Creatinine			**+0,20±0,25**	**+0,39±0,17**	**+0,93±0,30**	**-0,73**	**+0,54**
Urea			**-0,57±0,40**	**+0,02±0,27**	**+0,93±0,42**	**-1,50**	**+0,91**
T-helper Lymph	**0,054**	0,285	**-0,74±0,22**	**-1,17±0,22**	**-0,64±0,31**	**-0,10**	**+0,53**
ULF PSDr			**+1,06±0,52**	**+0,95±0,25**	**+0,07±0,35**	**+0,99**	**-0,88**
PWC_{150}	**-0,301**	-0,006	**-0,12±0,19**	**-0,44±0,18**	**-1,35±0,13**	**+1,23**	**-0,91**
Glomerular Filtr			**-0,93±0,26**	**-1,24±0,16**	**-1,70±0,15**	**+0,77**	**-0,46**
Reticulocytes	**-0,217**	0,062	**-0,39±0,23**	**-0,65±0,13**	**-0,87±0,13**	**+0,48**	**-0,22**
B-Lymphocytes	**-0,143**	-0,115	**-0,40±0,30**	**-0,58±0,24**	**-0,91±0,19**	**+0,51**	**-0,43**
Bilirubin	**-0,106**	-0,014	**-0,38±0,16**	**-0,49±0,21**	**-0,70±0,21**	**+0,32**	**-0,21**
Malondyaldehid			**+0,03±0,26**	**-0,10±0,21**	**-0,38±0,29**	**+0,41**	**-0,28**
Root 2 (30,3 %)	**Root 1**	**Root 2**	+0,98	**-0,83**	+0,68	+0,30	+1,51
F8-θ PSDr	0,102	**-0,481**	-0,72±0,18	**+0,06±0,17**	-0,34±0,25	**-0,38**	**-0,40**
Fp2-θ PSDr	0,007	**-0,372**	-0,37±0,19	**+0,14±0,17**	-0,27±0,22	**-0,10**	**-0,41**
T5-θ PSDr			-0,68±0,18	**-0,06±0,16**	-0,49±0,21	**-0,19**	**-0,43**
Frequency-β			-0,11±0,23	**+0,68±0,21**	+0,43±0,31	**-0,54**	**-0,25**
O2-δ PSDr			+0,28±0,56	**-0,55±0,15**	-0,33±0,20	**+0,61**	**+0,22**
O1-δ PSDr			+0,70±**0,55**	**-0,21±0,20**	-0,20±**0,24**	**+0,90**	**+0,01**
Γ-globulins			-0,15±0,11	**-0,57±0,20**	-0,49±0,30	**+0,34**	**+0,08**

Although the distinction between the integrated states of patients at admission and after the two therapy schemes is not sufficiently clear, the differences are statistically significant, which is documented by the calculation of Mahalanobis distances (Table 7.17).

Table 7.17. Squares of Mahalanobis distances between groups (above the diagonal) and F-criteria (df=10,3) with p-levels (below the diagonal)

Groups	Before ST (22)	After ST + Balm (11)	After ST (11)
Before therapy	***	5,41	6,68
After Combined therapy	3,10; p=0,007	***	12,8
After Standard therapy	3,83; p=0,002	5,48; $p=10^{-4}$	***

Selected discriminant variables were used to identify the affiliation of a patient to a particular groups. This goal of discriminant analysis is realized with the help of classification functions (Table 7.18).

Table 7.18. Coefficients and constants of classification functions

Groups	Before Standard therapy	After Standard Therapy + Balm	After Standard therapy
Variables	p=,50	p=,25	p=,25
Heart Rate, beats/min-	2,208	2,231	2,457
LF PSD, %	0,200	0,069	0,279
F8-θ PSD, %	-1,716	-2,145	-2,040
T-helper Lymphocytes, %	1,873	2,134	2,029
Bilirubin, μM/L	3,204	3,602	2,781
Fp2-θ PSD, %	-1,292	-1,416	-1,670
T6 PSD Entropy	79,97	80,98	89,33
B-Lymphocytes, %	2,356	2,600	2,178
Physical Working Capacity, W/kg	1,492	1,580	1,460
Reticulocytes, ‰	10,82	11,58	11,07
Constant	-253,5	-276,0	-271,7

The classification accuracy is quite high (Table 7.19).

Table 7.19. Classification Matrix

Group	Rows: Observed classifications Columns: Predicted classifications			
	Percent Correct	Before therapy p=,50	After comb therapy p=,25	After stand therapy p=,25
Before	86,4	19	2	1
Comb therapy	81,8	2	9	0
Stand therapy	90,9	1	0	10
Total	86,4	22	11	11

CONCLUSION

Phytocomposition «Balm Truskavets'» by modulating the parameters of the nervous system limits the adverse effects of standard balneotherapy at the Truskavets' Spa in patients with post-radiation encephalopathy.

Chapter 8

SEXUAL DIMORPHISM IN THE NEURO-ENDOCRINE REGULATION OF BICYCLE ERGOMETRIC TEST PARAMETERS IN INDIVIDUALS WITH MALADAPTATION

Summary

Background. Ergometric physical working capacity (PWC) testing has a long tradition in occupational medicine. PWC can be tested, using performance indicators like VO_2max or the mechanical power. However, the calculated by bicycle ergometry PWC in reality reflects the reaction of the autonomic nervous system to muscle load, which, in turn, is strong, but still not absolutely complete, correlates with VO_2max as a real indicator of cardiorespiratory fitness. The purpose of this study is to clarify the relationship between PWC, calculated based on the result of two-stage bicycle ergometry, and the parameters of neuro-endocrine regulation as well as sexual differences in such relationships.

Materials and Methods. The object of observation were 30 women 29-76 (49,4±11,0) years and 30 men 24-69 (47,4±12,0) years without a clinical diagnosis, but with the deviations from the norm in a number of parameters of the neuro-endocrine-immune complex as a manifestation of maladaptation. For estimation of PWC a two-stage bicycle ergometry used. Parameters of EEG, HRV and adaptation hormones levels registered twice with an interval of 4 or 7 days.

Results. In men, PWC correlates negatively with serum levels of cortisol (r=-0,52) and triiodothyronine (r=-0,47), but positively with levels of calcitonin (r=0,25) and testosterone (r=0,22). The coefficient of multiple correlation R=0,705. In women, the correlation of the twice lower PWC with cortisol is weaker (r=-0,31), and is absent with testosterone, calcitonin and triiodothyronine, instead it was found in relation to aldosterone (r=-0,24); R=0,378. The PWC regression model for men includes 6 HRV and 11 EEG parameters (R=0,846), while for women only the mode HRV (r=-0,56) and two EEG parameters (R=0,608).

Conclusion. PWC levels in men are generally downregulated by cortisol, triiodothyronine, sympathetic tone, and θ-rhythm generating

neurons, but upregulated by testosterone, calcitonin, vagal tone, and related α-rhythm generating neurons. In women, PWC levels are borderline downregulated by cortisol and aldosterone, but significantly upregulated by circulating catecholamines and β-rhythm generating neurons.

INTRODUCTION

Ergometric physical working capacity (PWC) testing has a long tradition in occupational medicine for assessing whether a sufficiently high level of physical performance for coping with the daily work requirements is given [Sammito S et al., 2020; Steinhilber B et al., 2022]. PWC can be tested maximally or submaximally, using performance indicators like VO_2max [Bugajska J et al., 2011] or the mechanical power [Farazdaghi GR & Wohlfart B, 2001; Wohlfart B & Farazdaghi GR, 2003]. In the case of submaximal PWC testing measuring the mechanical power, the achieved power at a given heart rate serves as performance indicator. There are age- and sex-specific norm values [Stemper T, 1988] that can be used to judge whether differences or changes are within the normal range or can be considered significant. In addition, cardiorespiratory fitness is considered an attribute of health in general and non-specific resistance in particular [Amosov MV & Bendet YaA, 1989; Gozhenko AI, 2010; Fil V et al., 2021; Daniela M et al., 2022], and is also an important target of adaptogenic agents [Ruzhylo SV et al., 2003; Popovych IL et al., 2005; Panossian AG et al., 2021; Zukow W et al., 2020; Zukow W et al., 2021; Zukow W et al., 2022].

However, it has been known for a long time that although the calculated submaximal PWC is considered as an indicator of cardiorespiratory fitness [Finger JD et al., 2013], in reality it reflects the reaction of the autonomic nervous system to muscle load, which, in turn, is strong, but still not absolutely complete, correlates with VO_2max as a real indicator of cardiorespiratory fitness. By the way, the correlation is significantly affected by the use of adrenergic and/or cholinergic blockers, as well as autonomic dysfunction as a manifestation of maladaptation [Popovych IL, 2011; Popovych IL et al., 2014; Gozhenko **AI** et al., 2021].

The purpose of this study is to clarify the relationship between PWC, calculated based on the result of two-stage bicycle ergometry, and the parameters of neuro-endocrine regulation and sexual differences in such relationships.

MATERIAL AND RESEARCH METHODS

The object of observation was employees of the clinical sanatorium "Moldova" and PrJSC "Truskavets' Spa": 30 women 29-76 (49,4±11,0) years and 30 men 24-69 (47,4±12,0) years. The volunteers were considered practically healthy (without a clinical diagnosis), but the initial testing revealed deviations from the norm in a number of parameters of the neuro-endocrine-immune complex (details follow) as a manifestation of maladaptation, which actually prompted them to participate in the study with the hope of recovery.

In the morning in basal condition we recorded simultaneosly HRV and EEG as well as calculated for HRV and each locus EEG the Entropy (h) of normalized PSD.

At last in portion of venous blood determined serum levels of major hormones of adaptation: Cortisol, Testosterone, Aldosterone, Triiodothyronine and Calcitonin (by the ELISA with the use of analyzer "RT-2100C" and corresponding sets of reagents from "Алкор Био", XEMA Co, Ltd and DRG International Inc).

For estimation of PWC a bicycle ergometer "Tunturi" (Finland) is used. The power of the first load was 0,5 W/kg (HR±SD: 100±11 beats/min) at a pedaling frequency of 60-75 rpm. The power of the second load (after 3 min) was 1,5 W/kg (131±15 beats/min). This corresponded to the recommendations for ergometer testing in occupational medicine, particular for patients with maladaptation [Amosov MV & Bendet YaA, 1989; Trappe H-J & Löllgen H, 2000; Finger JD et al., 2013; Chatterjee M et al., 2017]. Calculated submaximal PWC_{150} with the mechanical power in Watt per kilogram body weight (W/kg) as indicator of cardiorespiratory fitness [Finger JD et al., 2013].

Testing was performed twice with an interval of 4 or 7 days.

Reference values of hormones and HRV are taken from the instructions for the kits and the device, respectively. Instead, EEG reference values due to their absence in the instructions are taken from the database of the Truskavetsian Scientific School of Balneology (n=112).

RESULTS AND DISCUSSION

Both cohorts were almost identical in terms of age and body mass index (Table 8.1). The latter slightly exceeded the norm (by 8% in men and by 11% in women). Aldosterone and triiodothyronine serum levels

were equally normal, and cortisol levels were equally reduced (by 19% in men and by 18% in women). The actual levels of calcitonin did not differ, however, taking into account the significant sexual dimorphism (males/females average ratio is 2,76), it was found to be reduced by 25% in men and increased by 76% in women. A similar excess of the average norm (by 62%) in the latter was also found for testosterone, while in men its level corresponded to the age norm.

Table 8.1. Comparative characteristics of antropometric parameters and levels of adaptation hormones in men and women

Variable	Men (n=59)	Women (n=59)	Reference (n=30)		t/p for sexes	t/p for M reference	t/p for F reference
Age, years	47,4 1,6	49,4 1,7					
Hight, cm	178,2 0,7	163,8 1,1					
Weight, kg	83,0 0,7	71,5 1,3					
Body mass index, kg/m^2	26,2 0,3	26,8 0,6	24,2 0,6		0,94 ns	2,99 <0,01	3,07 <0,01
Aldosterone, pM/L	226 4	222 3	238 8		-0,68 ns	-1,39 ns	-1,82 >0,05
Triiodothyronine, nM/L	2,02 0,12	2,16 0,12	2,20 0,09		0,86 ns	-1,22 ns	-0,27 ns
Cortisol, nM/L	299 16	303 14	370 20		0,20 ns	-2,77 <0,01	-2,73 <0,01
			M	F			
Calcitonin, ng/L	10,51 0,89	5,62 0,42	13,95 1,26	5,05 0,45	-5,06 10^{-6}	-2,24 <0,05	0,91 ns
Testosterone, nM/L	13,1 0,8	3,83 0,42	14,4 0,5	2,37 0,14	-10,6 $<10^{-4}$	-1,46 ns	3,29 <0,01

In men, the level of PWC is significantly negatively correlated with serum levels of cortisol (Fig. 8.1) and triiodothyronine (Fig. 8.2), on the other hand, at the limit of significance (for a sample of n=59, critical module r=0,26) positively with levels of calcitonin and testosterone (Table 8.2) in the complete absence of correlation with aldosterone (r=-0,03).

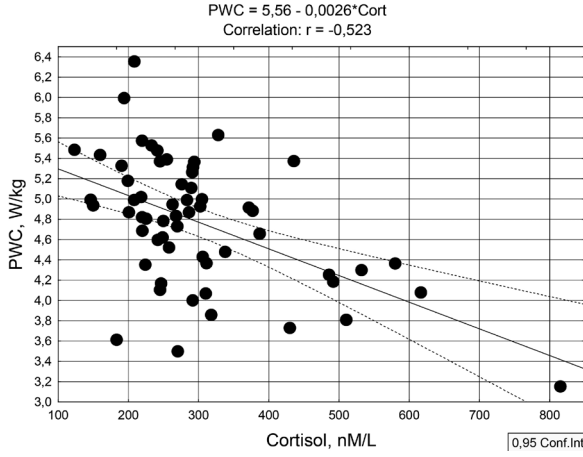

Fig. 8.1. Scatterplot of correlation between serum cortisol level (line X) and PWC (line Y) in men

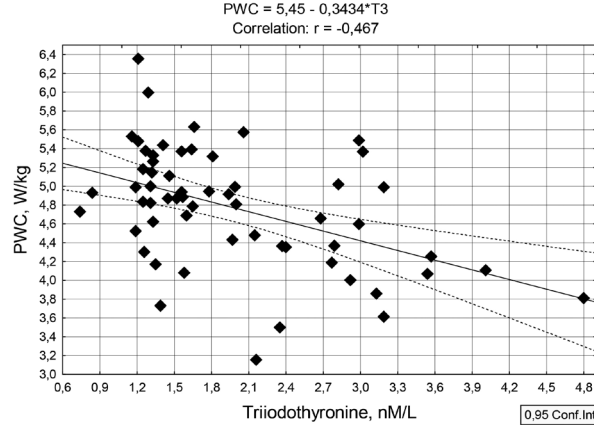

Fig. 8.2. Scatterplot of correlation between serum triiodothyronine level (line X) and PWC (line Y) in men

Judging by the coefficient of multiple correlation, this hormonal constellation determines the level of PWC by 49,7% (Table 8.2 and Fig. 8.2).

Table 8.2. Regression Summary for PWC_{150} (W/kg) in men
$R=0,705$; $R^2=0,497$; Adjusted $R^2=0,460$; $F_{(4,5)}=13,3$; $p<10^{-6}$; SD=0,46 W/kg

N=59		Beta	St. Err. of Beta	B	St. Err. of B	$t_{(54)}$	p-level
Variables	**r**		**Intercpt**	**5,446**	**0,275**	**19,8**	10^{-6}
Cortisol, nM/L	**-0,52**	-0,376	0,1037	-0,0019	0,0005	-3,63	0,001
Triiodothyronine, nM/L	**-0,47**	-0,432	0,0998	-0,3179	0,0735	-4,33	10^{-4}
Calcitonin, ng/L	**0,25**	0,160	0,1014	0,0147	0,0094	1,58	0,121
Testosterone, nM/L	**0,22**	0,262	0,0982	0,0282	0,0106	2,67	0,010

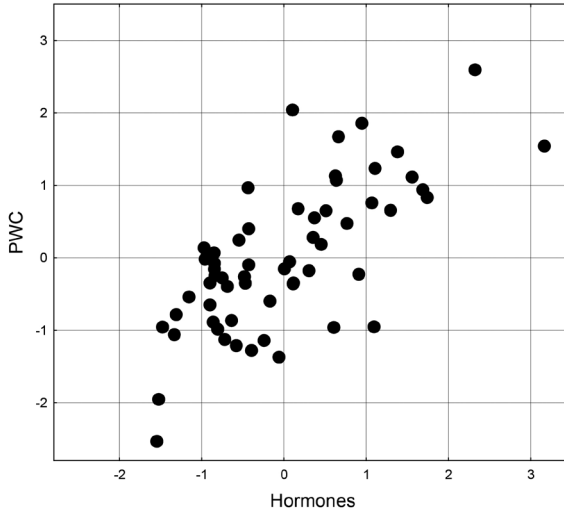

$R=0,705$; $R^2=0,497$; $\chi^2_{(4)}=38$; $p<10^{-6}$; Λ Prime=0,503
Fig. 8.2. Scatterplot of canonical correlation between hormonal variables (X-line) and PWC (Y-line) in men

As a result of the regression analysis with stepwise exclusion of variables until reaching the maximum value of Adjusted R^2, 6 HRV and 11 EEG parameters were included in the model (Table 8.3). The first 4 parameters of HRV are generally recognized markers of vagal tone, and Baevsky's stress index is a marker of sympathetic tone. The physiological interpretation of the VLF band remains a matter of debate, but in this situation it is a marker of sympathetic tone too.

Table 8.3. Regression Summary for PWC_{150} (W/kg) in men
$R=0,846$; $R^2=0,717$; Adjusted $R^2=0,599$; $F_{(17)}=6,1$; $p=10^{-6}$; SD=0,40 W/kg

N=59		Beta	St. Err. of Beta	B	St. Err. of B	$t_{(41)}$	p-level
Variables	**r**		**Intercpt**	**-1,952**	**2,098**	**-0,93**	**0,358**
Triangular index, units	**0,45**	0,976	0,304	0,1475	0,0459	3,21	0,003
MxDMn, msec	**0,41**	0,578	0,349	0,0043	0,0026	1,66	0,105
SDNN, msec	**0,38**	0,990	0,369	0,0287	0,0107	2,68	0,010
RMSSD, msec	**0,28**	-1,043	0,240	-0,0428	0,0098	-4,35	10^{-4}
P3-α PSD, %	**0,33**	-0,938	0,296	-0,0269	0,0085	-3,16	0,003
P3-α PSD, μV²/Hz	**0,32**	1,749	0,497	0,0027	0,0008	3,52	0,001
P4-α PSD, μV²/Hz	**0,32**	-1,375	0,610	-0,0022	0,0010	-2,25	0,030
T5-α PSD, %	**0,32**	-0,280	0,208	-0,0088	0,0066	-1,34	0,187
O2-α PSD, μV²/Hz	**0,31**	0,898	0,407	0,0011	0,0005	2,20	0,033
Amplitude α, μV	**0,31**	-1,118	0,595	-0,0610	0,0325	-1,88	0,067
O1-α PSD, %	**0,30**	0,305	0,264	0,0082	0,0071	1,16	0,253
T6-α PSD, %	**0,29**	1,024	0,223	0,0321	0,0070	4,59	10^{-4}
Laterality β, %	**0,29**	0,279	0,107	0,0043	0,0017	2,60	0,013
VLF PSD, %	**-0,41**	-0,156	0,109	-0,0055	0,0039	-1,43	0,161
O2-θ PSD, %	**-0,36**	-0,377	0,108	-0,0524	0,0150	-3,49	0,001
Stress index, ln units	**-0,32**	1,316	0,357	1,0556	0,2866	3,68	0,001
T3-θ PSD, μV²/Hz	**-0,31**	-0,179	0,117	-0,0058	0,0038	-1,53	0,135

Akselrod S et al. [1981] in pioneering experiment illustrated that after parasympathetic blockade the amplitude of the VLF peak is reduced; β-sympathetic blockade tends to reduce the VLF peak's amplitude, but this effect is not consistent because of the low tonic level of sympathetic activity in the resting dog. Increasing the activity of either the sympathetic or parasympathetic nervous system augments the area under the VLF peak. Therefore, both SNS and PSNS may mediate the VLF fluctuations. Selective blockade of renin-angiotensin system (by converting enzyme inhibitor) lead to 2-4.5-fold increase in the area under the VLF peak. Taylor JA et al. [1998] in young healthy subjects observed

that β-adrenergic blockade had no significant effect on VLF power. ACE blockade modestly (approximately 21%) increased VLF power in the supine (but not upright tilt) position; atropine, given alone or with atenolol, decreased VLF band by 92%. Authors concluded that although VLF band are influenced by the renin-angiotensin-aldosterone system, they depend primarily on the presence of parasympathetic outflow. Recently Del Valle-Mandragon L et al. [2022] showing that during hemodialysis angiotensin II had a **positive** correlation with VLF band (r=0.390) and with LF/HF (r=0.359) while a negative correlation with LF (r=-0.262) and HF (r=-0.383) bands. Therefore, the contradictions regarding the nature of VLF connections with vagal and sympathetic tone as well as the renin-angiotensin-aldosterone system remain unresolved. Besides it was shown that low VLF power has been correlated with low levels of testosterone, while cortisol has not [Theorell T et al., 2007; Hasson D et al., 2009]. In the cohort observed by us, the **relative** PSD of VLF band correlates negatively with markers of vagal tone (r=-0.44÷-0.54), but positively with the stress index (r=0.27) and AMo (r=0.31), as well as cortisol (r=0.44) in the complete absence of a connection with both aldosterone (r=-0.05) and testosterone (r=-0.03). So, in this specific situation, the **relative** PSD of VLF band acts as a marker of sympathetic tone and cortisol.

Among the EEG parameters included in the regression model, the activity of the α-rhythm generating neural structures, which project to the temporal, parietal and occipital both right and left loci of the scalp, are positively correlated with PWC.

Judging by the scheme of Winkelmann T et al. [45], on the P3/P4 loci is projected supramarginal gyrus, on the T5/T6 loci – transverse temporal cortex, and on the O1/O2 loci – lingual gyrus of left/right hemisphere, the **thickness** of which are positively correlated (r=0.43 for P3; 0.51 for T6 and 0.47 for O2 resrectively) with vagally mediated HRV (HF band and RMSSD). This is in excellent agreement with our data on vagal upregulation of PWC. At the same time, the activity of θ-rhythm-generating neurons of right lingual gyrus (O2) and leftt superior temporal gyrus (T3) makes down regulation of PWC. Taken together, neurogenic influences determine the level of PWC in men by 71.7% (Table 8.3 and Fig. 8.3).

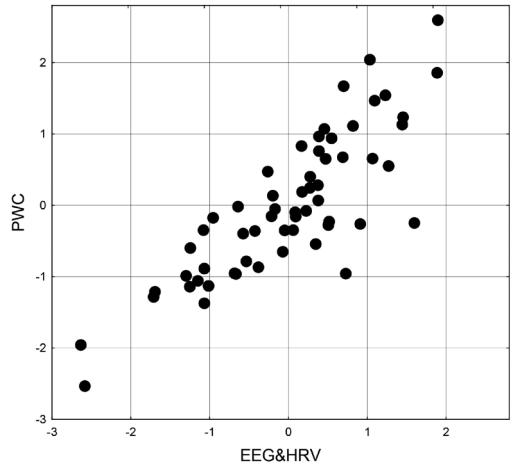

R=0,846; R^2=0,717; $\chi^2_{(16)}$=58; p=10^{-6}; Λ Prime=0,307

Fig. 8.3. Scatterplot of canonical correlation between EEG&HRV variables (X-line) and PWC (Y-line) in men

In women, the neuro-endocrine regulation of PWC differs from that in men both quantitatively and qualitatively. In particular, downregulation on the part of cortisol weaker, and on the part of triiodothyronine, calcitonin and testosterone they come to nothing (r=-0.13; 0.07 and -0.04 respectively), instead there is a weak downregulation on the part of aldosterone, absent in men. Accordingly, the measure of hormonal determination is very weak (14,3%), but statistically significant (Table 8.4 and Fig. 8.4).

Table 8.4. Regression Summary for PWC_{150} (W/kg) in women
R=0,378; R^2=0,143; Adjusted R^2=0,111; $F_{(2,6)}$=4,6; p=0,015; SD=0,17 W/kg

N=59		**Beta**	**St. Err. of Beta**	**B**	**St. Err. of B**	**$t_{(55)}$**	**p-level**
Variables	**r**		**Intercpt**	**2,692**	**0,216**	**12,5**	**10^{-6}**
Cortisol, nM/L	**-0,31**	-0,293	0,125	-0,0005	0,0002	-2,34	0,023
Aldosterone, pM/L	**-0,24**	-0,218	0,125	-0,0016	0,0009	-1,74	0,088

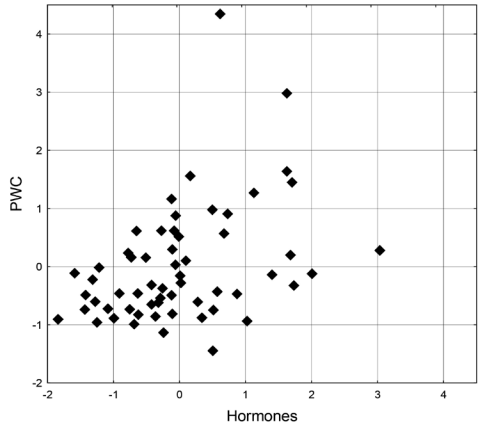

R=0,378; R^2=0,143; $\chi^2_{(3)}$=9,3; p=0,015; Λ Prime=0,845

Fig. 8.4. Scatterplot of canonical correlation between hormonal variables (X-line) and PWC (Y-line) in women

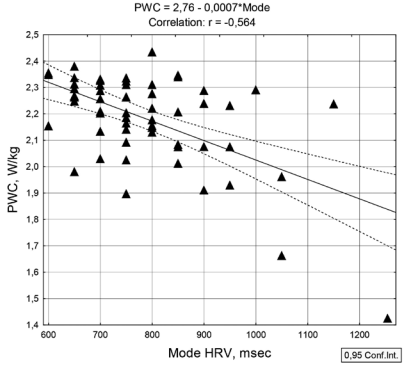

Fig. 8.5. Scatterplot of correlation between Mode HRV (line X) and PWC (line Y) in women

Among the HRV parameters, the connection with the Mode (Fig. 8.5), which is an inverse marker of the level of circulating catecholamines, turned out to be the most significant. A significant positive correlation was also found with the sympathetic tone marker LFnu (r=0.30) and P3-β PSD (0.27), but these parameters were formally outside the model. Instead, PSD entropy at the P3 locus and T5-β PSD were included in the model. As a result, the measure of neurogenic determination of PWC turned out to be very strong (37.0%), but significantly weaker than that in men.

Table 8.5. Regression Summary for PWC_{150} (W/kg) in women
R=0,608; R^2=0,370; Adjusted R^2=0,336; $F_{(3,6)}$=10,8; $p=10^{-5}$; SD=0,14 W/kg

N=59		Beta	St. Err. of Beta	B	St. Err. of B	$t_{(55)}$	p-level
Variables	**r**		**Intercpt**	**2,524**	**0,162**	**15,5**	10^{-6}
1/Mode HRV, msec^{-1}	**0,56**	-0,523	0,109	-0,0007	0,0001	-4,80	10^{-5}
P3 PSD Entropy	**0,24**	0,1825	0,108	0,2169	0,1286	1,69	0,097
T5-β PSD, μV2/Hz	**0,23**	0,136	0,109	0,0002	0,0002	1,26	0,214

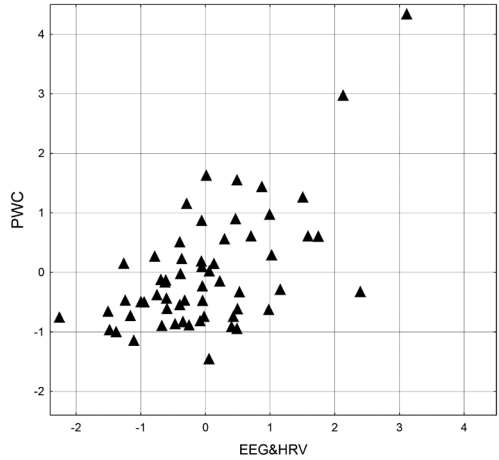

R=0,608; R^2=0,370; $\chi^2_{(3)}$=26; $p=10^{-5}$; Λ Prime=0,629
Fig. 8.6. Scatterplot of canonical correlation between EEG&HRV variables (X-line) and PWC (Y-line) in women

It is very interesting that in the already cited study of Winkelmann T et al. [2017] a negative correlation (r=-0.45) was found between the thickness of the isthmus cingulate cortex LH, which also projects to the P3 locus, and vagally mediated HRV. This suggests that the β-rhythm generating neurons of this area of the cortex, as well as of transverse temporal cortex RH (T6) are responsible for increasing the sympathetic tone and/or the level of circulating catecholamines through medullary sympathoexcitatory neurons [Verberne AJ, 1996; Verberne AJ et al., 1997] and other structures of the central autonomic network [Benarroch EE, 1993; Thayer JF & Lane RD, 2009; Vanneste S & De Ridder D, 2013; Palma JA & Benarroch EE, 2014; Popovych IL et al, 2013; Popovych IL et al, 2014; Sakaki M et al., 2016].

The described sexual dimorphism in the neuro-endocrine regulation of PWC is visualized in the form of profiles of correlation coefficients (Fig. 8.7).

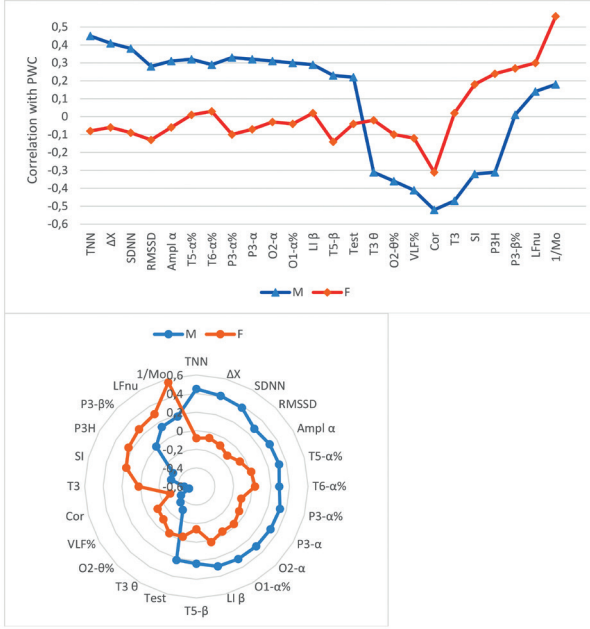

Fig. 8.7. Profiles of correlation coefficients between EEG&HRV parameters and PWC in men and women

The sexual dimorphism in the neuro-endocrine regulation of PWC is manifested against the background of the absence of significant differences in the HRV parameters involved, with the exception of a 9% higher sympathetic tone in men, which, in turn, exceeded the norm in both sexes in combination with a decrease in vagal tone and an increase the level of circulating catecholamines (Table 8.6).

Among the EEG parameters (Table 8.7), the PSD of the θ-rhythm in the T3 locus was found to be more than two times lower in men than in women, as well as a 32% lower PSD of the β-rhythm in the T5 locus, which, however, did not differ from the average norm, and in women exceeded it by 84% and 35%, respectively.

In addition, males had 16-20% lower than normal PSDs of the α-rhythm at all 4 loci, while females only at the P3 locus.

Table 8.6. Comparative characteristics of HRV parameters correlated with PWC

Variable	Males (n=59)	Females (n=59)	Reference (n=118)	t/p for sexes	t/p for M reference	t/p for F reference
Mode, msec	775 18	787 18	870 9	0,44 ns	-4,24 <0,001	-4,24 <0,001
MxDMn, msec	209 11	232 10	245 6	1,58 >0,05	-2,88 <0,01	-1,15 ns
Stress index, units	203 24	171 24	134 5	-0,97 ns	2,86 <0,01	1,53 >0,05
Stress index, ln units	5,01 0,10	4,83 0,10	4,89 0,09	-1,28 ns	0,85 ns	-0,49 ns
Triangular index, units	10,8 0,5	11,7 0,5	11,2 0,2	1,09 ns	-0,65 ns	0,80 ns
SDNN, msec	44,2 2,8	48,7 2,5	56,2 2,5	1,19 ns	-3,21 <0,01	-2,12 <0,05
RMSSD, msec	22,9 2,1	27,5 2,3	30,1 1,3	1,48 ns	-2,94 <0,01	-1,01 ns
LFnu PSD, %	81,7 1,4	74,8 1,7	64,4 1,5	-3,10 <0,01	8,44 $<10^{-4}$	-4,24 <0,001
VLF PSD, %	47,2 2,4	43,4 2,2	53,6 1,8	-1,18 ns	-2,19 <0,05	-4,24 <0,001

Table 8.7. Comparative characteristics of EEG parameters correlated with PWC

Variable	Males (n=59)	Females (n=59)	Reference (n=112)	t/p for sexes	t/p for M reference	t/p for F reference
1	2	3	4	5	6	7
T3-θ PSD, μV^2/Hz	26,4 2,5	55,4 7,9	30 3	3,51 <0,01	-0,92 ns	3,01 <0,01
T5-β PSD, μV^2/Hz	65 5	96 13	71 5	2,20 <0,05	-0,81 ns	1,80 >0,05
P3-α PSD, %	35,7 2,8	35,3 2,7	42,7 2,0	-0,09 ns	-2,03 <0,05	-2,18 <0,05
O1-α PSD, %	33,5 3,0	36,7 2,8	42,0 2,0	0,78 ns	-2,35 <0,05	-1,55 >0,05
T6-α PSD, %	28,6 2,6	31,8 2,4	35,5 1,7	0,92 ns	-2,25 <0,05	-1,24 ns
T5-α PSD, %	28,6 2,6	32,7 2,4	35,1 1,7	1,16 ns	-2,10 <0,05	-0,82 ns

Table 8.7 (cont)

1	2	3	4	5	6	7
P3-β PSD, %	20,4 1,5	20,1 1,4	22,7 1,1	-0,18 ns	-1,21 ns	-1,51 >0,05
Laterality β, %	-4 5	-6 4	-1 3	-0,35 ns	-0,53 ns	-1,11 ns
P3 PSD Entropy	0,79 0,02	0,80 0,02	0,80 0,01	0,10 ns	-0,29 ns	-0,17 ns
Amplitude α, μV	16,3 1,5	18,3 1,6	17,4 1,0	0,93 ns	-0,67 ns	0,47 ns
P3-α PSD, μV²/Hz	279 53	326 67	287 36	0,56 ns	-0,13 ns	0,51 ns
O2-α PSD, μV²/Hz	292 65	332 67	301 43	0,42 ns	-0,12 ns	0,38 ns
O2-θ PSD, %	7,4 0,6	8,0 0,6	7,1 0,4	0,71 ns	0,41 ns	1,26 ns

Identified deviations from the norm are, apparently, a manifestation of dysfunction of the neuro-endocrine-immune complex and maladaptation [Popovych IL, 2009; Popovych IL et al., 2014; Gozhenko **AI** et al., 2021].

CONCLUSION

PWC levels in men are generally downregulated by cortisol, triiodothyronine, sympathetic tone, and θ-rhythm generating neurons, but upregulated by testosterone, calcitonin, vagal tone, and related α-rhythm generating neurons. In women, PWC levels are borderline downregulated by cortisol and aldosterone, but significantly upregulated by circulating catecholamines and β-rhythm generating neurons.

Chapter 9

PREVENTION BY PHYTOADAPTOGENE OF UNFAVOURABLE ACTOTROPIC EFFECT OF BALNEOFACTORS OF TRUSKAVETS' SPA ON GASTROENTEROLOGIC PATIENTS AND ITS MECHANISMS

Summary

Background. The effect of standard balneotherapeutic complex of the Truskavets' Spa on the physical performance of both rats and resort patients is ambiguous. We have previously explored that phytoadaptogen "Balm Truskavets'" reverses the adverse effects of Naftussya bioactive water on dynamic muscle performance both in healthy rats and in patients with post-radiation encephalopathy. The purpose of this study is to test the ability of this phytocomposition prevention of unfavourable actotropic effect of balneofactors of Truskavets' Spa on gastroenterologic patients. **Material and methods.** The object of observation were 40 women (age 30÷76 years, body weight 55÷98 kg) with chronic cholecystitis in remission phase, who came for rehabilitation at Truskavets' Spa. Registered PWC_{150}, adaptation hormones levels, parameters of HRV, EEG, immunity, metabolism as well as gas discharge visualization (GDV). Members of the control group received for two weeks standard balneotherapy: drinking of Naftussya bioactive water, application of Ozokerite, baths with mineral water, therapeutic physical education. Members of the main group additionally received a phytoadaptogen.

Results. The analysis of individual changes revealed that normal levels of PWC in control group fell to the lower zone of the norm. Phytoadaptogen prevents PWC decrease. This is accompanied by the prevention of both a decrease in power spectral density (PSD) T4-θ EEG and VLF HRV, leukocytes level as well as area and symmetry of GDV, as well as an increase in vagal tone and entropy of HRV as well as a rightward shift in the symmetry of the virtual first Chakra of GDV. In addition, phytoadaptogen reverses balneotherapy-induced moderate decrease in the frequency of α-rhythm, PSD O1-β, sympathetic tone, serum levels of catecholamines, testosterone and IgG, activity of Na,K-ATPase of erythrocyte shadows as

well as Energy of the first, third and fourth virtual Chakras. Phytoadaptogen potentiates the reduction of PSD P4-β, IgM and cholesterol as well as initiates the reduction of δ-rhythm variability, PSD of α-rhythm in C3, C4, P4 and Fp2 loci, entropy in F4 locus as well as serum potassium while increasing in serum cortisol and calcitonin, blood B-lymphocytes levels as well as PSD Fp2-δ.

Conclusion. The phytoadaptogen «Balm Truskavets'» prevents the adverse effect of the standard balneotherapeutic complex of the Truskavets' Spa on PWC by, apparently, its neuro-endocrine effects.

Introduction

We have previously explored effects of phytocomposition "Balm Truskavets'", which is analogous to the "Balm Kryms'kyi", on parameters of neuro-endocrine-immune complex and biophotonics in humans with maladaptation. It was shown, that this phytoadaptogen reverses the adverse effects of Naftussya bioactive water on dynamic muscle performance both in healthy rats.

The purpose of this study is to test the ability of this phytocomposition prevention of unfavourable actotropic effect of balneofactors of the Truskavets' Spa on gastroenterologic patients.

Material and methods

At the preliminary stage, for 8 days, we examined 63 women with chronic cholecystitis in remission phase (age 29÷76 years, body weight 48÷105 kg), who came for rehabilitation at the Truskavets' Spa. For estimation of physical working capacity (PWC) a bicycle ergometer "Tunturi" (Finland) was used. The power of the first load was 0.5 W/kg, the second load (after 3 min) 1.5 W/kg at a pedaling frequency of 60-75 rpm. This corresponded to the recommendations for ergometer testing in occupational medicine (Trappe H-J & Löllgen H, 2000; Farazdaghi GR & Wohlfart B, 2001; Finger JD et al., 2013; Chatterjee M & Schmeißer G, 2017). We calculated submaximal PWC_{150} with the mechanical power in Watt per kilogram body weight (W/kg) as indicator of cardiorespiratory fitness (Finger JD et al., 2013).

The range of cardiorespiratory fitness was 1.30÷4.42 W/kg. The next study purposefully included women with fitness in the upper normal range

(2.04÷4.42 W/kg), of which 40 were found (age 30÷76 years, body weight 55÷98 kg).

The next day after bicycle ergometry, we recorded simultaneosly HRV and qEEG. Than we registered kirlianogram by the method of gas discharge visualization (GDV) by the device "GDV Chamber" ("Biotechprogress", SPb, RF). In portion of the venous blood the serum levels of major hormones of adaptation: Cortisol, Testosterone, Aldosterone, Triiodothyronine and Calcitonin was assayed with ELISA kits according to the SOP provided by the manufacturer ("Алкор Био", XEMA Co Ltd and DRG International Inc.) with the use of analyzer "RT-2100C".

Immune status evaluated as described in the manual [Lapovets' LYe & Lutsyk BD, 2004]. For phenotyping subpopulations of lymphocytes used the methods of rosette formation with sheep erythrocytes on which adsorbed monoclonal antibodies against receptors CD3, CD4, CD8, CD22 and CD56 (company "Granum", Kharkiv) with visualization under light microscope with immersion system.

Entropy of Immunocytogram (ICG) was calculated by formula:

$hICG = -[CD4 \bullet \log_2 CD4 + CD8 \bullet \log_2 CD8 + CD22 \bullet \log_2 CD22 + CD56 \bullet \log_2 CD56]/\log_2 4$.

The state of humoral immunity judged by the concentration in serum of Immunoglobulins of classes G, A, M (ELISA, analyser "Immunochem", USA) and circulating immune complexes (by polyethylene glycol precipitation method).

We estimated lipoprotein profile of serum: total cholesterol (by a direct method after the classic reaction by Zlatkis-Zack) and content of it in composition of HDL (by the enzyme method by Hiller); VLDL (calculated by the level of triglycerides, estimated by meta-periodate method, as ratio TG/2.1834); LDL (calculated by a difference between a total cholesterol and cholesterol in composition HD and VLD lipoproteins) according to instructions [Goryachkovskiy AM, 1998].

On sodium and potassium exchange judged by their levels in the serum and erythrocytes (flame photometry method) as well as activity of Na,K-ATPase of erythrocyte shadows, determined by the increase of Pi in the supernatant of the incubation medium [Makarenko YeV, 1987].

An analyzers "Reflotron" (BRD) and "Pointe-180" (USA) and corresponding sets of reagents as well as flame photometer "СФ-47" was used for biochemical studies.

According to the data of daily bicycle ergometry of eight patients, two groups were formed from them with approximately the same levels of PWC, body weight and age, followed by blind allocation into the control or main group.

Members of the control group received for two weeks standard balneotherapy: drinking of Naftussya bioactive water by 3 mL/kg for 1 hour before meals three times a day; application of Ozokerite on the lumbar region (temperature 45^0C, exposure 30 minutes, every other day, 5 procedures); baths with mineral water (Cl^--SO_4^{2-}-Na^+-Mg^{2+} containing salt concentration 25 g/L, temperature 36-37^0C, duration 8-10 minutes, every other day, 5 procedures); therapeutic physical education (motion mode II). Members of the main group additionally received a phytoadaptogen (5 mL pre-diluted in 200 mL of Naftussya water according to a similar scheme).

Phytoadaptogen Balm "Truskavets'" produced by private research-production enterprise "Ukrainian Balms" (Mykolaïv, Ukraine). Here are the components of the phytocomposition: *Nepeta cataria, Mentha* × ***piperita,*** *Salvia officinalis, Echinacea purpurea, Cichorium inthybus, Achillea millefolium, Artemisia balchanorum, Acorus calamus, Althaea officinalis, Silybum marianum, Rubus idaeus, Rosa majalis* (ТУ У 15.8-24055046-005:2009).

The next morning after completing the treatment, retesting was performed.

Statistical processing was performed using a software package "Microsoft Excell" and "Statistica 6.4 StatSoft Inc" (Tulsa, OK, USA).

Results

The starting positions of the members of the control and main groups turned out to be almost the same (Mean±SE): age 49.9±2.8 vs 47.3±2.6 years; body weight 71.6±3.1 vs 73.8±3.2 kg; PWC_{150} 2.45±0.13 vs 2.38±0.16 W/kg; cortisol 367±28 vs 322±20 nM/L; aldosterone 227±5 vs 221±6 pM/L; testosterone 3.17±0.50 vs 3.58±0.54 nM/L; triiodothyronine 2.05±0.22 vs 1.81±0.15 nM/L; calcitonin 5.33±0.69 vs 6.14±0.73 ng/L. A similar situation was established also with regard to the parameters of HRV, EEG, immunity and metabolism. This gave us the reason to combine members of both treatment groups into one.

As expected on the basis of previous studies, after standard balneotherapy, the PWC level dropped from the upper normal zone to its middle: from 2.45±0.10 to 2.02±0.08 W/kg. Additional use of phytoadaptogen minimized the adverse actotropic effect of standard balneotherapy to 2.24±0.10 W/kg.

Reference values are taken from the database of the Truskavetsian Scientific School of Balneology (EEG, GDV, immunity) or instructions (HRV, ELISA, metabolism).

Further, profiles (Fig. 9.1) of normalized parameters were created, the levels of which differ significantly before and after standard or combined therapy, as well as several parameters which according to the following discriminant analysis were still recognizable, despite the insignificant value of Student's t criterion.

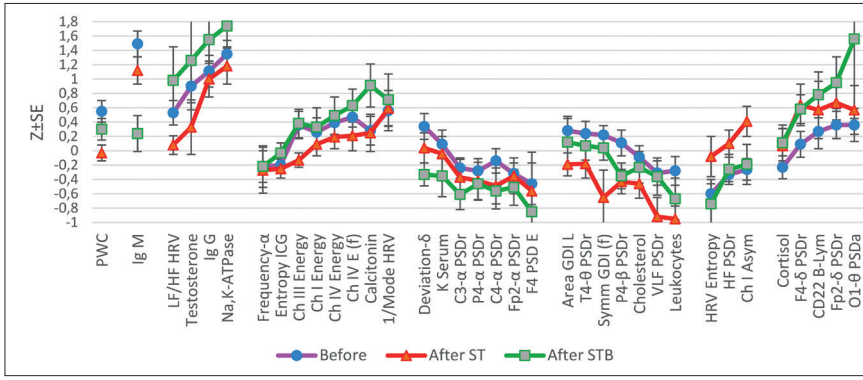

Fig. 9.1. Profiles of Z-scores of variables before and after standard therapy (ST) or supplemented with Balm

Next, the profiles were grouped into more or less homogeneous clusters (Fig. 2). It can be seen that, under the influence of standard balneotherapy, the increased levels of IgM, IgG and testosterone serum as well as Na,K-ATPase of erythrocyte shadows and LF/HF ratio as sympathetic tone decrease. Standard balneotherapy has practically no effect on the normal levels of the parameters of the two following clusters. On the other hand, the reduced entropy levels of HRV and PSD of HF band as vagal tone increase. That is, there is a **normalizing** (ambivalence-equilibratory) effect as one of the attributes of adaptogens (Balanovskyi VP et al., 1993; Kostyuk PG et al., 2006; Panossian AG et al., 2021) according to the good old "law of initial level".

At the same time, contrary to this law, the normal levels of cortisol, PSD of delta- and theta-rhythms in Fp2, F4 and O1 loci as well as B-lymphocytes also increase, and the normal levels of relative PSD of VLF band HRV, theta-rhythm in T4 locus and beta-rhythm in P4 locus, cholesterol, leukocytes as well as area and symmetry of GDI decrease. In addition, the left-sided asymmetry of the first Chakra is transformed into a right-sided one, which is evidenced by the transformation of a negative value into a positive one.

Supplementation of the balneotherapeutic complex with a phytoadaptogen potentiates both its inhibiting and enhancing effects on a number of parameters, instead it weakens or even reverses the effects on other constellations of parameters. A more detailed analysis will be conducted during the discussion.

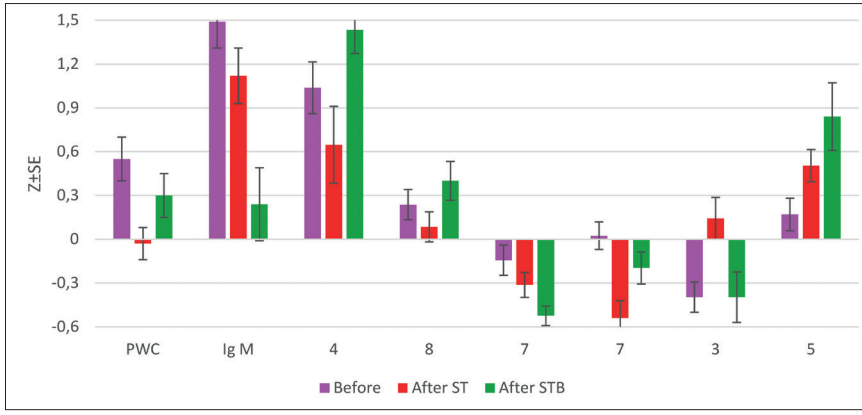

Fig. 2. Clusters of variables before and after standard therapy (ST) or combined with Balm (STB). *The number of variables is indicated under the clusters*

In order not only to find out which of the listed parameters are characteristic (recognizable) for the three groups, but primarily to visualize each patient in the information field, the constellation of these parameters was subjected to a discriminant analysis).

The forward stepwise program included, except PWC by definition, 30 variables in the discriminant model (Tables 9.1-9.2). Among them, 12 relate to **EEG**, 5 – **GDV**, 3 – **Hormones**, 3 – **Immunity**, 3 – **Metabolism** and 4 – **GDV**.

Table 9.1. Discriminant Function Analysis Summary

Step 31, N of vars in model: 31; Grouping: 3 grps; Wilks' Λ: 0,1593; approx. $F_{(63)}$=2,3; $p<10^{-4}$

Variables currently in the model	Groups (n) and Means±SE			Parameters of Wilks' Statistics					
	After Standard Therapy (20)	After Standard Therapy + Balm (20)	Before Therapy (40)	Wilks' Λ	Partial Λ	F-remove (2,47)	p-level	Tolerancy	Reference (Norm) (40) Cv; SD
1	2	3	4	5	6	7	8	9	10
Phys Working Capacity, W/kg	2,02 0,08	2,24 0,07	2,42 0,10	0,191	0,834	4,66	0,014	0,709	2,04 0,333
Frequency-α, Hz	10,36 0,30	10,42 0,27	10,41 0,21	0,178	0,894	2,78	0,072	0,450	10,62 0,088
Fp2-α PSD, %	27,8 3,6	25,3 3,7	28,3 2,2	0,194	0,822	5,09	0,010	0,058	32,9 0,448
C4-α PSD, %	27,4 3,8	26,4 3,7	32,6 2,5	0,179	0,891	2,88	0,066	0,046	34,8 0,432
C3-α PSD, %	29,3 4,2	25,2 3,6	31,5 2,3	0,174	0,916	2,16	0,127	0,071	35,4 0,468
P4-α PSD, %	36,8 4,9	35,9 4,5	39,5 3,2	0,167	0,957	1,06	0,353	0,047	44,8 0,428
Deviation-δ, Hz	0,68 0,06	0,58 0,04	0,76 0,05	0,179	0,890	2,91	0,064	0,408	0,67 0,395
Fp2-δ PSD, %	38,7 4,4	43,8 6,6	33,1 3,5	0,240	0,663	11,9	10^{-4}	0,164	26,5 0,687
F4-δ PSD, %	43,8 5,7	46,9 5,3	33,0 3,4	0,178	0,894	2,80	0,071	0,072	31,25 0,624
T4-θ PSD, %	8,9 0,9	10,0 0,9	10,8 0,8	0,198	0,806	5,66	0,006	0,332	9,7 0,482
O1-θ PSD, μV²/Hz	53 11	83 34	46 7	0,187	0,851	4,13	0,022	0,255	35 0,878
P4-β PSD, %	17,9 1,9	18,8 2,0	24,1 2,1	0,183	0,872	3,45	0,040	0,169	22,8 0,503
Entropy of PSD in F4 locus	0,799 0,050	0,772 0,041	0,809 0,027	0,179	0,889	2,94	0,062	0,114	0,851 0,139

Table 9.1 (cont)

1	2	3	4	5	6	7	8	9	10
VLF band PSD, %	41,7 3,4	48,7 3,0	49,3 2,4	0,178	0,896	2,71	0,077	0,144	53,2 0,288
HF band PSD, %	15,3 1,9	11,9 1,7	11,4 1,0	0,195	0,816	5,28	0,008	0,557	15,1 0,682
HF/LF HRV ratio	3,01 0,26	4,73 0,88	3,91 0,36	0,168	0,949	1,27	0,290	0,188	2,84 0,717
Entropy of PSD of HRV bands	0,797 0,022	0,740 0,020	0,757 0,016	0,179	0,889	2,93	0,063	0,116	0,807 0,109
Mode HRV, msec	815 26	797 36	815 28	0,169	0,940	1,50	0,234	0,607	871 0,115
Testosterone, nM/L	2,74 0,42	3,77 0,65	3,36 0,37	0,217	0,734	8,51	0,001	0,111	2,37 0,468
Cortisol, nM/L	378 27	383 28	345 17	0,170	0,939	1,52	0,229	0,232	370 0,303
Calcitonin, ng/L	5,66 0,64	7,31 0,75	5,74 0,49	0,179	0,891	2,88	0,066	0,529	5,05 0,490
Leukocytes, 10^9/L	5,05 0,18	5,33 0,29	5,72 0,20	0,167	0,955	1,10	0,342	0,372	6,00 0,167
CD22 B-Lymphocytes, %	22,0 1,4	22,8 1,1	20,9 0,8	0,175	0,913	2,25	0,116	0,136	20,0 0,175
Immunoglobulins M, g/L	1,46 0,05	1,22 0,07	1,56 0,05	0,168	0,946	1,34	0,273	0,404	1,15 0,239
Na,K-ATPase Erythr, M/L•h	1,02 0,05	1,14 0,06	1,06 0,04	0,169	0,944	1,38	0,260	0,802	0,76 0,288
Potassium Serum, mM/L	4,53 0,11	4,39 0,14	4,59 0,10	0,168	0,949	1,26	0,293	0,728	4,55 0,104
Cholesterol, mM/L	5,11 0,25	5,25 0,25	5,45 0,19	0,183	0,873	3,42	0,041	0,446	5,54 0,193
Symmetry of GDI (filter), %	92,29 0,53	93,25 0,24	93,50 0,19	0,185	0,861	3,80	0,029	0,542	93,20 0,015
Chakra I Asymmetry	0,01 0,05	-0,14 0,07	-0,16 0,04	0,177	0,902	2,55	0,089	0,485	-0,09 **0,25**
Chakra I Energy	0,13 0,06	0,22 0,10	0,20 0,07	0,167	0,954	1,14	0,329	0,132	0,10 **0,37**
Chakra III Energy	-0,13 0,04	0,08 0,09	0,07 0,08	0,178	0,896	2,71	0,077	0,161	-0,08 **0,42**

Table 9.2. Summary of stepwise analysis of discriminant variables ranked by criterion Λ

Variables currently in the model	F to enter	p-level	Λ	F-value	p-level
Immunoglobulins M, g/L	5,27	0,007	0,880	5,27	0,007
Physical Working Capacity, W/kg	3,83	0,026	0,799	4,51	0,002
Symmetry of GDI (filter), %	3,29	0,043	0,735	4,17	0,001
VLF band PSD, %	3,29	0,043	0,675	4,02	0,001
P4-β PSD, %	3,26	0,044	0,619	3,95	10^{-4}
Deviation-δ, Hz	2,20	0,119	0,584	3,71	10^{-4}
Na,K-ATPase Erythrocyte, M/L•h	1,79	0,174	0,556	3,46	10^{-4}
Fp2-δ PSD, %	1,70	0,190	0,530	3,27	10^{-4}
Testosterone, nM/L	2,40	0,098	0,495	3,23	10^{-4}
HF/LF HRV ratio	2,03	0,139	0,467	3,15	10^{-4}
Chakra I Asymmetry	1,91	0,157	0,442	3,07	10^{-4}
Cortisol, nM/L	1,73	0,185	0,420	2,98	10^{-4}
CD22 B-Lymphocytes, %	1,60	0,210	0,401	2,90	10^{-4}
Chakra III Energy	1,77	0,179	0,380	2,85	10^{-4}
O1-θ PSD, μV^2/Hz	1,60	0,210	0,361	2,79	10^{-4}
T4-θ PSD, %	2,10	0,131	0,338	2,79	10^{-4}
HF band PSD, %	1,95	0,151	0,318	2,77	10^{-4}
Frequency-α, Hz	1,35	0,266	0,304	2,71	10^{-4}
Fp2-α PSD, %	1,31	0,279	0,291	2,65	10^{-4}
Chakra I Energy	1,17	0,317	0,280	2,58	10^{-4}
F4-δ PSD, %	1,02	0,368	0,270	2,51	10^{-4}
Entropy of PSD in F4 locus	1,61	0,209	0,256	2,49	10^{-4}
Entropy of PSD of HRV bands	2,35	0,105	0,236	2,54	10^{-4}
Cholesterol, mM/L	1,19	0,311	0,226	2,49	10^{-4}
Mode HRV, msec	1,14	0,327	0,216	2,44	10^{-4}
C4-α PSD, %	1,69	0,195	0,203	2,44	10^{-4}
Calcitonin, ng/L	1,14	0,327	0,194	2,40	10^{-4}
C3-α PSD, %	1,57	0,219	0,183	2,39	10^{-4}
Potassium Serum, mM/L	1,22	0,303	0,174	2,36	10^{-4}
Leukocytes, 10^9/L	1,11	0,338	0,167	2,32	0,001
P4-α PSD, %	1,06	0,353	0,159	2,28	0,001

Other 5 variables, despite their recognizable properties, were outside the discriminant model, apparently due to duplication and/or redundancy of information (Table 9.3).

Table 9.3. Variables currently not in the model

Variables	Groups (n) and Means±SE			Parameters of Wilks' Statistics					
	After Standard Therapy (20)	After Standard Therapy + Balm (20)	Before Therapy (40)	Wilks' Λ	Partial Λ	F to enter	p-level	Tolerancy	Reference (Norm) (40) Cv; SD
Entropy of Immunocytogram	0,946 0,007	0,959 0,008	0,948 0,006	0,156	0,980	0,47	0,629	0,559	0,960 0,059
Immunoglobulins G, g/L	15,39 0,65	16,82 0,86	15,68 0,58	0,158	0,993	0,16	0,853	0,345	12,75 0,206
Area GDI Left, kPixels	23,97 0,54	25,01 0,50	25,55 0,65	0,157	0,984	0,38	0,683	0,105	24,47 0,150
Ch IV Energy	0,35 0,06	0,47 0,10	0,43 0,07	0,158	0,993	0,17	0,848	0,179	0,28 **0,38**
Ch IV Energy (filtered)	0,43 0,06	0,57 0,07	0,52 0,04	0,155	0,975	0,59	0,557	0,171	0,37 **0,31**

The identifying information contained in the 31 discriminant variables is condensed into two roots (Table 9.4). The first root contains 54,4% of discriminatory opportunities ($r^*=0,788$; Wilks' $\Lambda=0,159$; $\chi^2_{(62)}=114$; $p<10^{-4}$), and second root 45,6% ($r^*=0,761$; Wilks' $\Lambda=0,421$; $\chi^2_{(30)}=54$; $p=0,005$).

Calculating the values of discriminant roots for each patient by raw coefficients and constants given in Table 9.4 allows visualization of each patient in the information space of roots (Fig. 9.3).

Table 9.4. Standardized and raw coefficients and constants for discriminant variables

Coefficients	Standardized		Raw	
Variables	**Root 1**	**Root 2**	**Root 1**	**Root 2**
Immunoglobulins M, g/L	-0,269	0,390	-1,174	1,698
Physical Working Capacity, W/kg	0,562	0,254	1,053	0,476
Symmetry of GDI (filtered), %	0,590	0,264	0,505	0,226
VLF band PSD, %	0,409	-1,030	0,035	-0,087
P4-β PSD, %	1,103	-0,015	0,131	-0,002
Deviation-δ, Hz	0,419	0,527	2,090	2,630
Na,K-ATPase Erythrocyte, M/L•h	0,080	-0,336	0,365	-1,534
Fp2-δ PSD, %	0,447	-1,827	0,001	-0,004
Testosterone, nM/L	1,124	-1,672	42,81	-63,67
HF/LF HRV ratio	0,601	0,288	0,001	0,001
Chakra I Asymmetry	-0,402	0,418	-2,083	2,164
Cortisol, nM/L	0,370	-0,552	0,005	-0,008
CD22 B-Lymphocytes, %	-0,226	1,029	-0,056	0,253
Chakra III Energy	0,962	-0,347	2,976	-1,073
O1-θ PSD, μV^2/Hz	-0,804	0,562	-0,012	0,009
T4-θ PSD, %	0,969	0,031	0,280	0,009
HF band PSD, %	0,703	-0,199	0,057	-0,016
Frequency-α, Hz	0,400	-0,484	0,413	-0,499
Fp2-α PSD, %	1,247	-1,914	0,109	-0,168
Chakra I Energy	-0,687	0,311	-2,188	0,989
F4-δ PSD, %	0,556	-1,485	0,030	-0,080
Entropy of PSD in F4 locus	-0,497	-1,191	-3,535	-8,465
Entropy of PSD of HRV bands	-0,465	-1,191	-6,377	-16,35
Cholesterol, mM/L	0,659	0,159	0,566	0,137
Mode HRV, msec	0,339	0,218	0,002	0,001
C4-α PSD, %	1,926	0,303	0,158	0,025
Calcitonin, ng/L	0,479	-0,331	0,133	-0,092
C3-α PSD, %	-0,978	1,008	-0,081	0,083
Potassium Serum, mM/L	-0,226	0,257	-0,490	0,557
Leukocytes, 10^9/L	-0,281	0,350	-0,310	0,386
P4-α PSD, %	-1,064	-0,607	-0,069	-0,039
		Constants	-111,9	68,10
		Eigenvalues	1,641	1,377
		Cumulative Proportion	0,544	1

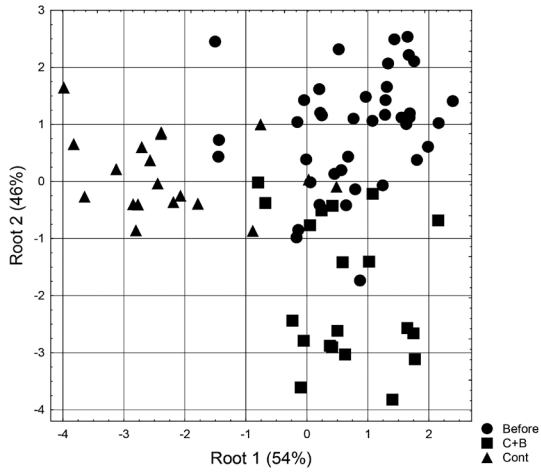

Fig. 9.3. Scattering of individual values of the first and second discriminant roots of patients before (**circles**) and after the course of standard balneotherapy (control, **triangles**) and in combination with Balm «Truskavets'» (**squares**)

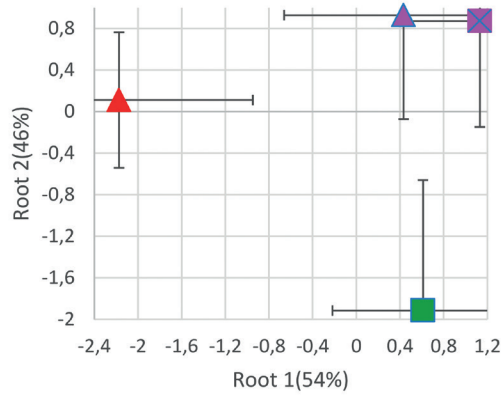

Fig. 9.4. Scattering of average values (M±SD) of the first and second discriminant roots of patients **before** and after the course of standard balneotherapy (**triangles**) and in combination with Balm «Truskavets'» (**squares**)

The shift along the axis of the first root of patients after standard balneotherapy to the left relative to their initial state reflects both a decrease in PWC and a constellation of other parameters positively related to the root (Table 9.5), as well as an increase in the inversely related entropy of

HRV and vagal tone as well as a transformation of the left-sided asymmetry of the virtual first Chakra to the right.

Additional use of phytoadaptogen, firstly, prevents or minimizes changes in PWC and another 15 related parameters, as evidenced by the shuffling of the projections of patients on the axis of the first root; secondly, it causes an increase in 12 parameters correlated with the second root inversely, and a decrease in 8 parameters correlated with it directly, as evidenced by the lower position of patients of the main group along the axis of the second root.

The demarcation of three clusters in the information field of two discriminant roots is visualized more clearly by their centroids (Fig. 9.4) and is documented by calculating Mahalanobis distances (Table 9.6).

Table 9.5. Correlations between variables and roots; centroids of clusters and Z-scores of variables

Variables	Correlations Variables-Roots		After Standard therapy (20)	After Standard Therapy + Balm (20)	Before Therapy (40)
1	2	3	4	5	6
Root 1 (54,4 %)	**Root 1**	**Root 2**	**-2,17**	0,61	0,78
PWC_{150}	**0,224**	0,101	**-0,03**	0,30	0,55
VLF PSDr	**0,206**	-0,027	**-0,92**	-0,36	-0,31
Symmetry GDI (filter)	**0,187**	0,032	**-0,65**	0,04	0,22
Ch III Energy	**0,123**	-0,015	**-0,13**	0,38	0,36
Leukocytes	**0,119**	0,080	**-0,95**	-0,67	-0,28
P4-β PSDr	**0,106**	0,122	**-0,43**	-0,35	0,11
T4-θ PSDr	**0,095**	0,042	**-0,18**	0,07	0,24
Cholesterol total	**0,083**	0,057	**-0,46**	-0,23	-0,09
Ch I Energy	**0,044**	-0,020	**0,09**	0,33	0,26
Frequency-α	**0,010**	-0,002	**-0,27**	-0,22	-0,22
Area GDI Left			**-0,19**	0,12	0,28
Ch IV Energy			**0,19**	0,49	0,39
Ch IV Energy (filter)			**0,21**	0,63	0,47
HRV Entropy	**-0,191**	0,085	**-0,08**	-0,74	-0,60

Table 9.5 (cont)

1	2	3	4	5	6
Ch I Asymmetry	**-0,163**	-0,008	**0,41**	-0,19	-0,26
HF PSDr	**-0,092**	0,073	**0,10**	-0,26	-0,33
Root 2 (45,6 %)	**Root 1**	**Root 2**	0,11	**-1,91**	0,90
Fp2-δ PSDr	0,044	**-0,256**	0,67	**0,95**	0,36
F4-δ PSDr	-0,047	**-0,178**	0,64	**0,58**	0,09
Na,K-ATPase Erythroc	0,106	**-0,128**	1,18	**1,74**	1,35
O1-θ PSDa	0,012	**-0,119**	0,57	**1,56**	0,36
Cortisol	-0,112	**-0,112**	0,07	**0,11**	-0,23
Calcitonin	0,011	**-0,100**	0,25	**0,91**	0,28
CD22 B-Lymphocytes	-0,026	**-0,092**	0,57	**0,78**	0,27
1/Mode HRV	-0,017	**-0,086**	0,59	**0,71**	0,56
Testosterone	0,039	**-0,084**	0,33	**1,26**	0,90
LF/HF HRV	0,011	**-0,057**	0,08	**0,98**	0,53
Entropy of ICG			-0,25	**-0,03**	-0,20
Immunoglobulines G			1,00	**1,55**	1,11
Immunoglobulines M	0,003	**0,315**	1,12	**0,24**	1,49
Deviation-δ	0,027	**0,184**	0,04	**-0,33**	0,34
Potassium Serum	-0,026	**0,110**	-0,04	**-0,35**	0,09
C3-α PSDr	0,006	**0,109**	-0,37	**-0,61**	-0,24
C4-α PSDr	0,055	**0,104**	-0,49	**-0,56**	-0,14
Fp2-α PSDr	-0,006	**0,054**	-0,35	**-0,51**	-0,32
F4 PSD Entropy	-0,001	**0,054**	-0,56	**-0,85**	-0,46
P4-α PSDr	0,021	**0,047**	-0,42	**-0,46**	-0,28

Table 9.6. Squared Mahalanobis distances between groups (above the diagonal) and F-criteria (df=31,5) with p-levels (below the diagonal)

Groups	**Before T (40)**	**After ST + Balm (20)**	**After ST (20)**
Before Therapy	***	5,56	7,80
After Combined therapy	2,09; p=0,011	***	9,18
After Standard therapy	2,46; p=0,003	2,33; p=0,004	***

Until now, the object of discriminant analysis was actual parameters of patients before and after therapy. Our previous experience suggests that a more sensitive approach to estimating effects is to calculate individual direct differences between postprandial and basal parameter levels. In addition, the calculation of direct differences between the effects on individual parameters of standard balneotherapy and supplemented with phytoadaptogen allows to simulate the essential (per se) effects of the latter. The results of this approach are visualized in Figs. 9.5 and 9.6.

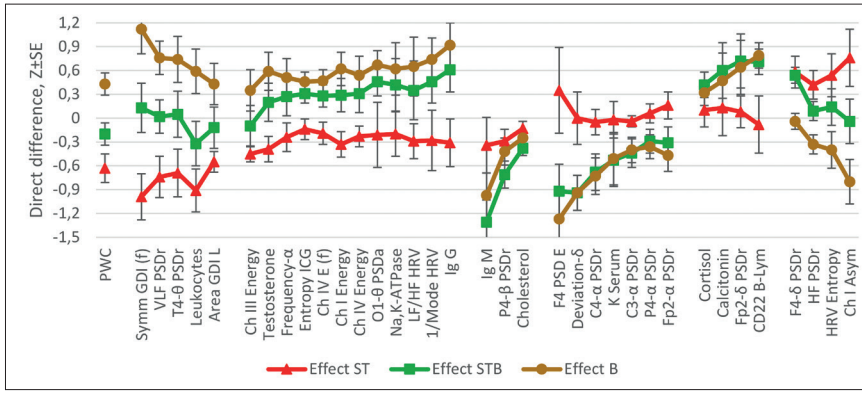

Fig. 9.5. Profiles of changes (direct differences) in PWC and accompanying parameters after standard (ST) and combined (STB) therapy as well as simulated essential effects of Balm (B**)**

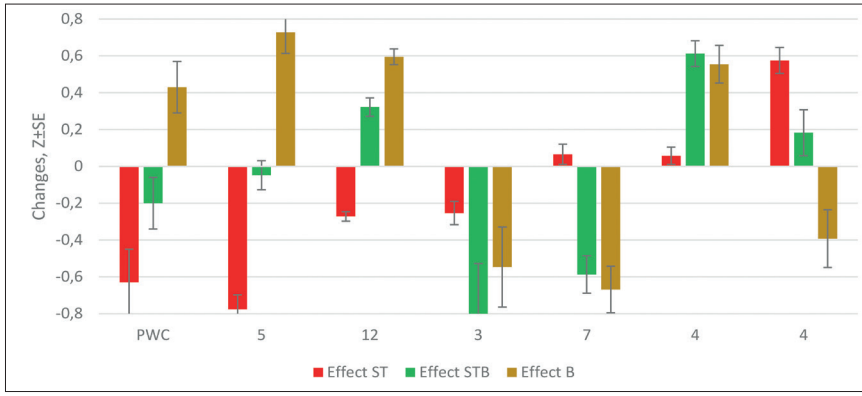

Fig. 9.6. Clusters of changes (direct differences) in PWC and accompanying parameters (number in parentheses) after standard (ST) and combined (STB) therapy as well as simulated essential effects of Balm (B)

Discussion

The decrease in the PWC_{150} level caused by standard balneotherapy reflects, in fact, an increase of 6.2±2.6 bpm in the HR response to a load of 1.5 W/kg, i.e., an increase in the autonomic reactivity of the heart. This is accompanied by a vagotonic shift in the sympatho-vagal balance (marker: LF/HF), an increase in vagal tone (marker: HF relative) and a decrease in the level of circulating catecholamines (marker: 1/Mode). In our situation, a decrease in **relative** PSD of VLF band is accompanied by a decrease in LF/HF (r=0.34) and testosterone level (r=0.26) in combination with an increase in relative PSD of HF (r=-0.60), i.e. it is a marker of sympathetic tone and testosterone.

Based on the nonoverlapping, bimodal distribution of circulating testosterone concentration with 95% references ranges of 7.7 to 29.4 nM/L in healthy men and 0 to 1.7 nM/L in healthy premenopausal women – making an allowance for women with the mild hyperandrogenism of polycystic ovary syndrome, who are overrepresented in elite athletics – the eligibility criterion for female athletic events should be a circulating testosterone concentration of <5.0 nM/L [Handelsman DJ et al., 2018]. Greater increases in serum testosterone, but not fat-free mass, resulted in larger effects on performance. Larger increases in testosterone were observed in young males, but performance only improved in diseased and older males [Varanoske AN et al., 2020].

In our women, the initial level of PWC in the upper normal range was also combined with a moderately increased level of testosterone, and balneotherapy reduced both parameters.

A vagotonic shift in the sympatho-vagal balance is accompanied by a decrease in the PSD of θ-rhythm in the T4 locus, which probably projects to the right amygdala [Romodanov AP, 1993]. The changes in PSD T4-θ are positively correlated with changes in the level of circulating catecholamines (r=0.48) and LF/HF (r=0.34), but negatively with changes in relative PSD HF (r=-0.32). This is consistent with the concept of the central autonomic network [Benarroch EE, 1993]. The amygdala is under tonic inhibitory control via prefrontal vagal pathways to intercalated cells in the amygdala. The activation of the central amygdala nucleus (CeA) inhibits the nucleus of the solitary tract which in turn inhibits inhibitory caudal ventrolateral medullary inputs to the rostral ventrolateral medullary (RVLM) sympathoexcitatory neurons, and simultaneously inhibits vagal

motor neurons in the nucleus ambiguus and the dorsal vagal motor nucleus. In addition, the CeA can directly activate the sympathoexcitatory neurons in the RVLM. The enhancing of prefrontal activity (projected on F3/F4 loci) leads to the vagotonic shift in sympatho-vagal balance [Palma JA & Benarroch EE, 2014; Sakaki M et al., 2016; Carnevali L et al., 2020].

It is interesting that the decrease in PSD T4-θ is positively correlated with the decrease in testosterone level (r=0.57), and changes in the latter are directly related to changes in LF/HF (r=0.23), the level of circulating catecholamines (r=0.26), and PSD O1-θ (r=0.40), but inversely with changes in PSD F4-δ (r=-0.30).

In our patients, after standard balneotherapy, a decrease in testosterone level, CeA activity and sympathetic tone and an increase in vagal tone and prefrontal activity were found.

In a previous study of our group [Kozyavkina NV et al., 2021] it was also shown that the level of testosterone in both women and men is inversely correlated with PSD F3-θ (r=-0.29) and relative HF (r=-0.22), instead directly – with LFnu (r=0.21). That is, testosterone acts as a sympathoexcitatory factor by inhibiting prefrontal activity, which leads to disinhibition of the CeA.

From the evolutionary perspective testosterone is a **precursor** of estradiol, dihydrotestoterone and other metabolites rather than a hormone *per se.* Testosterone does not only act per se, but also *via* the products of its metabolism. Reduction to dihydrotestosterone by 5-alpha reductase increases the androgen activity, conversion to estradiol by aromatase converts the androgen to estrogen activity [review: Celec P et al., 2015]. Estrogen receptors Eα and Eβ are widely expressed in the brain along with androgen receptors. Thus, circulating testosterone and estradiol levels are intrinsically related [review: Almeida M et al., 2017].

It is obvious that the revealed neurotropic effects of testosterone are realized through androgen receptors which are widely expressed in the brain [review: Gillies GE & McArthur, 2010].

The publications on the effect of testosterone on EEG are collected in excellent review [Riddle J et al., 2021]. Top-down signals from prefrontal cortex are theorized to converge with signals generated by reproductive steroid hormones in the medial temporal lobe. The amygdala, hippocampus, and bed nucleus of the stria terminalis within the medial temporal lobe include a large population of neurons with estrogen and androgen receptors.

The medial temporal lobe projects to and regulates the periventricular nucleus of the hypothalamus, which is responsible for initiating the stress response. Thus, reproductive steroid hormones are theorized to exercise their anxiolytic effects via the **medial temporal** lobe. Similarly, connectivity between the prefrontal cortex and the medial temporal lobe has been identified in emotion regulation and is decreased in anxiety and depression. Activation of the HPA-axis via a stressful task or administration of cortisol both increases frontal alpha asymmetry and inhibits the production of anxiolytic reproductive steroid hormones in the gonads. Riddle J et al. [2021] shown that low levels of testosterone or E2 related to greater pathological frontal activity, left greater than right. Multiple linear regression revealed that **low levels of testosterone** correlated with greater frontal alpha asymmetry in women. Source localization found that frontal asymmetry was driven by **decreased alpha power in right inferior frontal gyrus** that correlated with increased behavioral inhibition in women. From this we conclude that in this study the level of testosterone was positively associated with frontal activity. This is not consistent with our data or with the concept that androgens are associated with sympathetic hyperactivity in females. Even the postmenopausal ovary continues to produce androgens; serum testosterone or other androgen levels do not change significantly across menopause. In polycystic ovary syndrome patients, who often suffer from hyperandrogenism, sympathetic activity was enhanced whereas parasympathetic signaling was suppressed [review: So SY & Savidge TC, 2021].

Unfortunately, we did not have the opportunity to determine the level of estradiol in the observed women. However, there are reasons to assume that in this situation standard balneotherapy increased the level of estradiol.

So SY & Savidge TC [2021] in the excellent review note that sympathetic activity is often increased in the luteal phase of the menstrual cycle or during menopause when estrogen levels are reduced. Surgical-induced menopause reduced parasympathetic nervous system activity and shifted this towards sympathetic hyperactivity. Although some studies found no effect, others reported that estrogens in hormone replacement therapy facilitate parasympathetic activity and suppress sympathetic signaling in postmenopausal women. Estrogen may reduce sympathetic fiber density directly through affecting Eα receptor expressed in sympathetic neurons, or indirectly through affecting target tissue or specific molecules.

However, another study reported that estrogen is positively correlated to sympathetic activity in men. Nevertheless, estrogens are generally reported to inhibit sympathetic activity while sex could possibly influence the effect. However, several studies reported that androgens are positively correlated with parasympathetic activity in males. Also, a study found that males with low testosterone levels were unable to maintain cardiosympathetic and cardiovagal responses. These inconsistent findings suggest that autonomic control mediated by sex steroids could be sex-dependent, as well as modulated by health and hormonal status of the individual.

Hence, we conclude that the observed decrease in sympathetic tone combined with an increase in vagal tone may be caused not only by the documented decrease in testosterone level, but also by a hypothetical increase in estradiol level.

In our imagination, we get the impression that the decrease in the level of PWC caused by standard balneotherapy is accompanied, first of all, by a decrease in the activity of the right amygdala (PSD T4-θ as marker) and serum testosterone level as well as PSD O1-θ and frequency of alpha-rhythm while enhancing in prefrontal activity (PSD F4-δ as marker). We consider the vagotonic shift of the sympatho-vagal balance due to an increase in vagal tone (PSD HFr as marker) and a decrease in sympathetic tone (PSD VLFr as marker) as well as the level of circulating catecholamines (1/Mode HRV as marker) as second-order effects. The effects of the third order seem to us to be a decrease in the level of leukocytes and immunoglobulins G and M in the blood as well as serum cholesterol and activity of Na,K-ATPase of erythrocyte shadows.

Such ideas fit into classical concepts of the central autonomic network [Benarroch EE, 1993; Palma JA & Benarroch EE, 2014], neuro-endocrine-immune network [Besedovsky H & Sorkin E, 1977; Besedovsky H & del Rey A, 1996; Nance DM & Sanders VM, 2007; Tracey KJ, 2007; Thayer JF & Sternberg EM, 2010; Chavan SS et al., 2017; Pavlov VA et al., 2018; Korneva EA, 2020] and functional-metabolic continuum [Gozhenko AI, 2016]. By the way, all these concepts are cornerstones of Truskavetsian Scientific School of Balneology [Popovych IL, 2009; Popovych IL, 2011; Popovych IL et al., 2020; Popovych IL et al., 2022; Popovych IL et al., 2023].

The decrease in PWC and accompanying changes in other parameters provide grounds for comparing the condition of our patients with overtraining syndrome.

Armstrong LE et al. [2022] in review about overtraining syndrome noted that complex systems in nature are not aptly characterized or successfully analyzed using the classic scientific method (i.e., simplifying complex problems into single variables in a search for cause-and-effect) because they result from myriad (often non-linear) concomitant interactions of multiple determinants. Authors proposes evidence-based areas for future overtraining syndrome investigations, including concomitant multi-domain analyses incorporating brain neural networks, dysfunction of hypothalamic-pituitary-adrenal responses to training stress, the intestinal microbiota, immune factors, and low energy availability. As you can see, such recommendations are implemented in our study.

Overtraining syndrome is characterised by diminished sport-specific physical performance, accelerated fatiguability and subjective symptoms of stress. In addition to the determination of substrates and enzymes, the possibilities for monitoring of training by measuring hormonal levels in blood are currently being investigated. Endogenous hormones are essential for physiological reactions and adaptations during physical work and influence the recovery phase after exercise by modulating anabolic and catabolic processes. Testosterone and cortisol are playing a significant role in metabolism of protein as well as carbohydrate metabolism. Both are competitive agonists at the receptor level of muscular cells. The **testosterone/cortisol** ratio is used as an indication of the anabolic/catabolic balance. This ratio **decreases** during periods of intense training or repetitive competition, and can be **reversed** by regenerative measures. It seems more likely that the testosterone/cortisol ratio indicates the actual physiological strain in training, rather than overtraining syndrome. The sympatho-adrenergic system might be involved in the pathogenesis of overtraining. Overtraining appears as a disturbed autonomic regulation, which in its **parasympathicotonic** form shows a diminished maximal secretion of catecholamines [Urhausen A et al., 1995]. We will remind that in our patients vagotonic shift of sympatho-vagal balance and decrease in testosterone level, but without increase in cortisol level.

Uusitalo AL et al. [1998] examined different hormonal responses to heavy endurance training and overtraining in female athletes. Hormone responses to exercise load indicated decreased sympathoadrenal and/or adrenocortical activity (or exhaustion of the adrenal gland or the central

nervous system). Marked individual differences were found in training- and overtraining-induced hormonal changes.

The so-called informational (non-material) parameters require special attention. We assume that the decrease in the Entropy of the immunocytogram and the increase in the HRV Entropy will be accepted by readers at least tolerantly, similar to our previous publications regarding the physiological correlates of Entropy [Popadynets OO et al., 2020; Gozhenko AI et al., 2021; Popovych IL et al., 2022]. We also hope for an understanding regarding the reduction of GDI symmetry and its Area in the left projection. Although there is still skepticism about the GDV/PEI method, it has a biophysical basis [Korotkov KG et al., 2010; Muehsam et al., 2015; Korotkov KG, 2018; Korotkov KG, 2018a] and physiological correlates [Babelyuk VYe et al., 2017; Babelyuk VE et al., 2017; Babelyuk VY et al., 2021; Babelyuk VY et al., 2022; Bista S et al., 2022; Babelyuk VY et al., 2023]. Instead, the reduction of the Energy of the third, fourth and first *virtual* Chakras, as well as the rightward shift of the symmetry of the first Chakra, we predict, will be criticized by readers, but will be accepted by the adepts of the Eastern medicine paradigm.

According to Ayurvedic medicine, Chakras are power centers, related to the endocrine glands and neural plexus as well as to some organs. Chase CR [2018] provides a table according to which the **first** Chakra is associated with **adrenals**, pelvic nerve plexus, spine, kidneys, bladder, large intestine; **second** Chakra with testes/**ovaries**, inferior mesenteric ganglion, ileum, organs of reproduction; **third** Chakra with [endocrine] pancreas, celiac plexus ganglion, liver, gall bladder, stomach, duodenum, pancreas, **spleen**; **fourth** Chakra with **thymus**, celiac plexus, heart, circulation, **vagus nerve**; **fifth** Chakra with thyroid and parathyroid glands, inferior cervical ganglion, lungs, bronchus, larynx, pharynx, large intestine, **vagus nerve**; **sixth** Chakra with pituitary and pineal glands, thalamus, hypothalamus, superior cervical ganglion, left and lower **brain**, ears/nose, left eye; **seventh** Chakra with pineal gland, right and upper **brain**, right eye.

Korotkov KG [2007] believes that GDV method measures the distribution of electron densities in human systems and organs. These electron densities are the main basis of physiological energy, so there is reason to say that the GDV method allows us to measure the body's potential energy reserve. At the same time, the GDV method is a bridge between the logical science of the West and the intuitive science of the

East. It allows us to represent the same phenomena in different languages, in different systems, to look at the same things from different points of view. Author put forward the concept that each Chakra is associated with a part of the finger. This approach is embodied in the "GDV Chakras" program, which allows us to quantify the state of **virtual** Chakras.

A decrease in the Energy of the third Chakra associated with the thymus and the fourth Chakra associated with the spleen and vagus nerve, respectively, is consistent with a decrease in blood leukocytes and Igg G&M, but not with an increase in vagal tone. In this study, no changes in the Energy of the fifth to seventh Chakras, which are associated with the vagus nerve, pituitary gland and brain, were found, but such correlations were found in other studies [Babelyuk VY et al., 2021; Babelyuk VY et al., 2023]. A decrease in testosterone level is accompanied by a decrease in the Energy of the first Chakra, which is associated with the adrenals, but not the second Chakra, which is associated with the ovaries. However, it should be borne in mind that the reticular zone of the adrenal glands is a source of androgens. In women, 50% of testosterone is produced by the conversion of androgens in the periphery, while the ovaries and the adrenal glands contribute equally to the rest of the testosterone that circulates in the blood (25% each) [Kanakis GA et al., 2019; Witchel SF et al., 2020; Dumontet T & Martinez A, 2021].

Phytoadaptogen, mixed with Naftussya bioactive water, prevents the decrease of PWC. This is accompanied by the prevention of both a decrease in PSD T4-θ and VLFr, leukocytes level as well as area and symmetry of GDI, as well as an increase in vagus tone and entropy of HRV as well as a rightward shift of the symmetry of the first Chakra. In addition, phytoadaptogen reverses balneotherapy-induced moderate decrease in the frequency of α-rhythm, PSD O1-β, sympathetic tone, serum levels of catecholamines, testosterone and IgG, activity of Na,K-ATPase of erythrocyte shadows as well as Energy of the first, third and fourth virtual Chakras. Phytoadaptogen potentiates the reduction of PSD P4-β, IgM and cholesterol as well as initiates the reduction of δ-rhythm variability, PSD of α-rhythm in C3, C4, P4 and Fp2 loci, entropy in F4 locus as well as serum potassium while increasing in serum cortisol and calcitonin, blood B-lymphocytes levels as well as PSD Fp2-δ.

Screening for correlations between changes in PWC and the listed parameters revealed the following. PWC varied unidirectionally with

changes in PSD T4-θ (r=0.46), Fp2-δ (r=0.30), VLFr (r=0.32), 1/Mode (r=0.41), testosterone (r=0.41), B-lymphocytes (r=0.53) as well as Energy of first (r=0.39) and fourth (r=0.34) Chakras, however varied opposite of changes in deviation of δ-rhythm (r=-0.36), PSD Fp2-α (r=-0.37), HFr (r=-0.35), HRV entropy (r=-0.31), IgM (r=-0.31) as well as Asymmetry of first Chakra (r=-0.23).

Meta-analysis carried out by Riiser A et al. [2023] testified that glucocorticoids had a small positive effect on maximal physical performance compared to placebo and improved aerobic performance but not anaerobic performance. According to the authors, these results are consistent and should be of interest to WADA and anyone concerned about fair play. And will these authors and/or WADA be interested in Ukrainian phytoadaptogen?

Nordsborg N et al. [2008] investigated the effect of dexamethasone (2x2 mg per day or placebo for 5 days) on Na^+,K^+ pump subunit expression and muscle exchange of K^+ during exercise in nine healthy male. It was found, that catalytic alpha1 and alpha2 subunit expression was approximately 17% higher and the structural beta1 and beta2 subunit expression was approximately 6-8% higher after dexamethasone compared with placebo. During one-legged knee-extension for 10 min femoral venous K^+ and thigh K^+ release was lower in dexamethasone compared with placebo. In our women, phytoadaptogen also increased serum cortisol and activity of Na,K-ATPase and decreased serum potassium.

There is a well-founded opinion that the adaptogenic properties of classical phytoadaptogens are caused by polyphenolic compounds [Panossian AG et al., 2021]. The latter are also present both in the phytocomposition «Balm Kryms'kyi» [Alyeksyeyev OI et al., 1996] and Naftussya bioactive water [Dats'ko OR et al., 2008; Ivassivka SV et al., 1994; Ivassivka SV, 1997; Zukow W et al., 2022], which also have adaptogenic ability [Popovych IL, 2011; Popovych IL, 2022; Popovych IL et al., 2022]. It is interesting that Ozokerite, an integral component of the standard balneotherapeutic complex of the Truskavets' Spa, has a number of effects similar to those of Naftussya, both when taken orally and when applied to the skin [Popovych AI, 2018; Popovych AI, 2019; Ruzhylo SV et al., 2021], as well as in vitro [Ivassivka SV, 1997]. According to the hypothesis of the Truskavetsian Scientific School of Balneology, polyphenolic compounds of adaptogens of various nature are ligands of aryl hydrocarbon receptors (AhR) [Popovych IL, 2022], which are known

to be expressed by almost all types of cells of all organisms, starting from unicellular. Although the AhR was initially recognized as the receptor mediating the pathologic effects of dioxins and other pollutants, the activation of AhR by endogenous and environmental factors has important physiologic effects, including the regulation of the neural, endocrine and immune response [Esser C & Rannug, 2015; Murray IA & Perdew GH, 2020; Kou Z & Dai W, 2021; Rejano-Gordillo CM et al., 2022].

Taking into account literature data on the direct neurotropic effect of phytoadaptogens in vitro and in vivo [Panossian AG et al., 2021], previously data on changes in EEG&HRV parameters as well as relationships between EEG and HRV, EEG&HRV and adaptogene hormones, EEG&HRV and immunity parameters, the neurogenic mechanism of the revealed effects of balneotherapy factors and phytoadaptogens seems to be very real.

At the same time, there is a right to the hypothesis that the primary target of polyphenolic compounds are immunocytes, which through their cytokines affect neurons of the central and autonomic nervous and endocrine systems [reviews: Besedovsky H & del Rey A, 1996; Popovych IL, 2022; Popovych IL et al., 2022].

The presence of polyphenols in the composition of both the phytoadaptogen and the balneotherapy complex, it would seem, should enhance the effects of the latter when they are used simultaneously. However, contrary to expectations, the phytoadaptogen exerted effects opposite to those of the balneotherapeutic complex on PWC and 21 other parameters, and also affected 14 other parameters that did not respond to the balneotherapeutic complex (see please Figs 9.5 and 9.6). The reasons for this situation should be sought in differences in the composition of both factors. First, the term polyphenols covers hundreds of compounds with different properties, including both AhR agonists and blockers [Murray IA & Perdew GH, 2020]. Secondly, the composition of Naftussya bioactive water contains autochthonous microflora, which can significantly affect the neuro-endocrine-immune complex [Bilas VR & Popovych IL, 2009; Popovych IL et al., 2022].

Conclusion

The phytoadaptogen «Balm Truskavets'» prevents the adverse effect of the standard balneotherapeutic complex of the Truskavets' Spa on PWC by, apparently, its neuro-endocrine effects.

References

1. Aguwa CN. Effects of exogenous administration of female sex hormones on gastric secretion and ulcer formation in the rat. Eur J Pharmacol. 1984; 104(1-2): 79-84.
2. Ai HH, Zhou ZL, Sun LG, et al. 20 (S)-25-methoxyl-dammarane-3b, 12b, 20-triol negatively regulates activation of STAT3 and ERK pathways and exhibits anti-cancer effects in HepG2 cells. Apoptosis. 2017; 22: 1404-1418.
3. Akselrod S, Gordon D, Ubel FA, Shannon DC, Barger AC, Cohen RJ. Power spectrum analysis rate fluctuation: a quantitative probe of beat-to-beat cardiovascular control. Science (NY). 1981; 213(4504): 220-222.
4. Alexander S, Baranovskaya I, Tubalinal B, Cherezova A, Buncha V, Formin M, Mamenko M. A sexually dimorphic response to aldosterone antagonism in the kidney of spontaneously hypertensive rat. Physiology. 2023; 38(S1): 5734316.
5. Almeida M, Laurent M, Dubois V, Claessens F, O'Brien C, Bouillon R, Vanderschueren D, Manolagas S. Estrogens and Androgens in Skeletal Physiology and Pathophysiology. Physiological Reviews. 2017; 97(1): 135–187.
6. Alyeksyeyev OI, Popovych IL, Panasyuk YeM, Barylyak LG, Saranca SN, Shumakov MF. Adaptogens and Radiation [in Ukrainian]. Kyïv. Naukova dumka; 1996: 126.
7. Amsterdam JD, Panossian AG. *Rhodiola rosea* L. as a putative botanical antidepressant. Phytomedicine. 2016; 23: 770-783.
8. Andric SA, Kostic TS, Stojilkovic SS, Kovacevic RZ. Inhibition of rat testicular androgenesis by a polychlorinated biphenyl mixture aroclor 1248. Biol Reprod. 2000; 62(6): 1882-1888.
9. Armstrong L, Bergeron M, Lee E, Mershon J, Armstrong E. Overtraining Syndrome as a Complex Systems Phenomenon. Frontiers in Network Physiology. 2022; 1: 794392
10. Asea A, Kaur P, Panossian A, Wikman G. Evaluation of molecular chaperons Hsp72 and neuropeptide Y as characteristic markers of adaptogenic activity of plant extracts. Phytomedicine. 2013; 20: 1323-1329.
11. Asea A, Kaur P, Panossian A, Wikman KG. Evaluation of molecular chaperons Hsp72 and neuropeptide Y as characteristic markers of adaptogenic activity of plant extracts. Phytomedicine. 2013; 20(14): 1323-1329.
12. Ashton N, Balment RJ. Sexual dimorphism in renal function and hormonal status of New Zealand genetically hypertensive rats. European Journal of Endocrinology. 1991; 124(1): 91-97.
13. Aslanyan G, Amroyan E, Gabrielyan E, Nylander M, Wikman G, Panossian A. Double-blind, placebo-controlled, randomized study of single dose effects of ADAPT-232 on cognitive functions. Phytomedicine. 2010; 17: 494-499.
14. Avilla MN, Malecki KMC, Hahn ME, et al. The Ah Receptor: Adaptive Metabolism, Ligand Diversity, and the Xenokine Model. Chem Res Toxicol. 2020; 33(4) :860-879.
15. Ayati Z, Sarris J, Chang D, Emami SA, Rahimi R. Herbal medicines and phytochemicals for obsessive-compulsive disorder. Phytother Res. 2020; 2020(34): 1889-1901.

16. Babelyuk V, Dubkowa G, Korolyshyn T, Holubinka S, Dobrovolskyi Y, Zukow W, Popovych I. Operator of Kyokushin Karate via Kates increases synaptic efficacy in the rat Hippocampus, decreases C3-θ-rhythm SPD and HRV Vagal markers, increases virtual Chakras Energy in the healthy humans as well as luminosity of distilled water in vitro. Preliminary communication. Journal of Physical Education and Sport. 2017; 17(1): 383-393.
17. Babelyuk V, Gozhenko A, Dubkova G, Babelyuk N, Zukow W, Kovbasnyuk M, Popovych I. Causal relationships between the parameters of gas discharge visualization and principal neuroendocrine factors of adaptation. Journal of Physical Education and Sport. 2017; 17(2): 624-637.
18. Babelyuk V, Popovych I, Gozhenko A, Dubkova G, Kozyavkina O, Korolyshyn T, Babelyuk N, Kovbanyuk M, Fihura O, Dobrovolskyi Y, Zukow W, Yanchij R. Gas Discharge Vizualization (Electrophotonic Imaging, Kirlianography). Theoretical and Applied Aspects. Odesa. Feniks; 2023: 186.
19. Babelyuk V, Tserkovniuk R, Babelyuk N, Zukow X, Ruzhylo S, Dubkova G, Korolyshyn T, Hubytskyi V, Kikhtan V, Gozhenko A, Popovych I. The parameters of gas discharge visualization (biophotonics) correlated with parameters of acupuncture points, EEG, HRV and hormones. Journal of Education, Health and Sport. 2021; 11(12): 359–373.
20. Babelyuk V, Tserkovniuk R, Dubkova G, Kruhliy Y, Korolyshyn T, Babelyuk N, Zukow W, Ruzhylo S, Fihura O, Gozhenko A, Popovych I. Relationships between the neuro-endocrine parameters and virtual chakras energy and asymmetry. Journal of Education, Health and Sport. 2022; 12(1): 235-249.
21. Babelyuk VE, Gozhenko AI, Dubkova GI, Babelyuk NV, Zukow W, Kovbasnyuk MM, Popovych IL. Causal relationships between the parameters of gas discharge visualization and principal neuroendocrine factors of adaptation. Journal of Physical Education and Sport. 2017; 17(2): 624-637.
22. Babelyuk VY, GozhenkoAI, Dubkova GI, Babelyuk NV, Zukow W, Kindzer BM, Kovbasnyuk MM, Popovych IL. Causal relationships between the parameters of gas discharge visualization and phagocytosis. Journal of Education, Health and Sport. 2021; 11(6): 268-276.
23. Babelyuk VY, Tserkovniuk RG, Babelyuk NV, **Ź**ukow X, Ruzhylo SV, Dubkova GI, Korolyshyn TA, Hubyts'kyi VY, Kikhtan VV, Gozhenko AI, Popovych IL. The parameters of gas discharge visualization (biophotonics) correlated with parameters of acupuncture points, EEG, HRV and hormones. Journal of Education, Health and Sport. 2021; 11(12): 359-373.
24. Babelyuk VY, Tserkovniuk RG, Dubkova GI, Kruhliy YS, Korolyshyn TA, Babelyuk NV, Zukow W, Ruzhylo SV, Fihura OA, Gozhenko AI, Popovych IL. Relationships between the neuro-endocrine parameters and virtual chakras energy and asymmetry. Journal of Education, Health and Sport. 2022; 12(1): 235-249.
25. Babelyuk VY, Tserkovnyuk RG, Ruzhylo SV, Dubkova GI, Babelyuk NV, Zukow W, Popovych IL. Causal relationships between the parameters of gas discharge visualization and leukocytogram. Journal of Education, Health and Sport. 2021; 11(7): 258-269.

26. Babelyuk VYe, Gozhenko AI, Dubkova GI, Zukow W, Hubyts'kyi VY, Ruzhylo SV, Fedyayeva SI, Kovalchuk HY, Popovych IL. Causal relationships between the parameters of gas discharge visualization and immunity. Pedagogy and Psychology of Sport. 2021; 7(1): 115-134.
27. Babelyuk VYe, Popadynets' OO, Dubkova GI, Zukow W, Muszkieta R, Gozhenko OA, Popovych IL. Entropy of gas-discharge image correlates with the entropies of EEG, immunocytogram and leukocytogram but not HRV. Pedagogy and Psychology of Sport. 2020; 6(2): 30-39.
28. Baek JH, Heo JY, Fava M, et al. Effect of Korean Red Ginseng in individuals exposed to high stress levels: a 6-week, double-blind, randomized, placebo-controlled trial. J Ginseng Res. 2019; 43: 402-407.
29. Baevsky RM, Berseneva AP. Use KARDIVAR system for determination of the stress level and estimation of the body adaptability. Standards of measurements and physiological interpretation. Moscow-Prague; 2008: 41.
30. Balanovs'kyi VP, Popovych IL, Karpynets' SV. About ambivalence-equilibratory character of influence of curative water Naftussya on organism of human [in Ukrainian]. Dopovidi ANU. Mat pryr tekhn nauky. 1993; 3: 154-158.
31. Baraboy VA, Reznikov OH. Physiology, Biochemistry and Psychology of Stress [in Ukrainian]. Kyïv: Interservis; 2013: 314.
32. Benarroch EE. The central autonomic network: functional organization, dysfunction, and perspective. Mayo Clin Proc. 1993; 68(10): 988-1001.
33. Berezovskyi VYa. Personality traits in response to hypoxia [in Ukrainian]. Fiziol Zhurn. 1975; 21(3): 371-376.
34. Berntson GG, Bigger JT jr, Eckberg DL, Grossman P, Kaufman PG, Malik M, Nagaraja HN, Porges SW, Saul JP, Stone PH, Van der Molen MW. Heart Rate Variability: Origines, methods, and interpretive caveats. Psychophysiology. 1997; 34: 623-648.
35. Bertoglio JC, Baumgartner M, Palma R, et al. *Andrographis paniculata* decreases fatigue in patients with relapsing-remitting multiple sclerosis: a 12-month double-blind placebo-controlled pilot study. BMC Neurol. 2016; 16: 77.
36. Besedovsky H & del Rey A. Immune-neuro-endocrine interactions: facts and hypotheses. Endocrine reviews. 1996; 17(1): 64-102.
37. Besedovsky H & Sorkin E. Network of immune-neuroendocrine interaction. Clin Exp Immunol. 1977; 27(1): 1-12.
38. Bilas VR, Popadynets' OO, Flyunt ISS, et al. Entropies of thymocytogram, splenocytogram, immunocytogram and leukocytogram in rats are regulated by sex and the neuroendocrine parameters while regulates immune parameters. Journal of Education, Health and Sport. 2020; 10(7): 266-288.
39. Bilas VR, Popovych IL. Role of microflora and organic substances of water Naftussya in its modulating influence on neuroendocrine-immune complex and metabolism [in Ukrainian]. Medical Hydrology and Rehabilitation. 2009; 7(1): 68-102.
40. Bisson J, McAlpine JB, Friesen JB, Chen SN, Graham J, Pauli GF. Can invalid bioactives undermine natural product-based drug discovery? J Med Chem. 2016; 59: 1671-1690.

41. Bista S, Jasti N, Bhargav H, Sinha S, Gupta S, Ramarao P, Chaturvedi S, Gangadhar B. Applications of Gas Discharge Visualization Imaging in Health and Disease: A Systematic Review. Altern Ther Health Med. 2022; AT6764. PMID: 35648690.
42. Bjelobaba I, Janjic MM, Kucka M, Stojilkovic SS. Cell type-specific sexual dimorphism in rat pituitary gene expression during maturation. Biology of reproduction. 2015; 93(1): 1-9.
43. Bogatova RI, Shlykova LV, Salnitsky VP, Wikman G. Evaluation of the effect of a single dose of a phytoadaptogen on the working capacity of human subjects during prolonged isolation. Aerosp Environ Med. 1997; 31: 51-54.
44. Boon-Niermeijer EK, van den Berg A, Vorontsova ON, Bayda LA, Malyshev IY, Wiegant FAC. Enhancement of adaptive resistance against a variety of chronic stress conditions by plant adaptogens: protective effects on survival and embryonic development of *Lymnaea stagnalis*. Adapt Med. 2012; 4: 233-244.
45. Brekhman II, Dardymov IV. New substances of plant origin which increase nonspecific resistance. Annu Rev Pharmacol. 1969; 9: 419-430.
46. Brekhman II. Eleutherococcus. Leningrad: Nauka; 1968: 188.
47. Brekhman II. Ginseng. Leningrad: State Publishing House of Medical Literature MEDGIZ; 1957: 182.
48. Brown GC. Regulation of mitochondrial respiration by nitric oxide inhibition of cytochrome c oxidase. Biochim Biophys Acta. 2001; 1504: 46-57.
49. Buettner C, Yeh GY, Phillips RS, Mittleman MA, Kaptchuk TJ. Systematic review of the effects of ginseng on cardiovascular risk factors. Ann Pharmacother. 2006; 40: 83-95.
50. Bugajska J, Makowiec-Dabrowska T, Bortkiewicz A, Gadzicka E, Marszalek A, Lewandowski Z, Konarska M. Physical capacity of occupationally active population and capability to perform physical work. Int J Occup Saf Ergon. 2011; 17: 129–138.
51. Busbee PB, Rouse M, Nagarkatti M, Nagarkatti PS. Use of natural AhR ligands as potential therapeutic modalities against inflammatory disorders. Nutrition reviews. 2013; 71(6): 353–369.
52. Calabrese EJ, Bachmann KA, Bailer AJ, et al. Biological stress response terminology: Integrating the concepts of adaptive response and preconditioning stress within a hormetic dose-response framework. Toxicol Appl Pharmacol. 2007; 222: 122-128.
53. Calabrese V, Cornelius C, Dinkova-Kostova AT, Calabrese EJ, Mattson MP. Cellular stress responses, the hormesis paradigm, and vitagenes: novel targets for therapeutic intervention in neurodegenerative disorders. Antioxid Redox Signal. 2010; 13: 1763-1811.
54. Cannon WB. Stresses and strains of homeostasis. Am J Med Sci. 1935; 189: 1-14.
55. Carnevali L, Pattini E, Sgoifo A, Ottaviani C. Effects of prefrontal transcranial direct current stimulation on autonomic and neuroendocrine responses to psychosocial stress in healthy humans. Stress. 2020; 23(1): 26-36.
56. Castle C, Tietjens J. Perforated gastric ulcer as the initial manifestation of hyperparathyroidism. BMJ Case Rep. 2021; 14(4): e240570.
57. Cave AE, Chang DH, Münch GW, Steiner GZ. Efficacy of Cognition SupportFormula® on cognitive function in older adults with subjective cognitive impairment: a protocol

for a 26-week, randomised, double-blind, placebo-controlled trial. Trials. 2019; 20: 345.
58. Celec P, Ostatniková D, Hodosy J. On the effects of testosterone on brain behavioral functions. Frontiers in Neuroscience. 2015; 9(12).
59. Chase CR. The Geometry of Emotions: Using Chakra Acupuncture and 5-Phase Theory to Describe Personality Archetypes for Clinical Use. Med Acupunct. 2018; 30(4): 167-178.
60. Chatterjee M, Schmeißer G. Aktualisierter Leitfaden für die Ergometrie im Rahmen arbeitsmedizinischer Untersuchungen. Arb. Soz. Umweltmed. 2017; 52: 913–921.
61. Chavan SS, Pavlov VA, Tracey KJ. Mechanism and therapeutic relevance of neuro-imune communication. Immunity. 2017; 46(6): 927-942.
62. Chavan SS, Tracey KJ. Essencial neuroscience in immunology. J Immunol. 2017; 198: 3389-3397.
63. Chebanenko OI, Flyunt IS, Popovych IL, Balanovskyi VP, Lakhin PV. Water Naftussya and Water-salt Exchange [in Ukrainian]. Kyïv: Naukova dumka; 1997: 141.
64. Chen WC, Chang LH, Huang SS, et al. Aryl hydrocarbon receptor modulates stroke-induced astrogliosis and neurogenesis in the adult mouse brain. J Neuroinflamm. 2019; 16: 187.
65. Chen Y, Xu L, Xie HQH, et al. Identification of differentially expressed genes response to TCDD in rat brain after long-term low-dose exposure. J Environ Sci. 2017; 62: 92-99.
66. Chrousos GP, Gold PW. The concept of stress system disorders: overview of behavioral and physical homeostasis. JAMA. 1992; 267: 1244-1252.
67. Chrousos GP. Stressors, stress and neuroendocrine integration of the adaptive response. The 1997 Hans Selye memorial lecture. In: Stress of life: from molecules to man. Ed by P Csermely. Ann NYAS. 1998; 851: 311-335.
68. Chrousos GP. The stress response and immune function: Clinical implications: Novera H. Spector Lecture. In: Neuroimmunomodulation. Perspectives at the new millennium. Ed by A Conti et al. Ann NYAS. 2000; 917: 38-67.
69. Clavenna G, Musci R, Dorigotti L. Antiulcer and mineralocorticoid activities of carbenoxolone and desoxycorticosterone in rats. J Pharm Pharmacol. 1982; 34(8): 517-519.
70. Clementi G, Caruso A, Fiore CE, Leone MG, Prato A. Effect of parathyroid hormone, centrally or peripherally injected, on gastric activity in male rats. Eur J Pharmacol. 1989; 166(3): 549-552.
71. Clementi G, Prato A, Rapisarda E, Conforto G, Mangano O, Caruso A, Scapagnini U. Inhibition of restraint stress by systemic (Asu1,7) eel-calcitonin. J Endocrinol Invest. 1985; 8(6): 543-546.
72. Coon JT, Ernst E. Panax ginseng: a systematic review of adverse effects and drug interactions. Drug Saf. 2002; 25: 323-344.
73. Dai X, Yin C, Guo G, et al. Schisandrin B exhibits potent anticancer activity in triple negative breast cancer by inhibiting STAT3. Toxicol Appl Pharmacol. 2018; 358: 110-119.

74. Dajani EZ, Bianchi RG, Casler JJ, Weet JF. Gastric antiulcer and antisecretory effects of carbenoxolone, aldosterone and desoxycorticosterone in rats. Arch Int Pharmacodyn Ther. 1979; 242(1): 128-138.
75. Daniela M, Catalina L, Ilie O, Paula M, Daniel-Andrei I, Ioana B. Effects of Exercise Training on the Autonomic Nervous System with a Focus on Anti-Inflammatory and Antioxidants Effects. Antioxidants (Basel, Switzerland). 2022; 11(2): 350.
76. Darbinyan V, Aslanyan G, Amroyan E, Gabrielyan E, Malmström C, Panossian A. Clinical trial of *Rhodiola rosea* L. extract SHR-5 in the treatment of mild to moderate depression. Nord J Psychiatry. 2007; 61: 343-348. Erratum in: *Nord J Psychiatry*. 61, 503.
77. Darbinyan V, Kteyan A, Panossian A, Gabrielian E, Wikman G, Wagner H. *Rhodiola rosea* in stress induced fatigue – a double blind cross-over study of a standardized extract SHR-5 with a repeated low-dose regimen on the mental performance of healthy physicians during night duty. Phytomedicine. 2000; 7: 365-371.
78. Dats'ko, OR, Bubnyak, AB, Ivassivka SV. The organic part in mineral water Naftussya. Development of knowledges about its composition and origination [in Ukrainian]. Medical Hydrology and Rehabilitation. 2008; 6(1): 168-174.
79. Davies KJ. Adaptive homeostasis. Mol Aspects Med. 2016; 49 :1-7.
80. Del Valle-Mondragón L, Becerra-Luna B, Cartas-Rosado R, Infante O, Pérez-Grovas H, Lima-Zapata LI, Lerma C, Rodríguez-Chagolla J, Martínez-Memije R. Correlation between Angiotensin Serum Levels and Very-Low-Frequency Spectral Power of Heart Rate Variability during Hemodialysis. Life. 2022; 12(7): 1020.
81. Denison MS, Pandini A, Nagy SR, et al. Ligand binding and activation of the Ah receptor. Chem Biol Interact. 2002; 141(1-2): 3-24.
82. Denison MS, Soshilov AA, He G, et al. Exactly the same but different: promiscuity and diversity in the molecular mechanisms of action of the aryl hydrocarbon (dioxin) receptor. Toxicol Sci. 2011; 124: 1–22.
83. Desiderato O, Testa M. Shock-stress, gastric secretion and habituation in the chronic gastric fistula rat. Physiol Behav. 1976; 16(1): 67-73.
84. Deyama T, Nishibe S, Nakazawa Y. Constituents and pharmacological effects of Eucommia and Siberian ginseng. Acta Pharmacol Sin. 2001; 22: 1057-1070.
85. Dhabhar FS, McEwen BS. Acute stress enhances while chronic stress suppresses immune function in vivo: a potential role for leukocyte trafficking. Brain Behav Immun. 1997; 11: 286–306.
86. Dhabhar FS. Enhancing versus suppressive effects of stress on immune function: implications for immunoprotection and immunopathology. NeuroImmunoModulation. 2009; 16: 300–317.
87. Dhabhar FS. The short-term stress response – mother nature's mechanism for enhancing protection and performance under conditions of threat, challenge, and opportunity. Front Neuroendocrinol. 2018; 49: 175–192.
88. Dhabhar FS. The short-term stress response – mother nature's mechanism for enhancing protection and performance under conditions of threat, challenge, and opportunity. Front Neuroendocrinol. 2018; 49: 175-192.
89. Dumontet T, Martinez A. Adrenal androgens, adrenarche, and zona reticularis: A human affair? Molecular and Cellular Endocrinology. 2021; 528: 111239.

90. Durg S, Bavage S, Shivaram SB. *Withania somnifera* (Indian ginseng) in diabetes mellitus: a systematic review and meta-analysis of scientific evidence from experimental research to clinical application. Phytother Res. 2020; 34: 1041-1059.
91. Eckers A, Jakob S, Heiss C, et al. The aryl hydrocarbon receptor promotes aging phenotypes across species. Sci Rep. 2016; 6: 19618.
92. Elsenbruch S, Enck P. The stress concept in gastroenterology: from Selye to today. F1000Res. 2017; 6: 2149.
93. EMEA/HMPC/102655/2007. Reflection paper on the adaptogenic concept. London; 2008.
94. Esmaealzadeh N, Iranpanah A, Sarris J, Rahimi R. A literature review of the studies concerning selected plant-derived adaptogens and their general function in body with a focus on animal studies. Phytomedicine. 2022; 105: 154354.
95. Esplugues J, Lloris JM, Martí-Bonmatí E, Morcillo EJ. Effects of beta-adrenoceptor drug stimulation on various models of gastric ulcer in rats. Br J Pharmacol. 1982; 76(4): 587-94.
96. Esser C, Rannug A. The aryl hydrocarbon receptor in barrier organ physiology, immunology, and toxicology. Pharmacol Rev. 2015; 67(2): 259-279.
97. Evangelista S, Renzi D. A protective role for calcitonin gene-related peptide in water-immersion stress-induced gastric ulcers in rats. Pharmacol Res. 1997; 35(4): 347-350.
98. Evangelista S. Role of calcitonin gene-related Peptide in gastric mucosal defence and healing. Curr Pharm Des. 2009; 15(30): 3571-3576.
99. Facchinetti F, Neri I, Tarbusi M. *Eleutherococcus senticocus* reduces cardiovascular stress response in healthy subjects: randomized, placebo-controlled trial. Stress Health. 2002; 18: 11-17.
100. Fan F, Li L, Liu W, Yang M, Ma X, Sun H. Astrocytes and neurons in locus coeruleus mediate restraint water immersion stress-induced gastric mucosal damage through the ERK1/2 signaling pathway. Neurosci Lett. 2018; 675: 95-102.
101. Fan F, Yang M, Geng X, Ma X, Sun H. Effects of Restraint Water-Immersion Stress-Induced Gastric Mucosal Damage on Astrocytes and Neurons in the Nucleus Raphe Magnus of Rats via the ERK1/2 Signaling Pathway. Neurochem Res. 2019; 44(8):1841-1850.
102. Farazdaghi GR, Wohlfart B. Reference values for the physical work capacity on a bicycle ergometer for women between 20 and 80 years of age. Clin. Physiol. 2001; 21: 682–687.
103. Farnsworth NR, Waller D, Strelkova LM. Use of *Eleutherococcus senticosus* in United States: problems, prospects and literature update. *Proceedings of the Second International Symposium on Eleutherococcus* Vladivostok: Far Eastern Scientific Center, USSR Academy of Sciences; 1986: 47-51.
104. Fihura O, Melnyk O, Ruzhylo S, Zakalyak N, Kondratska H, Zukow W, Popovych I. Relationships between neuro-endocrine, electrocardiogram, and gastric mucosal damage parameters in naïve and stressed rats. Journal of Education, Health and Sport. 2023; 18(1): 162-190.
105. Fihura O, Ruzhylo S, Korda M, Klishch I, Żukow X, Popovych I. The influence of the Ukrainian phytocomposition «Balm Truskavets'» on parameters of neuro-

endocrine-immune complex and biophotonics in humans with maladaptation. Journal of Education, Health and Sport. 2023; 13(1): 326–337.
106. Fihura O, Ruzhylo S, Popovych I. Ukrainian adaptogenic phytocomposition “Balm Truskavets’” modulate EEG, HRV and biophotonics (GDV) parameters. Visnyk Morskoї Medytsyny. 2022; 2(95): 99-108.
107. Fihura O, Ruzhylo S, Zakalyak N. Phytoadaptogen reverses the adverse effects of Naftussya bioactive water on dynamic muscle performance in healthy rats. Quality in Sport. 2022; 8(2): 45–55.
108. Fihura O, Ruzhylo S, Żukow X, Popovych I. Immediate effects of Ukrainian phytocomposition on biophotonics (GDV), EEG and HRV parameters. Journal of Education, Health and Sport. 2021; 11(7): 349–365.
109. Fihura OA, Korda MM, Klishch IM, Ruzhylo SV, Melnyk OI, Zukow W, Yanchij RI, Vorobienko AA, Plyska OI, Popovych IL. Metabolic and immune accompaniments of electrocardiographic and morphologic gastric mucosa parameters in naïve and stressed rats. Journal of Education, Health and Sport. 2024; 61: 54947.
110. Fihura OA, Korda MM, Popovych DV, Ruzhylo SV. Plasma levels of main adaptogene hormones and EEG&HRV parameters are closely correlated. In: Materials of the XIII All-Ukrainian Science and Practice. conf. “Actual issues of pathology under the conditions of action of extraordinary factors on the body”. (Ternopil, October 26-28, 2022). Ternopil; 2022: 81-81.
111. Fihura OA, Melnyk OI, Ruzhylo SV, et al. Relationships between neuro-endocrine, electrocardiogram, and gastric mucosal damage parameters in naïve and stressed rats. Journal of Education, Health and Sport. 2023; 18(1): 162-190.
112. Fihura OA, Ruzhylo SV, Korda MM, Klishch IM, **Ż**ukow X, Popovych IL. The influence of the Ukrainian phytocomposition «Balm Truskavets’» on parameters of neuro-endocrine-immune complex and biophotonics in humans with maladaptation. Journal of Education, Health and Sport. 2023; 13(1): 326-337.
113. Fihura OA, Ruzhylo SV, Popovych IL. Ukrainian adaptogenic phytocomposition “Balm Truskavets’” modulate EEG, HRV and biophotonics (GDV) parameters. Journal of marine medicine. 2022; 2(95): 99-108.
114. Fihura OA, Ruzhylo SV, Zakalyak NR. Phytoadaptogen reverses the adverse effects of Naftussya bioactive water on dynamic muscle performance in healthy rats. Quality in Sport. 2022; 8(2): 45-55.
115. Fihura OA, Ruzhylo SV, **Ż**ukow X, Popovych IL. Immediate effects of Ukrainian phytocomposition on biophotonics (GDV), EEG and HRV parameters. Journal of Education, Health and Sport. 2021; 11(7): 349-365.
116. Fihura OA. Amelioration by phytoadaptogene of effects of balneofactors of Truskavets’ Spa on patients with post-radiation encephalopathy. Journal of Education, Health and Sport. 2023; 19(1): 36-58.
117. Fil V, Zukow W, Kovalchuk G, Voloshyn O, Kopko I, Lupak O, Stets V. The role of innate muscular endurance and resistance to hypoxia in reactions to acute stress of neuroendocrine, metabolic and ECGs parameters and gastric mucosa in rats. Journal of Physical Education and Sport. 2021; 21(Sup. 5): 3030-3039.
118. Filaretova L, Komkova O, Sudalina M, Yarushkina N. Non-Invasive Remote Ischemic Preconditioning May Protect the Gastric Mucosa Against Ischemia-Reperfusion-

Induced Injury Through Involvement of Glucocorticoids. Front Pharmacol. 2021; 12: 682643.
119. Filaretova L, Makara G. The surprising dual action of glucocorticoids. Ideggyogy Sz. 2014; 67(3-4): 121-123.
120. Filaretova L, Podvigina T, Bagaeva T, Morozova O. From gastroprotective to ulcerogenic effects of glucocorticoids: role of long-term glucocorticoid action. Curr Pharm Des. 2014; 20(7): 1045-1050.
121. Filaretova LP, Bagaeva TR, Amagase K, Takeuchi K. Contribution of glucocorticoids to protective influence of preconditioning mild stress against stress-induced gastric erosions. ANYAS. 2008; 1148: 209–212.
122. Filaretova LP, Filaretov AA, Makara GB. Corticosterone increase inhibits stress-induced gastric erosions in rats. Am J Physiology. 1998; 274(6): G1024–G1030.
123. Filaretova LP. The hypothalamic-pituitary-adrenocortical system: Hormonal brain-gut interaction and gastroprotection. Auton Neurosci. 2006; 125(1-2): 86-93.
124. Finger JD, Krug S, Gößwald A, Härtel S, Bös K. English Version: Kardiorespiratorische Fitness bei Erwachsenen in Deutschland. Ergebnisse der Studie zur Gesundheit Erwachsener in Deutschland (DEGS1) Bundesgesundheitsbl. 2013; 56: 772–778.
125. Flyunt IS, Chebanenko LO, Chebanenko OI, Kyjenko VM, Fil' VM. Experimental Balneophytotherapy [in Ukrainian]. Kyïv. UNESCO-SOCIO; 2008: 196.
126. Flyunt IS, Chebanenko OI, Hrinchenko BV, Barylyak LG, Popovych IL. Balneophytoradiodefensology. Influence of therapeutic factors of Truskavets' spa on the state of adaptation and protection systems of the victims of the Chernobyl disaster [in Ukrainian]. Kyïv. Computerpress; 2002: 112.
127. Foo YZ, Nakagawa S, Rhodes G, Simmons LW. The effects of sex hormones on immune function: a meta-analysis. Biological Reviews. 2017; 92(1): 551-571.
128. Forbes S, Herzog H, Cox H. A role for neuropeptide Y in the gender-specific gastrointestinal, corticosterone and feeding responses to stress. *Br J Pharmacol.*2012; **166:** 2307-2316.
129. Gaillard RC, Spinedi E. Sex-and stress-steroids interactions and the immune system: evidence for a neuroendocrine-immunological sexual dimorphism. Domestic animal endocrinology. 1998; 15(5): 345-352.
130. Gannon JM, Brar J, Rai A, Chengappa KNR. Effects of a standardized extract of *Withania somnifera* (Ashwagandha) on depression and anxiety symptoms in persons with schizophrenia participating in a randomized, placebo-controlled clinical trial. Ann Clin Psychiatry. 2019; 31: 123-129.
131. Gao W, Wang Z, Wang H, Li H, Huang C, Shen Y, Ma X, Sun H. Neurons and Astrocytes in Ventrolateral Periaqueductal Gray Contribute to Restraint Water Immersion Stress-Induced Gastric Mucosal Damage via the ERK1/2 Signaling Pathway. Int J Neuropsychopharmacol. 2021; 24(8): 666-676.
132. Gerontakos SE, Casteleijn D, Shikov AN, Wardle J. A critical review to identify the domains used to measure the effect and outcome of adaptogenic herbal medicines. Yale J Biol Med. 2020; 93(2): 327-346.
133. Giani Tagliabue S, Faber SC, Motta S, et al. Modeling the binding of diverse ligands within the Ah receptor ligand binding domain. Sci Rep. 2019; 9(1): 10693.

134. Gillies G, McArthur S. Estrogen Actions in the Brain and the Basis for Differential Action in Men and Women: A Case for Sex-Specific Medicines. Pharmacological Reviews. 2010; 62(2): 155–198.
135. Ginseng Radix. WHO monographs on selected medicinal plants. World Health Organization; 1999; 1:168-182.
136. Goldstein DS, Bentho O, Park MY, Sharabi Y. Low-frequency power of heart rate variability is not a measure of cardiac sympathetic tone but may be a measure of modulation of cardiac autonomic outflows by baroreflexes. Exp Physiol. 2011; 96(12): 1255-1261.
137. Gozhenko AI, Korda MM, Popadynets OO, Popovych IL. Entropy, Harmony, Synchronization and Their Neuro-Endocrine-Immune Correlates [in Ukrainian]. Odesa: Feniks; 2021: 232.
138. Gozhenko AI, Sydoruk NO, Babelyuk VYe, Dubkowa GI, Flyunt VR, Hubyts'kyi VYo, Zukow W, Barylyak LG, Popovych IL. Modulating effects of bioactive water Naftussya from layers Truskavets' and Pomyarky on some metabolic and biophysic parameters at humans with dysfunction of neuro-endocrine-immune complex. Journal of Education, Health and Sport. 2016; 6(12): 826-842.
139. Gozhenko AI, Zukow W, Polovynko IS, Zajats LM, Yanchij RI, Portnichenko VI, Popovych IL. Individual Immune Responses to Chronic Stress and their Neuro-Endocrine Accompaniment. RSW. UMK. Radom. Torun; 2019: 200.
140. Gozhenko **AI,** Korda MM, Popadynets' OO, Popovych IL. Entropy, Harmony, Synchronization and Their Neuro-Endocrine-Immune Correlates [in Ukrainian]. Odesa. Feniks; 2021: 232.
141. Gozhenko **AI,** Korda MM, Smagliy SS, Badiuk NS, Zukow W, Klishch IM, Korda IV, Bombushkar IS, Popovych IL. Uric Acid, Metabolism, Neuro-Endocrine-Immune Complex [in Ukrainian]. Odesa: Feniks; 2023: 266.
142. Guidobono F, Netti C, Pagani F, Bettica P, Sibilia V, Pecile A, Zanelli J. Effect of unmodified eel calcitonin on gastric acid secretion and gastric ulcers in the rat. Farmaco. 1991; 46(4): 555-563.
143. Han S, Jeong AJ, Yang H, et al. Ginsenoside 20(S)-Rh2 exerts anti-cancer activity through targeting IL-6-induced JAK2/STAT3 pathway in human colorectal cancer cells. J Ethnopharmacol. 2016; 194: 83-90.
144. Handelsman D, Hirschberg A, Bermon S. Circulating Testosterone as the Hormonal Basis of Sex Differences in Athletic Performance. Endocr Rev. 2018; 39(5): 803-829.
145. Hara MR, Cascio MB, Sawa A. GAPDH as a sensor of NO stress. Biochim Biophys Acta. 2006; 1762: 502-509.
146. Harrington EC. The Desirability Function. Industrial Quality Control. 1965; 21: 494-498.
147. Hartz AJ, Bentler S, Noyes R, et al. Randomized controlled trial of Siberian ginseng for chronic fatigue. Psychol Med. 2004; 34: 51-61.
148. Hasson D, Theorell T, Liljeholm-Johansson Y, Canlon B. Psychosocial and physiological correlates of self-reported hearing problems in male and female musicians in symphony orchestras. Int J Psychophysiol. 2009; 74(2): 93-100.
149. Heart Rate Variability. Standards of Measurement, Physiological Interpretation, and Clinical Use. Task Force of ESC and NASPE. Circulation. 1996; 93(5): 1043-1065.

150. Herbison AE, Spratt DP. Sexually dimorphic expression of calcitonin gene-related peptide (CGRP) mRNA in rat medial preoptic nucleus. Molecular brain research. 1995; 34(1): 143-148.
151. Hildebrandt G. Chronobiological aspects of cure treatment. Journal of Japanese Society of Balneology, Climatology and Physical Medicine. 1980; 44(1-2): 1-37.
152. Hiller G. Test for the quantitative determination of HDL cholesterol in EDTA plasma with Reflotron®. Klin Chem. 1987; 33: 895-898.
153. Holzer P, Reichmann F, Farzi A. Neuropeptide Y, peptide YY and pancreatic polypeptide in the gut-brain axis. *Neuropeptides*. 2012;46(6):261-274. doi: 10.1016/j.npep.2012.08.005.
154. Hotta H, Onda A, Suzuki H, Milliken P, Sridhar A. Modulation of Calcitonin, Parathyroid Hormone, and Thyroid Hormone Secretion by Electrical Stimulation of Sympathetic and Parasympathetic Nerves in Anesthetized Rats. Front Neurosci. 2017; 11: 375.
155. Hrinchenko BV, Ivanyts'ka OM, Safyanyk TV. Influence of balm "Kryms'kyi" on gastric secretion, cholekinetics and mineralocorticoid activity [in Ukrainian]. Medical Hydrology and Rehabilitation. 2006; 4(4): 30-36.
156. Hrinchenko BV, Ruzhylo SV, Flyunt IS, Alyeksyeyev AI, Huchko BYa. The effect of complex balneotherapy at the Truskavets' resort with the use of phytoadaptogen on psychophysiological functions and physical performance [in Ukrainian]. Medical Hydrology and Rehabilitation.1999; 2(1): 31-35.
157. Hrinchenko BV. A comparative study of the effect of balneotherapy with the use of Krymskyi and Bittner balms on physical performance and central hemodynamics [in Ukrainian]. Ukrainian Balneological Journal. 1998; 1(4): 36-38.
158. Hrinchenko BV. A comparative study of the effect of balneotherapy with the use of Krymskyi and Bittner balms on physical performance and central hemodynamics [in Ukrainian]. Ukrainian Balneological Journal. 1998; 1(4): 36-38.
159. Hrinchenko BV. Adaptive balneophytotherapy as a sanogenetic basis for rehabilitation of neuro-endocrine-immune system dysfunction [in Ukrainian]. Medical Hydrology and Rehabilitation. 2008; 6(1): 85-97.
160. Hsu JH, Chang PM, Cheng TS, et al. Identification of Withaferin A as a potential candidate for anti-cancer therapy in non-small cell lung cancer *Cancers* (Basel). 2019; 11 :1003.
161. Hu Q, He G, Zhao J, et al. Ginsenosides are novel naturally-occurring aryl hydrocarbon receptor ligands. PLoS One. 2013; 8(6): e66258.
162. Iseger TA, van Bueren NER, Kenemans JL, Gevirtz R, Arns M. A frontal-vagal network theory for Major Depressive Disorder: Implications for optimizing neuromodulation techniques. Brain Stimul. 2020; 13(1): 1-9.
163. Ivassivka SV, Bubnyak AB, Kovbasnyuk MM, Popovych IL. Genesis and role of phenols in waters from Naftussya layer [in Ukrainian]. In: Problems of pathology in experiment and clinic. Scientific works of Drohobych Medical Institute. Vol. XV. Drohobych. 1994: 6-11.
164. Ivassivka SV, Popovych IL, Aksentiychuk BI, Bilas VR. Nature of Balneofactors of Water Naftussya and the Essence of its Therapeutic and Preventive Action [in Ukrainian]. Truskavets'. Truskavets'kurort; 1999: 125.

165. Ivassivka SV, Popovych IL, Yaremenko MS, Kovbasnyuk MM. Mineral water Naftussya as a xenobiotic [in Russian]. Fiziol Zhurn. 1990; 36(3): 40-45.
166. Ivassivka SV. Biologically Active Substances of Naftussya Water, their Genesis and Mechanisms of Physiological Action [in Ukrainian]. Kyïv. Naukova dumka; 1997: 110.
167. Jaillon S, Berthenet K, Garlanda C. Sexual dimorphism in innate immunity. Clinical reviews in allergy & immunology. 2019; 56: 308-321.
168. Jeong HG, Ko YH, Oh SY, Han C, Kim T, Joe SH. Effect of Korean Red Ginseng as an adjuvant treatment for women with residual symptoms of major depression. Asia Pac Psychiatry. 2015; 7: 330-336.
169. Jin W, Ma R, Zhai L, et al. Ginsenoside Rd attenuates ACTH-induced corticosterone secretion by blocking the MC2R-cAMP/PKA/CREB pathway in Y1 mouse adrenocortical cells. Life Sci. 2020; 245: 117337.
170. Joseph-Bravo P, Lazcano I, Jaimes-Hoy L, Gutierrez-Mariscal M, Sanchez-Jaramillo E, Uribe RM, Charli JL. Sexually dimorphic dynamics of thyroid axis activity during fasting in rats. Frontiers in Bioscience-Landmark. 2020; 25(7): 1305-1323.
171. Kaestner CL, Smith EH, Peirce SG, Hoover DB. Immunohistochemical analysis of the mouse celiac ganglion: an integrative relay station of the peripheral nervous system. J Comp Neurol. 2019; 527: 2742–2760.
172. Kanakis G, Tsametis Ch, Goulis D. Measuring testosterone in women and men. Maturitas. 2019; 125: 41-44.
173. Kawashima D, Asai M, Katagiri K, Takeuchi R, Ohtsuka K. Reinvestigation of the effect of carbenoxolone on the induction of heat shock proteins. Cell Stress Chaperones. 2009; 14(5): 535-543.
174. Kelly CD, Stoehr AM, Nunn C, Smyth KN, Prokop ZM. Sexual dimorphism in immunity across animals: a meta-analysis. Ecology Letters. 2018; 21(12): 1885-1894.
175. Keshavarzi M, Khoshnoud MJ, Ghaffarian Bahraman A, Mohammadi-Bardbori A. An Endogenous Ligand of Aryl Hydrocarbon Receptor 6-Formylindolo[3,2-b] Carbazole (FICZ) Is a Signaling Molecule in Neurogenesis of Adult Hippocampal Neurons. J Mol Neurosci. 2020; 70: 806–817.
176. Keshavarzi Z, Mohebbati R, Mohammadzadeh N, Alikhani V. The protective role of estradiol & progesterone in male rats, following gastric ischemia-reperfusion. Acta Endocrinol (Buchar). 2018; 14(1): 30-35.
177. Kim D, Park M, Haleem I, et al. Natural product ginsenoside 20(S)-25-methoxyl-dammarane-3β, 12β, 20-triol in cancer treatment: a review of the pharmacological mechanisms and pharmacokinetics. Front Pharmacol. 2020;1: 521.
178. Kim MH, Lee SH, Hwang DY, Park YB, Ham SH, Yang WM. Protective effects of Banhasasim-tang, a herbal medicine, against cold restraint stress-induced gastric ulcers. Pak J Pharm Sci. 2022; 35(1): 9-13.
179. Kimura E, Tohyama C. Embryonic and Postnatal Expression of Aryl Hydrocarbon Receptor mRNA in Mouse Brain. Front Neuroanat. 2017; 11: 4.
180. Konturek PC, Brzozowski T, Konturek SJ, et al. Influence of bacterial lipopolysaccharide on healing of chronic experimental ulcer in rat. Scand J Gastroenterol. 2001; 36(12): 1239-47.

181. Koo MW, Ogle CW, Cho CH. Effects of verapamil, carbenoxolone and N-acetylcysteine on gastric wall mucus and ulceration in stressed rats. Pharmacology. 1986; 32(6): 326-34.
182. Korda M, Gozhenko A, Fihura O, Popovych D, **Ż**ukow X, Popovych I. Relationships between plasma levels of main adaptogene hormones and EEG&HRV parameters at human with dysadaptation. Journal of Education, Health and Sport. 2021; 11(12): 492-512.
183. Korda MM, Gozhenko AI, Fihura OA, Popovych DV, **Ż**ukow X, Popovych IL. Relationships between plasma levels of main adaptogene hormones and EEG&HRV parameters at human with dysadaptation. Journal of Education, Health and Sport. 2021; 11(12): 492-512.
184. Korda MM, Gozhenko AI, Popovych IL, Klishch IM, Bombushkar IS, Korda IV, Badiuk NS, Zukow WA, Smagliy VS. Neurotropic, Hormonal and Immunotropic Activity of Uric Acid. Ternopil': Ukrmedknyha; 2024: 206.
185. Korkushko OV, Pysaruk AV, Shatylo VB. The value of heart rate variability analysis in cardiology: age aspects [in Russian]. Circulation and Hemostase. 2009; 1-2: 127-139.
186. Korotkov K, Matravers P, Orlov D, Williams B. Application of electrophoton capture (EPC) analysis based on gas discharge visualization (GDV) technique in medicine: a systematic review. J Altern Complement Med. 2010; 16(1): 13-25.
187. Korotkov K. Principles of the human body functioning and their applications in integrative medicine (review). J Appl Biotechnol Bioeng. 2018; 5(6): 346–348.
188. Korotkov K. Review of EPI papers on medicine and psychophysiology published in 2008-2018. Int J Complement Alt Med. 2018; 11(5): 311-315.
189. Kostyuk PG, Popovych IL, Ivassivka SV (Editors). Chornobyl, Adaptive and Protection Systems, Rehabilitation. Adaptive, metabolic, hemostasis and immunological aspects of diagnostics and balneo- and phytorehabilitation in Truskavets' spa of persons exposed to Chornobyl accident factors [in Ukrainian]. Kyïv: Computerpress; 2006: 348.
190. Kou Z, Dai W. Aryl hydrocarbon receptor: Its roles in physiology. Biochem Pharmacol. 2021; 185: 114428.
191. Kozyavkina NV, Gozhenko AI, Barylyak LG., Korolyshyn TA, Popovych IL. Variety immediate thyrotropic effects of bioactive water Naftussya, their neuroendocrine-immune accompaniment and possibility of forecast [in Ukrainian]. Medical Hydrology and Rehabilitation. 2013; 11(4): 27-54.
192. Kozyavkina NV, Popovych IL, Popovych DV, Zukow W, Bombushkar IS. Sexual dimorphism in some psycho-neuro-endocrine parameters at human. Journal of Education, Health and Sport. 2021; 11(5): 370-391.
193. Kozyavkina OV, Kozyavkina NV, Gozhenko OA, Gozhenko AI, Barylyak LG., Popovych IL. Bioactive Water Naftussya and Neuro-Endocrine-Immune Complex [in Ukrainian]. Kyïv. UNESCO-SOCIO; 2015: 349.
194. Kozyavkina OV, Popovych IL, Zukow W. Immediate vegetotropic effects of bioactive water Naftussya and their neuro-endocrine-immune accompaniment in healthy men. Journal of Health Sciences. 2013; 3(5): 391-408.

195. Kozyavkina OV. The state of post-stress parameters of autonomic homeostasis and endocrine, metabolic and immune status and the relationship between them in rats with alternative types of pre-stress autonomic homeostasis induced by bioactive water Naftussya [in Ukrainian]. Medical Hydrology and Rehabilitation. 2009; 7(2): 40-56.
196. Kristt DA, Freimark SJ. Histopathology and pathogenesis of behaviorally induced gastric lesions in rats. Am J Pathol. 1973; 73(2): 411-424.
197. Kuehl P, Baczako K, Stanescu A, Malfertheimer P. Loss of alkaline phosphatase activity in duodenal mucosa: a marker for precursorsof gastric metaplasia? J Pathol. 1990; 162(4): 317-322.
198. Kul'chyns'kyi AB, Gozhenko AI, Zukow W, Popovych IL. Neuro-immune relationships at patients with chronic pyelonephritis and cholecystitis. Communication 3. Correlations between parameters EEG, HRV and Immunogram. Journal of Education, Health and Sport. 2017; 7(3): 53-71.
199. Kul'chyns'kyi AB, Kovbasnyuk MM, Korolyshyn TA, Kyjenko VM, Zukow W, Popovych IL. Neuro-immune relationships at patients with chronic pyelonephrite and cholecystite. Communication 2. Correlations between parameters EEG, HRV and Phagocytosis. Journal of Education, Health and Sport. 2016; 6(10): 377-401.
200. Kul'chyns'kyi AB**,** Kyjenko VM, Zukow W, Popovych IL. Causal neuro-immune relationships at patients with chronic pyelonephritis and cholecystitis**.** Correlations between parameters EEG, HRV and white blood cell count. Open Medicine. 2017; 12(1): 201-213.
201. Kul'chyns'kyi AB**,** Zukow W, Korolyshyn TA, Popovych IL. Interrelations between changes in parameters of HRV, EEG and humoral immunity at patients with chronic pyelonephritis and cholecystitis. Journal of Education, Health and Sport. 2017; 7(9): 439-459.
202. Kumar P, Banik SP, Goel A, Chakraborty S, Bagchi M, Bagchi D. Chemical, microbial and safety profiling of a standardized Withania somnifera (Ashwagandha) extract and Withaferin A, a potent novel phytotherapeutic of the millennium. Functional Foods in Health and Disease. 2023; 13(2): 36-51.
203. Kurt D, Saruhan BG, Kanay Z, Yokus B, Kanay BE, Unver O, Hatipoglu S. Effect of ovariectomy and female sex hormones administration upon gastric ulceration induced by cold and immobility restraint stress. Saudi Med J. 2007; 28(7): 1021-1027.
204. Kwiecien S, Magierowska K, Magierowski M, et al. Role of sensory afferent nerves, lipid peroxidation and antioxidative enzymes in the carbon monoxide-induced gastroprotection against stress ulcerogenesis. J Physiol Pharmacol. 2016; 67(5): 717-729.
205. Lapovets L, Lutsyk B. Handbook of Laboratory Immunology [in Ukrainian]. 2004; Lviv: 173.
206. László F, Varga C, Montoneri C, Drago F. Damaging actions of testosterone on cysteamine-induced gastroduodenal ulceration and vascular leakage in the rat. Eur J Pharmacol. 1997; 337(2-3): 275-278.
207. Lazarev NV, Ljublina EI, Ljublina MA. State of nonspecific resistance. Patol Fiziol Exp Terapia. 1959; 3: 16-21.

208. Lazarev NV. General and specific in action of pharmacological agents. Farmacol Toxicol. 1958; 21: 81-86.
209. Lee NH, Son CG. Systematic review of randomized controlled trials evaluating the efficacy and safety of ginseng. J Acupunct Meridian Stud. 2011; 4: 85-97.
210. Lee TJ, Chang HH, Lee HC, Chen PY, Lee YC, Kuo JS, Chen MF. Axo-axonal interaction in autonomic regulation of the cerebral circulation. Acta Physiol (Oxf). 2011; 203(1): 25-35.
211. Lee TJ, Liu J, Evans MS. Cholinergic-nitrergic transmitter mechanisms in the cerebral circulation. Microsc Res Tech. 2001; 53(2): 119-128.
212. Li J, Liu T, Zhao L, et al. Ginsenoside 20(S)Rg3 inhibits the Warburg effect through STAT3 pathways in ovarian cancer cells. Int J Oncol. 2015; 46: 775-781.
213. Li Lih-Ann, Wang Pei-Wen. PCB126 Induces Differential Changes in Androgen, Cortisol, and Aldosterone Biosynthesis in Human Adrenocortical H295R Cells. *Toxicological Sciences.* 2005; 85(1): 530–540.
214. Li W, Liu M, Feng S, et al. Acanthopanax for acute ischaemic stroke. Cochrane Database Syst Rev. 2009; 3: CD007032.
215. Lin X, Liu Y, Ma L, et al. Amelioration of experimental autoimmune encephalomyelitis by *Rhodiola rosea*, a natural adaptogen. Biomed Pharmacother. 2020; 125: 109960.
216. Lopresti AL, Smith SJ, Malvi H, Kodgule R. An investigation into the stress-relieving and pharmacological actions of an ashwagandha (*Withania somnifera*) extract: a randomized, double-blind, placebo-controlled study. Medicine. 2019; 98: e17186.
217. Lu S, Wu D, Sun G, et al. Gastroprotective effects of Kangfuxin against water-immersion and restraint stress-induced gastric ulcer in rats: roles of antioxidation, anti-inflammation, and pro-survival. Pharmaceutical biology. 2019; 57(1): 770–777.
218. Lukovych YuS, Popovych AI, Kovbasnyuk MM, Korolyshyn TA, Barylyak LG, Popovych IL. Neuroendocrine and immune support of the diuretic effect of balneotherapy at the Truskavets resort [in Ukrainian]. Kidneys. 2015; 2(12): 7-14.
219. Luo XJ, Liu B, Dai Z, Yang ZC, Peng J. Stimulation of calcitonin gene-related peptide release through targeting capsaicin receptor: a potential strategy for gastric mucosal protection. Dig Dis Sci. 2013; 58(2): 320-325.
220. Machowska A, Brzozowski T, Sliwowski Z, et al. Gastric secretion, proinflammatory cytokines and epidermal growth factor (EGF) in the delayed healing of lingual and gastric ulcerations by testosterone. Inflammopharmacology. 2008; 16(1): 40-47.
221. Machowska A, Szlachcic A, Pawlik M, et al. The role of female and male sex hormones in the healing process of preexisting lingual and gastric ulcerations. J Physiol Pharmacol. 2004; 55(Suppl 2): 91-104.
222. Man C, Dai Z, Fan Y. Dazhu Hongjingtian preparation as adjuvant therapy for unstable Angina Pectoris: a meta-analysis of randomized controlled trials. Front Pharmacol. 2020; 11: 213.
223. Mao JJ, Xie SX, Zee J, et al. *Rhodiola rosea* versus sertraline for major depressive disorder: a randomized placebo-controlled trial. Phytomedicine. 2015; 22: 394-399.

224. Marassi MP, Fortunato R.S, da Silva ACM, Pereira VS, Carvalho DP, Rosenthal D, da Costa VM. Sexual dimorphism in thyroid function and type 1 iodothyronine deiodinase activity in pre-pubertal and adult rats. Journal of Endocrinology. 2007; 192(1): 121-130.
225. Markova OO, Popovych IL, Tserkovnyuk AV, Barylyak LG. Adrenaline Myocardiodystrophy and Reactivity of the Organism [in Ukrainian]. Kyïv: Computerpress; 1997: 126.
226. Marrone GC, Silen W. Pathogenesis, diagnosis and treatment of acute gastric mucosal lesions. Clin Gastroenterol. 1984; 13(2): 635-650.
227. Mattson MP, Cheng A. Neurohormetic phytochemicals: Low-dose toxins that induce adaptive neuronal stress responses. Trends Neurosci. 2006; 29: 632-639.
228. Mattson MP, Son TG, Camandola S. Viewpoint: mechanisms of action and therapeutic potential of neurohormetic phytochemicals. Dose Response. 2007; 5: 174-186.
229. Mattson MP. Dietary factors, hormesis and health. Ageing Res Rev. 2008; 7: 43-48.
230. Mattson MP. Hormesis and disease resistance: activation of cellular stress response pathways. Hum Exp Toxicol. 2008; 27: 155-162.
231. Megna M, Amico AP, Cristella G, Saggini R, Jirillo E, Ranieri M. Effects of herbal supplements on the immune system in relation to exercise. Int J Immunopathol Pharmacol. 2012; 25: 43S-49S.
232. Melnyk OI, Chendey IV, Zukow W, Plyska OI, Popovych IL. The features of reactions to acute stress of neuro-endocrine-immune complex, metabolome, ECG and gastric mucosa in rats with various state of innate muscular endurance and resistance to hypoxia. Journal of Education, Health and Sport. 2023; 38(1): 96-128.
233. Melnyk OI, Lukyanchenko OI, Gozhenko OA, Popovych IL. Features of the parameters of EEG in persons whose immune status is susceptible or resistant to chronic stress. Experimental and Clinical Physiology and Biochemistry. 2019; 86(2): 11-23.
234. Melnyk OI, Struk ZD, Zukow W, Popovych IL. Vegetative, endocrine and metabolic accompaniments of individual immune responses to adaptogenic balneotherapy. Journal of Education, Health and Sport. 2019; 9(12): 207-229.
235. Melnyk OI, Struk ZD, Zukow W, Popovych IL. Vegetative, endocrine and metabolic accompaniments of individual immune responses to adaptogenic balneotherapy. Journal of Education, Health and Sport. 2019; 9(12): 207-229.
236. Melnyk OI, Zukow W, Hrytsak MV, et al. Canonical analysis of neuroendocrine-metabolic and neuroendocrine-immune relationships at female rats. Journal of Education, Health and Sport. 2021; 11(5): 356-369.
237. Mizunashi K, Furukawa Y, Katano K, et al. Effect of omeprazole, an inhibitor of H^+,K^+-ATPase, on bone resorption in humans. Calcif Tissue Int. 1993; 53(61): 21-25.
238. Moghadam ZM, Henneke P, Kolter J. From flies to men: ROS and the NADPH oxidase in phagocytes. Front Cell Dev Biol. 2021; 9: 628991.
239. Mohanan P, Subramaniyam S, Mathiyalagan R, Yang DC. Molecular signaling of ginsenosides Rb1, Rg1, and Rg3 and their mode of actions. J Ginseng Res. 2018; 42: 123-132.

240. Muehsam D, Chevalier G, Barsotti T, Gurfein B. An overview of biofield devices. Global Advances in Health and Medicine. 2015; 4(Suppl): 42-51.
241. Murakami A. Non-specific protein modifications may be novel mechanism underlying bioactive phytochemicals. J Clin Biochem Nutr. 2018; 62: 115-123.
242. Murray IA, Perdew GH. How Ah receptor ligand specificity became important in understanding its physiological function. Int J Mol Sci, 2020; 21(24): 9614.
243. Nakamura J, Takada S, Ohtsuka N, Heya T, Ueda S, Hamaura T, et al. An assessment of gastric ulcers in vivo: enhancement of urinary recovery after oral administration of phenolsulfonphthalein in rats. J Pharmacobiodynamics. 1984; 7(7): 485–491.
244. Nance DM, Sanders VM. Autonomic innervation and regulation of immune system (1987-2007). Brain Behav Immun. 2007; 21(6): 736-745.
245. Nebert DW, Bausserman LL. Genetic differences in the extent of aryl hydrocarbon hydroxylase induction in mouse fetal cell cultures. J Biol Chem. 1970; 245(23): 6373-82.
246. Newberg AB, Alavi A, Baime M, Pourdehnad M, Santanna J, d'Aquili E. The measurement of regional cerebral blood flow during the complex cognitive task of meditation: a preliminary SPECT study. Psychiatry Research: Neuroimaging Section. 2001; 106: 113-122.
247. Nordsborg N, Ovesen J, Thomassen M, Zangenberg M, Jøns C, Iaia FM, Nielsen JJ, Bangsbo J. Effect of dexamethasone on skeletal muscle Na^+,K^+ pump subunit specific expression and K^+ homeostasis during exercise in humans. J Physiology. 2008; 586(5): 1447–1459.
248. Nunn CL, Lindenfors P, Pursall ER, Rolff J. On sexual dimorphism in immune function. Philosophical Transactions of the Royal Society B: Biological Sciences. 2009; 364(1513): 61-69.
249. Oh ES, Steele CN, You Z, et al. Sex hormones and the risk of cardiovascular disease and mortality in male and female patients with chronic kidney disease: A systematic review and meta-analysis. Physiol Rep. 2022; 10(22): e15490.
250. Ohno H, Noguchi M, Takayanagi N. Effect of elcatonin on experimental gastric and duodenal ulcers. Jpn J Pharmacol. 1985; 37(1): 67-75.
251. Ojo ES, Tischkau SA. The Role of AhR in the Hallmarks of Brain Aging: Friend and Foe. Cells. 2021; 10(10): 2729.
252. Olsson EM, von Schéele B, Panossian AG. A randomized double-blind placebo controlled parallel group study of SHR-5 extract of *Rhodiola rosea* roots as treatment for patients with stress related fatigue. Planta Med. 2009; 75: 105-112.
253. Ordynskyi YuM, Riabokon MO, Denefil OV, Bolyukh OO. Stress-limiting mechanisms of adaptation to immobilization stress in high-resistant and low-resistant to hypoxic hypoxia female and male rats [in Ukrainian]. Art of Medicine. 2019; 1(9): 95-99.
254. Ordynskyi YuM, Riabokon MO, Denefil OV. Stress effect on male and female rats' organism with various hypoxia resistance [in Ukrainian]. Bukovinian Medical Herald. 2017; 21(3): 36-43.

255. Palma JA, Benarroch EE. Neural control of the heart: recent concepts and clinical correlations. Neurology. 2014; 83(3): 261-271.
256. Panasyuk YM, Levkut LH, Popovych IL, Alekseyev OI, Kovbasnyuk MM, Balanovskyi VP. Experimental study of adaptogenic properties of “Crimean” balm [in Ukrainian]. Fiziol Zh. 1994; 40(3-4): 25-30.
257. Panossian A, Amsterdam J. Chapter 8: Adaptogens in psychiatric practice In: Gerbarg PL, Muskin PR, Brown RP, eds. Complementary and Integrative Treatments in Psychiatric Practice. Arlington, VA: American Psychiatric Publishing; 2017: 155-181.
258. Panossian A, Efferth T. Network Pharmacology of Adaptogens in the Assessment of Their Pleiotropic Therapeutic Activity. Pharmaceuticals (Basel). 2022; 15(9): 1051.
259. Panossian A, Gabrielian E, Wagner H. On the mechanism of action of plant adaptogens with particular reference to cucurbitacin R diglucoside. Phytomedicine. 1999; 6: 147-155.
260. Panossian A, Hambartsumyan M, Hovanissian A, Gabrielyan E, Wilkman G. The adaptogens Rhodiola and Schizandra modify the response to immobilization stress in rabbits by suppressing the increase of phosphorylated stress-activated protein kinase, nitric oxide and cortisol. Drug Targets Insights. 2007; 2: 39-54.
261. Panossian A, Seo EJ, Efferth T. Effects of anti-inflammatory and adaptogenic herbal extracts on gene expression of eicosanoids signaling pathways in isolated brain cells. Phytomedicine. 2019; 60: 152881.
262. Panossian A, Seo EJ, Efferth T. Novel molecular mechanisms for the adaptogenic effects of herbal extracts on isolated brain cells using systems biology. Phytomedicine. 2018; 50: 257-284.
263. Panossian A, Seo EJ, Efferth T. Novel molecular mechanisms for the adaptogenic effects of herbal extracts on isolated brain cells using systems biology. Phytomedicine. 2018; 50: 257-284.
264. Panossian A, Wagner H. Adaptogens. A review of their history, biological activity, and clinical benefits. HerbalGram. 2011; 90: 52-63.
265. Panossian A, Wagner H. Stimulating effect of adaptogens: an overview with particular reference to their efficacy following single dose administration. Phytother Res. 2005; 19: 819-838.
266. Panossian A, Wikman G, Kaur P, Asea A. Adaptogens stimulate neuropeptide Y and Hsp72 expression and release in neuroglia cells. Front Neurosci. 2012; 6: 6.
267. Panossian A, Wikman G, Wagner H. Plant adaptogens III. Earlier and more recent aspects and concepts on their mode of action. Phytomedicine. 1999; 6: 287-300.
268. Panossian A, Wikman G. Effects of adaptogens on the central nervous system and the molecular mechanisms associated with their stress-protective activity. Pharmaceuticals. 2010; 3: 188-224.
269. Panossian A, Wikman G. Effects of adaptogens on the central nervous system and the molecular mechanisms associated with their stress-protective activity. Pharmaceuticals (Basel). 2010; 3(1): 188-224.
270. Panossian A, Wikman G. Evidence-based efficacy of adaptogens in fatigue, and molecular mechanisms related to their stress-protective activity. Curr Clin Pharmacol. 2009; 4: 198-219.

271. Panossian A. Adaptogens in mental and behavioral disorders. Psychiatr Clin North Am. 2013; 36: 49-64.
272. Panossian A. Challenges in phytotherapy research. Front Pharmacol. 2023; 14: 1199516.
273. Panossian A. Understanding adaptogenic activity: specificity of the pharmacological action of adaptogens and other phytochemicals. Ann NY Acad Sci. 2017; 1401: 49-64.
274. Panossian AG, Efferth T, Shikov AN, Pozharitskaya ON, Kuchta K, Mukherjee PK, Banerjee S, Heinrich M, Wu W, Guo DA, Wagner H. Evolution of the adaptogenic concept from traditional use to medical systems: Pharmacology of stress- and aging-related diseases. Med Res Rev. 2021; 41(1): 630-703.
275. Panossian AG. Adaptogens: tonic herbs for fatigue and stress. Altern Complement Ther. 2003; 9: 327-332.
276. Park S, Lee HJ, Jeong SJ, et al. Inhibition of JAK1/STAT3 signaling mediates compound K-induced apoptosis in human multiple myeloma U266 cells. Food Chem Toxicol. 2011; 49: 1367-1372.
277. Pat. 10271 Ukraine MKI A 61 K 31/00. Adaptogenic agent [in Ukrainian]. Panasyuk YM, Levkut LG, Popovych IL, Shumakov MF, Sychova AO, Alekseyev OI, Bakova MM. 1996. Bull № 4.
278. Pavlov VA, Chavan SS, Tracey KJ. Molecular and functional neuroscience in immunity. Annu Rev Immunol. 2018; 36: 783-812.
279. Pawlik MW, Kwiecien S, Ptak-Belowska A, Pajdo R, Olszanecki R, Suski M, Madej J, Targosz A, Konturek SJ, Korbut R, Brzozowski T. The renin-angiotensin system and its vasoactive metabolite angiotensin-(1-7) in the mechanism of the healing of preexisting gastric ulcers. The involvement of Mas receptors, nitric oxide, prostaglandins and proinflammatory cytokines. J Physiol Pharmacol. 2016; 67(1): 75-91.
280. Peck JR, Waxman D. What is adaptation and how it should be measured? J Theor Biol. 2018; 447: 190-198.
281. Pérez-Gómez J, Villafaina S, Adsuar JC, Merellano-Navarro E, Collado-Mateo D. Effects of Ashwagandha (*Withania somnifera*) on VO_{2max}: a systematic review and meta-analysis. Nutrients. 2020; 12: 1119.
282. Peskar BM. Neural aspects of prostaglandin involvement in gastric mucosal defense. J Physiol Pharmacol. 2001; 52(4 Pt 1): 555-568.
283. Pharmacopoeia of the People's Republic of China 2015. 1st ed., HM He, L Cui, (Eds). Beijing: China Medical Science Press. 2017.
284. Phelan D, Winter GM, Rogers WJ, et al. Activation of the Ah receptor signal transduction pathway by bilirubin and biliverdin. Arch Biochem Biophys. 1988; 357(1): 155-163.
285. Poland A, Glover E, Kende AS. Stereospecific, high affinity binding of 2,3,7,8-tetrachlorodibenzo-p-dioxin by hepatic cytosol. Evidence that the binding species is receptor for induction of aryl hydrocarbon hydroxylase. J Biol Chem. 1976; 251(16): 4936-4946.

286. Polovynko IS, Zajats LM, Popovych AI, Popovych IL. **I**ntegral quantification of neuroendocrine and immune responses to chronic stress in male rats [in Ukrainian]. In: Pathophysiology and Pharmacy: ways of integration: Abstracts VII National Congress pathophysiologists Ukraine with international participation (5-7 October 2016). Kharkiv: NPhU; 2016: 182-182.
287. Polovynko IS, Zajats LM, Zukow W, et al. Quantitative evaluation of integrated neuroendocrine and immune responses to chronic stress in rat male. Journal of Education, Health and Sport. 2016; 6(8): 154-166.
288. Polovynko IS, Zayats LM, Zukow W, Popovych IL. Neuro-endocrine-immune relationships by chronic stress at male rats. Journal of Health Sciences. 2013; 3(12): 365-374.
289. Polovynko IS, Zukow W. Variety of immune responses to chronic stress in rat male. Journal of Education, Health and Sport. 2016; 6(12): 843-856.
290. Popadynets O, Gozhenko A, Badyuk N, Popovych I, Skaliy A, Hagner-Derengowska M, Napierata M, Muszkieta R, Sokołowski D, Zukow W, Rybałko L. Interpersonal differences caused by adaptogen changes in entropies of EEG, HRV, immunocytogram, and leukocytogram. Journal of Physical Education and Sport. 2020; 20(Suppl. 2): 982-999.
291. Popovych AI. Features of the immunotropic effects of partial components of the balneotherapeutic complex of spa Truskavets'. Journal of Education, Health and Sport. 2018; 8(12): 919-935.
292. Popovych AI. Features of the neurotropic effects of partial components of the balneotherapeutic complex of spa Truskavets'. Journal of Education, Health and Sport. 2019; 9(1): 396-409.
293. Popovych I, Flyunt I. (Editors). Sanogenetic Bases of Rehabilitation on Spa Truskavets' Urological Patients from Chornobylian Contingent [in Ukrainian]. Kyïv: Computerpress; 2003: 192.
294. Popovych I, Mysula I, Popovych A, Mysula Y, Sydliaruk N, Bilas V, Zukow W. Role of organic carbon and nitrogen of mineral waters in their immunomodulating effects at female rats. Journal of Education, Health and Sport. 2021; 11(9): 886-894.
295. Popovych I, Ruzhylo S, Ivassivka S, Aksentiychuk B. (Editors). Balneocardioangiology. The impact of balneotherapy in the spa Truskavets' on the cardiovascular system and physical performance [in Ukrainian]. Kyïv. Computerpress; 2005: 239.
296. Popovych I. Similarity effects of two types of adaptogens (transcutaneous electrical stimulation with the device "VEB" ® and using of bioactive Naftussya water) on the human body. Journal of Education, Health and Sport. 2022; 12(4): 213-258.
297. Popovych I. Similarity of adaptogenic effects of bioactive Naftussya water and phytocomposition "Balm Truskavets'". Journal of Education, Health and Sport. 2022; 12(12): 344-356.
298. Popovych IL, Babelyuk VYe, Dubkova GI. Relations between the parameters bioelectrography (kirlianography) and heart rate variability and blood pressure [in Ukrainian]. Medical Hydrology and Rehabilitation. 2010; 8(1): 4-16.
299. Popovych IL, Bombushkar IS, **Ż**ukow X, Kovalchuk HY. Uric acid, neuroendocrine-immune complex and metabolism: relationships. Journal of Education, Health and Sport. 2023; 36(1): 135-159.

300. Popovych IL, Gozhenko AI, Korda MM, Klishch IM, Popovych DV, Zukow W (editors). Mineral Waters, Metabolism, Neuro-Endocrine-Immune Complex. Odesa: Feniks; 2022: 252.
301. Popovych IL, Gozhenko AI, Zukow W, Polovynko IS. Variety of Immune Responses to Chronic Stress and their Neuro-Endocrine Accompaniment. Riga: Scholars' Press; 2020: 172.
302. Popovych IL, Ivassivka SV, Barylyak LG, Fil VM, Korolyshyn TA, Shologin AI, Datsko OR. Features of stress-induced changes in the gastric mucosa, neuroendocrine-immune complex and metabolism in rats with different resistance to hypoxia [in Ukrainian]. Medical Hydrology and Rehabilitation. 2010; 8(2): 96-109.
303. Popovych IL, Ivassivka SV. The role of organic matter in Naftussya water in its physiological activity [in Ukrainian]. Medical hydrology and rehabilitation. 2009; 7(2): 6-26.
304. Popovych IL, Kozyavkina OV, Kozyavkina NV, Korolyshyn TA, Lukovych YuS, Barylyak LG. Correlation between Indices of the Heart Rate Variability and Parameters of Ongoing EEG in Patients Suffering from Chronic Renal Pathology. Neurophysiology. 2014; 46(2): 139-148.
305. Popovych IL, Kozyavkina OV. Immediate vegetotropic effects of bioactive water Naftussya and their neuro-endocrine-immune accompaniment in apparently healthy men [in Ukrainian]. Medical Hydrology and Rehabilitation. 2012; 10(3): 32-65.
306. Popovych IL, Kulchynskyi AB**,** Gozhenko AI, Zukow W, Kovbasnyuk MM, Korolyshyn TA**.** Interrelations between changes in parameters of HRV, EEG and phagocytosis at patients with chronic pyelonephritis and cholecystitis. Journal of Education, Health and Sport. 2018; 8(2): 135-156.
307. Popovych IL, Kulchynskyi AB, Korolyshyn TA, Zukow W. Interrelations between changes in parameters of HRV, EEG and cellular immunity at patients with chronic pyelonephritis and cholecystitis. Journal of Education, Health and Sport. 2017; 7(10): 11-23.
308. Popovych IL, Lukovych YuS, Korolyshyn TA, Barylyak LG, Kovalska LB, Zukow W. Relationship between the parameters heart rate variability and background EEG activity in healthy men. Journal of Health Sciences. 2013; 3(4): 217-240.
309. Popovych IL, Polovynko IS, Zajats LM, Melnyk OI. Sexual dimorphism of the neuroendocrine-immune complex and its reactions on chronic stress at rats. Experimental and Clinical Physiology and Biochemistry. 2018; 3(83): 5-17.
310. Popovych IL, Ruzhylo SV, Ivassivka SV, Aksentiychuk BI (editors). Balneocardioangiology [in Ukrainian]. Kyïv. Computerpress; 2005: 229.
311. Popovych IL, Vistak (Markevych) HI, Humega MD, Ruzhylo SV. Vegetotropic Effects of Bioactive Water Naftussya and their Neuroendocrine-Immune, Metabolic and Hemodynamic Accompaniments [in Ukrainian]. Kyïv. UNESCO-SOCIO; 2014: 162.
312. Popovych IL, Zavidnyuk YV, Korda MM, Mysula IR, Klishch IM, Zukow W. Role of organic carbon and nitrogen of mineral waters in their metabolic effects at female rats. Journal of Education, Health and Sport. 2018; 8(12): 793-802.
313. Popovych IL. Factor and canonical analyzes of the parameters of the neuro-endocrine-immune complex, metabolism and erosive-ulcerative lesions of the gastric mucosa

in rats under acute water-immersion stress [in Ukrainian]. Medical Hydrology and Rehabilitation. 2007; 5(2): 68-80.
314. Popovych IL. Immediate responses of the autonomic nervous system to the balneofactors, their neuro-endocrine-immune accompaniments and predictors. Experimental and Clinical Physiology and Biochemistry. 2018; 1(81): 11-26.
315. Popovych IL. Similarity of adaptogenic effects of bioactive Naftussya water and phytocomposition "Balm Truskavets'". Journal of Education, Health and Sport. 2022; 12(12): 344-356.
316. Popovych IL. Stresslimiting Adaptogene Mechanism of Biological and Curative Activity of Water Naftussya [in Ukrainian]. Kyïv. Computerpress; 2011: 300.
317. Popovych IL. The concept of neuro-endocrine-immune complex (review) [in Russian]. Medical Hydrology and Rehabilitation. 2009; 7(3): 9-18.
318. Portnychenko AG. Ukrainian balneology: scientific trends of the last decade (scientometric analysis) [in Ukrainian]. Medical Hydrology and Rehabilitation. 2015; 13(4): 41-52.
319. Qi HY, Li L, Ma H. Cellular stress response mechanisms as therapeutic targets of ginsenosides. Med Res Rev. 2018; 38: 625-654.
320. Qi LW, Wang CZ, Du GJ, Zhang ZY, Calway T, Yuan CS. Metabolism of ginseng and its interactions with drugs. Curr Drug Metab. 2011; 12: 818-822.
321. Qi Z, Qi S, Ling L, Lv J, Feng Z. Salidroside attenuates inflammatory response via suppressing JAK2-STAT3 pathway activation and preventing STAT3 transfer into nucleus. Int Immunopharmacol. 2016; 35: 265-271.
322. Quintana FJ, Sherr DH. Aryl hydrocarbon receptor control of adaptive immunity. Pharmacol Rev. 2013; 65(4): 1148-61.
323. Radchenko OM. Adaptation reactions in the clinic of internal diseases [in Ukrainian]. Lviv. Liga-Press; 2004: 232.
324. Rao SS, Saifi AQ. Relevance of male hormonal status with antiulcer effect of cimetidine in pylorus ligated rats. Indian J Physiol Pharmacol. 1987; 31(4): 263-266.
325. Rejano-Gordillo C, Marín-Díaz B, Ordiales-Talavero A, Merino J, González-Rico F, Fernandez-Salguero P. From Nucleus to Organs: Insights of Aryl Hydrocarbon Receptor Molecular Mechanisms. International J Molecular Sciences. 2022; 23(23): 14919.
326. Reyes del Paso GA, Langewitz W, Mulder LJ, van Roon A, Duschek S. The utility of low frequency heart rate variability as an index of sympathetic cardiac tone: a review with emphasis on a reanalysis of previous studies. Psychophysiology. 2013; 50(5): 477-487.
327. Reznikov AG, Nosenko ND, Tarasenko LV, Sinitsyn PV, Polyakova LI. Early and Long-Term Neuroendocrine Effects of Prenatal Stress in Male and Female Rats. Neuroscience and Behavioral Physiology. 2001; 31(1):1–5.
328. Reznikov AG, Nosenko ND. Perinatal stress modification of the reactivity of the hypothalamic-pituitary-adrenal system (HPAS) [in Ukrainian]. Fiziol Zhurn. 2000; 46(2): 146-158.
329. Reznikov OG. Perinatal programming of disorders of endocrine functions and behavior [in Ukrainian]. Kyïv. Naukova dumka; 2019: 272.

330. Ribeiro Júnior RF, Ronconi KS, Jesus ICG, Almeida PWM, Forechi L, Vassallo DV, Guatimosim S, Stefanon I, Fernandes AA. Testosterone deficiency prevents left ventricular contractility dysfunction after myocardial infarction. Mol Cell Endocrinol. 2018; 460: 14-23.
331. Riddle J, Rubinow D, Girdler S, Frohlich F. Disinhibition of right inferior frontal gyrus underlies alpha asymmetry in women with low testosterone. Biological Psychology. 2021; 161: 108061.
332. Riiser A, Stensrud T, Andersen L. Glucocorticoids and physical performance: A systematic review with meta-analysis of randomized controlled trials. Frontiers in Sports and Active Living. 2023; 5.
333. Romano TA, Felten SY, Felten DL, Olschowka JA. Neuropeptide-Y innervation of the rat spleen: another potential immunomodulatory neuropeptide. Brain Behav Immun. 1991; 5(1): 116-31.
334. Romodanov AP (Editor). Postradiation Encephalopathy. Experimental Researches and Clinical Observations [in Ukrainian and Russian]. Kyïv. USRI of Neurosurgery; 1993: 224.
335. Romodanov AP. Status of the brain during internal radiation by small doses and chronic radiation sickness [in Ukrainian and Russian]. In: Post-radiation encephalopathy. Experimental studies and clinical observations. (Editor Romodanov AP). Kyïv. USRI of Neurosurgery; 1993: 5-17.
336. Ruzhylo SV, Fihura OA, Zakalyak NR, Kovalchuk GY, **Ż**ukow X, Popovych DV. Sexual dimorphism in the neuro-endocrine regulation of bicycle ergometric test parameters in untrained individuals with dysfunction of the neuro-endocrine-immune complex. Journal of Education, Health and Sport. 2022; 12(9): 971-984.
337. Ruzhylo SV, Fihura OA, Zukow W, Popovych IL. Immediate neurotropic effects of Ukrainian phytocomposition. Journal of Education, Health and Sport. 2015; 5(4): 415-427.
338. Ruzhylo SV, Popovych AI, Zakalyak NR, Chopyk RV, Fihura OA, Bilas VR, Badiuk NS, Gozhenko AI, Popovych IL, Zukow W. Bioactive water Naftussya and ozokerite have the same neuro-endocrine-immune effects in male rats caused by aryl hydrocarbons. PharmacologyOnLine. 2021; 3: 213-226.
339. Ruzhylo SV, Tserkovnyuk AV, Hrebinyuk OV, Kovbasko HR. Cluster and discriminant analysis of the influence of balneotherapy at the Truskavets' resort on resistance to hypoxia and physical performance of school-age children [in Ukrainian]. Medical hydrology and rehabilitation. 2003; 1(2): 82-86.
340. Ruzhylo SV, Tserkovnyuk AV, Popovych IL. Actotropic Effects of Balneotherapeutic Complex of Truskavets spa [in Ukrainian]. Kyïv. Computerpress; 2003: 131.
341. Ruzhylo SV, Tserkovnyuk AV. Variants of actotropic effects of balneotherapy at the Truskavets resort and the possibility of their prediction by the method of discriminant analysis [in Ukrainian]. Ukrainian Balneological Journal. 2003; 2: 41-47.
342. Ruzhylo SV, Zakalyak NR, Ivanikiv N, Popovych DV, **Ż**ukow X, Popovych IL. Features of EEG&HRV in 1997 in humans exposed to the factors of the accident at the Chornobylian nuclear power plant in 1986. Journal of Education, Health and Sport. 2022; 12(10): 214-224.

343. Sabbadin C, Bordin L, Donà G, Manso J, Avruscio G, Armanini D. Licorice: From Pseudohyperaldosteronism to Therapeutic Uses. Front Endocrinol (Lausanne). 2019; 10: 484.
344. Sakaki M, Yoo HJ, Nga L, Lee TH, Thayer JF, Mather M. Heart rate variability is associated with amygdala functional connectivity with MPFC across younger and older adults. Neuroimage. 2016; 139: 44-52.
345. Sammito S, Heblich F, Güttler N. Die Fahrradergometrie in der arbeitsmedizinischen Vorsorge. Zbl Arbeitsmed. 2020; 70: 240–246.
346. Samuelsson G, Bohlin L. Drugs of Natural Origin: A Treatise of Pharmacognosy. 6th ed. Stockholm: Swedish Academy of Pharmaceutical Sciences; 2009:776.
347. Saratikov AS, Krasnov EA. Rhodiola rosea (Golden root). Tomsk: Tomsk State University Publishing House; 2004: 292.
348. Sarris J, Panossian A, Schweitzer I, Stough C, Scholey A. Herbal medicine for depression, anxiety and insomnia: a review of psychopharmacology and clinical evidence. Eur Neuropsychopharmacol. 2011; 21: 841-860.
349. Selye H. Forty years of stress research: principal remaining problems and misconceptions. Can Med Assoc J. 1976; 115(1): 53-56.
350. Selye H. Stress and inflammation. Am J Proctol. 1953; 4(3): 229-230.
351. Selye H: A syndrome produced by diverse nocuous agents. 1936. *J Neuropsychiatry Clin Neurosci.* 1998; 10(2): 230–231.
352. Sergeeva I, Kiseleva T, Pomozova V, Shkrabtak N, Frolova N, Vereshchagin A. Experimental studies of the effect of schisandra chinensis extract on the state of adaptive capabilities of rats under chronic and general exposure to cold. Int J Environ Res Public Health. 2021; 18(22): 11780.
353. Shaffer F, Ginsberg JP. An Overview of Heart Rate Variability Metrics and Norms. Front Public Health. 2017; 5: 258.
354. Shannon CE. A mathematical theory of information. Bell Syst Tech J. 1948; 27: 379-423.
355. Shen CY, Jiang JG, Yang L, Wang DW, Zhu W. Anti-ageing active ingredients from herbs and nutraceuticals used in traditional Chinese medicine: pharmacological mechanisms and implications for drug discovery. Br J Pharmacol. 2017; 174: 1395-1425.
356. Shepherd R, Cheung AS, Pang K, Saffery R, Novakovic B. Sexual Dimorphism in Innate Immunity: The Role of Sex Hormones and Epigenetics. Front Immunol. 2021; 11: 604000.
357. So S, Savidge T. Sex-Bias in Irritable Bowel Syndrome: Linking Steroids to the Gut-Brain Axis. Front Endocrinol (Lausanne). 2021;12: 684096.
358. Son TG, Camandola S, Mattson MP. Hormetic dietary phytochemicals. NeuroMolecular Med. 2008; 10: 236-246.
359. Song E, Jeon MJ, Yoo HJ, Bae SJ, Kim TY, Kim WB, Shong YK, Kim HK, Kim WG. Gender-Dependent Reference Range of Serum Calcitonin Levels in Healthy Korean Adults. Endocrinol Metab (Seoul). 2021; 36(2): 365-373.
360. Song F, Zeng K, Liao L, Yu Q, Tu P, Wang X. Schizandrin A inhibits microglia-mediated neuroninflammation through inhibiting TRAF6-NF-κB and Jak2-Stat3 signaling pathways. PLOS One. 2016; 11:e0149991.

361. Spratt DP, Herbison AE. Sexually dimorphic effects of testosterone on preoptic area calcitonin gene-related peptide mRNA expression depend upon neuron location and differential estrogen and androgen receptor activation. Endocrinology. 2001; 142(8): 3397-3404.
362. Steinhilber B, Seibt R, Gabriel J, Brountsou J, Muljono M, Downar T, Bär M, Bonsch R, Brandt A, Martus P, Rieger MA. Effects of Face Masks on Physical Performance and Physiological Response during a Submaximal Bicycle Ergometer Test. International journal of environmental research and public health. 2022; 19(3): 1063.
363. Stemper T. Gesundheit, Fitness, Freizeitsport: Praxis des Modernen Gesundheitssports. Köln. Bund; 1988: 144.
364. Sternberg EM. Neural regulation of innate immunity: a coordinated nonspecific response to pathogens. Nat Rev Immunol. 2006; 6(4): 318-328.
365. Stewart PM, Wallace AM, Atherden SM, Shearing CH, Edwards CR. Mineralocorticoid activity of carbenoxolone: contrasting effects of carbenoxolone and liquorice on 11 beta-hydroxysteroid dehydrogenase activity in man. Clin Sci (Lond). 1990; 78(1): 49-54.
366. Stiel D, Murray DJ, Peters TJ. Mucosal enzyme activities, with special reference to enzymes implicated in bicarbonate secretion, in the duodenum of rats with cysteamine-induced ulcers. Clin Sci (Lond). 1983; 64(63): 341-347.
367. Stranahan AM, Mattson MP. Recruiting adaptive cellular stress responses for successful brain ageing. Nat Rev Neurosci. 2012; 13: 209-216.
368. Stratakis CA, Chrousos GP. Neuroendocrinology and pathophysiology of the stress system. Ann N Y Acad Sci. 1995; 771: 1-18.
369. Suleyman H, Halici Z, Cadirci E, Hacimuftuoglu A, Keles S, Gocer F. Indirect role of α2-adrenoreceptors in anti-ulcer effect mechanism of nimesulide in rats. Naunyn-Schmiedeberg's archives of pharmacology. 2007; 375: 189-198.
370. Sun XB, Matsumoto T, Yamada H. Anti-ulcer activity and mode of action of the polysaccharide fraction from the leaves of Panax ginseng. Planta Med. 1992; 58(5): 432-435.
371. Szabo S, Yoshida M, Filakovszky J, Juhasz G. "Stress" is 80 Years Old: From Hans Selye Original Paper in 1936 to Recent Advances in GI Ulceration. Curr Pharm Des. 2017; 23(27): 4029-4041.
372. Taché Y, Kolve E, Maeda-Hagiwara M, Kauffman GL Jr. Central nervous system action of calcitonin to alter experimental gastric ulcers in rats. Gastroenterology. 1988; 94(1): 145-150.
373. Taché Y, Saperas E. Potent inhibition of gastric acid secretion and ulcer formation by centrally and peripherally administered interleukin-1. Ann N Y Acad Sci. 1992; 664: 353-68.
374. Taché Y. Brainstem neuropeptides and vagal protection of the gastric mucosal against injury: role of prostaglandins, nitric oxide and calcitonin-gene related peptide in capsaicin afferents. Curr Med Chem. 2012; 19(1): 35-42.
375. Taylor JA, Carr DL, Myers CW, Eckberg DL. Mechanisms underlying very-low-frequency RR-interval oscillations in humans. Circulation. 1998; 98(6): 547-555.

376. Thayer JF, Lane RD. Claude Bernard and the heart-brain connection: further elaboration of a model of neurovisceral integration. Neurosci Biobehav Rev. 2009; 33: 81-88.
377. Thayer JF, Sternberg EM. Neural aspects of immunomodulation: Focus on the vagus nerve. Brain Behav Immun. 2010; 24(8): 1223-1228.
378. Theorell T, Liljeholm-Johansson Y, Björk H, Ericson M. Saliva testosterone and heart rate variability in the professional symphony orchestra after "public faintings" of an orchestra member. Psychoneuroendocrinology. 2007; 32(6): 660-668.
379. Thorin-Trescases N, Thorin E. Vascular aging and oxidative stress: Hormesis and adaptive cellular pathways In: Bondy S, Maiese K, eds. Aging and Age-Related Disorders. Berlin Heidelberg: Springer Science + Business Media, LLC; 2010: 309-321.
380. Todorova V, Ivanov K, Ivanova S. Comparison between the biological active compounds in plants with adaptogenic properties (Rhaponticum carthamoides, Lepidium meyenii, Eleutherococcus senticosus and Panax ginseng). Plants (Basel). 2021; 11(1): 64.
381. Tracey KJ. Physiology and immunology of the cholinergic antiinflammatory pathway. J Clin Invest. 2007; 117(2): 289-296.
382. Tracey KJ. Understanding immunity requires more than immunology. Nature Immunology. 2010; 11(7): 561-564.
383. Trappe H-J, Löllgen H. Leitlinien zur Ergometrie. Z Kardiol. 2000; 89: 16.
384. Trego ML, Hoh E, Kellar NM, et al. Comprehensive Screening Links Halogenated Organic Compounds with Testosterone Levels in Male Delphinus delphis from the Southern California Bight. Environ Sci Technol. 2018; 52(5): 3101-3109.
385. Tserkovnyuk AV, Ruzhylo SV, Aksentiychuk MI, Misko OI. The influence of balneotherapy at the Truskavets resort on vegetative and hemodynamic maintenance of physical capacity [in Ukrainian]. Halyts'kyi Medical Herald. 2002; 9(1): 100-102.
386. Tserkovnyuk AV, Ruzhylo SV. Aerobic training optimization of the effect of balneotherapy at the Truskavets' resort on physical performance and its support systems [in Ukrainian]. Ukrainian Balneological Journal. 2001; 2: 39-45.
387. Tserkovnyuk AV, Ruzhylo SV. The influence of aerobic training against the background of balneotherapy at the Truskavets' resort on physical performance and its hemodynamic and metabolic support [in Ukrainian]. Ukrainian Balneological Journal. 2001; 1: 55-64.
388. Tserkovnyuk AV. Determination of muscle performance by parameters of cation exchange [in Ukrainian]. Ukrainian Balneological Journal. 2002; 1: 40-44.
389. Uehara A, Okumura T, Kitamori S, et al. Gastric antisecretory and antiulcer actions of interleukin-1. Evidence for the presence of an "immune-brain-gut" axis. J Clin Gastroenterol. 1992; 14 Suppl 1: S149-S155.
390. Urhausen A, Gabriel H, Kindermann W. Blood hormones as markers of training stress and overtraining. Sports Med. 1995; 20(4): 251-276.
391. Uribe-Querol E, Rosales C. Phagocytosis: Our Current Understanding of a Universal Biological Process. Frontiers in immunology. 2020; 11: 1066.

392. Uusitalo A, Huttunen P, Hanin Y, Uusitalo A, Rusko H. Hormonal responses to endurance training and overtraining in female athletes. Clin J Sport Med. 1998; 8(3): 178-186.
393. Vanneste S, De Ridder D. Brain Areas Controlling Heart Rate Variability in Tinnitus and Tinnitus-Related Distress. PloS ONE. 2013; 8(3): e59728.
394. Varanoske A, Margolis L, Pasiakos S. Effects of Testosterone on Serum Concentrations, Fat-free Mass, and Physical Performance by Population: A Meta-analysis. J Endocr Soc. 2020; 4(9): bvaa090.
395. Verberne AJ, Lam W, Owens NC, Sartor D. Supramedullary modulation of sympathetic vasomotor function. Clin Exp Pharmacol Physiol. 1997; 24(9-10): 748-754.
396. Verberne AJ. Medullary sympathoexcitatory neurons are inhibited by activation of the medial prefrontal cortex in the rat. Am J Physiol. 1996; 270(4Pt2): R713-R719.
397. Vetvik K, Schrumpf E, Andersen KJ. et al. Effect of misoprostol and antacids on gastric and duodenal mucosal enzyme activities in duodenal ulcer patients. Scand J Gastroenterol. 1991; 26(64): 385-391.
398. Vetvik K, Schrumpf E, Mowinckel P, et al. Effects of omeprazole and eradication of Helicobacter pylory on gastric and duodenal mucosal enzyme activities and DNA in duodenal ulcer patients. Scand J Gastroenterol. 1994; 29(611): 995-1000.
399. Vistak HI, Popovych IL. Vegetotropic effects of bioactive water Naftussya and their endocrine-immune support in female rats [in Ukrainian]. Medical Hydrology and Rehabilitation. 2011; 9(2): 39-57.
400. Vogler BK, Pittler MH, Ernst E. The efficacy of ginseng. A systematic review of randomised clinical trials. Eur J Clin Pharmacol. 1999; 55: 567-575.
401. Wagner H, Nörr H, Winterhoff H. Plant adaptogens. Phytomedicine. 1994; 1: 63-76.
402. Wang M, Gu H, Brewster BD, Huang C. Role of endogenous testosterone in TNF-induced myocardial injury in males. Int J Clin Exp Med. 2012; 5(2): 96-104.
403. Wang X, Hawkins BT, Miller DS. Aryl hydrocarbon receptor-mediated up-regulation of ATP-driven xenobiotic efflux transporters at the blood-brain barrier. FASEB J. 2011; 25: 644–652.
404. Wang Y, Ye X, Ma Z, et al. Induction of cytochrome P450 1A1 expression by ginsenoside Rg1 and Rb1 in HepG2 cells. Eur J Pharmacol. 2008; 601(1-3): 73-78.
405. Ward TL, Watkins KL, Southern LL, et al. Interactive effects of sodium zeolite-A and copper in growing swine: growth, and bone and tissue mineral concentrations. J Anim Sci. 1991; 69(62): 726-733.
406. Winkelmann T, Thayer JF, Pohlak ST, Nees F, Grimm O, Flor H. Structural brain correlates of heart rate variability in healthy young adult population. Brain Structure and Function. 2017; 222(2): 1061-1068.
407. Witchel S, Pinto B, Burghard A, Oberfield S. Update on adrenarche. Curr Opin Pediatr. 2020; 32(4): 574-581.
408. Wohlfart B, Farazdaghi GR. Reference values for the physical work capacity on a bicycle ergometer for men – a comparison with a previous study on women. Clinical physiology and functional imaging. 2003: 23(3): 166–170.

409. Yanes LL, Romero DG, Iles JW, Iliescu R, Gomez-Sanchez C, Reckelhoff JF. Sexual dimorphism in the renin-angiotensin system in aging spontaneously hypertensive rats. American Journal of Physiology-Regulatory, Integrative and Comparative Physiology. 2006; 291(2) :R383-R390.
410. Yang X, Liu H, Ye T, et al. AhR activation attenuates calcium oxalate nephrocalcinosis by diminishing M1 macrophage polarization and promoting M2 macrophage polarization. Theranostics. 2020; 10(26): 12011-12025.
411. Yaremenko MS, Ivassivka SV, Popovych IL, Bilas VR, Yassevych HP, Zahorodnyuk VP et al. Physiological Bases of Curative Effect of Water Naftussya [in Russian]. Kyïv. Naukova dumka; 1989: 144.
412. Ye L, Zhao B, Hu G, et al. Inhibition of human and rat testicular steroidogenic enzyme activities by bisphenol A. Toxicol Lett. 2011; 207(2): 137-142.
413. Yoo HJ, Thayer JF, Greenig S, Lee TH, Ponzio A, Min J, Sakaki M, Nga L, Mater M, Koenig J. Brain structural concomitants of resting state heart rate variability in the young and old: evidence from two independent samples. Brain Structure and Function. 2018; 223(2): 727-737.
414. Yue PY, Mak NK, Cheng YK, et al. Pharmacogenomics and the Yin/Yang actions of ginseng: antitumor, angiomodulating and steroid-like activities of ginsenosides. Chin Med. 2007; 2: 6.
415. Zajats LM, Polovynko IS, Zukow W, et al. Neuroendocrine-immune relatioships in rat females. Journal of Education, Health and Sport. 2017; 7(10): 59-78.
416. Zhang X, Zhang S, Sun Q, Jiao W, Yan Y, Zhang X. Compound K induces endoplasmic reticulum stress and apoptosis in human liver cancer cells by regulating STAT3. Molecules. 2018; 23: 1482.
417. Zhang YY, Xie N, Sun XD, Nice EC, Liou YC, Huang C, ... & Shen Z. Insights and implications of sexual dimorphism in osteoporosis. Bone research. 2024; 12(1): 8.
418. Zhao DQ, Xue H, Sun HJ. Nervous mechanisms of restraint water-immersion stress-induced gastric mucosal lesion. World J Gastroenterology. 2020; 26(20): 2533–2549.
419. Zukow W, Fihura OA, Korda MM, Klishch IM, Ruzhylo SV, Melnyk OI, Yanchij RI, Popovych IL. Modulating effects of Ukrainian phytocomposition "Balm Truskavets'" on post stress changes in neuroendocrine-immune complex, metabolome, electrocardiogram, and gastric mucosa at rats. Journal of Education, Health and Sport. 2024; 64: 55171.
420. Zukow W, Fihura OA, Żukow X, Muszkieta R, Hagner-Derengowska M, Smoleńska O, Michalska A, Melnyk OI, Ruzhylo SV, Zakalyak NR, Kondratska HD, Voloshyn OR, Popovych IL. Prevention of adverse effects of balneofactors at Truskavets' Spa on gastroenterologic patients through phytoadaptogens and therapeutic physical education: mechanisms of rehabilitation. Journal of Physical Education and Sport. 2024; 24(4): 791-810.
421. Zukow W, Fil VM, Kovalchuk HY, Voloshyn OR, Kopko IY, Lupak OM, Ivasivka AS, Musiyenko OV, Bilas VR, Popovych IL. The role of innate muscular endurance and resistance to hypoxia in reactions to acute stress of immunity in rats. Journal of Physical Education and Sport. 2022; 22(7): 1608-1617.

422. Zukow W, Flyunt I-S S, Ponomarenko RB, Rybak NY, Fil' VM, Kovalchuk HY, Sarancha SM, Nahurna YV. Polyvariant change of step-test under the influence of natural adaptogens and their accompaniments. Pedagogy and Psychology of Sport. 2020; 6(2): 74-84.
423. Zukow W, Flyunt I-S S, Ruzhylo SV, Kovalchuk HY, Nahurna YV, Popovych DV, Sarancha SM. Forecasting of multivariant changes in step test under the influence of natural adaptogens. Pedagogy and Psychology of Sport. 2021; 7(1): 85-93.
424. Zukow W, Gozhenko OA, Zavidnyuk YV, Korda MM, Mysula IR, Klishch IM, Zhulkevych IV, Popovych IL, Muszkieta R, Napierata M, Hagner-Derengowska M, Skaliy A. Role of organic carbon and nitrogen of mineral waters in their neuro-endocrine effects at female rats. International J of Applied Exercise Physiology. 2020; 9(4): 20-25.
425. Zukow W, Muszkieta R, Hagner-Derengowska M, Smoleńska O, Żukow X, Fil VM, Kovalchuk HY, Voloshyn OR, Kopko IY, Lupak OM, Ivasivka AS, Musiyenko OV, Ruzhylo SV, Kindrat V, Popovych IL. Role of organic substances of Naftussya bioactive water in its effects on dynamic and static fitness in rats. Journal of Physical Education and Sport. 2022; 22(11): 2733-2742.
426. Zukow W, Muszkieta R, Hagner-Derengowska M, Smoleńska O, Żukow X, Melnyk OI, Popovych DV, Tserkoniuk RG, Hryhorenko AM, Yanchij RI, Kindrat V, Popovych IL. Effects of rehabilitation at the Truskavets' spa on physical working capacity and its neural, metabolic, and hemato-immune accompaniments. Journal of Physical Education and Sport. 2022; 22(11), 2708-2722.

Наукове видання

Mykhaylo M. Korda
Oksana A. Fihura
Oksana I. Melnyk
Ivan M. Klishch
Roman I. Yanchij
Walery A. Zukow
Sofiya V. Ruzhylo
Dariya V. Popovych
Igor L. Popovych

UKRAINIAN PHYTOCOMPOSITION «BALM TRUSKAVETS'», METABOLISM, PHYSICAL WORKING CAPACITY AND NEURO-ENDOCRINE-IMMUNE COMPLEX

Монографія

В авторській редакції

Комп'ютерна верстка *Ю. Гандера*

Підписано до друку 27.01.2025 р. Формат 60x84/16
Папір офсетн. Умовн.друк. арк. 20,5.
Тираж 100 прим.

Державне підприємство
«Всеукраїнське спеціалізоване видавництво «Світ»
79008 Львів, вул. Галицька, 21
Свідоцтво суб'єкта видавничої справи
ДК №2980 від 19.09.2007 р.
www.svit.gov.ua
e-mai: office@svit.gov.ua